

Old Drugs in a New Light, Investigating the Gold Rheumatoid Arthritis Medications as Novel  
Inhibitors of Neuroinflammation

by

Jocelyn Marie Madeira

B.Sc., The University of British Columbia, 2010

A THESIS SUBMITTED IN PARTIAL FULFILLMENT OF  
THE REQUIREMENTS FOR THE DEGREE OF

Master of Science

in

The College of Graduate Studies

(Biology)

THE UNIVERSITY OF BRITISH COLUMBIA  
(Okanagan)

November 2012

© Jocelyn Marie Madeira, 2012

## Abstract

Several degenerative disorders of the central nervous system including Alzheimer's and Parkinson's diseases are characterized by chronic inflammation. The main contributors to this inflammation are glial cells, including microglia and astrocytes. Even though they are normally protective, disease specific stimuli can activate glial cells to start secreting neurotoxic molecules. There is no effective treatment for neurodegenerative diseases, though it is hypothesized that reducing neuroinflammation may diminish neuronal loss. Chronic use of non-steroidal anti-inflammatory drugs (NSAIDs) has been linked with lower incidence of neurodegenerative disorders, though mixed results have been obtained in clinical trials of NSAIDs when these drugs are used for treatment of established disease. Gold thiol compounds, including aurothiomalate, aurothioglucose, and auranofin, comprise another class of medications effective at reducing peripheral inflammation in rheumatoid arthritis patients. Their effects on neuroinflammation are unknown. In this thesis I demonstrate that 0.1 – 5  $\mu\text{M}$  auranofin, but not the other gold thiol compounds, inhibits human microglia and astrocyte-mediated neurotoxicity *in vitro*. The anti-neurotoxic properties of auranofin are selective; treatment with auranofin does not inhibit expression or secretion of several cytokines by glia but does upregulate heme-oxygenase (HOX)-1. Interestingly, low micromolar concentrations of auranofin directly protect neuronal cells from toxicity induced by hydrogen peroxide or stimulated glial supernatants, possibly through the upregulation of HOX-1. Lastly, laser ablation inductively coupled plasma mass spectrometry (LA-ICP-MS) was used to demonstrate that auranofin reaches low micromolar concentrations in mouse brains following daily oral administration for one week. Since auranofin can protect against neuroinflammation by inhibiting glial toxicity and is directly

neuroprotective, it may be useful in neurodegenerative diseases where sustained inflammation contributes to disease progression including neuronal loss.

**Keywords:** Auranofin, Alzheimer's Disease, Parkinson's Disease, Neuroinflammation

## **Preface**

To date, part of my research on AF has been described in two manuscripts. One of them has been accepted for publication in *Inflammopharmacology* (see Appendix B) and the other manuscript is under review by the *European Journal of Pharmacology* (see Appendix C).

The data described in this thesis was also presented as a poster at the International Alzheimer's Association Conference in Vancouver, BC and UBC Okanagan Biochemistry Departmental seminars.

I underwent training required to work with Biosafety Level 1 and Level 2 materials including various human cell lines and primary human astrocytes and obtained appropriate certification.

I am responsible for all experimental data obtained and writing presented in this thesis, except for laser ablation inductively coupled plasma mass spectroscopy (LA-ICP-MS) experiments which were performed by Colby Renschler and Bert Mueller, Sulforhodamine B (SRB) cell viability assays performed by Jenelle Lamothe and experiments with primary human microglia which were performed by Dr. Sadayuki Hashioka. In addition, for the publication included in Appendix D, I only performed enzyme-linked immunosorbent assays, in addition to writing parts of the manuscript. Dr. Jonathan Little was the lead author of the manuscript and performed all other experiments. Drs. Little and Klegeris designed the study, and wrote the manuscript.

# Table of Contents

<b>Abstract</b> .....	ii
<b>Preface</b> .....	iv
<b>Table of Contents</b> .....	v
<b>List of Tables</b> .....	ix
<b>List of Figures</b> .....	x
<b>List of Abbreviations and Symbols</b> .....	xi
<b>Acknowledgements</b> ....	xvii
<b>Dedication</b> .....	xviii
<b>1.0. Introduction</b> .....	1
<b>1.1. Background</b> .....	1
<b>1.1.1. Neurodegenerative Disorders</b> .....	1
<b>1.1.2. The Central Nervous System</b> .....	3
<b>1.1.3. Neuroinflammation</b> .....	4
<b>1.1.4. Rheumatoid Arthritis and Disease-Modifying Anti-Rheumatic Medications</b> .....	6
<b>1.1.5. Gold Drugs and their Potential Therapeutic Uses</b> .....	7
<b>1.1.6. Cell Culture Model of Neuroinflammation</b> .....	8
<b>1.1.7. Molecular Targets for Auranofin</b> .....	10
<b>1.1.8. <i>In Vivo</i> Distribution of Auranofin</b> .....	11
<b>1.2. Biological Activity of Auranofin</b> .....	12
<b>1.2.1. Anti-Inflammatory Activity of Auranofin</b> .....	12
<b>1.2.2. Anti-Neoplastic Activity of Auranofin</b> .....	13
<b>1.2.3. Protective Effects of Auranofin</b> .....	15
<b>1.3. Research Overview and Hypothesis</b> .....	17
<b>2.0. Materials and Methods</b> .....	22
<b>2.1. Reagents</b> .....	22
<b>2.2. Equipment</b> .....	23
<b>2.3. Model Cells</b> .....	24

<b>2.4. Plating Glial Cells for Supernatant Transfer and Neuroprotective Experiments</b> .....	24
<b>2.4.1. THP-1 Human Promonocytic Cells</b> .....	24
<b>2.4.2. Primary Human Microglia</b> .....	25
<b>2.4.3. U-373 MG and U-118 MG Astrocytoma Cells</b> .....	26
<b>2.4.4. Primary Human Astrocytes</b> .....	27
<b>2.5. Plating Human SH-SY5Y Neuronal Cells for Supernatant Transfer and Neuroprotective Experiments</b> .....	27
<b>2.6. Cell Viability Assay: Lactate Dehydrogenase</b> .....	28
<b>2.7. Cell Viability Assay: 3-(4, 5-Dimethylthiazol-2-Yl)-2, 5-Diphenyltetrazolium Bromide</b> .....	30
<b>2.8. Cell Viability Assay: Sulforhodamine B Colorimetric Assay</b> .....	31
<b>2.9. Enzyme-Linked Immunosorbent Assay</b> .....	32
<b>2.10. Plating and Differentiating HL-60 Cells for Use in Experiments</b> .....	34
<b>2.11. Chemiluminescence Assay (Measuring Respiratory Burst)</b> .....	35
<b>2.12. mRNA Extraction And cDNA Synthesis</b> .....	37
<b>2.12.1. mRNA Extraction From SH-SY5Y Cells</b> .....	37
<b>2.12.2. mRNA Extraction From Astrocytic Cells</b> .....	37
<b>2.12.3. mRNA Spin Column Protocol</b> .....	38
<b>2.12.4. cDNA Synthesis</b> .....	39
<b>2.13. Quantitative Polymerase Chain Reaction</b> .....	39
<b>2.14. Treatment of Mice With Auranofin and Preparation Of Tissues For Laser Ablation Inductively Coupled Plasma Mass Spectroscopy</b> .....	42
<b>2.15. Laser Ablation Inductively Coupled Plasma Mass Spectroscopy</b> .....	44
<b>2.16. Statistical Analysis</b> .....	44
<b>3.0. Results</b> .....	46
<b>3.1. Anti-Neurotoxic Activity Of Gold Compounds</b> .....	46
<b>3.1.1. Inhibition of Microglial Toxicity by Gold Compounds</b> .....	46
<b>3.1.1.1. Effects of Gold Compounds on Human THP-1 Promonocytic Cell Viability and Cytotoxicity after 24 H Incubation</b> .....	46

<b>3.1.1.2.</b> Effects of Gold Compounds on THP-1 Cell Viability and Cytotoxicity after 48 H Incubation .....	50
<b>3.1.1.3.</b> Effects of Auranofin on Primary Human Microglia Cell Viability and Cytotoxicity after 48 H Incubation .....	54
<b>3.1.2. Inhibition of Astrocyte Toxicity by Gold Compounds</b> .....	56
<b>3.1.2.1.</b> Effects of Gold Compounds on U-373 MG Astrocytoma Cell Viability and Cytotoxicity.....	56
<b>3.1.2.2.</b> Effects of Auranofin on U-118 MG Astrocytoma Cell Viability and Cytotoxicity .....	63
<b>3.1.2.3.</b> Effects of Auranofin on Human Astrocyte Viability and Cytotoxicity .....	68
<b>3.2. Neuroprotective Activity of Auranofin</b> .....	70
<b>3.3. Mechanisms of Auranofin Action</b> .....	72
<b>3.3.1. Mechanisms of Action of Auranofin on Microglia</b> .....	72
<b>3.3.1.1.</b> Inhibition of the Phagocyte Respiratory Burst by Auranofin.....	72
<b>3.3.1.2.</b> Inhibition of the Priming of the Phagocyte Respiratory Burst by Auranofin .....	74
<b>3.3.1.3.</b> Effects of Auranofin on HL-60 Cell Viability .....	77
<b>3.3.1.4.</b> Effects of Gold Compounds on the Secretion of Monocyte Chemotactic Peptide-1 by THP-1 Cells .....	78
<b>3.3.2. Mechanisms of Action of Auranofin on Astrocytes</b> .....	80
<b>3.3.2.1.</b> Effects of Auranofin on the Inflammatory Mediator mRNA Expression in Astrocytic Cells .....	80
<b>3.3.2.2.</b> Effects of Auranofin on the Secretion of Interleukin-6, Interleukin-8, and Monocyte Chemotactic Peptide-1 by Astrocytic Cells .....	83
<b>3.3.2.3.</b> Effects of the Calmodulin Inhibitor Trifloroperazine on the Anti-Neurotoxic Activity of Auranofin.....	85
<b>3.3.2.4.</b> Effects of Auranofin on the Expression and Secretion of	

Interleukin-4 By Human Astrocytic Cells.....	87
<b>3.3.3. Mechanisms of Action of Auranofin in Neurons .....</b>	<b>90</b>
<b>3.3.3.1. Effect of Auranofin on Heme-Oxygenase-1 Expression</b>	
In Neurons .....	90
<b>3.3.3.2. Effects of the Calmodulin Inhibitor TFP on the</b>	
Neuroprotective Activity of Auranofin .....	92
<b>3.4. In Vivo Distribution of Auranofin after Oral Administration in Mice ..</b>	<b>93</b>
<b>4.0. Discussion .....</b>	<b>95</b>
<b>4.1. Anti-Neurotoxic Activity of Gold Compounds .....</b>	<b>95</b>
<b>4.1.1. Effect of Gold Compounds on Microglial Toxicity .....</b>	<b>95</b>
<b>4.1.2. Activity of Gold Compounds on Astrocyte Toxicity .....</b>	<b>95</b>
<b>4.2. Neuroprotective Activity of Auranofin .....</b>	<b>98</b>
<b>4.3. Mechanisms of Auranofin Action.....</b>	<b>100</b>
<b>4.3.1. Mechanisms of Action of Auranofin on Microglia.....</b>	<b>100</b>
<b>4.3.2. Mechanisms of Action of Auranofin on Astrocytes.....</b>	<b>101</b>
<b>4.3.3. Mechanisms of Action of Auranofin on Neurons .....</b>	<b>103</b>
<b>4.4. In Vivo Distribution of Auranofin after Oral Administration .....</b>	<b>104</b>
<b>5.0. Conclusions and Future Work.....</b>	<b>107</b>
<b>5.1. Limitations of Research.....</b>	<b>107</b>
<b>5.2. Future Work .....</b>	<b>108</b>
<b>5.3. Significance of Findings.....</b>	<b>108</b>
<b>References.....</b>	<b>110</b>
<b>Appendices .....</b>	<b>124</b>
<b>Appendix A: Enzyme Linked Immunosorbent Assay Reagents.....</b>	<b>124</b>
<b>Appendix B: Publication: The Biological Activity of Auranofin: Implications</b>	
<b>For Novel Treatment Of Diseases. Neuropharmacology</b>	
<b>(In Press).....</b>	<b>125</b>
<b>Appendix C: Publication: Auranofin Inhibits Astrocyte-Mediated</b>	
<b>Neuroinflammation <i>In Vitro</i> and is Directly Neuroprotective.</b>	
<b>Euro J Pharm (Submitted).....</b>	<b>150</b>

**Appendix D:** Publication: The Saturated Fatty Acid Palmitate Induces Human Monocytic Cell Toxicity towards Neuronal Cells: Exploring a Possible Link between Obesity-Related Metabolic Impairments and Neuroinflammation J. Alzheim. Dis. Vol. 30 Suppl. 2, S179-S183..... 176

## List of Tables

<b>Table 1:</b> The Anti-Neoplastic Molecular Mechanisms of AF .....	15
<b>Table 2:</b> Primer Sequences Used in qPCR Experiments .....	42
<b>Table 3:</b> Concentrations of Gold in Various Organs of Mice and Rats after Oral Gavage of Auranofin .....	94

## List of Figures

Figure 1: The chemical structures of AF, ATG, ATM and ATS.....	7
Figure 2: Flow chart of experiments .....	20
Figure 3: Example of chemiluminescence data .....	36
Figure 4: Example of primer efficiency data.....	41
Figure 5: Effect of 24 h incubation with gold compounds on the viability of human THP-1 promonocytic cells .....	47
Figure 6: 24 h incubation with AF reduces cytotoxic secretions of THP-1 promonocytic cells .....	49
Figure 7: Effect of 48 h incubation with gold compounds on the viability of human THP-1promonocytic cells .....	51
Figure 8: 48 h incubation with AF reduces cytotoxic secretions of THP-1 promonocytic cells.....	53
Figure 9: Effect of 24 h incubation with AF on the viability and cytotoxicity of primary human microglia.....	55
Figure 10: Effect of 48 h incubation with gold compounds on the viability of human U-373 MG astrocytoma cells .....	57
Figure 11: 48 h incubation with AF reduces cytotoxic secretions of U-373 MG astrocytoma cells .....	59
Figure 12: AF is not toxic to human U-373 MG astrocytoma cells and reduces toxicity of secretions from U-373 MG cells towards SH-SY5Y neuronal cells: confirmation by the SRB assay .....	61
Figure 13: AF prevents morphological changes induced in SH-SY5Y cells by stimulated U-373 MG cell supernatants .....	63
Figure 14: Effect of gold compounds on the viability of human U-118 MG astrocytoma cells after 48 h incubation .....	65
Figure 15: 48 h incubation with AF reduces cytotoxic secretions of U-118 MG astrocytoma cells .....	67
Figure 16: Effect of AF on the viability and cytotoxicity of primary human astrocytes after 24 h incubation .....	69

Figure 17: AF protects SH-SY5Y neuronal cells against toxicity induced by hydrogen peroxide and supernatants from stimulated glial cells.....	71
Figure 18: AF, but not ATM, ATG, or ATS, inhibits phagocyte respiratory burst activity.....	73
Figure 19: AF inhibits LPS and Tfm induced priming of the phagocyte respiratory burst .....	75
Figure 20: 24 h incubation with AF inhibits the phagocyte respiratory burst.....	76
Figure 21: Effect of AF on the viability of human HL-60 promyelocytic cells after 24 h incubation .....	78
Figure 22: Gold compounds have no significant effect on MCP-1 secretion by THP-1 cells .....	79
Figure 23: AF upregulates HOX-1 mRNA expression in unstimulated and stimulated U-373 MG astrocytic cells and primary human astrocytes.....	81
Figure 24: AF does not change IL-6, IL-8 or MCP-1 mRNA expression in unstimulated or IFN- $\gamma$ -stimulated U-373 MG astrocytic cells.....	82
Figure 25: AF has no significant effect on cytokine secretion by stimulated U-373 MG cells .....	84
Figure 26: AF has no significant effect on cytokine secretion by stimulated U-118 MG cells .....	85
Figure 27: Calmodulin inhibitor TFP does not affect the anti-neurotoxic activity of AF .....	87
Figure 28: AF has no effect on IL-4 expression in U-373 MG astrocytic cells; it also does not affect IL-4 secretion by primary human astrocytes .....	89
Figure 29: AF upregulates heme oxygenase (HOX-1) mRNA expression in stimulated SH-SY5Y cells .....	91
Figure 30: Effects of calmodulin inhibitor, TFP, on the neuroprotective activity of AF .....	93

## List of Abbreviations

A $\beta$ - Amyloid beta protein

AD- Alzheimer's Disease

AF- Auranofin

ANOVA- Analysis of Variance

ATG- Aurothioglucose

ATM- Sodium aurothiomalate

ATS- Aurothiosulfate

Au- Chemical element gold

BBB- Blood brain barrier

$\beta$ -NAD- Beta-nicotinamide adenine dinucleotide

BLAST- Basic local alignment search tool

BSA- Bovine serum albumin

CB2- Cannabinoid type 2

cDNA- Complementary DNA

CHL- Chemiluminescence

CNS- Central nervous system

CO- Carbon monoxide

COX – Cyclooxygenase

Ct- Cycle threshold

DAMP- Damage associated molecular patterns

DMARD- Disease-modifying anti-rheumatic drugs

DMEM- F12- Dulbecco's modified Eagle medium nutrient mixture F-12 Ham

DMF- N, N-Dimethylformamide

DMSO- Dimethyl sulfoxide

DNA- Deoxyribonucleic acid

EDTA - Ethylenediaminetetraacetic acid

ELISA- Enzyme linked immunoabsorbent assay

EtOH- Ethanol

F0- DMEM-F12 media without FBS

F5- DMEM-F12 media supplemented with 5% FBS

F10- DMEM-F12 media supplemented with 10% FBS

FBS- Fetal bovine serum

FLAP- 5-LOX activating protein

fMLP- N-formyl-methionine-leucine-phenylalanine

H<sub>2</sub>O<sub>2</sub>- Hydrogen peroxide

HOX - Heme-oxygenase

HL-60- Human promyelocytic leukemia cell line (microglial NADPH-oxidase model)

IFN- Interferon

IKK- IκB kinase

IL – Interleukin

INT- Iodonitrotetrazolium chloride

IRF- Interferon regulatory factor

JAK- Janus kinase

Lactate- Sodium L-lactate

LA-ICP-MS - Laser ablation inductively coupled plasma mass spectrometry

LDH- Lactate dehydrogenase

LOX- Lipoxygenase

LPS- Lipopolysaccharide

LSD- Least significant difference

MAPK- Mitogen-activated protein kinase

MCP- Monocyte chemotactic protein

MIQE- Minimum Information for Publication of Quantitative Real-Time PCR Experiments

MMP- Matrix metalloproteinase

mRNA- Messenger RNA

MTT- 3-(4,5-dimethylthiazol-2-yl)-2,5-diphenyl tetrazolium bromide

NADPH- Nicotinamide adenine dinucleotide phosphate

NCBI- National centre for biotechnology information

NF- $\kappa$ B- Nuclear factor kappa-light-chain-enhancer of activated-B-cells

NFT- Neurofibrillary tangles

Nrf2- Nuclear factor erythroid 2-related factor 2

NRT- No reverse transcriptase control

NSAIDS- Non-steroidal anti-inflammatory drugs

NTC- No template control

OD- Optical density

p- Probability

PBS- Phosphate-buffered saline

PD- Parkinson's disease

PG- Prostaglandin

RA- Rheumatoid arthritis

Rac1- Ras-related C3 botulinum toxin substrate 1

RAGE - Receptor for advanced glycation end products

RNA- Ribonucleic acid

RONS - Reactive oxygen and nitrogen species

ROS- Reactive oxygen species

RT- qPCR- real time quantitative polymerase chain reaction

SD- Standard deviation

SDS- Sodium dodecyl sulphate

SEM- Standard error of the mean

SH-SY5Y- Human dopaminergic neuroblastoma cell line (neuronal model)

SRB- Sulforhodamine B

STAT- Signal transducer and activator of transcription

TB- Tuberculosis

Tfam- Mitochondrial protein transcription factor A

TFP- Trifloroperazine

THP-1- Human promonocytic cell line (microglia model)

TIMP- Tissue inhibitor of matrix metalloproteinase

TIR- Toll/IL-1 receptor

TLR- Toll-like receptor

TNF - Tumor necrosis factor

TRIF- TIR-domain-containing adapter-inducing interferon- $\beta$

Tris- Tris (hydroxymethyl)aminomethane

TrxR- Thioredoxin reductase

U-118 MG- Human astrocytoma cell line (astrocyte model)

U-373 MG- Human astrocytoma cell line (astrocyte model)

## **Acknowledgements**

I would like to express both my appreciation and gratitude to my advisor, Dr. Andis Klegeris, for the patient guidance and mentorship he provided to me. I thank Dr. Klegeris for his continuous support despite several lab mishaps and my early attempts at writing. I am truly fortunate to have had the opportunity to work with him.

I would also like to thank my committee members, Drs. Joyce Boon, Deanna Gibson, and Bruce Mathieson for the friendly guidance, thought provoking suggestions, and the general collegiality that each of them offered to me over the years. Thank you to Dr. Mark Rheault's laboratory for the use of equipment, to Bert Mueller for his assistance with LA-ICP-MS work, and to the lab members of Drs. Gibson and Ghosh for their qPCR expertise. Special thanks to Dr. Jonathan Little who was a prodigious source of information and guidance. I would also like to thank my fellow colleagues at the Laboratory of Cellular and Molecular Pharmacology for helping me with my project and for providing a positive shared work space.

Lastly, I would like to thank my family and friends for supporting my continued academic endeavours. I could not maintain my perpetual student status if it wasn't for your support, patience, and valiant attempts to understand my research.

Thank you all so much, without your help I could not have completed this thesis.

*For my grandmother*

## **1.0. Introduction**

### **1.1. Neuroinflammation and Background**

#### **1.1.1. Neurodegenerative disorders**

Alzheimer's disease (AD) and Parkinson's disease (PD) are the two most common late-onset neurodegenerative disorders, both of which have devastating effects on patients and their families <sup>1</sup>. Unfortunately, there is not yet an effective treatment or cure for either of these conditions. Furthermore, the causes of the majority of cases of these disorders are currently unknown, making it difficult to pinpoint potential targets for treatment. AD alone accounts for 60-70% of all cases of progressive cognitive impairment in the elderly and costs the Canadian health care system approximately \$47,000 per patient per year <sup>2</sup>. A large aging population from the baby boomer generation combined with an increase in the average North American's lifespan will amplify the prevalence of these conditions in coming years, placing an enormous burden on healthcare systems. Therefore, it is now more important than ever to find an effective way to treat these conditions.

AD currently affects 20-30 million people worldwide, and its population-wide prevalence increases to above 40% in individuals over the age of 85 <sup>2</sup>. The symptoms of AD are progressive and include severe memory loss, inability to communicate, and the eventual loss of motor functioning <sup>2</sup>. The two major pathological features of AD include extracellular plaques containing amyloid beta protein (A $\beta$ ) and intracellular neurofibrillary tangles (NFT)'s composed of phosphorylated tau protein <sup>3</sup>. More recently, the influences of chronic inflammation and glial cell activation have been recognized as important factors in driving AD progression <sup>3,4</sup>. While

the cause of this inflammation remains unknown, the neurotoxic A $\beta$  plaques have been shown to activate microglia and astrocytes <sup>5,6</sup>.

PD also involves neuroinflammation and increases in prevalence with age, from 0.6% at age 65 to 4-5% at greater than 85 years of age <sup>1</sup>. Symptoms of PD include resting tremors, slow movement, rigidity, and dementia in late stages of the disease <sup>1</sup>. There is significant loss of dopaminergic neurons in the substantia nigra of PD patients, with the major pathological hallmark being the presence of Lewy bodies, which are brain inclusions composed mainly of  $\alpha$ -synuclein <sup>1,7</sup>. In PD, death or damage to dopaminergic neurons lead to excess production of reactive oxygen species (ROS), and the resulting oxidative stress contributes to neuroinflammatory processes <sup>8</sup>. The current treatment for PD is Levodopa, a dopamine precursor which supplements the central nervous system (CNS) with the dopamine that is no longer being produced by dead and damaged dopaminergic neurons <sup>8</sup>. While Levodopa is able to temporarily mask the symptoms of PD, it becomes less effective over time, causes increasing side effects, and it does not stop the progression of the disease and therefore cannot be considered a cure <sup>8</sup>.

AD and PD are not the only diseases in which neuroinflammation and neurodegeneration occur together. For example, Huntington's disease, multiple sclerosis, and amyotrophic lateral sclerosis involve both neuroinflammation and neurodegeneration <sup>9</sup>. Even non-progressive conditions such as fetal alcohol spectrum disorder are characterized by neuronal loss and activated microglia <sup>10</sup>. Neuroinflammation is a multi-faceted process involving many pathways, including production of toxic reactive species by immune cells of the CNS, inflammatory cascades involving cyclooxygenase (COX) and lipoxygenase (LOX) enzymes, and activation of caspases and subsequent apoptosis in neurons <sup>4,11</sup>. The additional complication of disease-specific triggers in neurodegenerative conditions makes finding a cure for these conditions

especially difficult, as a reductionist perspective attempting to summarize the whole based on individual parts cannot encompass the many interactions and synergies that occur in these diseases<sup>3</sup>. Obstacles such as these have prevented the development of successful treatments for neurodegenerative conditions to date. Further research investigating potential treatments may not only slow the progression of these diseases and elucidate novel mechanisms by which these diseases occur, but could also lead to the development of a cure.

### **1.1.2. The Central Nervous System**

The brain is primarily composed of two types of cells: neurons and glial cells. Neurons are excitable cells that respond to stimuli and transmit electrical and chemical signals. In addition to neurons, there are four main types of glial cells in the CNS: astrocytes, microglia, ependymal cells, and oligodendrocytes<sup>12</sup>. Astrocytes, the most abundant glial cell type in the brain, regulate the chemical environment surrounding neurons by taking up neurotransmitters and ions and providing neurons with glucose<sup>12</sup>. While astrocytes can support neurons and promote viability, they can become adversely activated by inflammatory mediators and start damaging neurons<sup>13</sup>.

Microglia account for approximately 12% of glial cells in the brain. They are members of the mononuclear phagocyte system and act as part of the innate immune system of the CNS<sup>7</sup>. While in a resting state, microglia provide protection from foreign pathogens and support neuronal growth and development by secreting various neurotrophic molecules such as endocannabinoids and neurotrophins<sup>7</sup>. However, upon stimulation with disease-specific misaggregated proteins such as A $\beta$  or  $\alpha$ -synuclein, microglia can become activated and begin to secrete cytotoxic molecules including reactive oxygen and nitrogen species (RONS) and proteases in an attempt to clear the misaggregated proteins<sup>3,14</sup>. These disease-specific proteins

stimulate microglia through various pathways and cell surface receptors. For example, the formyl peptide receptor and the receptor for advanced glycation end products (RAGE) have been implicated in A $\beta$ -dependent activation of microglia<sup>5</sup>. On the other hand, activation of microglia by  $\alpha$ -synuclein is mediated by phagocytosis of  $\alpha$ -synuclein and includes activation of nicotinamide adenine dinucleotide phosphate (NADPH) oxidase<sup>15</sup>.

### 1.1.3. Neuroinflammation

Cytotoxic secretions from microglia and astrocytes aid in the destruction of foreign pathogens. However, when activation of these cells becomes chronic and unchecked, as in neurodegenerative disorders, they can also harm healthy neurons surrounding the site of inflammation<sup>14,16</sup>. The resulting neuronal death and damage can in turn activate additional glial cells, which can lead to a cycle of inflammation and cell death that continues even in the absence of the initial trigger<sup>17</sup>.

In AD, the hallmark A $\beta$  plaques do not correlate strongly with cognitive decline and the NFTs alone cannot account for progression of the disease<sup>3</sup>. As mentioned previously, A $\beta$  plaques are capable of activating glial cells and initiating neuroinflammation, which could be partially responsible for the AD progression that cannot be explained by NFTs or A $\beta$  alone<sup>3</sup>.

In the case of PD, the initial stages of the disease are characterized by loss of dopaminergic neurons in the substantia nigra<sup>8</sup>. The death of these neurons is followed by the release of molecules including glutamine, RONS, and  $\alpha$ -synuclein, all of which have been shown to activate microglia<sup>15</sup>. In particular, the mutated form of  $\alpha$ -synuclein found in PD has been shown to activate both microglia and astrocytes, though the mechanism by which this occurs is

currently unknown<sup>18</sup>. While PD is known to have various causes, the role of chronic and excessive microglial activation in disease progression is well established<sup>1,15</sup>.

With the role of inflammation in neurodegenerative disorders becoming more established and widely accepted, various pilot tests involving anti-inflammatory medications have been performed in attempt to treat these conditions<sup>18</sup>. In their recent work, Lee *et al.* (2011) showed that stimulated THP-1 cell supernatants, which model the substances released from activated microglia, reduce neuronal cell viability by 45%. The effectors responsible for this reduction in neuronal viability included interleukin (IL)-1 $\beta$ , IL-8, and tumor necrosis factor (TNF)- $\alpha$ , which accounted for a combined total of 37-38% of neuronal death<sup>19</sup>. RONS accounted for another 37-38% of neuronal killing<sup>19</sup>. Additionally, post-mortem samples from patients with AD confirm upregulation of inflammatory cytokines, complement activation, and increased COX-2 expression in comparison to non-diseased brains<sup>20</sup>. Anti-inflammatory treatments that reduce the inflammation characteristic of neurodegenerative conditions could potentially reduce neuronal loss in AD and PD. People regularly consuming non-steroidal anti-inflammatory drugs (NSAIDs) are relatively spared from AD and PD, though clinical trials with COX-2 inhibitors have shown mixed results<sup>21,22</sup>. Early randomized clinical trials with indomethacin indicated a protective effect, though subsequent studies with indomethacin, diclofenac, nimesulide, and naproxen failed to demonstrate any benefit in cognitive performance<sup>22-25</sup>. Leoutsakos *et al.*, (2011) demonstrated that naproxen and celecoxib may inhibit cognitive decline in early, but not late, stages of AD indicating that stages of the disease may also play a role in the efficacy of anti-inflammatory interventions in AD. Despite these inconclusive data, it is possible that the low doses used in these studies and the relatively modest anti-inflammatory effects of NSAIDs are

not potent enough to inhibit chronic inflammation once it has begun and may account for the inconsistent findings.

#### **1.1.4. Rheumatoid Arthritis and Disease-Modifying Anti-Rheumatic Medications**

Rheumatoid Arthritis (RA) is a debilitating autoimmune disease characterized by inflammation and progressive deterioration of the joints <sup>26</sup>. While NSAIDs are prescribed for the pain associated with RA, there are also several disease-modifying anti-rheumatic drugs (DMARD)s that are used to control inflammation and prevent disease progression <sup>26</sup>. DMARD therapy is usually initiated with the drug methotrexate at the time of diagnosis, followed by physician-supervised DMARD supplementation which is adjusted and tailored to each individual patient <sup>27</sup>. In addition to methotrexate, common DMARDs include gold compounds, cyclosporine, and sulfasalazine <sup>27</sup>. While these medications all have different mechanisms of action and efficacies, they tend to be more potent inhibitors of inflammation than NSAIDs <sup>27</sup>.

Gold thiol compounds comprise the oldest category of DMARDs and include sodium aurothiomalate (ATM), aurothioglucose (ATG), and 2,3,4,6-tetra-*o*-acetyl-1-thio- $\beta$ -D-glucopyrano-sato-S-(triethyl-phosphine) manufactured as auranofin (AF) <sup>28</sup>. These gold-based compounds are the focus of this thesis and we hypothesize that they could be more potent inhibitors of inflammation in chronic inflammatory diseases such as AD and PD than the NSAIDs previously used in clinical trials. Aurothiosulfate (ATS); a gold-thiol complex similar to ATM, ATG and AF, was included in experiments as a control gold compound without anti-inflammatory activity. The structures of the gold compounds are illustrated in Figure 1.

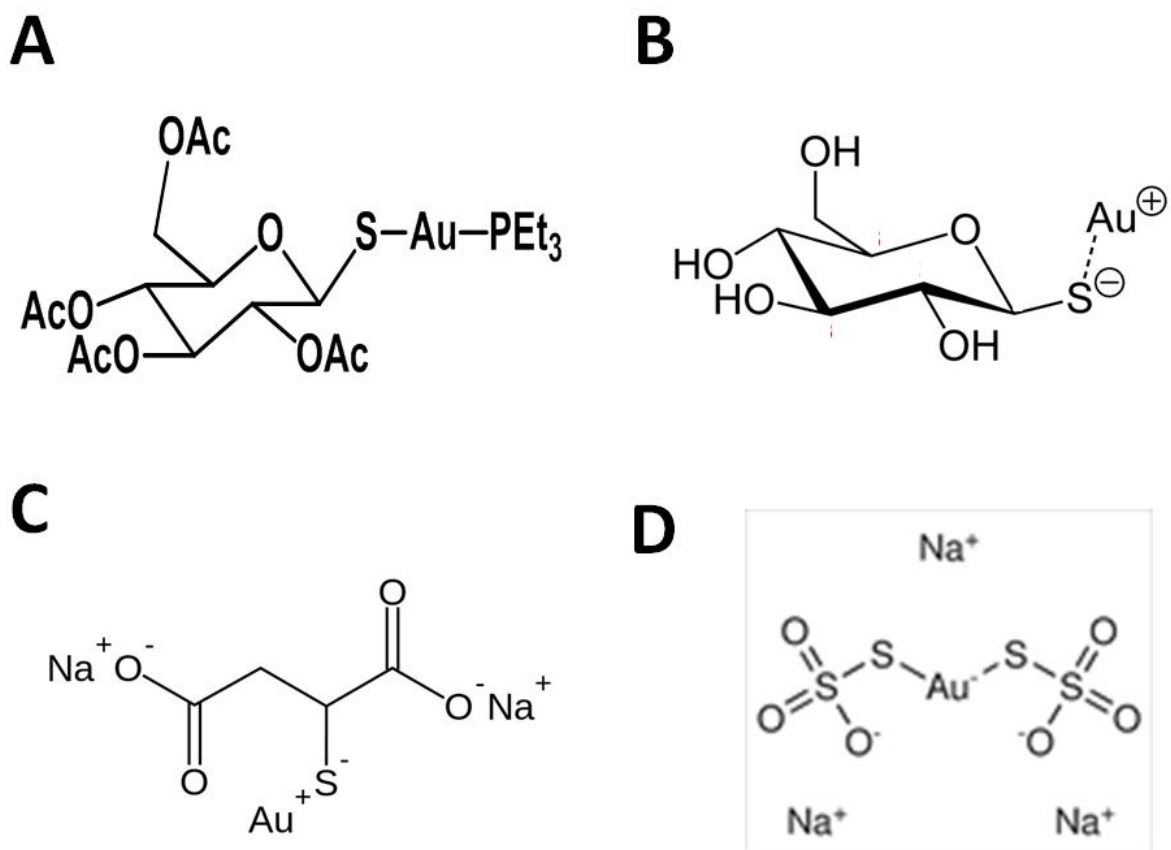


**Fig. 1:** The chemical structures of AF (**A**), ATG (**B**), ATM (**C**), and ATS (**D**). Ac, acetyl group; Et, ethyl group.

### 1.1.5. Gold Drugs and their Potential Therapeutic Uses

In the early 1890's, interest in gold therapy originated from the work of bacteriologist Dr. Koch who observed that gold cyanide was toxic toward the tubercle bacteria *in vitro*<sup>29</sup>. This led to increased research activity in this area and the establishment of tuberculosis (TB) treatments with various gold compounds, including ATM<sup>30</sup>. The potential anti-TB action of the gold drugs was eventually dismissed after the patients treated with these compounds were not cured of their infections. However, a serendipitous observation that RA improved with gold therapy led to the use of gold compounds in the treatment of RA, which is still widely used today<sup>26</sup>. In the 1980's

an oral gold drug, AF, was introduced to the market <sup>29</sup>. It was thought that the reduced side effects and easier oral administration of AF compared to other available gold compounds would make it a better candidate for treatment of RA <sup>31</sup>. Unfortunately, AF was not as effective at reducing RA symptoms as ATM and ATG, and despite having fewer side effects, clinicians eventually stopped prescribing it as frequently as the injectable gold compounds <sup>26</sup>.

AF has both anti-inflammatory and anti-neoplastic activities which are described in detail in recent literature reviews <sup>26,28-30</sup>. While clinicians generally view it as a safe drug, common side effects of AF include diarrhoea (the most common side effect and severe in 2-5% of cases involving mucosal lesions), skin rashes, stomatitis, conjunctivitis, proteinuria, and thrombocytopenia <sup>29</sup>. ATM and ATG have primarily anti-inflammatory properties and their main side effects include skin rash, proteinuria, and thrombocytopenia <sup>29</sup>.

#### **1.1.6. Cell Culture Model of Neuroinflammation**

Primary human glial cells and neurons are not readily available for use in laboratory experiments. While human astrocytes proliferate *in vitro*, human microglia and neurons do not, therefore immortalized cell lines were used in this thesis to model neuroinflammation. Experiments were replicated using primary human microglia and astrocytes when significant results were obtained.

Immortalized human cell lines are neoplastic cells derived from various tissues of interest. These cells are inexpensive, relatively easy to maintain, and are able to proliferate indefinitely. These properties make neoplastic cells ideal for drug studies, which often involve numerous experiments. A disadvantage of using cell lines is that they may differ in their function

and morphology from the original source tissue, hence important experiments need to be replicated using primary cells.

The following human cell lines were used to model neuroinflammation: THP-1 promonocytic cells as a model of microglia, U-373 MG and U-118 MG astrocytoma cells as astrocyte models, SH-SY5Y neuroblastoma cells as a model of neurons, and HL-60 promyelocytic cells to model the respiratory burst, which is a defence mechanism used by phagocytes including neutrophils, macrophages and microglia. All of these cell lines have been used extensively to model neuroinflammation<sup>32-34</sup>.

It has been found that stimulation of THP-1 cells and human microglia with a combination of lipopolysaccharide (LPS) and interferon (IFN)- $\gamma$  results in a pathological activation of these cells similar to activated microglia in disease states<sup>35</sup>. Stimulation of human U-373 MG cells and primary astrocytes with IFN- $\gamma$  alone induces cytotoxicity, whereas U-118 MG cells require stimulation with a combination of IFN- $\gamma$  and IL-1 $\beta$  to induce a pathological response<sup>32</sup>. We employed the widely accepted method of using the formyl peptide N-formyl-methionine-leucine-phenylalanine (fMLP) as the trigger of the respiratory burst in HL-60 cells<sup>36</sup>. Another well-known method using LPS to prime the NADPH-oxidase respiratory burst in HL-60 cells and the mitochondrial protein transcription factor A (Tfam) was employed to see if damage associated molecular patterns (DAMP)s could also prime the respiratory burst<sup>37</sup>. While neither LPS nor IFN- $\gamma$  are present in most CNS neuroinflammatory conditions, the cytotoxic and activated glial cell phenotypes they induce are similar to those induced by neuroinflammatory conditions in the brain and to A $\beta$ -induced activation of glial cells<sup>14,34</sup>. By simulating and inducing the inflammatory and cytotoxic phenotype of glial cells, the anti-cytotoxic and

neuroprotective properties of compounds can be investigated. The specific details of the experiments performed are explained in the methods section below.

#### **1.1.7. Molecular Targets for AF**

Several targets for anti-inflammatory activity exist, including inhibiting ROS production and pro-inflammatory cytokine expression and secretion, and increasing the expression of anti-inflammatory protective enzymes<sup>4,38,39</sup>. The effects of AF on each of these components were investigated in my research.

The ability of AF to inhibit the microglial respiratory burst was investigated using an HL-60 cell model of NADPH-oxidase<sup>36</sup>. Traditional NADPH-oxidase inhibitors effectively inhibit the whole enzyme and prevent the release of any ROS; however, this is not ideal as NADPH-oxidase activity is necessary for protection against microbes and other immune functions<sup>40</sup>. The NADPH-oxidase enzyme is comprised of several sub-units, each of which requires phosphorylation to activate the enzyme to produce ROS<sup>40</sup>. Several disease-specific mediators are capable of ‘priming’ the NADPH-oxidase enzyme by phosphorylating some, but not all, of the subunits<sup>37</sup>. This priming does not activate the enzyme to produce ROS, but does result in increased production of ROS upon full stimulation<sup>37</sup>. Decreasing the priming of the respiratory burst while not inhibiting NADPH-oxidase completely is an attractive target for anti-inflammatory therapy as it would inhibit the exacerbated disease responses while retaining immune functioning. AF was tested for effectiveness against two priming agents; LPS, a well-established priming agent, and Tfam, a novel DAMP priming agent.

Several inflammatory cytokines have been implicated in neuroinflammation, including IL-6, IL-8, and monocyte chemoattractant protein (MCP)-1<sup>3,4,14,20,41</sup>. The expression and secretion

of these molecules by microglia-like THP-1 and astrocytic cells was investigated. While the inhibition of pro-inflammatory cytokines is a traditional method used to treat inflammation, upregulating protective activity may be a better method as inflammation is necessary for tissue repair<sup>38</sup>. Both IL-4 and heme-oxygenase (HOX)-1 have anti-inflammatory activities and function by inducing protective phenotypes in glial cells, therefore their expression in astrocytic cells was also investigated<sup>42,43</sup>.

The targets and activities mentioned above could be beneficial in inhibiting the neuroinflammation associated with AD and PD, and previous research has shown several related activities of AF. AF has been shown to inhibit the production of pro-inflammatory cytokines IL-6 and IL-8 by activated immune cells<sup>50,51</sup>. Research has also shown protective activity of AF resulting from induced expression of HOX-1 in THP-1 cells<sup>49</sup>. The biological activity of AF is discussed in further detail in section 1.2.

#### **1.1.8. *In vivo* Distribution of AF**

AF is known to accumulate in various tissues throughout the body over time, with highest levels of gold (Au) accumulating in the kidneys, spleen, and lungs<sup>44,45</sup>. Previous studies by Walz *et al.* (1983) indicated low penetration of the blood brain barrier (BBB) by AF. As any agents intended for treatment of neuroinflammation would need to reach effective concentrations in the CNS, it was necessary to investigate the *in vivo* distribution of AF. The distribution of AF has been previously studied using radioactively labeled Au, sulfur (S) and phosphorus (P) atoms of AF. This technique involves administration of a mixture of labeled and unlabeled AF and several steps of sample preparation before measurements can be performed<sup>45</sup>. This technique does not

distinguish the active moiety of AF, it merely determines the distribution of the various components of the molecules.

For this thesis a different technique was used to measure Au concentrations in mice fed AF. Laser ablation inductively coupled plasma mass spectrometry (LA-ICP-MS) directly measures the total number of unlabeled Au atoms in a tissue sample by comparing the signals obtained from experimental tissue samples with those obtained from preparations with known Au concentrations. This technique has been used previously to detect platinum-containing drugs in animal tissues<sup>46</sup>. LA-ICP-MS is a more direct measurement of Au than the radioactively labeled technique used previously<sup>45</sup>. However, both these techniques measure Au concentration as opposed to concentration of intact AF molecules as neither of the techniques is able to distinguish between AF and its metabolites, including Au as a breakdown product of AF<sup>29,45</sup>.

## **1.2. Biological Activity of Auranofin**

### **1.2.1. Anti-Inflammatory Activity of AF**

AF has been studied extensively since it was first developed in the 1980's. While the precise mechanism of AF's anti-inflammatory activity has not been established, the effects of AF on peripheral inflammatory pathways have been well-documented<sup>47-51</sup>. AF affects the secretion of several cytokines and there have been reports of AF both increasing and decreasing the secretion of IL-1 $\beta$ , IL-6, and IL-8 from LPS-stimulated monocytes and macrophages<sup>48,50,52</sup>. In macrophages, AF increases the production of pro-inflammatory prostaglandin (PG) E<sub>2</sub> production by COX-1 while decreasing the production of PGE<sub>2</sub> by COX-2<sup>51,53</sup>. Additionally, AF has several effects on neutrophils including both increasing and decreasing the neutrophil

chemotactic response, stimulating and inhibiting secretion of inflammatory cytokines such as IL-1 $\beta$ , and inhibiting respiratory burst activity<sup>54-56</sup>.

AF also modulates several inflammatory pathways, including activating mitogen activated protein kinases (MAPK), preventing activation of nuclear factor kappa-light-chain-enhancer of activated-B-cells (NF- $\kappa$ B) and both increasing and decreasing the induction of pro-inflammatory cytokines<sup>53,57,58</sup>. These anti-inflammatory properties could potentially inhibit neuroinflammation, though this has not yet been investigated. In addition to these anti-inflammatory activities, AF exhibits anti-neoplastic and protective properties, and these studies have contributed to the understanding of the molecular mechanisms of action of AF<sup>53,57,58</sup>.

### 1.2.2 Anti-Neoplastic Activity of AF

The anti-inflammatory activity of AF is thought to be closely linked to the anti-neoplastic activity of AF, and this is important to consider as it makes AF toxic to the cell lines used in my research<sup>47,53,57</sup>. The anti-inflammatory and cytotoxic activities of a compound usually involve similar molecular pathways, with cytotoxic activity observed at higher concentrations (Yamamoto and Gaynor, 2001). Identifying these pathways is important in understanding how AF could be causing the effects observed in our model. Activation of NF- $\kappa$ B and its downstream pathways is linked with neoplastic growth and development since several anti-apoptotic factors are activated through this pathway<sup>59,60</sup>. AF inhibits NF- $\kappa$ B activation and nuclear translocation by preventing the breakdown of I $\kappa$ B- $\alpha$  and I $\kappa$ B- $\beta$  and inhibiting I $\kappa$ B kinase (IKK) activation in macrophages stimulated with LPS<sup>51,57</sup>. The effect of AF on NF- $\kappa$ B is specific to stimulus and cell type, although it may be mediated by the suppression of TNF- $\alpha$ <sup>57</sup>. Han *et al* . (2008) found that treating LPS-stimulated RAW 264.7 macrophages with AF decreased expression and

production of TNF- $\alpha$ , whereas Stern *et al.* (2005) found that treating LPS-stimulated human THP-1 promonocytic cells with AF had no effect on TNF- $\alpha$  production. The inhibition of TNF- $\alpha$ -dependent NF- $\kappa$ B activation by AF may be cell- and stimulus- specific, but AF also blocks other pathways that activate NF- $\kappa$ B, including inhibiting IL-1 $\beta$  and IL-6 expression and release<sup>47, 49</sup>.

In cultured human monocytes and synoviocytes, AF inhibits release of IL-1 $\beta$  and prevents NF- $\kappa$ B nuclear translocation<sup>61</sup>. AF has been shown to reduce IL-6 release and inhibit IL-6-dependent activation of Janus kinase (JAK)-1 and -2<sup>47,49</sup>. Inhibiting JAK-1 and -2 prevents phosphorylation of signal transducer and activator of transcription (STAT)-3 in multiple myeloma cell lines, and AF-induced reduction in STAT-3 activity leads to decreased NF- $\kappa$ B activation<sup>47,49</sup>. In combination, the inhibition of STAT-3 signalling and cellular release of TNF- $\alpha$  and IL-1 $\beta$  may contribute to the molecular mechanisms responsible for the cytotoxicity of AF towards neoplastic cells<sup>49</sup>. Blocking STAT-3 signalling and NF- $\kappa$ B activation could also be protective in neuroinflammation, hence AF may be a good candidate for treating these diseases<sup>62-64</sup>.

Angiogenesis is a key factor in the clonal evolution of solid tumors as proliferating neoplastic cells typically require a direct blood supply<sup>65</sup>. Increased angiogenesis and disruption of the BBB have also been linked to AD, and it is thought that compounds that inhibit angiogenesis and help maintain the endothelial cells surrounding the CNS could be protective<sup>66</sup>. AF has been shown to directly inhibit neovascularization, which would result in decreased blood supply to neoplasms<sup>67</sup>. A molecular basis for this activity could be inhibition of toll-like receptor (TLR)-3 activation and signalling<sup>68</sup>. Viral TLR-3 signalling through a toll/IL-1 receptor '(TIR)-domain-containing adapter-inducing interferon- $\beta$ ' (TRIF)-dependent pathway has been linked

with the angiogenesis induced by neoplastic cells <sup>69</sup>. AF inhibits the phosphorylation and transcription of interferon regulatory factor (IRF)-3 and prevents TRIF activation, which would also inhibit angiogenesis, the progression of solid tumors, and the pathological angiogenesis that has been reported in AD <sup>66,68,70</sup>.

AF inhibits many pathways that are critical to the development and progression of neoplasms, and these molecular effects are summarized in Table 1. Some of these activities could be beneficial in treating neuroinflammation, while some explain the toxicity of AF towards the cell lines used in experiments.

Table 1: The Anti-Neoplastic Molecular Mechanisms of AF

---

**Effects Related to NF- $\kappa$ B**

- Blocks breakdown of I $\kappa$ B- $\alpha$  and I $\kappa$ B- $\beta$  <sup>57</sup>
- Blocks IKK activation <sup>57</sup>
- ↓ TNF- $\alpha$  expression and secretion <sup>53,57</sup>
- ↓ IL-1 $\beta$  secretion <sup>61</sup>
- ↓ IL-6-induced STAT-3 activation <sup>47,49</sup>

**TLR-Mediated Effects**

- Blocks MyD88 and TRIF pathways in TLR-4 activation <sup>70,71</sup>
  - Blocks TRIF pathway in TLR-3 activation <sup>68,70</sup>
  - Blocks IRF-3 phosphorylation and transcription <sup>68,70</sup>
- 

**1.2.3. Protective effects of AF**

It has been well documented that AF is toxic towards a wide variety of cell types and organisms, but several protective activities of AF have also been documented (Ashino *et al* ., 2011, Shabani *et al* ., 1998). Under inflammatory conditions, such as RA, AD or PD, an ideal

treatment would involve stopping or slowing deleterious pro-inflammatory responses while stimulating innate protective mechanisms<sup>39</sup>. Inflammation can be beneficial, and treatments designed to decrease all inflammatory responses without stimulating protective mechanisms have yielded sub-optimal results. For example, negative outcomes were observed when multiple sclerosis patients were treated with TNF- $\alpha$  inhibitors, as some inflammation is required in the healing process<sup>38,77</sup>. Along with inhibiting pro-inflammatory pathways, AF induces several protective molecules, which may make AF a good candidate for the treatment of inflammatory conditions<sup>78,79</sup>.

Matrix metalloproteinase (MMP)-1 is an enzyme that aids wound repair by degrading collagen<sup>80</sup>. MMP-1 has been shown to contribute to inflammation by augmenting MCP-1 signalling, inducing the processing of stromal cell derived factor-1 into a potentially neurotoxic form, and enhancing the processing of pro-TNF- $\alpha$  into active TNF- $\alpha$ <sup>80</sup>. Due to its activity on collagen, MMP-1 has been implicated in the tissue destruction common in RA<sup>79</sup>. Tissue inhibitor of matrix metalloproteinase (TIMP)-1 is responsible for controlling MMP-1 enzymatic activity; TIMP-1 binds to and inactivates MMP-1<sup>79</sup>. In fact, upregulation or stabilization of TIMP-1 could be protective in MMP-1-associated destructive inflammation. TIMP-1 is susceptible to oxidative inactivation by hypochlorous acid, a by-product of the neutrophil respiratory burst, so the protective activity of TIMP-1 may be lost during chronic inflammation<sup>81</sup>. Shabani *et al.* (1998) demonstrated that AF, aurothiomalate, and aurothioglucose prevent the oxidative inactivation of TIMP-1. By preserving the protective activity of the TIMP-1 enzyme, AF may prevent tissue destruction by MMP-1 without impairing inflammatory processes.

Another protective molecule induced by AF is HOX-1<sup>78</sup>. HOX-1 catabolizes the heme molecule into carbon monoxide (CO), biliverdin, and free iron<sup>82</sup>. Additionally, HOX-1 has anti-

inflammatory activity, as evidenced by observations that transgenic mice lacking HOX-1 develop chronic inflammation and that the only known human born without HOX-1 enzymatic activity died of inflammatory syndrome<sup>82-84</sup>. The induction of HOX-1 has been implicated in the anti-inflammatory activity of alcohol and in the protective activities of several molecules, including IL-10, rapamycin, and heat shock proteins<sup>82</sup>. AF induces HOX-1 expression by increasing levels of nuclear factor erythroid 2-related factor 2 (Nrf2) through the activation of Ras-related C3 botulinum toxin substrate 1 (Rac1)<sup>48</sup>. The induction of HOX-1 has been linked to the beneficial effects of AF, including its ability to protect against cocaine-induced hepatic injury *in vivo*<sup>78</sup>. In fact, Ashino *et al.* (2011) found that AF was able to induce HOX-1 expression in mouse and human hepatocytes *in vitro*. Additionally, treating mice with AF prior to cocaine exposure significantly upregulated HOX-1 in the liver and protected mice from liver damage<sup>78</sup>.

The combined anti-inflammatory and protective activities of AF makes it a good candidate for the treatment of several diseases associated with inflammation and tissue damage<sup>78,79</sup>. The potential protective effects of AF are particularly exciting as many of the currently available anti-inflammatory treatments stop inflammation without inducing the protective mechanisms that enhance recovery<sup>39</sup>. By inducing several protective pathways, AF has the potential to be part of a new therapeutic approach aimed at achieving a balanced inflammatory response<sup>39</sup>.

### **1.3. Research Overview and Hypotheses**

There are currently no effective treatments available for neuroinflammation. However, diseases associated with neuroinflammation, such as AD and PD, are increasing in prevalence, therefore finding effective treatment options is a priority.

The main effector cells in neuroinflammation are microglia and astrocytes, which normally maintain neuronal viability by supplying neurotrophic molecules and regulating the chemical environment surrounding neurons <sup>4</sup>. However, upon stimulation by disease-specific misaggregated proteins, such as A $\beta$  or  $\alpha$ -synuclein, microglia and astrocytes can become activated to start secreting cytotoxic chemicals in an attempt to clear the threat <sup>85</sup>. This process is the main driving force of neuroinflammation and is believed to be responsible for some of the neuronal loss that is characteristic of several neurodegenerative disorders including AD and PD <sup>1,4,85</sup>. There are no published reports on the effects of the gold compounds in the CNS; however, significant evidence indicates that AF is a potent inhibitor of inflammation in the periphery <sup>29</sup>. Due to AF's potential as an inhibitor of glial cell-driven neuroinflammation and secretion of neurotoxic substances, **the central hypothesis of this research is that the gold rheumatoid arthritis medication AF is able to enter the brain where it reduces the neuronal death caused by toxins that are released by stimulated glial cells.**

**The hypotheses of this research are:**

- 1) Treatment of stimulated microglia and astrocytes with the gold compounds AF, ATM, or ATG reduces their toxicity towards neuronal SH-SY5Y cells.
- 2) Treatment of neuronal cells with the gold compounds AF, ATM, or ATG reduces the death of neurons exposed to H<sub>2</sub>O<sub>2</sub> or toxic supernatants from stimulated glial cells.
- 3) The molecular mechanisms by which the gold compounds exert their anti-inflammatory and neuroprotective effects include decreased expression and production of pro-inflammatory cytokines and increased expression and production of protective cytokines and enzymes.

4) After oral administration of AF to mice, increased levels of gold can be detected in their CNS by LA-ICP-MS.

Figure 2 describes different series of experiments performed by using cell lines and primary glial cells, their corresponding hypotheses, and the numbers of biological replicates per experiment.

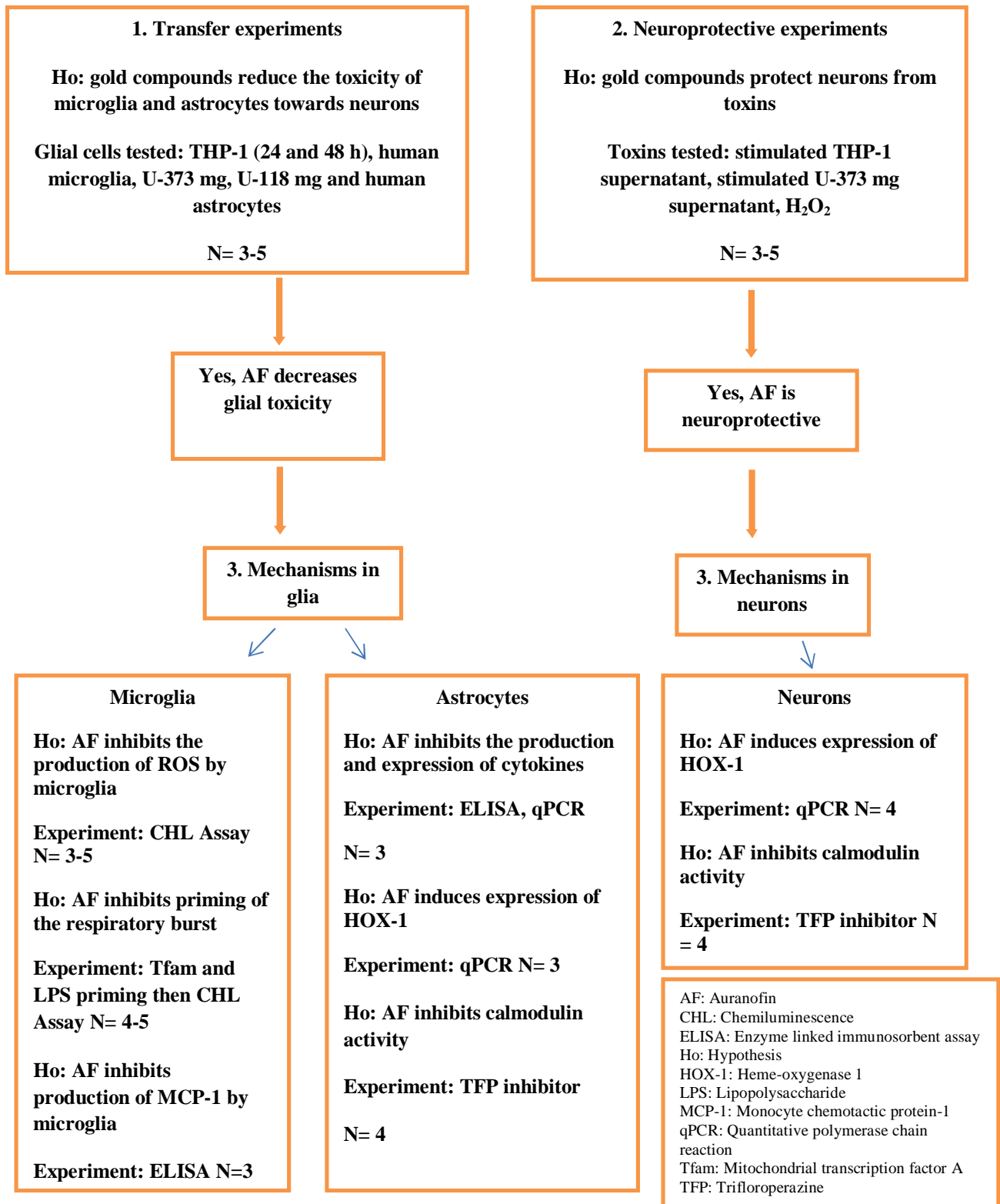


**Fig 2:** Flow chart of experiments performed, corresponding hypotheses, and numbers of

biological replicates per experiment.

The following human cell lines were used to model neuroinflammation: THP-1 promonocytic cells were used to model microglia, U-373 MG and U-118 MG astrocytic cells were used as astrocyte surrogates, SH-SY5Y neuroblastoma cells were used as a neuronal model, and HL-60 promyelocytic cells were used to model the microglial respiratory burst since these cells express NADPH oxidase at levels that are sufficient for measurements of ROS production. Primary human microglia and astrocytes obtained from surgical specimens were used to confirm key findings. The inhibitory effects of the gold compounds on astrocyte- and microglia-mediated neurotoxicity were investigated. The neuroprotective effect of AF against H<sub>2</sub>O<sub>2</sub>-, THP-1-, and U-373 MG-induced toxicity was investigated and the inhibition of respiratory burst activity and the effect of priming by gold compounds were examined. The effect of calmodulin inhibition on the neuroprotective and anti-neurotoxic activities of AF was examined as a potential mechanism of action of AF. In addition to these experiments, mechanistic studies on the expression and secretion of cytokines by microglial, astrocytic, and neuronal cells were carried out. Lastly, the distribution of gold to various tissues in mice that had been administered AF orally was investigated. Outcomes of this research may contribute to the development of AF as a treatment option for conditions associated with neuroinflammation.

## 2.0. Materials and Methods

### 2.1. Reagents

The following substances were used in various assays and obtained from Sigma-Aldrich (Oakville, ON, Canada): ATM, ATG, beta-nicotinamide adenine dinucleotide ( $\beta$ -NAD), diaphorase (from *Clostridium kluyveri*), dimethyl sulfoxide (DMSO), iodonitrotetrazolium chloride (INT), LPS (from *Escherichia coli* 055:B5), luminol sodium salt, 3-(4,5-dimethylthiazol-2-yl)-2,5-diphenyl tetrazolium bromide (MTT), fMLP, PD98059 (ERK/MEK1/2 inhibitor), SB202190 (p38 MAPK inhibitor), sodium L-lactate (lactate), SP600125 (JNK inhibitor), sulforhodamine B (SRB), and Triton X-100. The following reagents were obtained from ThermoFisher Scientific (Ottawa, ON, Canada): bovine serum albumin (BSA), diethanolamine, Dulbecco's modified Eagle medium nutrient mixture F-12 Ham (DMEM-F12), ethanol (EtOH), ethylenediaminetetraacetic acid (EDTA) sodium salt, glycine, HCl, H<sub>2</sub>O<sub>2</sub>, NaCl, N,N-Dimethylformamide (DMF), sodium dodecyl sulphate (SDS), trifloroperazine (TFP, calmodulin inhibitor) and tris (hydroxymethyl)aminomethane (Tris).

AF was obtained from Cedarlane Canada (Burlington, ON, Canada), the control salt ATS and qScript cDNA synthesis kit were obtained from VWR International (Mississauga, ON, Canada). Human recombinant IFN- $\gamma$ , human recombinant IL-1 $\beta$ , as well as anti-human IL-6 and IL-8 antibodies and recombinant protein standards used in the IL-6 and IL-8 enzyme linked immunoabsorbent assays (ELISA) were purchased from Peprotech (Rocky Hill, NJ, USA). Ssofast qPCR reaction mix and Aurum RNA extraction kit were purchased from Bio-Rad (Mississauga, ON, Canada). Trypsin/EDTA solution and fetal bovine serum (FBS) were obtained from ThermoFisher Scientific. Phosphate-buffered saline (PBS) tablets were purchased from

Takara Bio Incorporated (Madison, WI, USA). Recombinant Tfam and Tfam buffer was a kind gift from Dr. Kirsten Wolthers of the University of British Columbia – Okanagan (Kelowna, BC, Canada).

## **2.2. Equipment**

Tissue culture dishes (10 cm<sup>2</sup>) and sterile 96-well plastic plates (Corning Inc., Corning, NY, USA) were used when experiments involved collection of large volumes of supernatants or treatments in small volumes, respectively. All other cell culture experiments were conducted using sterile 6-well or 24-well plastic cell culture plates (Corning). Cell cultures were grown in T-75 flasks (Sarstedt, Montreal, QC, Canada) in a Steri-Cycle HEPA Class 100 carbon dioxide (CO<sub>2</sub>) incubator (Model#370, ThermoFisher). A hemocytometer (ChangBioscience, Castro Valley, CA, USA) was used for cell counting. The Sorvall RT1 Centrifuge (Cat#75002384, ThermoFisher) was used to centrifuge cell samples for use in experiments or for supernatant collection. The Fluostar Omega microplate reader used for cell viability and chemiluminescence experiments was purchased from BMG Labtech (Nepean, ON, Canada). A VistaVision phase contrast inverted microscope was used to visualize cells (Model #82026-630, VWR International). Phase contrast digital microscopy pictures were taken with a Motic inverted microscope (Model AE31) using a Moticom 3000 camera attachment (Motic, Richmond, BC, Canada).

RNA was quantified using NanoDrop 1000 (ThermoFisher) and a C1000 Thermal Cycler (Model#185-1048, Bio-Rad) was used to conduct reverse transcriptase reactions. White 96-well plates were used for real time quantitative polymerase chain reaction (RT-qPCR) (Bio-Rad) and RT-qPCR was performed using a CFX96 Real Time System (Bio-Rad).

### **2.3. Model cells**

The THP-1 human promonocytic cell line was used as a microglia model, U-373 MG and U-118 MG human astrocytoma cell lines were used as astrocyte models, the HL-60 human promyelocytic cell line was used as a neutrophil model, and the SH-SY5Y human dopaminergic neuroblastoma cell line was used to model neurons. All cell lines were obtained from the Kinsman Laboratory of Neurological Research at the University of British Columbia. Primary human microglia and astrocytes were isolated from surgical tissues and provided by the Kinsman Laboratory for Neurological Research at the University of British Columbia Vancouver campus. Cultures were grown at 37°C with 5% CO<sub>2</sub> and 100% humidity in DMEM-F12 media supplemented with 10% FBS (F10). Penicillin (100 U/ml) and streptomycin (100 µg/ml) were also added to media to inhibit bacterial growth.

### **2.4. Plating Glial Cells for Transfer and Neuroprotective Experiments**

Experiments using THP-1, U-118 MG, and U-373 MG cells were performed on at least three independently grown batches of cells. Human astrocytes and microglia isolated from two different human surgical cases were used. Fig. 2 provides an overview on all experiments performed including the number of independent replicates for each experiment.

#### **2.4.1. THP-1 human promonocytic cells**

For use in experiments, THP-1 cells were harvested from T-75 flasks and counted using a hemocytometer. Cells were then centrifuged at 450 g for 7 min and re-suspended in DMEM-F12 media supplemented with 5% FBS (F5) to a final concentration of 0.5 million cells/ml.

For transfer experiments, 1 ml of these resuspended THP-1 cells were plated per well in sterile 24 well plates which were kept in the incubator for 15 min before being treated with AF, ATM, ATG, ATS, or their respective vehicle controls. For AF 10% DMSO/95% F5 media v/v was the vehicle, for all other compounds the vehicle was 25% DMSO/75% PBS v/v. The treated cells were incubated for an additional 15 min period prior to stimulation with a combination of LPS (0.5  $\mu\text{g}/\mu\text{l}$ ) and IFN- $\gamma$  (150 U/ml). Following 24 or 48 h incubation at 37°C, cell supernatants were collected and cell viability was assessed using lactate dehydrogenase (LDH) and MTT assays.

For use in neuroprotective experiments, 15 ml of THP-1 cells were plated in 10 cm<sup>2</sup> sterile culture dishes at a concentration of 0.5 million cells/ml and kept in an incubator for 15 min prior to stimulation with LPS (0.5  $\mu\text{g}/\text{ml}$ ) and IFN- $\gamma$  (150 U/ml). Cells were then incubated for 48 h, at which point supernatants were collected for use in experiments.

#### **2.4.2. Primary human microglia**

Experiments with primary human microglia were performed at the Kinsman Laboratory for Neurological Research at the UBC Vancouver campus by Dr. Sadayuki Hashioka. Primary human microglia isolated from surgical samples were used. The previously described protocol was followed, which included spinning homogenized tissue on percoll gradients to separate microglia and astrocytes from myelin and tissue debris then culturing adherent cells<sup>86,87</sup>. Microglial supernatants were collected as described for THP-1 cell supernatant preparation above (see 2.4.1).

### 2.4.3. U-373 MG and U-118 MG astrocytoma cells

Adherent U-373MG and U-118 MG astrocytoma cells were detached from the bottom of the flask for use in experiments by incubating cells in 2 ml of 0.25% trypsin/EDTA solution for 5-10 min. The flask was washed with 10 ml of F10 medium and cell suspension was harvested for experiments. The cells were counted, centrifuged at 450 g for 7 min, and re-suspended in F5 media to a final concentration of 0.2 million cells/ml.

For use in transfer experiments, 0.9 ml of U-373MG or U-118MG cells were plated per well in sterile 24 well plates which were then incubated for 24 h to allow cells to adhere to the bottom of the plates. Following this incubation, cells were treated with AF, ATM, ATG, ATS, or their vehicle controls. For mechanism studies, the calmodulin inhibitor TFP was added 15 min prior to the addition of AF. After treatment, cells were allowed to incubate for 15 min; at which point U-373MG cells were stimulated with IFN- $\gamma$  (150 U/ml) and U-118MG cells were stimulated with a combination of IFN- $\gamma$  (150 U/ml) and IL-1 $\beta$  (100 U/ml). U-118 MG cells required the addition of IL-1 $\beta$  to stimulation mixture as IFN- $\gamma$  alone did not induce toxicity towards neurons. Treated and stimulated cells were then returned to the incubator for 48 h at 37°C. Following this incubation, supernatants were collected for use in experiments and cell viability was tested using the LDH and MTT assays. U-373 MG transfer experiments with AF were replicated using the SRB assay as an alternative method for assessment of cell viability.

For use in neuroprotective experiments, 15 ml of U-373MG cells were plated in 10 cm<sup>2</sup> sterile culture dishes and incubated for 24 h to allow cell adherence to the plate. After this incubation, cells were stimulated with IFN- $\gamma$  (150 U/ml) and incubated for an additional 48 h, after which supernatants were collected for use in experiments.

#### **2.4.4. Primary human astrocytes**

Primary astrocytes were isolated from human surgical tissues by Dr. Sadayuki Hashioka at the Kinsman Laboratory of Neurological Research at UBC Vancouver according to previously published procedures<sup>32</sup>. After astrocyte cultures were established, cells were frozen and transported to UBC Okanagan where they were stored in liquid nitrogen. Cells were thawed by removing vials from liquid nitrogen then immersing vials in room temperature water until contents were liquid. Astrocytes were then removed from the vial and suspended in 10 ml of F10 media and centrifuged for 10 minutes at 250 g. After centrifugation media was discarded and cells were suspended in 10 ml of fresh F10 media and transferred into a T-75 flask where they grew to confluence before use. For use in experiments, adherent primary human astrocytes were detached from T-75 flasks by removing cell supernatant and incubating cells with 2 ml of 0.25% trypsin/EDTA solution for 5-10 min at 37°C. Following cell detachment, the previously described protocol for collecting U-373 MG cell supernatants was followed (see 2.4.3).

#### **2.5. Plating Human SH-SY5Y Neuronal Cells for Transfer and Neuroprotective**

##### **Experiments**

Adherent SH-SY5Y cells were detached from the bottom of the flask by incubating cells in 2 ml of 0.05% trypsin/EDTA solution for 1-2 min. The flask was then washed with 10 ml of F10 medium and cell suspension was harvested for experiments. SH-SY5Y cells were counted, centrifuged at 450 g for 7 min, and re-suspended in F5 media to a final concentration of 0.2 million/ml for use in experiments. A volume of 0.4ml/well of re-suspended SH-SY5Y cells was plated in sterile 24-well plates and incubated for 24 h to allow cells to adhere to the plate prior to treatment.

For transfer experiments, SH-SY5Y supernatants were aspirated following 24 h incubation and replaced with gold compound-treated and/or stimulated glial cell supernatants. The SH-SY5Y cells were then incubated in a 37 °C CO<sub>2</sub> incubator for an additional 72 h, at which point cell viability was assessed using the MTT and LDH assays.

For use in neuroprotective experiments, SH-SY5Y supernatants were aspirated following 24 h incubation and replaced with stimulated glial cell supernatants that had not yet been treated with gold compounds. SH-SY5Y cells were then immediately treated with the drugs or their vehicle solution (DMSO) and returned to the 37 °C CO<sub>2</sub> incubator for 72 h. Cell viability was then assessed using the MTT and LDH assays.

For use in H<sub>2</sub>O<sub>2</sub> neuroprotective experiments, following the initial 24 h incubation, SH-SY5Y cells were treated with various concentrations of AF or a vehicle control and returned to the incubator for 15 min. SH-SY5Y cells were exposed to 0.5 mM hydrogen peroxide and allowed to incubate for 24 h. Cell viability was assessed 24 h later using the MTT and LDH assays.

## **2.6. Cell viability assay: LDH**

Cell supernatants from each experiment were collected for use in the LDH assay to measure cell death. LDH is a stable enzyme that converts lactate to pyruvate, a reaction essential to cell survival. LDH is normally present in the cytosol, but the extracellular concentration increases when it is released from cells with damaged membranes, such as those undergoing necrosis. The enzymatic activity of LDH released from dead/dying cells can be measured to estimate the percent cell death in comparison to a 100% lysis control in which untreated cells have been lysed with 1% Triton X-100. The catalytic activity of LDH requires the reduction of

$\beta$ -NAD, which can be coupled with the diaphorase-catalyzed reduction of INT to a purple product that can be measured spectrophotometrically in order to assess cell death.

For the LDH assay, 100  $\mu$ l of cell supernatants were collected in a 96-well plate. INT (260  $\mu$ g/mL) was added to each well and an initial measurement of optical density (OD) at 492 nm was made. A mixture of lactate (750  $\mu$ g/ml),  $\beta$ -NAD (60  $\mu$ g/ml) and diaphorase (55  $\mu$ g/ml) in PBS was added to each well and the reaction was incubated for 5-30 min on a bench top rocker at 37°C. A final measurement of OD at 492 nm was performed when the lysis well appeared orange in colour. Percent cell death for each sample was determined using a two-step equation:

$$1.) A_{\text{final}} - A_{\text{initial}} = cA$$

$$2.) (cA_{\text{sample}} - cA_{\text{media}}) / (cA_{\text{lysis}} - cA_{\text{media}}) * 100\% = \% \text{ death}$$

Where A refers to the absorbance measurement (OD) at 492 nm and cA indicates the corrected absorbance value. 'Initial' and 'final' refer to the first and final absorbance measurements, respectively.

Where  $A_{\text{initial}}$  represents the first absorbance value,  $A_{\text{final}}$  represents the final absorbance value, and cA represents the corrected absorbance value for each well. 'Media' refers to the absorbance measured for a control well containing only media and 'lysis' refers to the absorbance measured for cells treated with 1% Triton X-100, which served as a 100% cell death control .

## 2.7. Cell viability assay: MTT

Cell viability was assessed using the MTT assay. MTT is a yellow formazan dye that is reduced to a water-insoluble purple product by succinate dehydrogenase in the mitochondria of viable cells. The change in OD of the MTT is linearly correlated with the concentration of live cells in the sample (Hansen *et al.* . 1989; Mosmann 1983).

Following removal of 100  $\mu$ l of cell supernatants for the LDH assay, 30  $\mu$ l of 5mg/ml MTT was added to the 0.3 ml of cell suspensions remaining in each well of the 24-well cell culture plates. Plates were then placed in a 37°C 5% CO<sub>2</sub> incubator for 1-2 h, at which point 0.33 ml of 20% SDS/50% DMF in deionized water was added to each well to solubilise the product. The plates were then placed in a wet box and incubated in a dry incubator at 37°C for 2-3 h. Each plate was then vortexed for 10 min, following which 0.1 ml of each sample was reverse pipetted into a 96-well plate and the OD was measured at 570 nm. The percentage of viable cells was determined using the following equations:

$$1.) A_{\text{sample}} - A_{\text{media}} = cA$$

$$2.) (cA_{\text{sample}}/cA_{\text{untreated}}) * 100\% = \% \text{ viable}$$

Where  $A_{\text{sample}}$  represents the absorbance measurement in each well,  $A_{\text{media}}$  represents the absorbance of the wells containing media only, and  $cA$  represents the corrected absorbance values for each well. 'Sample', 'media', and 'untreated' refer to the absorbance measurements in a particular experimental sample well, a control well containing only media, and an untreated 100% cell viability control, respectively. All viability results are presented as a percentage of the 100% untreated control.

## 2.8. Cell viability assay: SRB Colorimetric Assay

The SRB assay is based on measuring total cellular protein and was performed as previously described by Skehan *et al.* (1990). All SRB assays were carried out by Jenelle Lamothe, an undergraduate student in Dr. Klegeris' lab. Supernatants from cell cultures were aspirated and 0.25 ml of 10% trichloroacetic acid:PBS solution was added to each well. Following a 1 h incubation at 4 °C, each well was aspirated and washed 4 x with H<sub>2</sub>O. 0.2 ml of 0.4% (w/v) SRB in 1% acetic acid was then added to each well and plates were incubated for 10 min at room temperature. Plates were aspirated and washed 4 x with 1% acetic acid followed by the addition of 0.2 ml of 10 mM Tris base solution (pH 10.5) to each well. Each plate was then incubated for 30 min at room temperature, and after transferring 0.1 ml aliquots of each sample to 96-well plates, the OD was measured at 492 and 620 nm using a microplate reader. The background measurement (620 nm) was subtracted from 492 nm values and these values were used to calculate percentage viability. The cell viability was calculated as a percent of the value obtained from cells incubated with fresh medium only using the equations below:

$$1.) A_{\text{sample}} - A_{\text{media}} = cA$$

$$2.) (cA_{\text{sample}}/cA_{\text{untreated}}) * 100\% = \% \text{ viable}$$

Where  $A_{\text{sample}}$  represents the absorbance measurement in each well,  $A_{\text{media}}$  represents the absorbance of the media only well, and  $cA$  represents the corrected absorbance for each well.  $cA_{\text{untreated}}$  refers to the 100% cell viability control.

## 2.9. ELISA

Concentrations of MCP-1, IL-4, IL-6 and IL-8 secreted by cells were measured using an ELISA development kit from Peptotech. The assay utilizes a double-antibody “sandwich” technique in which MCP-1, IL-4, IL-6 or IL-8 cytokines present in cell supernatants first bind a primary antibody attached to the well surface, and then are detected by the addition of a biotinylated secondary antibody. Previously collected, frozen and stored at -20°C cell-free supernatants from THP-1, U-373 MG and U-118 MG cell cultures were thawed for 24 h at 4°C prior to use in ELISA experiments.

Details on the composition of all solutions used in the ELISA assay are listed in Appendix 1. The ELISA was performed as follows: 50µl of primary capture antibody diluted 1:200 (or 1:100 for IL-6) in coating buffer (Na<sub>2</sub>CO<sub>3</sub>-NaCO<sub>3</sub>/H<sub>2</sub>O solution) was added to each well of a 96-well plate which was then covered with adherent tape and incubated at 4°C for 24 h. Following incubation, the coating buffer was discarded and the plate was blocked with 180µl of blocking solution (0.5% BSA/Skim milk powder w/v in PBS) per well and placed in a wet box on a bench top rocker for 1 h at 37°C. The blocking solution was then discarded and the plate was washed 2 x with PBS-Tween (0.05% Tween in PBS v/v). 0.1ml of each supernatant sample was added to each well of the plate along with a series of standards with concentrations of cytokines ranging from 0.032 - 10 ng/ml and four media only control wells. The plate was then covered with adherent tape and incubated at 4°C for 24 h.

Following incubation, samples were discarded, the plate was washed 3 x with PBS-Tween, and 0.1ml of secondary antibody diluted in blocking solution (1:400 for IL-4, IL-6, and IL-8 and 1:500 for MCP-1) was added to each well. The plate was then placed in a wet box and incubated for 45 min at 37°C. The secondary antibody solution was then discarded and the plate

was washed 4 x with PBS-Tween, following which 0.1ml of extravidin-alkaline phosphatase diluted 1:10 000 in blocking solution was added to each well. The plate was returned to a wet box and incubated for an additional 45 min period at 37°C. The plate was then washed 5 x with PBS-Tween and 0.1ml of detection solution (1 mg/ml phosphatase substrate tablets in substrate solution) was added to each well. The optical density was measured at 405 nm immediately after addition of the detection solution, following which the plate was incubated in a wet box at 37°C until the yellow colour has developed (0.5-24 h).

Data were analyzed as per ELISA manufacturer's instructions (Peprotech). The change in absorbance of samples ( $\Delta A_{\text{samples}}$ ) was measured by subtracting the initial absorbance ( $A_i$ ) from the final absorbance ( $A_f$ ). The media control change in absorbance ( $\Delta A_{\text{medium}}$ ) was then subtracted from the change in absorbance of the samples to get the adjusted change in absorbance ( $\Delta A_a$ ). The detection limit of the assay (ng/ml) was determined by multiplying the standard deviation of the two blank absorbance values ( $\Delta A_{\text{medium}}$ ) then adding the average of the blank absorbance values and calculating the corresponding cytokine concentrations. To calculate the amount of cytokine present in each sample, a calibration curve was plotted using the  $\Delta A_a$  of the standards (0.032 - 10ng/ml) and a trendline was fitted to this curve. The  $\Delta A_{a\text{-samples}}$  values were then divided by the slope of the trendline to calculate concentration values. The equations are demonstrated below.

1.)  $A_f - A_i = \Delta A$

2.)  $\Delta A - \Delta A_{\text{medium}} = \Delta A_a$

3.)  $\Delta A_{a\text{-samples}} / \text{slope of trendline} = \text{concentration of cytokine in ng/ml}$

## 2.10. Plating and Differentiating HL-60 cells for use in experiments

It was necessary to differentiate the HL-60 cell line into neutrophil-like cells prior to use in chemiluminescence experiments so the cells would express functional NADPH-oxidase enzymes. To do this, 10 ml of cell suspensions were collected and centrifuged at 450 g for 7 min to form a pellet. Cells were re-suspended in F5 media, counted and diluted to a concentration of 0.2 million cells/ml. The cells were plated onto 10cm<sup>2</sup> tissue culture dishes in a volume of 10-20 ml then placed in the CO<sub>2</sub> incubator for 15 min. After incubation, DMSO was added to the cells at a concentration of 1.3% (v/v) and the cells were allowed to differentiate for 5-7 days before use in chemiluminescence experiments.

Differentiated HL-60 cells were harvested from 10 cm<sup>2</sup> tissue culture dishes and centrifuged at 450 g for 7 min to form a pellet. The cells were then re-suspended in clear media without FBS (F0 media) for same day experiments or clear F5 media for use in 24 h priming experiments because the red indicator dye in regular cell culture media interferes with the chemiluminescence signal. The cells were then plated at a concentration of 1 million cells/ml in 0.08 ml in 96-well tissue culture plates.

Same day chemiluminescence experiments were performed by Colby Renschler, an undergraduate student in Dr. Klegeris' lab. For same day acute chemiluminescence experiments, the HL-60 cells in the 96-well plates were allowed to rest for 30 min in a dry heat (37°C) incubator. Following incubation, cells were treated with 5 µl vehicle controls (PBS or DMSO), or with gold compounds AF, ATM, ATG or ATS. The plate was then incubated for another 30 min before use in the assay.

For use in priming experiments, HL-60 cells were placed in a 37°C CO<sub>2</sub> incubator and incubated for 15 min prior to treatment with 1, 0.5, or 0.1µM concentrations of AF or a vehicle

control. The cells were then returned to the CO<sub>2</sub> incubator for 15 min before being exposed to LPS (0.5 µg/ml), Tfam (5 ug/ml) or Tfam buffer solution. The plates were then incubated for 24 h before use in the assay.

### **2.11. Chemiluminescence Assay (Measuring Respiratory Burst)**

Muranka *et al.* (2005) developed an assay to measure the production of ROS generated by HL-60 cells *in vitro*. This assay utilizes luminol, a compound that interacts with ROS to produce light that can be measured with a plate reader. fMLP, a component of bacterial cell walls, was used as a stimulant to induce the respiratory burst in HL-60 cells. Luminol was diluted in PBS to 50 mM, pre-heated to 37°C, and then loaded into the first injector of the FLUOstar Omega plate reader prior to each experiment. At the same time, fMLP was diluted to 20 µM in PBS, pre-heated to 37°C, and loaded into the second injector of the plate reader. The previously plated and treated HL-60 cells were then placed into the plate reader which was pre-set for cell incubation and chemiluminescence measurements at 37°C.

The plate reader was configured to measure luminescent light for 60 cycles, with each cycle lasting 30 s. At cycle 5, 10µl of luminol solution was injected into each well and at cycle 10, fMLP was injected. The production of light was then measured every 30 s generating a peak of light production which was plotted as a light production over time.

Data analysis was done using Mars Analysis Software provided by BMG Labtech. A baseline correction was done for each curve by adjusting the baseline production of light to the average value from cycles 40-60. This normalized the curves to the light emission values detected at the time when the cells were no longer producing ROS. The area under the curves of the CHL signals measured from cycles 15-39 was summated to produce a single CHL value for each well. The data was expressed as a percentage CHL of a PBS control well.

- 1.)  $CHL_{cycles\ 15-39} - CHL_{cycles\ 40-60} = CHL_{normalized}$
- 2.)  $(CHL_{normalized-sample} / CHL_{normalized-PBS-control}) * 100\% = \% CHL$

Where  $CHL_{cycles}$  represents the area under the light production curve in each well,  $CHL_{normalized}$  represents the baseline corrected CHL signal. Figure 3 illustrates the fluorescence curves generated by the Mars Analysis Software with a primed HL-60 cells versus non-primed cells.

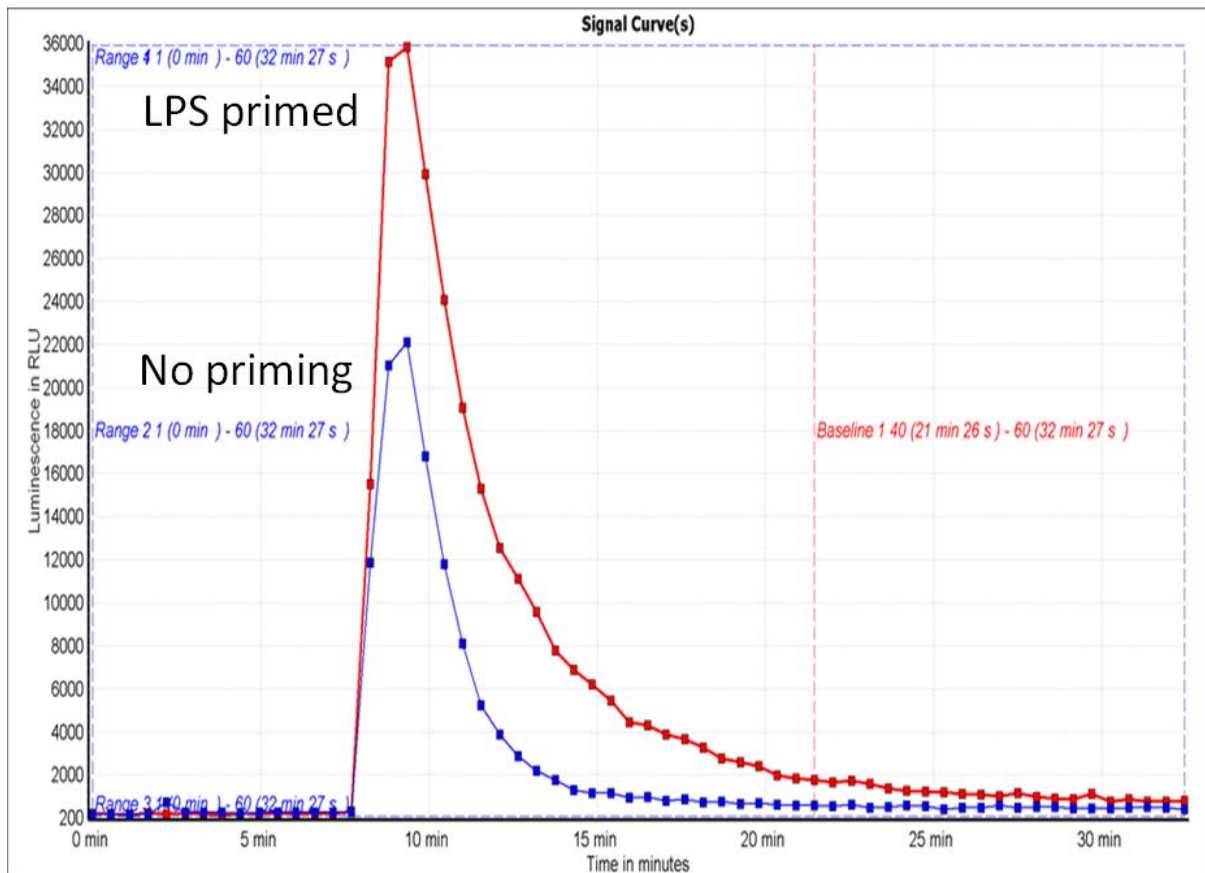


**Fig. 3:** Example of chemiluminescence data. Relative light units produced by LPS primed and non-primed HL-60 cells stimulated with fMLP were monitored over time.

## **2.12. mRNA Extraction and cDNA Synthesis**

### **2.12.1. mRNA Extraction from SH-SY5Y Cells**

For use in ribonucleic acid (RNA) extraction experiments, adherent SH-SY5Y cells were first removed from the bottom of the flask by incubating the cells in 2 ml of 0.05% trypsin/EDTA solution for 1-2 min. The flask was then washed with 10 ml of F10 medium and the cell suspension was harvested for experiments. SH-SY5Y cells were then counted, centrifuged at 450 g for 7 min, and re-suspended in F5 media to a final concentration of 1 million cells/ml. SH-SY5Y cells were then plated in 2 ml/well in sterile 6-well plates and left in the 37°C, 5% CO<sub>2</sub> incubator for 24 h to allow cells to adhere to the plate prior to treatment. Following incubation, SH-SY5Y cells were first treated with 0.5 μM AF or vehicle control (DMSO). The plates were then returned to the incubator for 15 min, after which SH-SY5Y cells were stimulated with 0.5 mM H<sub>2</sub>O<sub>2</sub> and then returned to the incubator for 24 h at 37°C. Following 24 h incubation RNA was extracted from cells.

### **2.12.2. mRNA Extraction from Astrocytic Cells**

Adherent U-373 MG cells were first removed from the bottom of the flask by incubating cells in 2 ml of 0.25% trypsin/EDTA solution for 5-10 min. The flask was then washed with 10 ml of F10 medium and cell suspension was harvested for experiments. The cells were then counted, centrifuged at 450 g for 7 min, and re-suspended in F5 media to a concentration of 1 million cells/ml. For use in RNA experiments, U-373 MG cells were then plated in 2 ml/well in sterile 6-well plates and left in the incubator for 24 h to allow cells to adhere to the bottom of the plates. Following 24 h incubation, cells were treated with AF, ATG, or their vehicle controls. Plates were then returned to the incubator for 15 min after which U-373 MG cells were

stimulated with IFN- $\gamma$  (150 U/ml). After stimulation, plates were returned to the incubator for 48 h at 37°C. RNA was extracted from cells following this incubation.

For use in RNA experiments, adherent primary human astrocytes were harvested and re-suspended according to the protocol for U-373 MG cells described above, with the exception that cells were plated at a concentration of 0.25 million cells/ml in 2 ml/well.

### 2.12.3. mRNA Spin Column Protocol

Messenger RNA (mRNA) was extracted using the Aurum mini-kit from Bio-Rad using the spin protocol provided by the manufacturer. Following the final incubation period previously described for each cell type, adherent cells were washed 2 x with ice-cold PBS. Cells were then lysed using 350  $\mu$ l of lysis solution provided in the kit, transferred to eppendorf tubes, and lysed with 350  $\mu$ l of 70% molecular grade ethanol. The solutions were then transferred to spin columns provided with the kit, which were subsequently placed into 2 ml capped tubes. The lids on the 2 ml tubes were closed over the spin columns and tubes were centrifuged for 30 s at 12 000 g to force the lysis/ethanol solution through the columns. The flow-through was discarded and 750  $\mu$ l of low stringency wash solution was added to the column. The lids were then sealed again and the columns and tubes were centrifuged for another 30 s at 12 000 g. This flow-through was also discarded. While columns were spinning, 5  $\mu$ l of DNase I; which was provided with the kit and re-constituted in 10mM Tris, was combined with 75  $\mu$ l of DNase dilution solution, and 80  $\mu$ l of this solution was added to each column. Columns containing this solution were then allowed to incubate at room temperature for 15 min to remove genomic deoxyribonucleic acid (DNA) contamination from samples. Following incubation, the DNase solution was deactivated with 700  $\mu$ l of high stringency wash solution. Columns were then centrifuged for 30 s at 12 000 g and

the flow-through was discarded. 700 µl of low stringency wash solution was added to each column. The columns were centrifuged for 1 min at 12 000 g and the flow-through was discarded. The empty columns were centrifuged for 2 min at 12 000 g to remove any residual liquid from the columns. Finally, 40 µl of RNA elution solution was added to the columns, which were then allowed to incubate for 1 min prior to centrifugation for 1 min at 12 000 g to remove RNA from the column. The RNA was quantified spectrophotometrically by measuring absorption at 260 and 280 nm using a NanoDrop 1000 (ThermoFisher). 1µg of RNA was converted to complementary DNA (cDNA) while the rest was frozen and stored at -80°C.

#### **2.12.4. cDNA synthesis**

mRNA samples were converted to cDNA using the qScript cDNA synthesis kit (Quanta Biosciences, Gaithersburg, MD). Approximately 1 µg of each mRNA sample was converted to cDNA. A mixture of 1 µg of sample mRNA, 1 µl of reverse transcriptase enzyme, 4 µl of qScript cDNA reaction mix (proprietary), and nuclease-free water were combined to a total of 20 µl in a 0.2 ml eppendorf tube. Tubes were centrifuged briefly to gather contents then placed in a thermocycler. Reactions were performed for 5 min at 25 °C, 30 min at 45 °C, 5 min at 85 °C, then held at 4 °C. Samples were diluted 1:5 in nuclease-free water and stored at -20 °C until use in qPCR.

#### **2.13. RT-qPCR**

Sequences of the primers obtained from previous publications and used in experiments are shown in Table 2. The primers were checked for specificity using national centre for biotechnology information (NCBI) primer basic local alignment search tool (BLAST) and were

tested for optimal annealing temperatures, primer dimer formation, and efficiency before use in experiments using Minimum Information for Publication of Quantitative Real-Time PCR Experiments (MIQE) guidelines<sup>88</sup>. PCR reactions were performed in duplicate on 3-5 independent biological samples in 96-well plates (Bio-Rad). The total volume of each reaction was 10  $\mu$ l, containing: 5 $\mu$ l Ssofast Evagreen Supermix (Bio-Rad), 0.8 $\mu$ l of each primer (5  $\mu$ M), approximately 1 ng of cDNA template, and 3.2  $\mu$ l nuclease-free water. Negative controls consisted of the PCR components of each 10  $\mu$ l reaction with water replacing cDNA (no template control, NTC) and a no-reverse transcriptase (NRT) cDNA synthesis control to ensure no DNA contamination was present. The PCR program of the CFX96 Real Time System (Bio-Rad) consisted of the following steps: 95°C for 5 min, followed by 40 cycles of 95°C for 5 s, 58°C for 5 s, followed by a dissociation stage of 95°C for 10 s, 65°C for 5 s, and 95°C for 5 s. Melting curve analysis was performed to confirm amplification specificity. The efficiency of each primer set was determined by plotting template dilutions against cycle threshold (Ct) values, and results were within standard accepted values<sup>88</sup>. An example of an efficiency curve is shown in Figure 4. The expression of genes for each treatment was first normalized to the reference gene beta-actin and then normalized to the mRNA found in unstimulated control samples exposed to DMSO vehicle solution only, which were assigned a value of one. 18s RNA was also used as an alternative reference gene but it was not included in analysis as a control due to fluctuations in the level of its expression. Relative expression values were calculated using GeneExMacro OM 3.0 software (Bio-Rad) and the results are shown as mean  $\pm$  standard error of the mean (SEM).

**Table 2: Primer Sequences Used in qPCR Experiments**

---

Primer Sequences	
IL-6 F	GAC CCA ACC ACA AAT GCC A
IL-6 R	GTC ATG TCC TGC AGC CAC TG
IL-8 F	CTG GCC GTG GCT CTC TTG
IL-8 R	CCT TGG CAA AAC TGC ACC TT
IL-4 F	CCG GCA GTT CTA CAG CCA CCA T
IL-4 R	CAG AGG TTC CTG TCG AGC CGT T
MCP-1 F	CTC TGC CGC CCT TCT GTG
MCP-1 R	TGC ATC TGG CTG AGC GAG
HOX-1 F	TGT GGC AGC TGT CTC AAA CCT CCA
HOX-1 R	TTG AGG CTG AGC CAG GAA CAG AGT
18S RNA F	GTA ACC CGT TGA ACC CCA TT
18S RNA R	CCA TCC AAT CGG TAG TAG CG
Beta-Actin F	GGA CTT CGA GCA AGA GAT GG
Beta-Actin R	AGC ACT GTG TTG GCG TAC AG

---

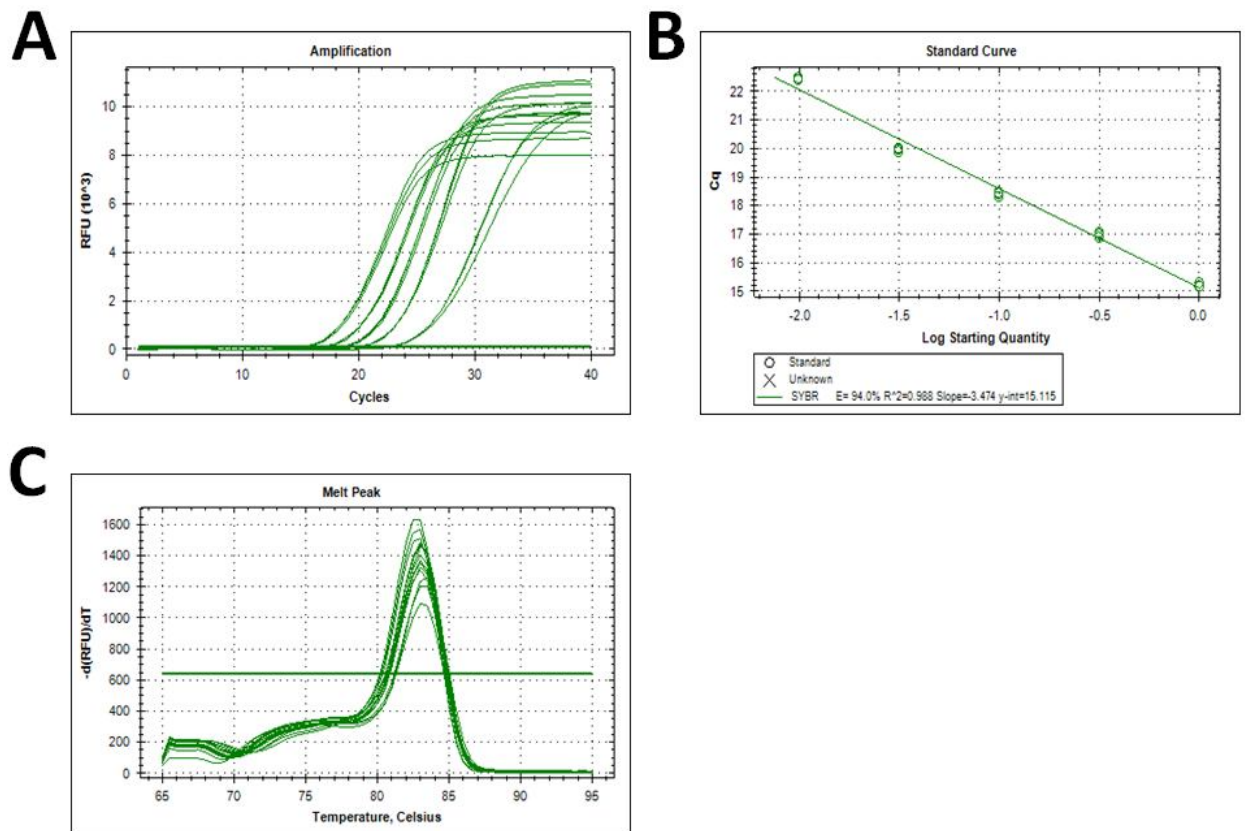


**Fig. 4:** Example of primer efficiency data. Primer efficiency data for MCP-1 is shown as a representative of primers used in this thesis. cDNA from 24 h LPS (0.5  $\mu$ g/ml) and IFN- $\gamma$  (150 U/ml) stimulated THP-1 cells was used to optimize primers. MCP-1 primer amplification curves (A), standard curve (B), and melt curve (C) are shown. All values are within standard accepted values for publishing<sup>88</sup>.

#### 2.14. Treatment of mice with AF and preparation of tissue for LA-ICP-MS

Mice were donated by Dr. D. Gibson and all *in vivo* experiments were performed by a technician in Dr. Gibson's lab. Eight-week-old female C57BL/6 mice obtained from Jackson Laboratories (Bar Harbor, ME, USA) were maintained at the Center for Disease Modelling at UBC Vancouver campus in sterilized, filter-topped cages in a temperature-controlled ( $22 \pm 2^\circ\text{C}$ )

facility with a 12 h light-dark cycle. Mice were maintained under pathogen-free conditions and fed a standard sterile chow (Laboratory Rodent Diet 5001, Purina Mills, St. Louis, MO, USA) with access to tap water *ad libitum* throughout the experiments. All procedures involving care and handling of mice were approved by the UBC Committee on Animal Care Ethics under the guidelines of the Canadian Council on the Use of Laboratory Animals. Three experimental mice were administered 0.1 ml of 2 mg/kg AF dissolved in 10% ethanol once daily for 7 days by oral gavage while 3 control mice were administered 10% ethanol solution only on the same schedule. Mice were euthanized on day 7 and the liver, spleen, kidneys, duodenum, lungs, and brain of each mouse were harvested, rinsed in PBS, and stored at -20 °C. Tissue preparation was done with assistance of Colby Renschler, an undergraduate student in Dr. Klegeris' lab. Small sections of frozen tissue were placed on a glass slide and homogenized by cutting repeatedly with a razor blade. The mass of the homogenized tissue was measured and 5 ppm platinum in 5% HNO<sub>2</sub> in PBS was added 1:1 (w/w). Each tissue/platinum sample was then vortexed and sonicated for 30 s. One µl of fully homogenized tissue/platinum suspension was pipetted on a glass slide with three replicate spots per tissue per experimental animal. Standards with known AF concentrations were also prepared by adding aliquots of serial dilutions of AF solutions to homogenized control tissues. The calibration curves for gold measured with these standards yielded R<sup>2</sup> correlation factor values between 0.9662 - 0.9995. The spots were allowed to dry for 24 h before being analyzed by LA-ICP-MS. Final concentrations of AF were determined by accounting for 50% loss of mass from the tissue homogenates due to drying following spotting on microscope slides.

## 2.15. LA-ICP-MS

LA-ICP-MS experiments were performed by an undergraduate student in Dr. Klegeris' lab, Colby Renschler, and Bert Mueller from the Fipke Laboratory for Trace Element Research (FILTER, UBC Okanagan campus). A procedure similar to the previously described method used to measure the distribution of platinum drug cisplatin in kidneys was developed for use with AF<sup>46</sup>. Murine tissues were ablated using an Analyte 193 argon-fluoride laser (Photon Machines Inc., Redmond, WA, USA). Aerosols generated were transported by 600 ml min<sup>-1</sup> He flow to an Element XR sector field ICP-MS (Thermo Scientific) for gold analysis. The wavelength of the laser was 193 nm (deep UV). It was focused to 148 µm spot diameter with 50% power equivalent to 3.63 J cm<sup>-2</sup>, fired at 10 pulses s<sup>-1</sup>, and scanned across samples at a speed of 370 µm s<sup>-1</sup>. Counts for isotopes <sup>194</sup>Pt, <sup>195</sup>Pt and <sup>197</sup>Au were acquired for 18 s in low mass resolution, 1 sample per peak, 0.01 s dwell time, in speed mode. Blank data were acquired before sampling each standard or sample in the manner described above, except that the laser was not fired. Signal counts for <sup>197</sup>Au were normalized to the <sup>194</sup>Pt counts prior to blank subtraction.

## 2.16. Statistical analysis

SPSS software (version 16.0, IBM SPSS, Chicago IL, USA) was used to conduct statistical analyses on the data. Due to considerable variability in the absolute values obtained from independent experiments performed on different days, randomized block design Analysis of Variance (ANOVA) was used to determine overall significance of findings. ANOVA was followed by Fisher's least significant difference (LSD) post hoc test to assess significant differences in all possible comparisons. For RT-qPCR experiments, due to different experimental design, ANOVA was performed on Ct values with Fisher's LSD as a post hoc test

<sup>89</sup>. This allowed for full comparisons between Ct values. Although ANOVA assumes normality, it is a robust enough test that the likelihood of false positives is low even with the non-normally distributed Ct values <sup>90</sup>.

ANOVA analyses were performed for each experiment; the dependent variable was the experimental results (MTT, LDH, CHL, or Ct values), the independent variables were the different concentrations of compounds, and the random factor blocked the data by the different days or independent replicates. Significance levels of Fisher's LSD comparisons between the solvent control and compound concentrations are shown on the graphs. Data are presented as means  $\pm$  SEM or standard deviation (SD). A probability (p) value less than 0.05 was considered statistically significant and indicated on graphs as \*p<0.05. Cases with a p value less than 0.01 are also shown on graphs as \*\*p<0.01.

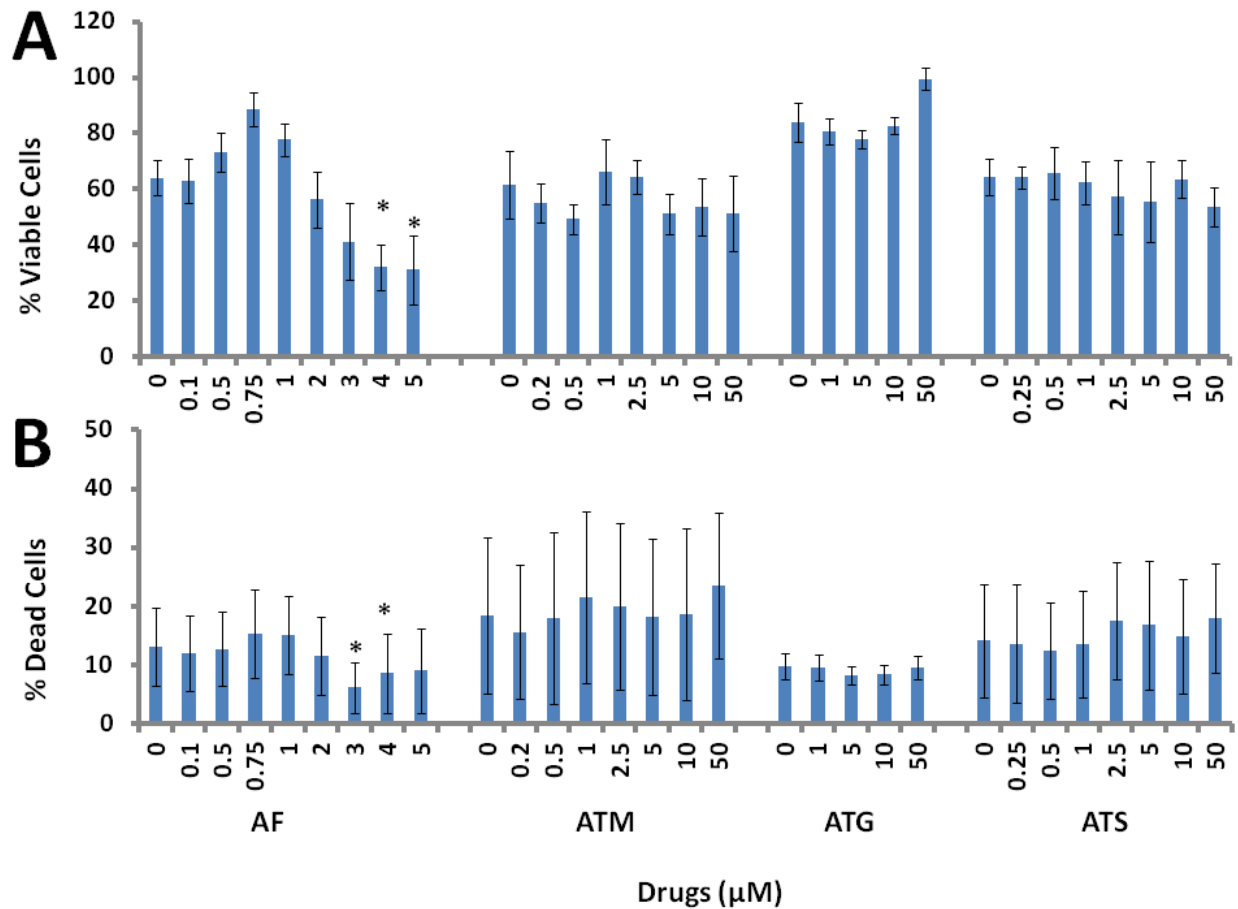
## **3.0. Results**

### **3.1. Anti-Neurotoxic Activity of Gold Compounds**

#### **3.1.1. Activity of Gold Compounds on Microglial Toxicity**

##### **3.1.1.1. Effects of 24 h incubation with gold compounds on human THP-1 promonocytic cell viability and cytotoxicity**

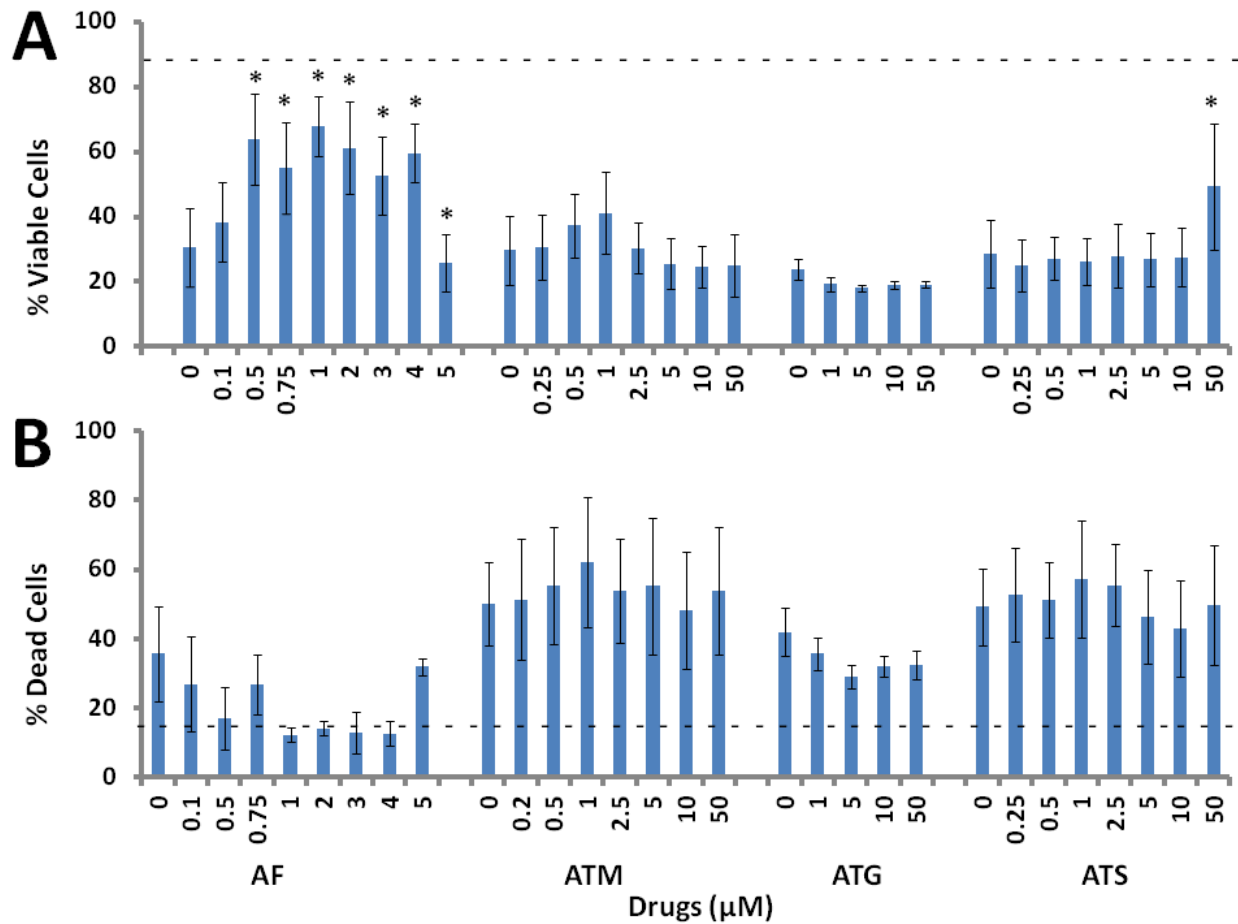
Gold compounds were tested for their ability to inhibit human THP-1 promonocytic cell toxicity towards human neuronal SH-SY5Y cells. Experiments were performed as described in materials and methods section 2.4.1. Compounds were tested at concentrations ranging from 0.1 – 50  $\mu$ M and results were compared to those obtained from samples treated with DMSO vehicle solution only. At the concentrations used (<0.13%, v/v), DMSO alone had no detectable effects in the assays used (data not shown). THP-1 cells were treated with the compounds for 15 min prior to stimulation with LPS plus IFN- $\gamma$ . Following 24 h incubation, viability of THP-1 cells was assessed using MTT cell viability (Fig. 5A) and LDH cell death (Fig. 5B) assays. AF was moderately toxic to THP-1 cells at 3 and 4  $\mu$ M according to the LDH assay (Fig. 5B) and at 4 - 5  $\mu$ M according to the MTT assay (Fig. 5A). Neither assay indicated toxicity of ATM, ATG, nor ATS towards stimulated THP-1 cells at the concentrations tested.



**Fig. 5:** Effect of 24 h incubation with gold compounds on the viability of human THP-1 promonocytic cells. Non-adherent THP-1 cells were pre-treated with various concentrations of the gold compounds or their vehicle solution (DMSO) for 15 min before stimulation with a combination of LPS (0.5 μg/ml) and IFN-γ (150 U/ml). After 24 h incubation, the THP-1 cell viability was assessed by the MTT (A) and LDH (B) assays. Data from 4 independent experiments are presented. The concentration-dependent effects of the compounds were assessed by the randomized block design ANOVA, followed by Fisher's LSD post hoc test. \* p<0.05, significantly different from samples treated with the vehicle solution only.

After the 24 h stimulation period, the cell-free supernatants from THP-1 cell cultures were transferred to SH-SY5Y neuroblastoma cells to assess their cytotoxic effects. Following a

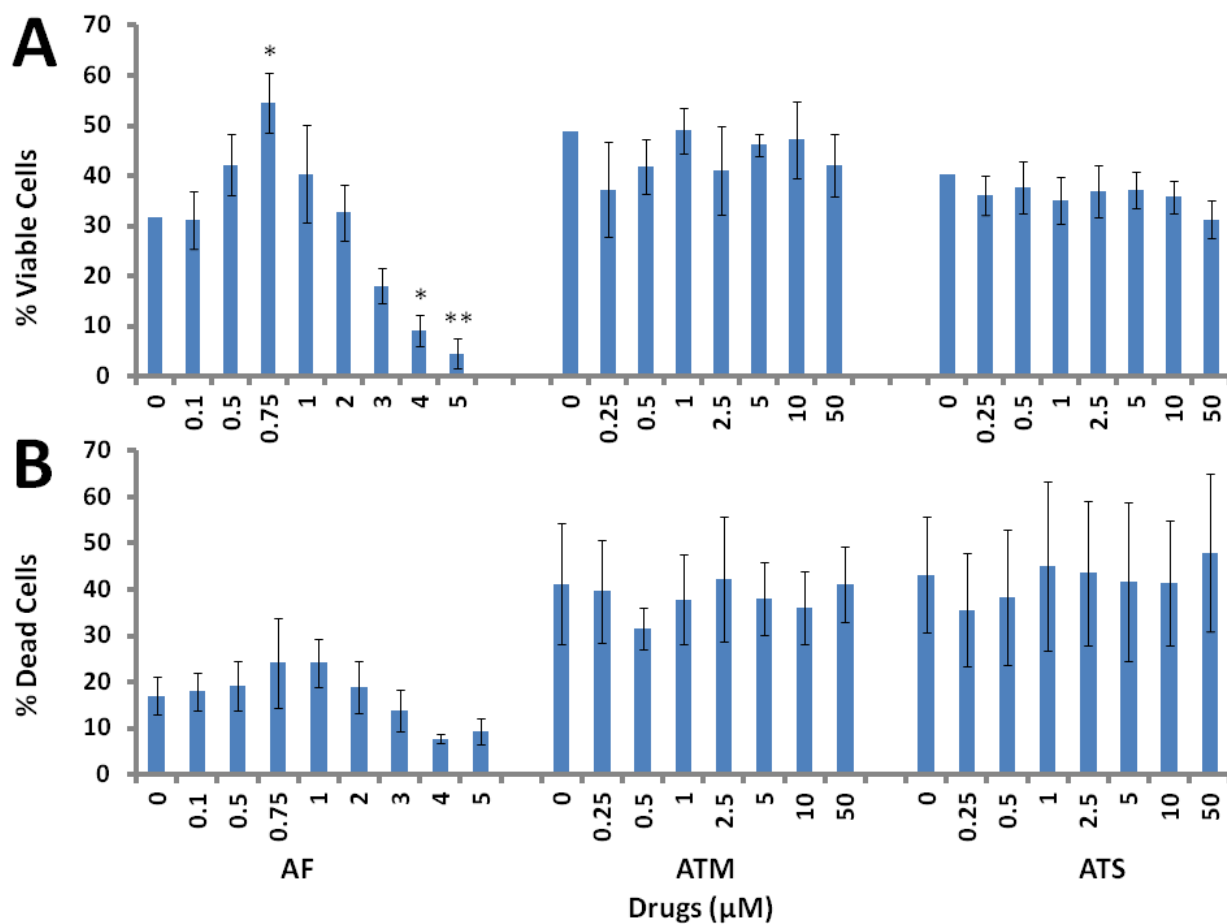
72 h incubation period with THP-1 supernatants, the viability of neuronal cells was assessed using MTT cell viability (Fig. 6A) and LDH cell death (Fig. 6B) assays. Supernatants from unstimulated THP-1 cells did not significantly affect the viability of SH-SY5Y cells (see dashed lines on Fig. 6A and 6B). Transfer of cell-free supernatants from stimulated THP-1 cells to SH-SY5Y cells resulted in significantly reduced neuronal cell viability (Fig. 6A and 6B). A combination of LPS and IFN- $\gamma$  was used to achieve maximal stimulation of cells<sup>91</sup>. As seen in Fig. 6A, the MTT assay indicated that neither ATM nor ATG exhibited any anti-neurotoxic activity while both AF and ATS inhibited the toxicity of stimulated THP-1 supernatants towards neuronal cells at the 0.5 – 5  $\mu$ M range and 50  $\mu$ M, respectively. The anti-neurotoxic activities of AF at 0.5 – 2  $\mu$ M and ATS at 50  $\mu$ M were not due to their toxicity towards THP-1 cells, but most likely due to specific inhibition of the cytotoxic secretions of THP-1 cells. On the other hand, the anti-neurotoxic activity of AF between 3 – 5  $\mu$ M was most likely mediated by direct toxicity towards THP-1 cells. The toxicity and anti-neurotoxic effects of AF were not confirmed in the LDH assay. AF has been shown to induce apoptosis in several cancer cell lines, and it could be that the cells are dying by apoptosis, which leads to intracellular degradation of LDH enzymes before the experiments are completed<sup>58</sup>.



**Fig. 6:** 24 h incubation with AF reduces cytotoxic secretions of THP-1 promonocytic cells. The effects of gold compounds on the viability of SH-SY5Y neuronal cells exposed to supernatants from THP-1 cells stimulated for 24 h with a combination of LPS and IFN- $\gamma$  in the presence or absence of four different gold compounds was assessed by the MTT (**A**) and LDH (**B**) assays. The horizontal dashed lines indicate viability of SH-SY5Y cells exposed to supernatants from unstimulated THP-1 cells. Data from 4 independent experiments are presented. The concentration-dependent effects of the compounds were assessed by the randomized block design ANOVA, followed by Fisher's LSD post hoc test. \*  $p < 0.05$  significantly different from samples treated with the vehicle solution only.

### **3.1.1.2. Effects of 48 h incubation with gold compounds on THP-1 cell viability and cytotoxicity**

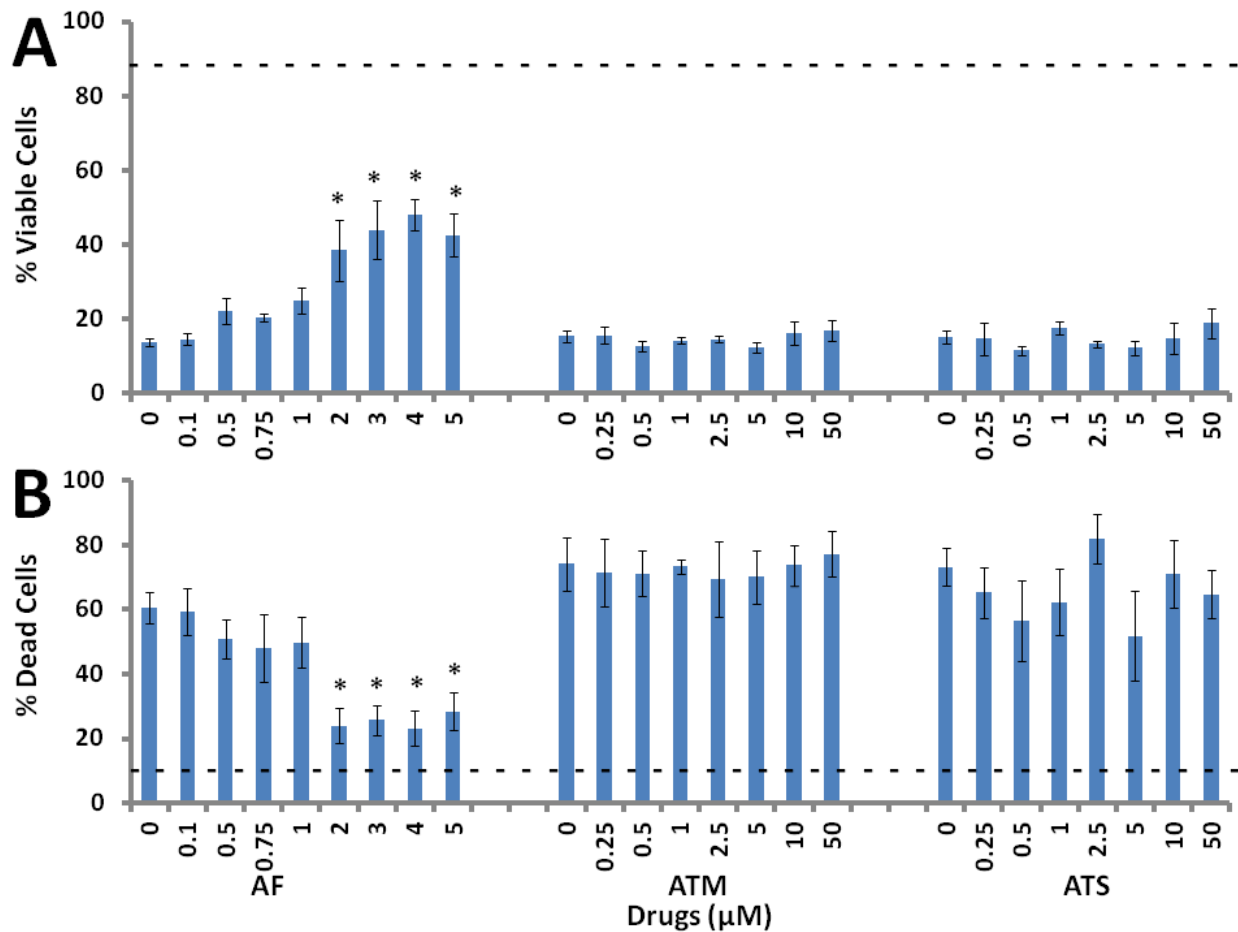
The anti-neurotoxic effect of gold compounds on THP-1 cells was also assessed after a 48 h incubation period. AF, ATM, and ATS were tested at concentrations ranging from 0.1 – 50  $\mu\text{M}$  and results were compared to those obtained from samples treated with DMSO vehicle solution only. Experiments were performed as described in materials and methods section 2.4.1. and in the section 3.1.1.1. above, except that treated THP-1 cells were allowed to incubate with the drugs for 48 h prior to transfer of supernatants and assessment of the monocytic cell viability by the MTT cell viability (Fig. 7A) and LDH cell death (Fig. 7B) assays. Similar to results obtained with the 24 h incubation period, AF was moderately toxic to THP-1 cells at 4 - 5  $\mu\text{M}$  and increased THP-1 cell viability at 0.75  $\mu\text{M}$  according to the MTT assay (Fig. 7A). ATM, ATG, and ATS did not affect viability of stimulated THP-1 cells at the concentrations tested according to either assay.



**Fig. 7:** Effect of 48 h incubation with gold compounds on the viability of human THP-1 promonocytic cells. Non-adherent THP-1 cells were pre-treated with various concentrations of the gold compounds or their vehicle solution (DMSO) for 15 min before stimulation with a combination of LPS (0.5 μg/ml) and IFN-γ (150 U/ml). After 48 h incubation, the THP-1 cell viability was assessed by the MTT (**A**) and LDH (**B**) assays. Data from 3-5 independent experiments are presented. The concentration-dependent effects of the compounds were assessed by the randomized block design ANOVA, followed by Fisher's LSD post hoc test. \*  $p < 0.05$ , \*\*  $p < 0.01$  significantly different from samples treated with the vehicle solution only.

Following 48 h incubation, cell-free supernatants from the THP-1 cell cultures were transferred to SH-SY5Y neuroblastoma cells to assess their cytotoxicity. Following a 72 h incubation period with THP-1 supernatants, the viability of neuronal cells was measured using

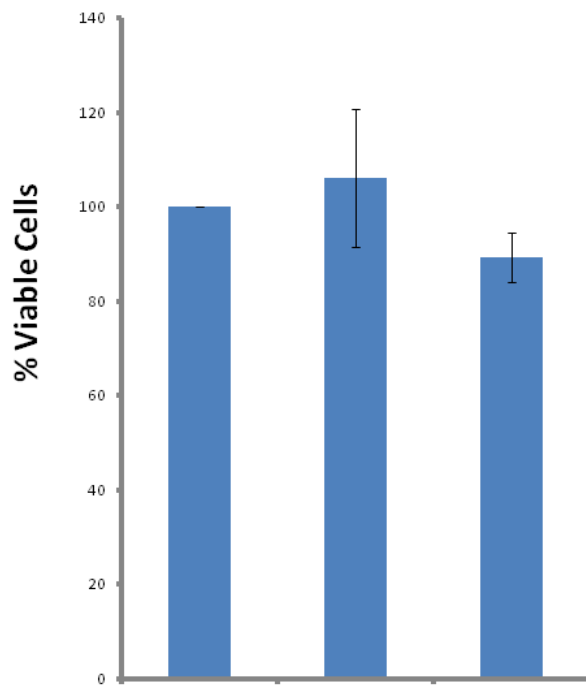
the MTT cell viability (Fig. 8A) and LDH cell death (Fig. 8B) assays. Supernatants from unstimulated THP-1 cells did not significantly affect the viability of SH-SY5Y cells (see dashed line on Fig. 8A and 8B). Both the MTT and LDH assays demonstrated that ATM and ATS did not have any anti-neurotoxic activity while AF inhibited the toxicity of stimulated THP-1 supernatants at the 2 – 5  $\mu$ M range (Fig. 8). The anti-neurotoxic activity of AF between 2 – 3  $\mu$ M was not due to its toxicity towards THP-1 cells but most likely due to specific inhibition of the THP-1 cytotoxic secretions. However, the anti-neurotoxic activity of AF between 4 – 5  $\mu$ M was most likely mediated by direct toxicity towards THP-1 cells.



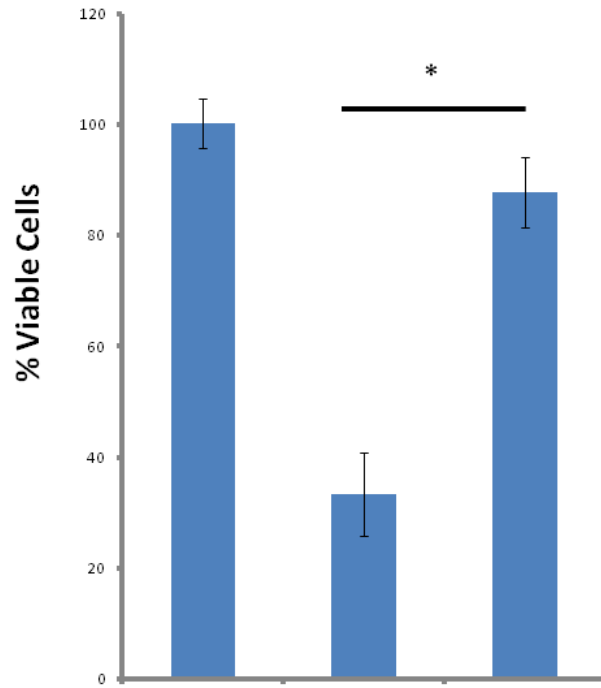
**Fig. 8:** 48 h incubation with AF reduces cytotoxic secretions of THP-1 promonocytic cells. The effects of gold compounds on the viability of SH-SY5Y neuronal cells exposed to supernatants from THP-1 cells stimulated for 48 h with a combination of LPS and IFN- $\gamma$  in the presence or absence of gold compounds was assessed by the MTT (**A**) and LDH (**B**) assays. The horizontal dashed lines indicate viability of SH-SY5Y cells exposed to supernatants from unstimulated THP-1 cells. Data from 3-5 independent experiments are presented. The concentration-dependent effects of the compounds were assessed by the randomized block design ANOVA, followed by Fisher's LSD post hoc test. \*  $p < 0.05$ , significantly different from samples treated with the vehicle solution only.

### 3.1.1.3. Effects of 48 h incubation with AF on primary human microglia cell viability and cytotoxicity

The anti-neurotoxic effects of AF were confirmed using primary human microglia prepared from post mortem brain tissue samples by Dr. S. Hashioka, Department of Psychiatry, UBC, Vancouver. AF was tested at 0.1  $\mu$ M and cell viability values were compared to those obtained from samples treated with DMSO vehicle solution only. Experiments were performed as described previously in materials and methods section 2.4.2. Following 48 h incubation with 0.1  $\mu$ M AF, or its vehicle control, the viability of primary human microglia was assessed using the MTT cell viability assay (Fig. 9A); AF was not toxic to microglial cells at this concentration. Cell-free supernatants from microglia cultures were transferred to SH-SY5Y neuroblastoma cells in order to assess possible cytotoxic effects. Following a 72 h incubation period with these supernatants, the viability of neuronal cells was measured using the MTT cell viability assay (Fig. 9B). MTT assay results demonstrate that 0.1  $\mu$ M AF inhibited the toxicity of stimulated human microglia towards neuronal cells (Fig. 9B), confirming results observed with the THP-1 microglia model.

**A** Human Microglia

AF 0.1  $\mu$ M     -     -     +  
LPS + IFN- $\gamma$    -     +     +

**B** SH-SY5Y Cells

AF 0.1  $\mu$ M     -     -     +  
LPS + IFN- $\gamma$    -     +     +

**Fig. 9:** Effect of 24 h incubation with AF on the viability and cytotoxicity of primary human microglia. Primary human microglia were pre-treated with 0.1  $\mu$ M AF or vehicle solution (DMSO) for 15 min before stimulation with a combination of LPS (0.5  $\mu$ g/ml) and IFN- $\gamma$  (150 U/ml). After 48 h incubation, microglial cell viability was assessed by the MTT assay (**A**). The effects of AF on the viability of SH-SY5Y neuronal cells exposed to supernatants from primary human microglia stimulated with a combination of LPS and IFN- $\gamma$  in the presence or absence of 0.1  $\mu$ M AF was also examined. Following 72 h incubation with microglial supernatants, SH-SY5Y viability was assessed by the MTT assay (**B**) Data from 3 independent experiments with cells obtained from two different surgical cases are presented. The effects of AF were assessed by one way ANOVA \*  $p < 0.05$ , significantly different from stimulated samples treated with the vehicle solution only.

### **3.1.2. Activity of Gold Compounds on Astrocyte Toxicity**

#### **3.1.2.1. Effects of gold compounds on U-373 MG astrocytoma cell viability and cytotoxicity**

Four gold compounds were tested for their ability to inhibit human astrocytic cell toxicity towards human neuronal SH-SY5Y cells. Experiments were performed as described in materials and methods section 2.4.3.. Compounds were tested at concentrations ranging from 0.1 – 50  $\mu\text{M}$  and results were compared to those obtained from samples treated with DMSO vehicle solution only. At the concentrations used ( $<0.13\%$ , v/v), DMSO alone had no detectable effects in the assays used (data not shown). The compounds were added to U-373 MG cells 15 min prior to stimulation with IFN- $\gamma$ . Following 48 h incubation, the viability of U-373 cells was assessed using MTT cell viability (Fig. 10A) and LDH cell death (Fig. 10B) assays. According to the MTT assay, ATS was moderately toxic to U-373 MG cells at 0.25, 10, and 50  $\mu\text{M}$  while AF, ATM, and ATG were not toxic to stimulated U-373 MG cells at the concentrations tested.

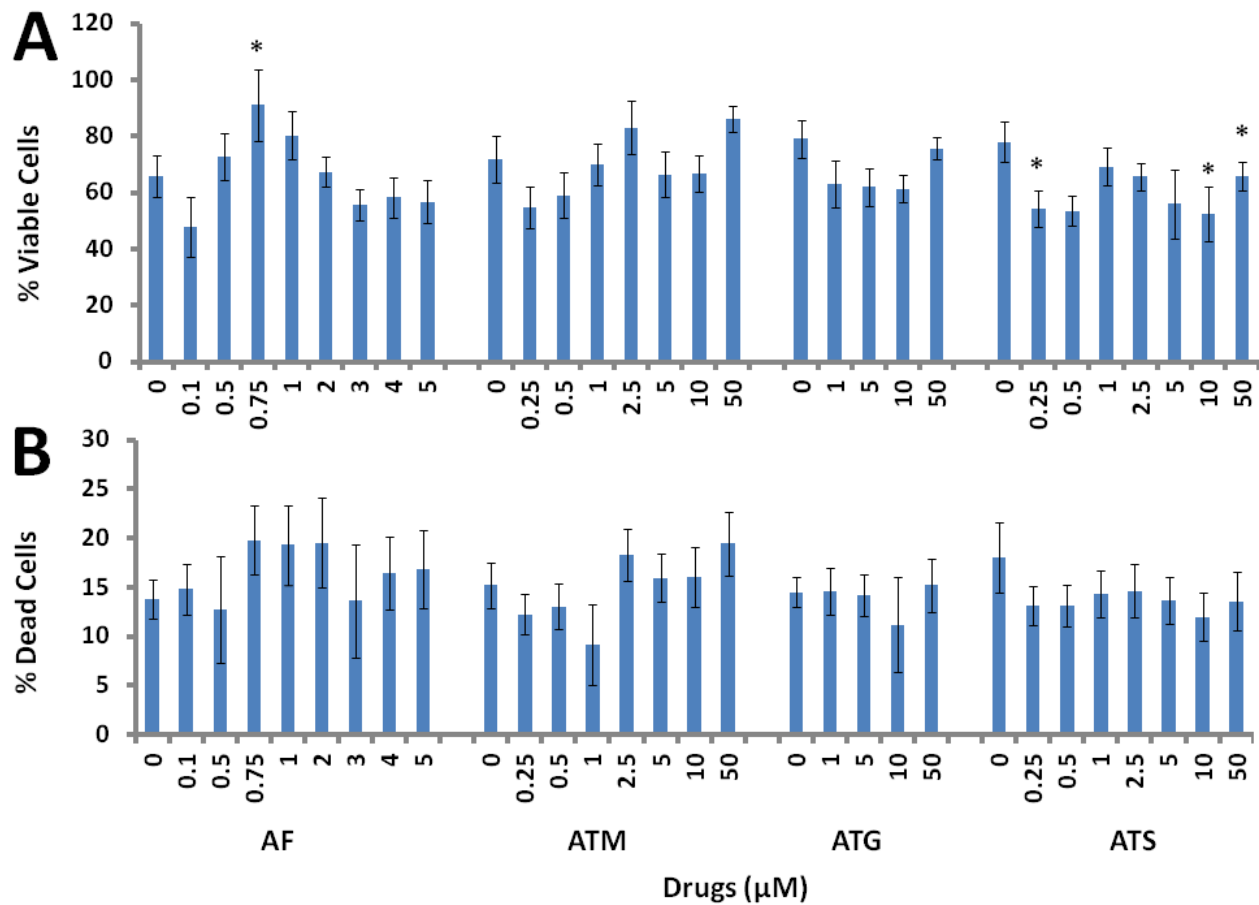


**Fig. 10:** Effect of 48 h incubation with gold compounds on the viability of human U-373 MG astrocytoma cells. Adherent U-373 MG cells were pre-treated with various concentrations of gold compounds or their vehicle solution (DMSO) for 15 min before stimulation with IFN- $\gamma$  (150 U/ml). After 48 h incubation, U-118 MG cell viability was assessed by the MTT (A) and LDH (B) assays. Data from 3-5 independent experiments are presented. The concentration-dependent effects of the compounds were assessed by the randomized block design ANOVA, followed by Fisher's LSD post hoc test. \*  $p < 0.05$ , significantly different from samples treated with the vehicle solution only.

Cell-free supernatants from the U-373 MG astrocytic cell cultures were transferred to SH-SY5Y neuroblastoma cells to assess their cytotoxicity. Following a 72 h incubation period,

the viability of neuronal cells was measured using MTT cell viability (Fig. 11A) and LDH cell death (Fig. 11B) assays. Supernatants from unstimulated U-373 MG cells did not significantly affect the viability of SH-SY5Y cells (see dashed lines on Fig. 11A and 11B). As reported previously<sup>32</sup>, transfer of cell-free supernatants from IFN- $\gamma$  stimulated U-373 MG cells to SH-SY5Y cells resulted in significantly reduced neuronal cell viability (Fig. 11A and 11B). Figures 11A and 11B illustrate that ATM, ATG or ATS did not have any anti-neurotoxic activity while AF inhibited the toxicity of stimulated U-373 MG supernatants towards neuronal cells at the 1 – 5  $\mu$ M range. The anti-neurotoxic activity of AF was not due to its toxicity towards astrocytic cells but most likely due to specific inhibition of the U-373MG cytotoxic secretions. According to the LDH assay, ATS exhibited anti-neurotoxic effects at 0.25 and 50  $\mu$ M, although this was most likely due to direct toxicity of ATS towards U-373 MG cells.

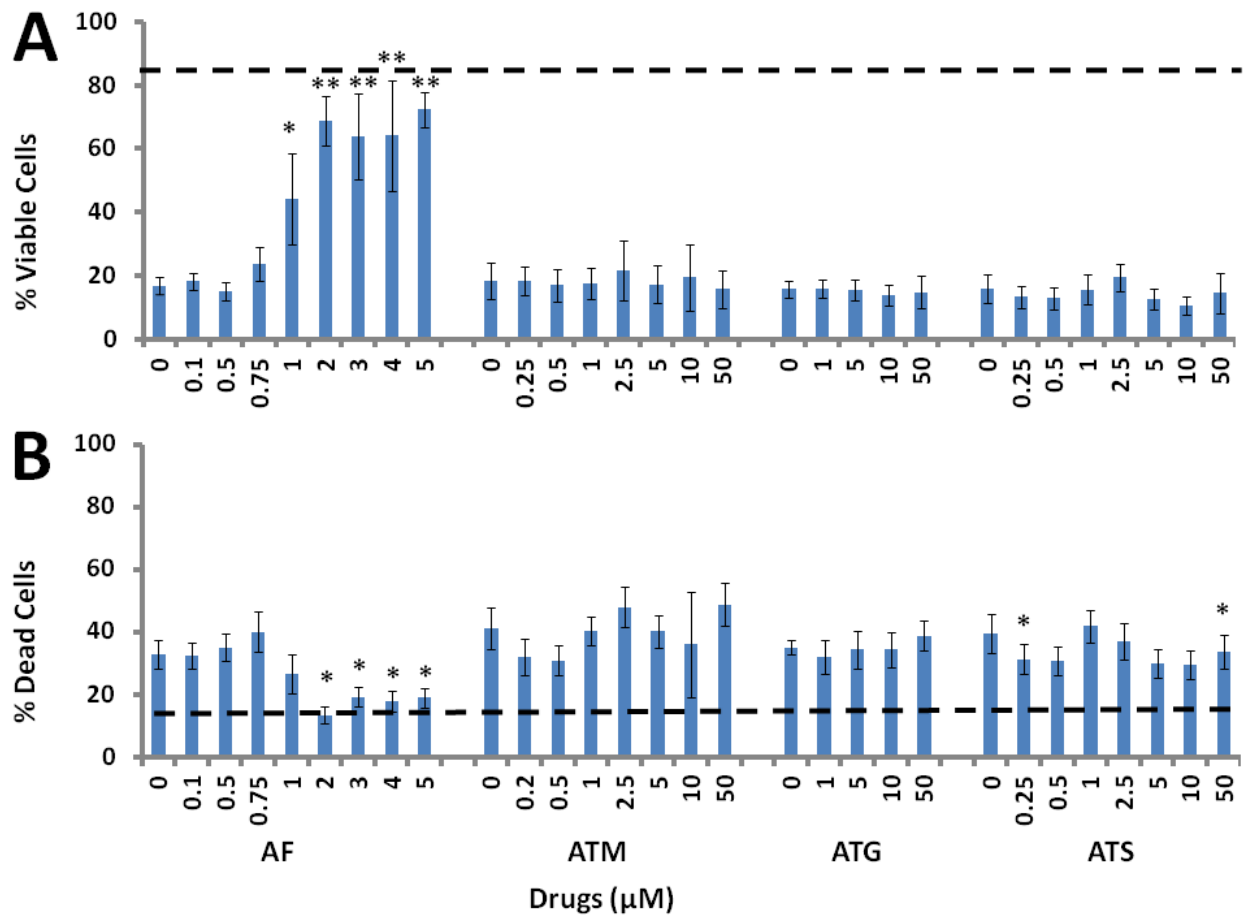


**Fig. 11:** 48 h incubation with AF reduces cytotoxic secretions of U-373 MG astrocytoma cells. The effects of gold compounds on the viability of SH-SY5Y neuronal cells exposed to supernatants from U-373 MG cells stimulated for 48 h with IFN- $\gamma$  in the presence or absence of AF was assessed by the MTT (**A**) and LDH (**B**) assays. The horizontal dashed lines indicate viability of SH-SY5Y cells exposed to supernatants from unstimulated U-373 MG cells. Data from 3-5 independent experiments are presented. The concentration-dependent effects of the compounds were assessed by the randomized block design ANOVA, followed by Fisher's LSD post hoc test. \*  $P < 0.05$ , \*\*  $P < 0.01$  significantly different from samples treated with the vehicle solution only.

The SRB cell viability assay was used to confirm anti-neurotoxic data obtained by the MTT and LDH assays. It yielded similar results. Experiments were performed as described previously in materials and methods section 2.8 and Fig. 10. At 0.5 - 5  $\mu$ M, AF had no significant effect on stimulated U-373 MG viability (Fig. 12A) but inhibited the toxicity of stimulated U-373 MG supernatants towards neuronal cells at 2 and 5  $\mu$ M (Fig. 12B).

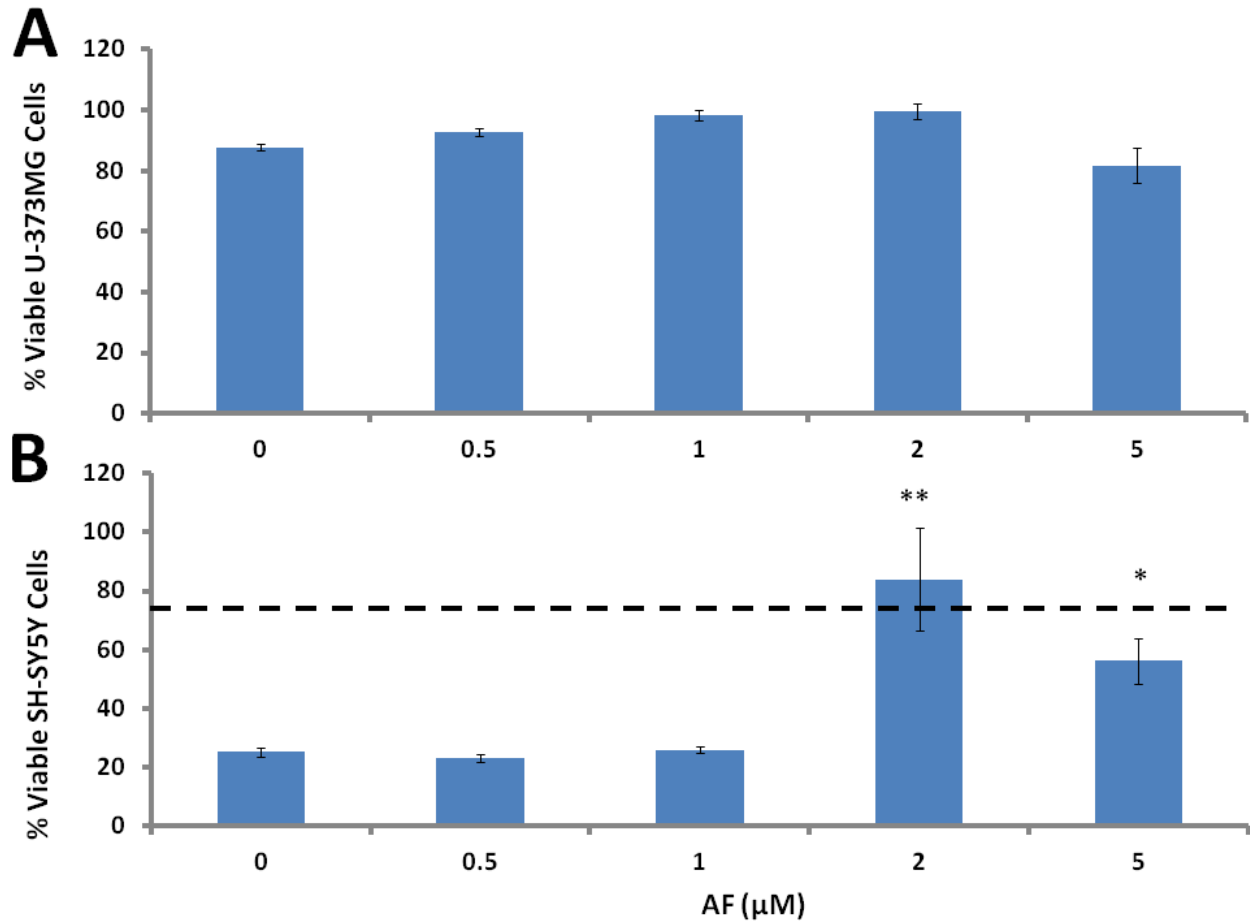


**Fig. 12:** AF is non-toxic to human U-373 MG astrocytoma cells and reduces toxicity of secretions from U-373 MG cells towards SH-SY5Y neuronal cells: confirmation by the SRB assay. Adherent astrocytoma cells were pre-treated with various concentrations of AF or its vehicle solution (DMSO) for 15 min before stimulation with IFN- $\gamma$  (150 U/ml). After 48 h incubation, the U-373 MG cell viability was assessed by the SRB assay (**A**) and 0.4 ml of cell-free supernatants was applied to SH-SY5Y cells. Survival of neuronal cells was assessed 72 h later by the SRB assay (**B**). Data from 3 independent experiments are presented. The horizontal dashed line indicates viability of SH-SY5Y cells exposed to supernatants from unstimulated U-373 MG cells (**B**). The concentration-dependent effects of the compound were assessed by the randomized block design ANOVA, followed by Fisher's LSD post hoc test. \*  $P < 0.05$ , \*\*  $P < 0.01$  significantly different from samples treated with the vehicle solution only.

Phase contrast microscopy images of SH-SY5Y cells were taken following their incubation with U-373 MG cell supernatants. Fig. 13 shows the density and morphology of SH-SY5Y cells following incubation with unstimulated supernatants (**A**), stimulated supernatants and DMSO vehicle control (**B**), and stimulated supernatants supplemented with 2  $\mu$ M AF (**C**). The morphology and density of SH-SY5Y cells treated with AF and stimulated supernatants appear more similar to SH-SY5Y cells exposed to unstimulated U-373 MG supernatants compared to those exposed to stimulated U-373 MG cell supernatants.

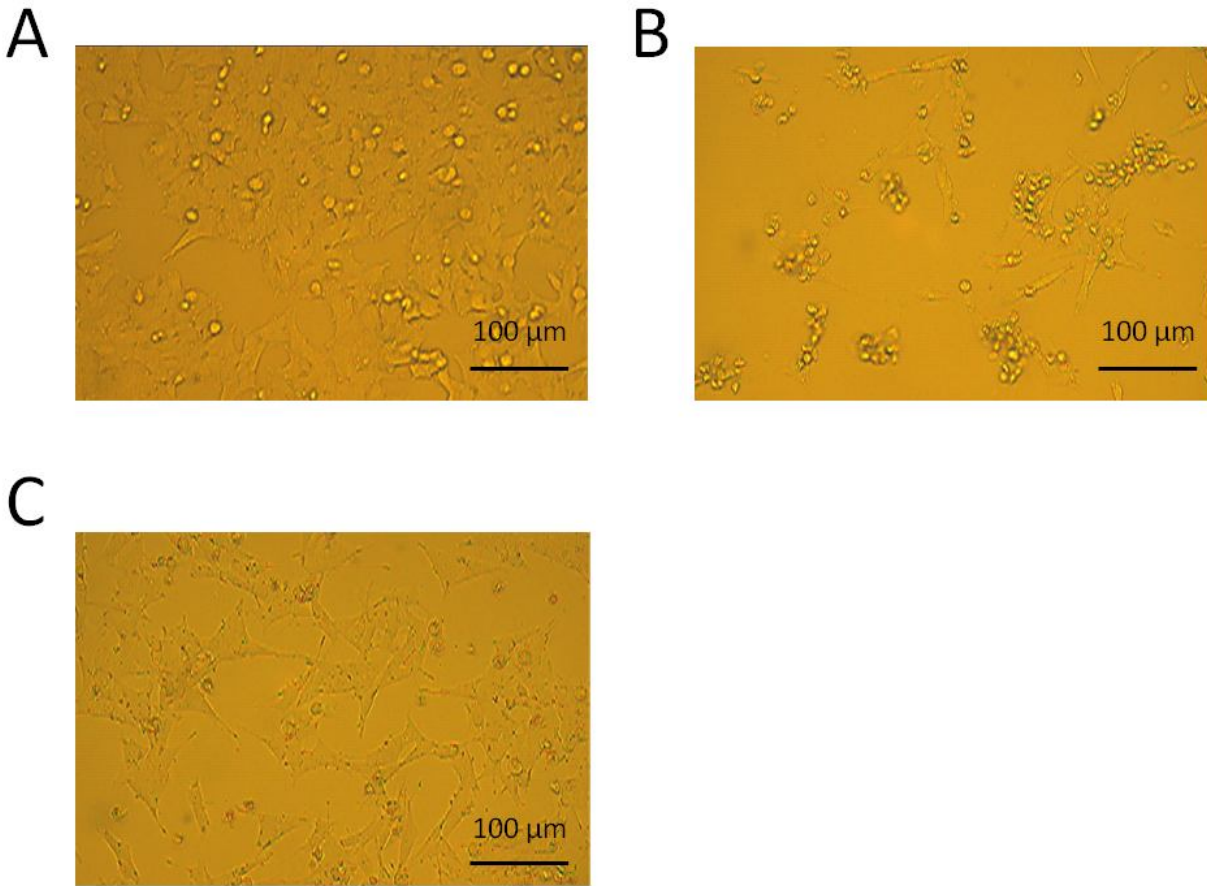


**Fig. 13:** AF restores SH-SY5Y morphology after treatment with stimulated U-373 MG cell supernatants. Phase contrast microscopy of SH-SY5Y cell cultures after incubation with unstimulated U-373 MG supernatant (**A**) IFN- $\gamma$ -stimulated U-373 MG supernatant (**B**) and IFN- $\gamma$ -stimulated U-373 MG supernatant supplemented with 2  $\mu$ M AF (**C**). Experiments were performed as described in Fig. 7 and 8. Photos are representative of 3 independent experiments. Magnification bars in A-C = 100  $\mu$ m.

### 3.1.2.2. Effects of AF on U-118 MG astrocytoma cell viability and cytotoxicity

AF was tested for its ability to inhibit human U-118 MG cell toxicity (another astrocytic cell model) towards human neuronal SH-SY5Y cells to confirm results obtained with U-373 MG astrocytic cells (see sections 3.1.2.1. above). AF concentrations ranging from 0.1 – 5  $\mu$ M were

tested and results were compared to those obtained from samples treated with DMSO vehicle solution only. AF was added to U-118 MG cells 15 min before stimulation with a combination of IL-1 $\beta$  and IFN- $\gamma$  as stimulation with IFN- $\gamma$  alone did not induce significant U-118 MG toxicity towards SH-SY5Y cells. Following 48 h incubation, the viability of U-118 cells was assessed by the MTT cell viability (Fig.14A) and LDH cell death (Fig. 14B) assays. According to both the MTT and LDH assays, AF was moderately toxic to U-118 MG cells at 4 and 5  $\mu$ M. The LDH assay also showed AF to be toxic to U-118 MG cells at 2  $\mu$ M and according to the MTT assay, AF increased U-118 MG cell viability at 0.75  $\mu$ M. The cell death rates according to the LDH assay appeared to be inconsistent with actual cell counts throughout all experiments and are probably not indicative of actual U-118 MG cell death. The significant increase in U-118 MG cell viability in the presence of 0.75  $\mu$ M AF is most likely valid as this is also observed in THP-1 cells. This increase in viability could be due to the inhibition of excitatory cell death caused by the stimulation; since AF is a potent anti-inflammatory molecule, it would prevent the release of non-specific cytotoxic molecules such as RONS<sup>45</sup>.

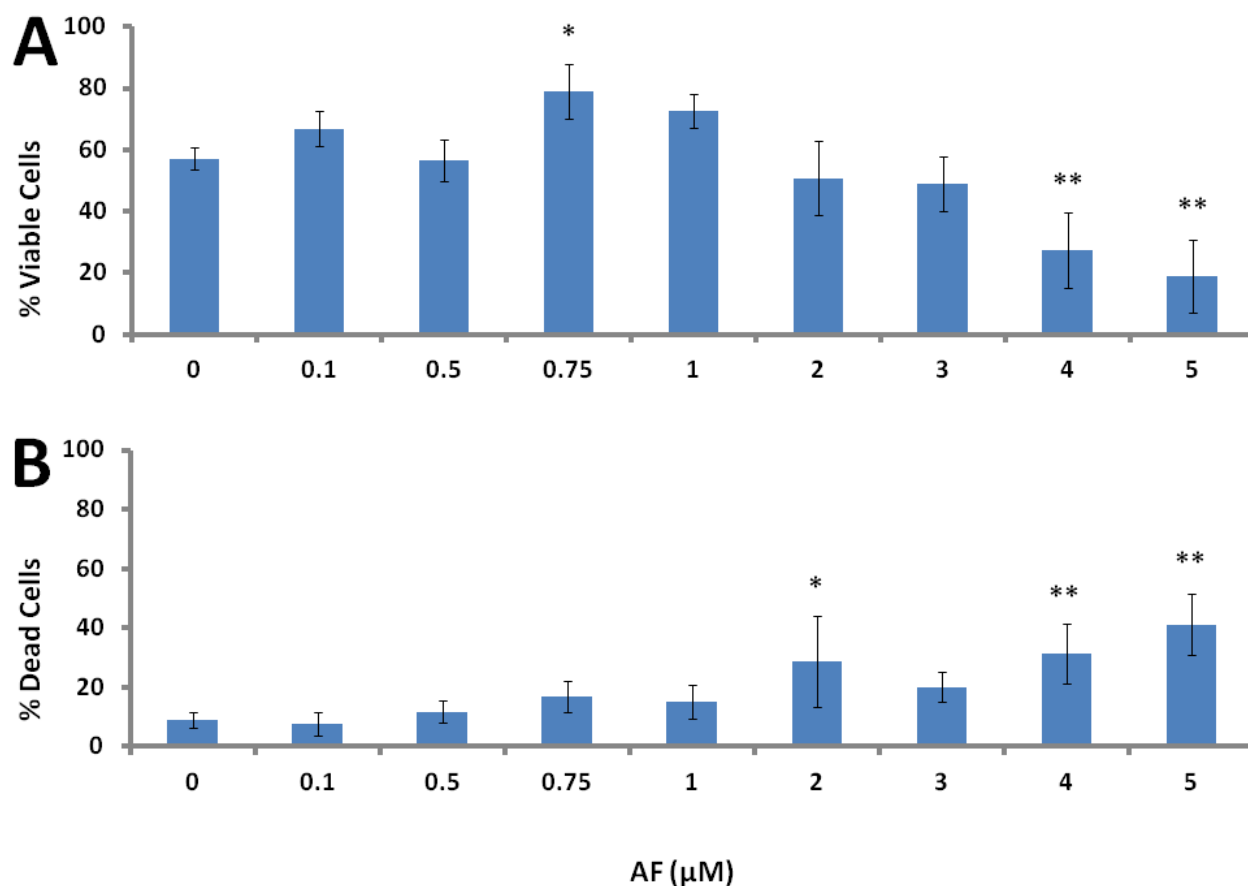


**Fig. 14:** Effect of 48 h incubation with gold compounds on the viability of human U-118 MG astrocytoma cells. Adherent U-118 MG cells were pre-treated with various concentrations of AF or vehicle solution (DMSO) for 15 min before stimulation with a combination of IL-1 $\beta$  (100U/ml) and IFN- $\gamma$  (150 U/ml). After 48 h incubation, U-118 MG cell viability was assessed by the MTT (**A**) and LDH (**B**) assays. Data from 3-5 independent experiments are presented. The concentration-dependent effects of the compound were assessed by the randomized block design ANOVA, followed by Fisher's LSD post hoc test. \*  $p < 0.05$ , \*\*  $p < 0.01$  significantly different from samples treated with the vehicle solution only.

Cell-free supernatants from U-118 MG astrocytic cells treated with AF were transferred to SH-SY5Y neuroblastoma cells to assess their cytotoxicity. Following a 72 h incubation

period, the viability of neuronal cells was measured using MTT cell viability (Fig. 14A) and LDH cell death (Fig. 15B) assays. Supernatants from unstimulated U-118 MG cells, unlike U-373 MG cells, significantly reduced the viability of SH-SY5Y cells according to both the MTT and LDH assays (see dashed lines on Fig. 15A and 15B). According to the MTT assay, transfer of cell-free supernatants from stimulated U-118 MG cells to SH-SY5Y cells resulted in significantly reduced neuronal cell viability (Fig. 15A); however, this effect was not seen in the LDH assay (Fig. 15B). Results from the MTT assay indicate that AF inhibited the toxicity of stimulated U-118 MG supernatants at the 0.75 – 2  $\mu$ M range and decreased the viability of SH-SY5Y cells at 3-5  $\mu$ M. The anti-neurotoxic activity of AF at the 0.75 – 2  $\mu$ M range was not due to its direct toxicity towards astrocytic cells but most likely due to specific inhibition of U-118 MG cytotoxic secretions.

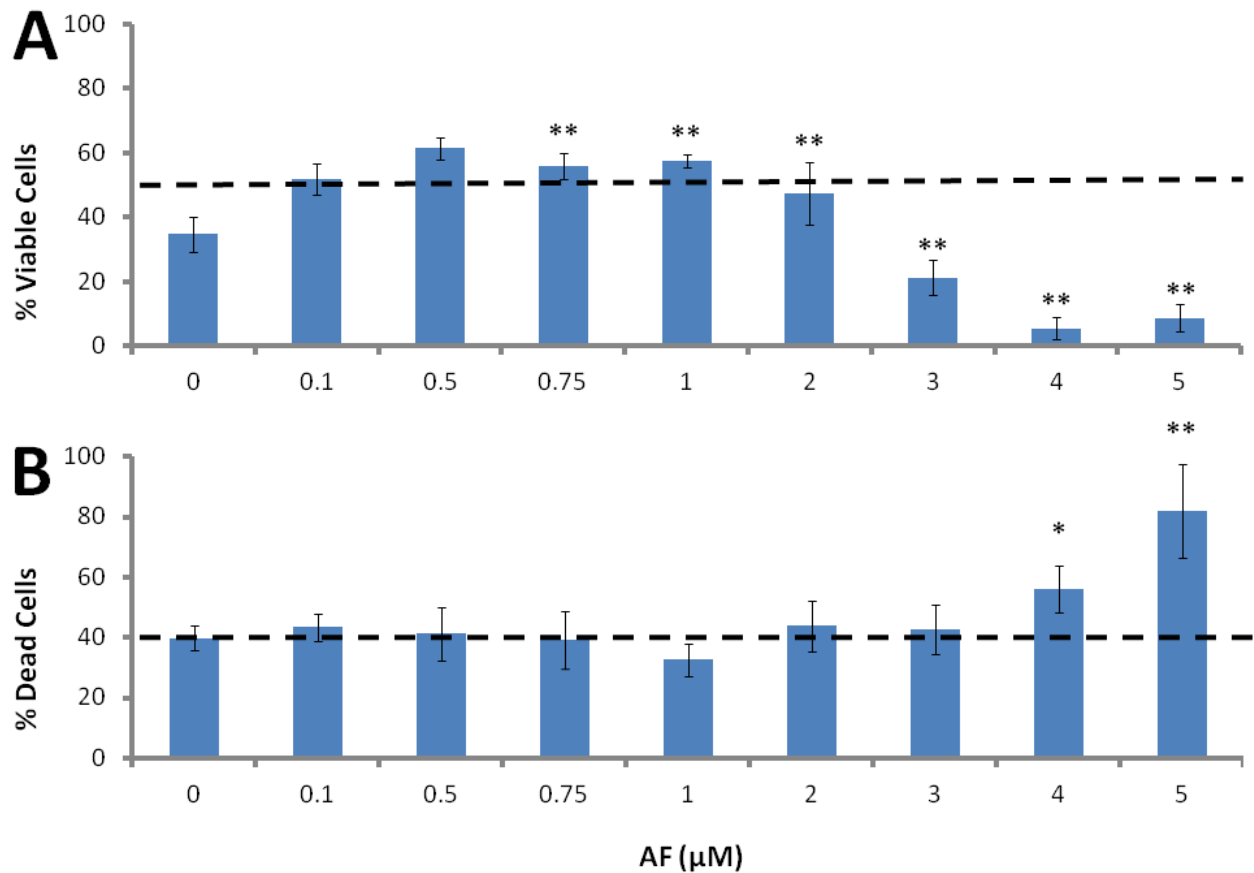


**Fig. 15:** 48 h incubation with AF reduces cytotoxic secretions of U-118 MG astrocytoma cells. The effects of AF on the viability of SH-SY5Y neuronal cells exposed to supernatants from U-118 MG cells stimulated for 48 h with a combination of IL-1 $\beta$  and IFN- $\gamma$  in the presence or absence of AF was assessed by the MTT (**A**) and LDH (**B**) assays. The horizontal dashed lines indicate viability of SH-SY5Y cells exposed to supernatants from unstimulated U-118 MG cells. Data from 5 independent experiments are presented. The concentration-dependent effects of the compound were assessed by the randomized block design ANOVA, followed by Fisher's LSD post hoc test. \*  $p < 0.05$ , \*\*  $p < 0.01$  significantly different from samples treated with the vehicle solution only.

### 3.1.2.3. Effects of AF on human astrocyte cell viability and cytotoxicity

The anti-neurotoxic effects of AF were confirmed using primary human astrocytes prepared from post mortem brain tissue samples by Dr. Sadayuki Hashioka, Department of Psychiatry, UBC, Vancouver. AF was tested at 0.1 - 5  $\mu$ M and results were compared to those obtained from samples treated with DMSO vehicle solution only. Experiments were performed as described previously for U-373 MG cells in section 3.1.2.1.. Following 48 h incubation with AF or its vehicle control, the viability of primary human astrocytes was assessed using the MTT cell viability assay (Fig. 16A). AF was not toxic to human astrocytes at these concentrations, and 5  $\mu$ M AF actually increased astrocyte viability. Cell-free supernatants from astrocyte cultures were transferred to SH-SY5Y neuroblastoma cells to assess their cytotoxicity. Following a 72 h incubation period, the viability of neuronal cells was measured using the MTT cell viability assay (Fig. 16B); MTT assay results demonstrated that 0.1  $\mu$ M AF inhibited the toxicity of stimulated human astrocytes, confirming results observed with U-373 and U-118 MG astrocytic cell models (see Figs. 10 - 16).

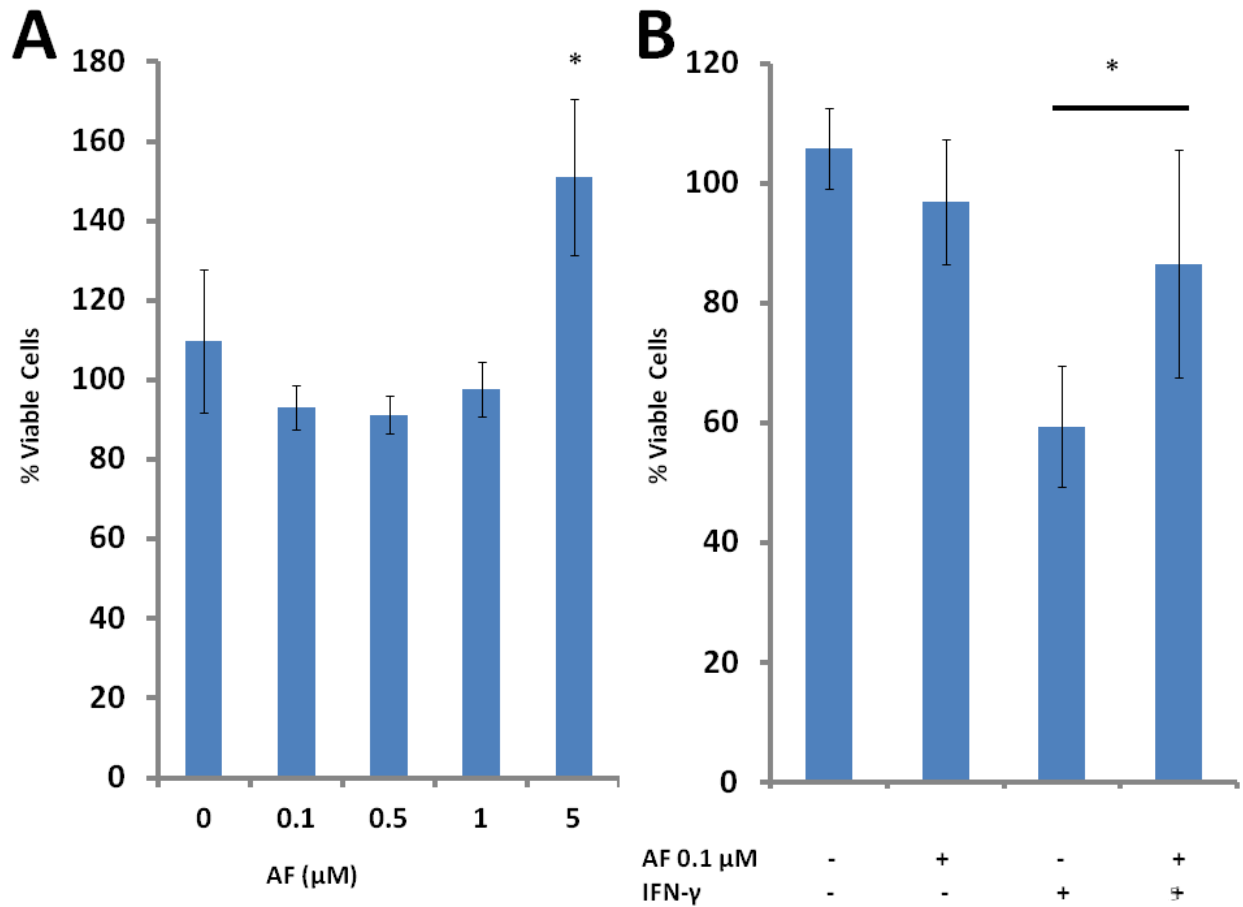


**Fig. 16:** Effect of 24 h incubation with AF on the viability and cytotoxicity of primary human astrocytes. Adherent primary human astrocytes were pre-treated with various concentrations of AF or vehicle solution (DMSO) for 15 min before stimulation with IFN- $\gamma$  (150 U/ml). After 48 h incubation, astrocyte viability was assessed by the MTT assay (**A**). AF reduced cytotoxic secretions of primary human astrocytes. The effects of AF on the viability of SH-SY5Y neuronal cells exposed to supernatants from primary human astrocytes stimulated with IFN- $\gamma$  in the presence or absence of 0.1  $\mu$ M AF was examined. Following 72 h incubation with astrocyte supernatants SH-SY5Y viability was assessed by the MTT assay (**B**). Data from 5 independent experiments with cells obtained from two different surgical cases are presented. The effects of AF were assessed by the randomized block design ANOVA, followed by Fishers LSD post-hoc test \*  $p < 0.05$ , significantly different from stimulated samples treated with the vehicle solution only. Note the difference in scales for the two panels.

### **3.2. Neuroprotective Activity of AF**

The direct neuroprotective effect of AF on cultured SH-SY5Y cells was assessed by: (1) exposing neuronal cells to hydrogen peroxide in the presence of 0.1 – 1  $\mu$ M AF (Fig. 17A), (2) adding AF to supernatants from stimulated U-373 MG cells at the time of their transfer to SH-SY5Y cells (Fig. 17B), and (3) adding AF to supernatants from stimulated THP-1 cells at the time of their transfer to SH-SY5Y cells (Fig. 17C). In all cases, AF at 0.5 and 1  $\mu$ M significantly increased the viability of treated SH-SY5Y cells compared to those not treated with AF. Figure 17D demonstrates that at the concentrations studied, AF had no direct effect on SH-SY5Y cell viability in the absence of hydrogen peroxide or toxins derived from THP-1 and U-373 MG cells.

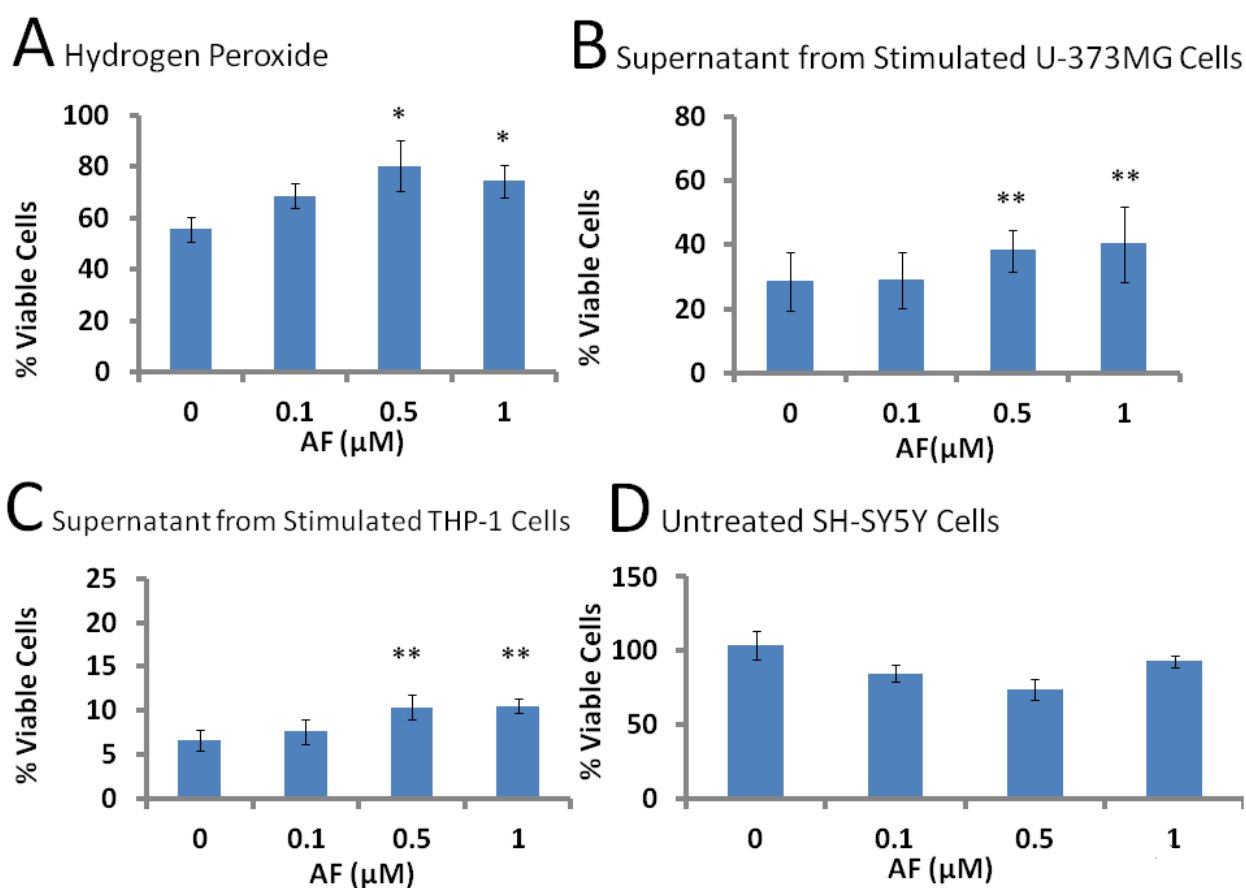


**Fig. 17:** AF protects SH-SY5Y neuronal cells against toxicity induced by hydrogen peroxide and supernatants from stimulated glial cells. The effects of gold compounds on viability of SH-SY5Y neuronal cells exposed to hydrogen peroxide, stimulated U-373 MG astrocytoma cell supernatants, stimulated THP-1 cell supernatants, or untreated neuronal cells were examined. **A** – AF (0.1 - 1 μM), or its vehicle solution (DMSO), was added 15 min prior to the addition of 0.5 mM hydrogen peroxide. **B** - AF (0.1 - 1 μM) or its vehicle solution (DMSO) were added to supernatants from stimulated U-373 MG cells at the time of their transfer to SH-SY5Y cell cultures. **C** - AF (0.1 - 1 μM) or its vehicle solution (DMSO) were added to supernatants from stimulated THP-1 MG cells at the time of their transfer to SH-SY5Y cell cultures. **D** - AF (0.1 - 1 μM), or its vehicle solution (DMSO), was added to unstimulated SH-SY5Y cells. Viability of neuronal cells was assessed by the MTT assay 24 h (**A**) or 72 h (**B, C, D**) later. Data from 3-5 independent experiments are presented; the concentration-dependent effects of the compounds were assessed by the randomized block design ANOVA, followed by Fishers LSD post-hoc test. \*  $p < 0.05$ , \*\* $p < 0.01$  significantly different from samples treated with the vehicle solution only.

### **3.3. Mechanisms of AF action**

#### **3.3.1. Mechanisms of action of AF on microglia**

##### **3.3.1.1. Inhibition of the respiratory burst by AF**

The four gold compounds; AF, ATG, ATM, and ATS, were tested for their ability to inhibit the NADPH oxidase-dependent respiratory burst. DMSO-differentiated human HL-60 cells were used as a model of the microglial respiratory burst as THP-1 cells do not express enough of the NADPH enzyme to generate detectable levels of ROS. Experiments were performed as described in materials and methods section 2.10. and 2.11. Gold compounds were tested at concentrations ranging from 0.1– 5  $\mu$ M and results were compared to those obtained from samples treated only with DMSO vehicle control. At the concentrations used (<0.13%, v/v), DMSO alone had no detectable effects in the assays. Fig. 18A illustrates that 30 min incubation with 5  $\mu$ M AF significantly reduced the luminol-dependent chemiluminescence of HL-60 cells induced by the formyl peptide fMLP. However, viability experiments indicated that concentrations above 1  $\mu$ M AF are significantly toxic towards HL-60 cells (Fig. 21); therefore, the inhibition of respiratory burst activity was most likely due to the direct toxicity of AF. The other gold compounds tested did not significantly affect the luminol-dependent chemiluminescence of HL-60 cells (Fig. 18B, 18C and 18D).

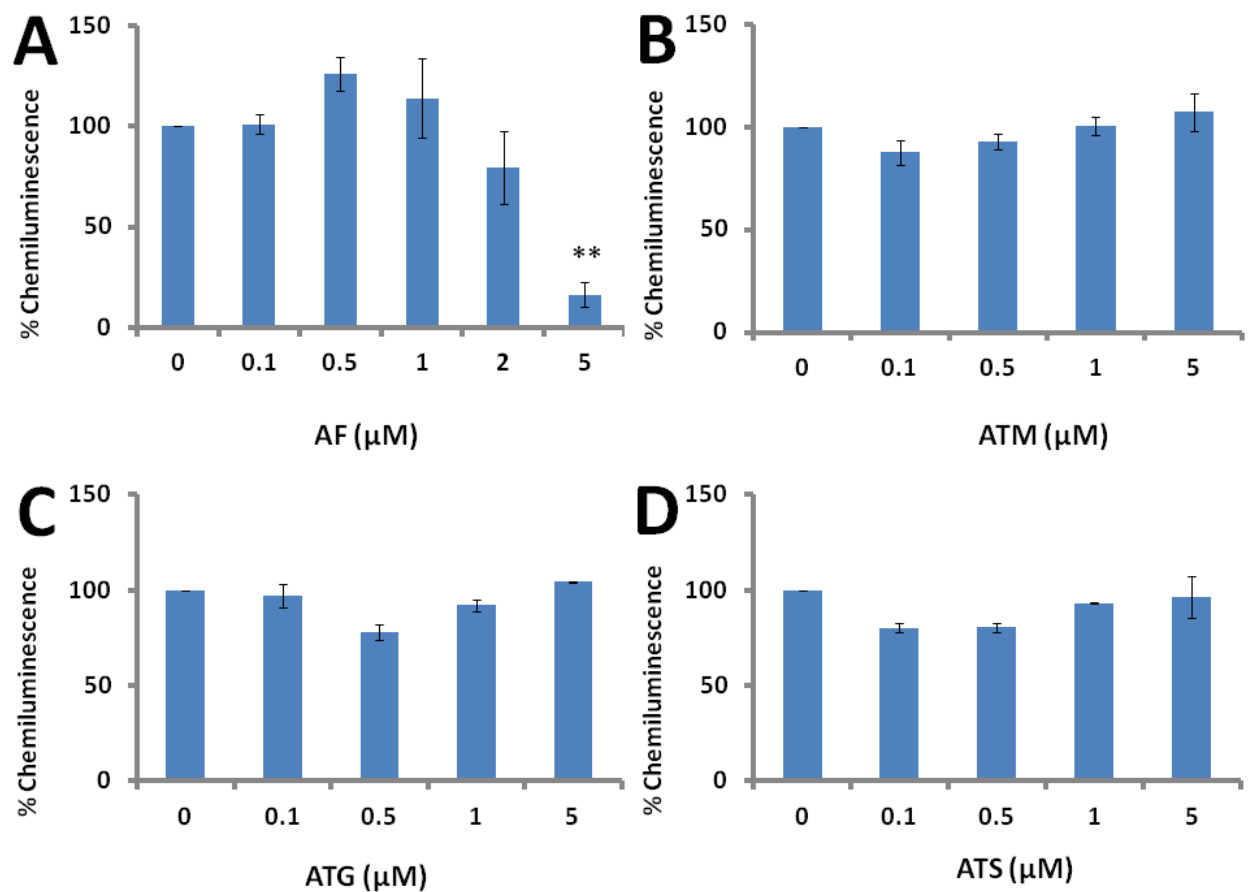


**Fig. 18:** AF, but not ATM, ATG, or ATS, inhibits phagocyte respiratory burst activity. HL-60 cells were first differentiated in the presence of DMSO before use in experiments. They were then washed and transferred into DMEM-F12 media without phenol red and seeded into 96-well plates at a concentration of  $8 \times 10^4$  cells/well. Luminol-dependent chemiluminescence response of HL-60 cells in the presence or absence of compounds was recorded for 30 min after injection of 1  $\mu\text{M}$  FMLP. Data from 3-5 independent experiments are presented; the concentration-dependent effects of the compounds were assessed by the randomized block design ANOVA, followed by Fishers LSD post-hoc test. \*\*  $p < 0.01$  significantly different from samples treated with the vehicle solution only.

### 3.3.1.2. AF inhibits the priming of the neutrophil respiratory burst by LPS and Tfam

The ability of AF to inhibit priming of the neutrophil respiratory burst by 24 h co-treatment with LPS or Tfam was investigated using DMSO-differentiated human HL-60 cells. AF was tested at concentrations ranging from 0.1 – 1  $\mu$ M and results were compared to those obtained from samples treated with the DMSO vehicle control (indicated by dashed lines in Fig. 19A and 19B). At the concentrations used (<0.13%, v/v), DMSO alone induced no detectable effects in the assays used. AF was added to HL-60 cells 15 min before cells were exposed to LPS, Tfam, or Tfam buffer. Recombinant Tfam was dissolved in Tfam buffer and this buffer was added as a control group to eliminate the possibility that the ingredients of buffer were priming HL-60 cells. LPS was dissolved in the media used for cell plating and therefore a vehicle control was not included in this case. Following 24 h incubation, fMLP-induced production of ROS by HL-60 cells was measured as increase in luminol-dependent chemiluminescence signal. Incubation of DMSO-differentiated HL-60 cells with LPS and Tfam for 24 h was found to increase their ROS production by as much as 400% (Fig. 19A and 19B). Addition of AF at time of priming, at 0.1 – 1  $\mu$ M, significantly reduced the production of ROS in cells primed with LPS (Fig. 19A) or Tfam (Fig. 19B). Furthermore, 24 h incubation with 1  $\mu$ M AF alone reduced the production of ROS by HL-60 cells that had not been primed (Fig. 20) though 24 h incubation with AF and Tfam buffer had no significant effect on ROS production (Fig. 19B). Acute 30 min treatment with AF had no effect on ROS production in 24 h LPS-primed, 24 h Tfam-primed or control conditions in the absence of a priming agent (Fig. 19A and 19B). However, viability experiments (see section 3.3.1.3. below) indicated that 24 h incubation with 1  $\mu$ M AF was toxic towards HL-60 cells; therefore, inhibition of the respiratory burst activity at this concentration is most likely due to the direct toxicity of AF (Fig. 21).

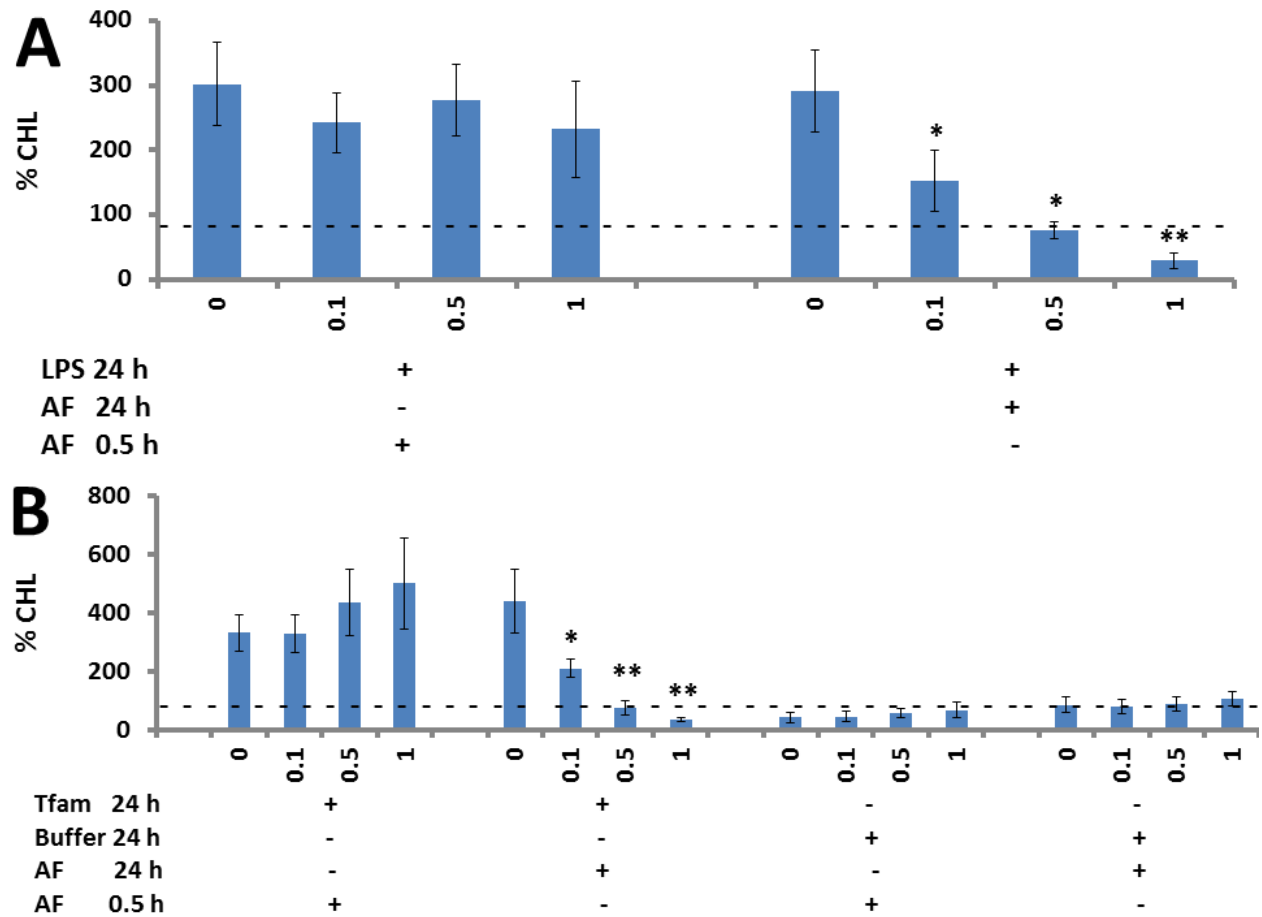


**Fig. 19:** AF inhibits LPS and Tfam priming of the phagocyte respiratory burst. HL-60 cells were differentiated in the presence of DMSO before use in experiments. They were then washed and transferred into DMEM-F12 media without phenol red and seeded into 96-well plated at a concentration of  $8 \times 10^4$  cells/well. Cells were pre-treated with various concentrations of the AF or vehicle solution (DMSO) for 15 min before their exposure to either LPS (0.5  $\mu\text{g/ml}$ ) (**A**) or Tfam (5  $\mu\text{g/ml}$ ) (**B**) and were incubated for 24 h. Following 24 h incubation cells that were not incubated with AF were treated with AF for 0.5 h. Following incubation, luminol-dependent chemiluminescence response of HL-60 cells in the presence or absence of compounds was recorded for 30 min after injection of 1  $\mu\text{M}$  fMLP. Data from 4-5 independent experiments are presented; the concentration-dependent effects of the compounds were assessed by the randomized block design ANOVA, followed by Fishers LSD post-hoc test. \*  $p < 0.05$ , \*\* $p < 0.01$  significantly different from samples treated with the vehicle solution only.

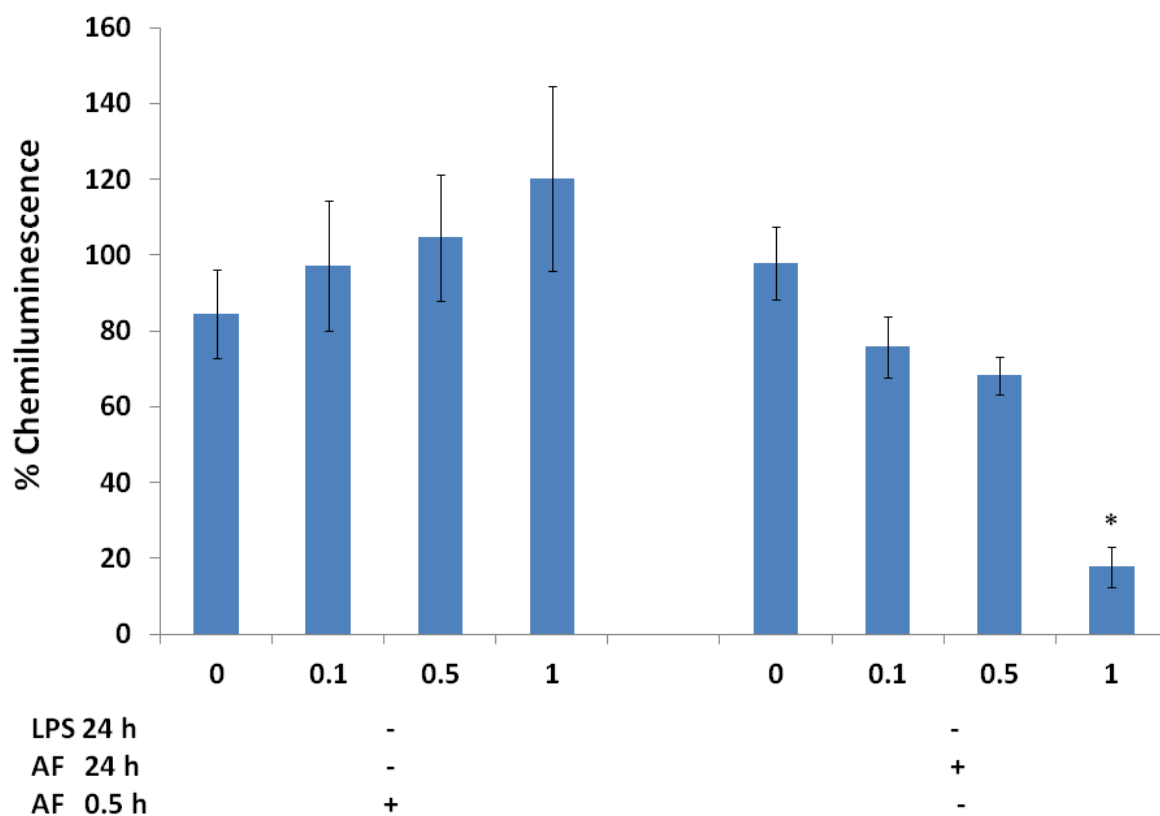


**Fig. 20** 24 h incubation with AF inhibits the phagocyte respiratory burst. HL-60 cells were differentiated in the presence of DMSO before use in experiments. Cells were then washed and transferred into DMEM-F12 media without phenol red and seeded into 96-well plated at a concentration of  $8 \times 10^4$  cells/well. Cells were pre-treated with various concentrations of the AF or vehicle solution (DMSO) for 15 min and were incubated for 24 h. Following 24 h incubation cells that were not incubated with AF were treated with AF for 0.5 h. Following treatment with AF, luminol-dependent chemiluminescence response of HL-60 cells in the presence or absence of compounds was recorded for 30 min after injection of  $1 \mu\text{M}$  fMLP. Data from 4 independent experiments are presented; the concentration-dependent effects of the compounds were assessed by the randomized block design ANOVA, followed by Fishers LSD post-hoc test. \*  $p < 0.05$  significantly different from samples treated with the vehicle solution only.

### **3.3.1.3. Effects of AF on HL-60 cell viability**

AF was tested for its toxicity towards human HL-60 cells at concentrations ranging from 0.1 – 1  $\mu$ M and results were compared to those obtained from samples treated with DMSO vehicle solution only. At the concentrations used (<0.13%, v/v), DMSO alone had no detectable effects in the assays (data not shown). AF was added to HL-60 cells, and following 24 or 0.5 h incubation, viability of HL-60 cells was assessed using the MTT cell viability assay (Fig. 21). 24 h incubation with 1  $\mu$ M AF caused a significant reduction in the viability of HL-60 cells.

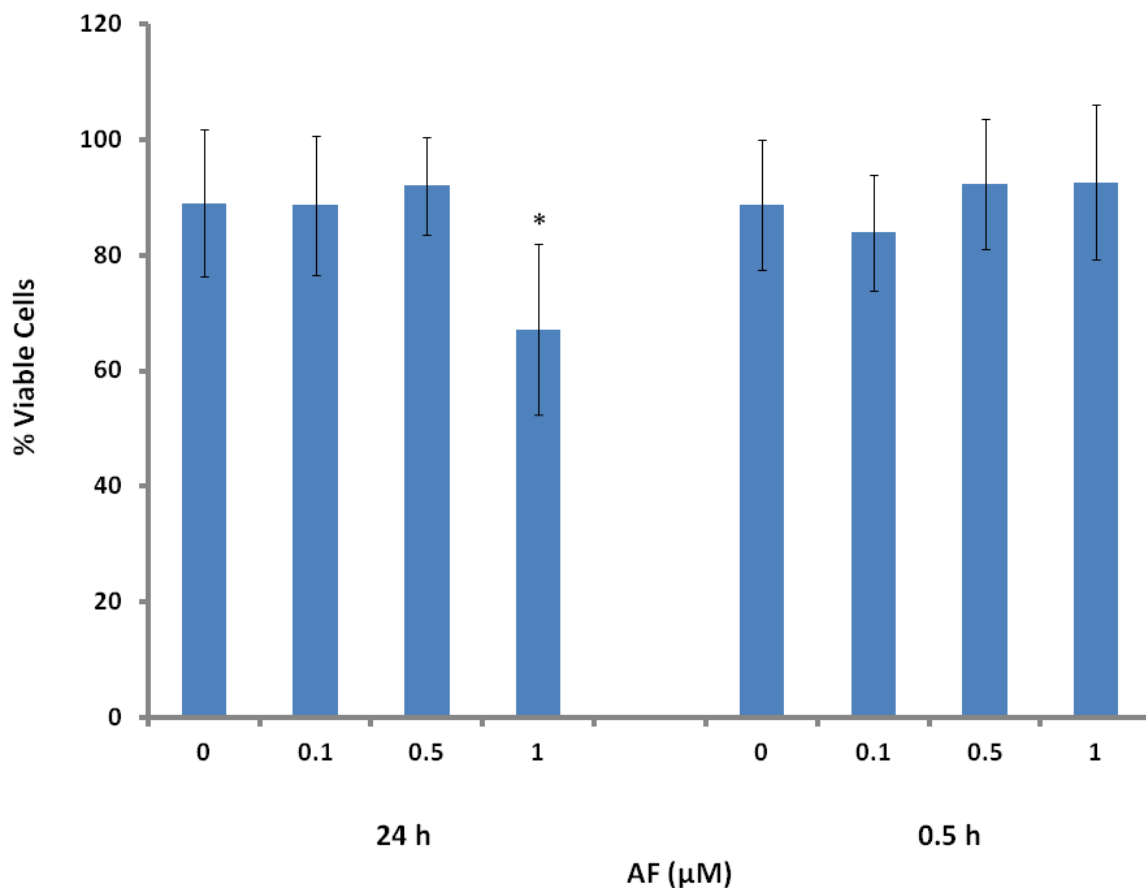
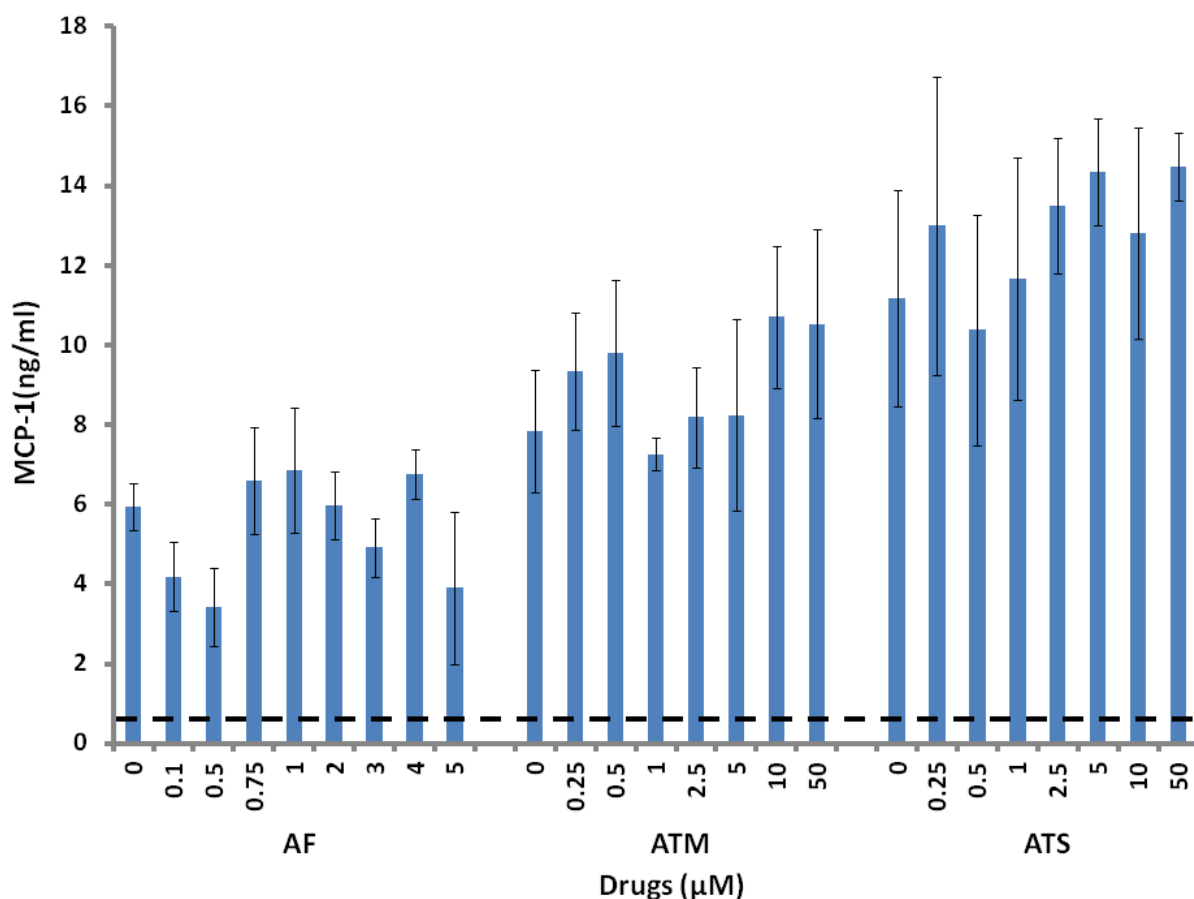


**Fig. 21:** Effect of 24 h incubation with AF on the viability of human HL-60 promyelocytic cells. HL-60 cells were incubated with AF or vehicle solution (DMSO) for 24 h. Following incubation, the cell viability was assessed by the MTT assay. Data from 4 independent experiments are presented. The concentration-dependent effects of the compound were assessed by the randomized block design ANOVA, followed by Fisher’s LSD post hoc test. \*  $p < 0.05$ , significantly different from samples treated with the vehicle solution only.

### 3.3.1.4. Effects of gold compounds on the secretion of MCP-1 by THP-1 cells

The effect of three of the gold compounds on the secretion of the pro-inflammatory cytokine MCP-1 by stimulated THP-1 cells was investigated by ELISA analysis of 24 h stimulated THP-1 supernatants. Gold compounds were tested at concentrations ranging from

0.1 – 50  $\mu\text{M}$  and results were compared to those obtained from samples treated with DMSO vehicle solution only. Figure 22 shows that stimulation of THP-1 cells with LPS and IFN- $\gamma$  increased the secretion of MCP-1; the baseline secretion of MCP-1 by unstimulated cells is indicated on Fig. 22 by a dashed line. None of the gold compounds studied significantly affected the production of MCP-1 by stimulated THP-1 cells (Fig. 22).

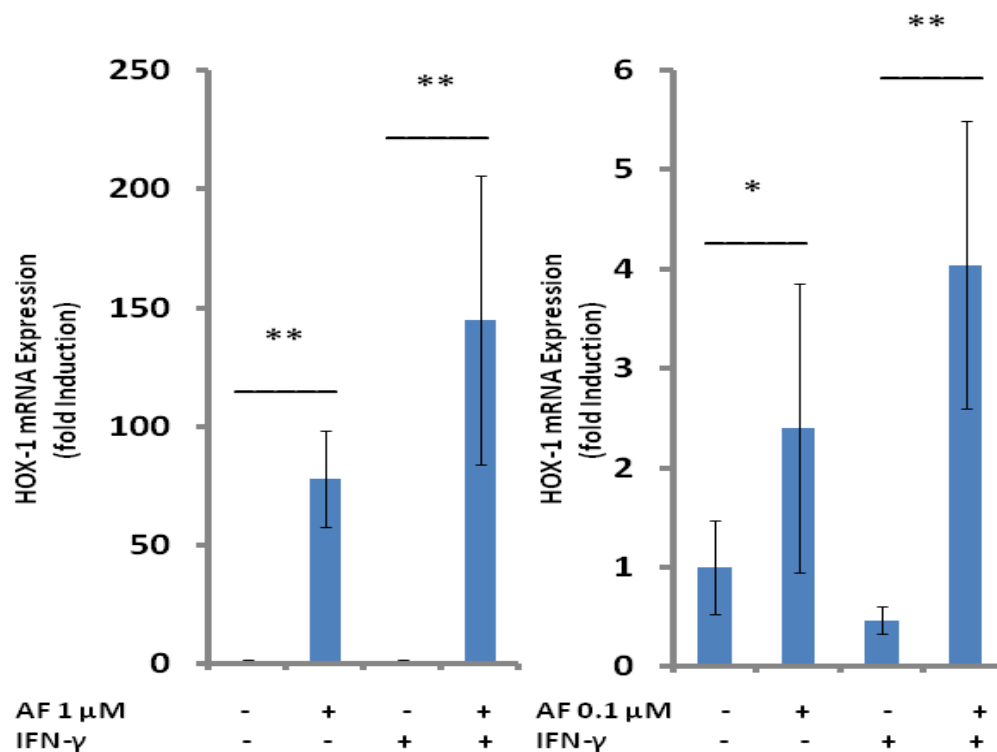


**Fig. 22** Gold compounds have no significant effect on MCP-1 secretion by THP-1 cells. THP-1 cells were stimulated as described in the legend of Fig. 2. Following a 24 h incubation period, MCP-1 concentration in THP-1 culture supernatants was measured by ELISA. Data from 3 independent experiments are presented. The horizontal dashed line indicates MCP-1 concentration in supernatants from unstimulated THP-1 cells. The concentration-dependent effects of the compound were assessed by the randomized block design ANOVA, no significance was found.

### **3.3.2. Mechanisms of Action of AF on Astrocytes**

#### **3.3.2.1. Effects of AF on the expression of inflammatory mediators in astrocytic cells**

Expression of the inflammatory mediators HOX-1, IL-6, IL-8, and MCP-1 were measured in the presence or absence of AF. RT-qPCR was used to measure the fold changes in the expression of inflammatory genes of interest. Figure 23 illustrates that 24 h incubation of U-373 MG cells and human astrocytes in the presence of AF significantly upregulated HOX-1 mRNA expression. RT-qPCR results indicated that 1  $\mu$ M AF upregulated HOX-1 expression in unstimulated U-373 MG cells more than 75 fold, compared to DMSO solvent-treated cells (Fig. 23A). Similarly, treatment of human astrocytes with 0.1  $\mu$ M AF resulted in more than 2 fold upregulation of HOX-1 (Fig. 23B). Stimulation of U-373 MG cells or human astrocytes with IFN- $\gamma$  alone did not induce a significant increase in HOX-1 expression. However, combining AF and IFN- $\gamma$  treatments resulted in further doubling of HOX-1 mRNA levels compared to treatment with AF alone. This resulted in a nearly 150 fold increase in HOX-1 expression in U-373 MG cells and a more than 7 fold increase in HOX-1 expression in human astrocytes compared to unstimulated cells (Fig. 23). 24 h treatment with AF did not significantly affect the expression of IL-6 (Fig. 24A), IL-8 (Fig. 24B), or MCP-1 (Fig. 24C) in either unstimulated or stimulated U-373 MG cells. Due to the induction of HOX-1 expression by AF, the effect of treating U-373 MG cells with ATG was also investigated to determine if the effect on HOX-1 was specific to AF. ATG did not induce HOX-1 expression in either stimulated or unstimulated U-373 MG cells (data not shown).

**A**- U373 MG Cells**B**- Human Astrocytes

**Fig. 23:** AF upregulates heme oxygenase (HOX-1) mRNA expression in unstimulated and stimulated U-373 MG astrocytic cells and primary human astrocytes. U-373 MG cells (**A**) and human astrocytes (**B**) were treated with either AF or DMSO vehicle solutions. Astrocytic cells were either left unstimulated or were stimulated with IFN- $\gamma$  (150 U ml<sup>-1</sup>). Total RNA was extracted 24 h later and the HOX-1 mRNA expression was analyzed by using specific primers and RT-qPCR. Results were normalized to a reference gene  $\beta$ -actin and are presented as a fold increase compared to the HOX-1 mRNA level in control unstimulated cells not exposed to AF (expression level = 1). Data from 3-4 independent experiments are presented; the observed differences in expression levels were assessed by the randomized block design ANOVA, followed by Fishers LSD post-hoc test. \* p<0.05; \*\* p<0.01, significantly different from samples treated with the vehicle solution only.

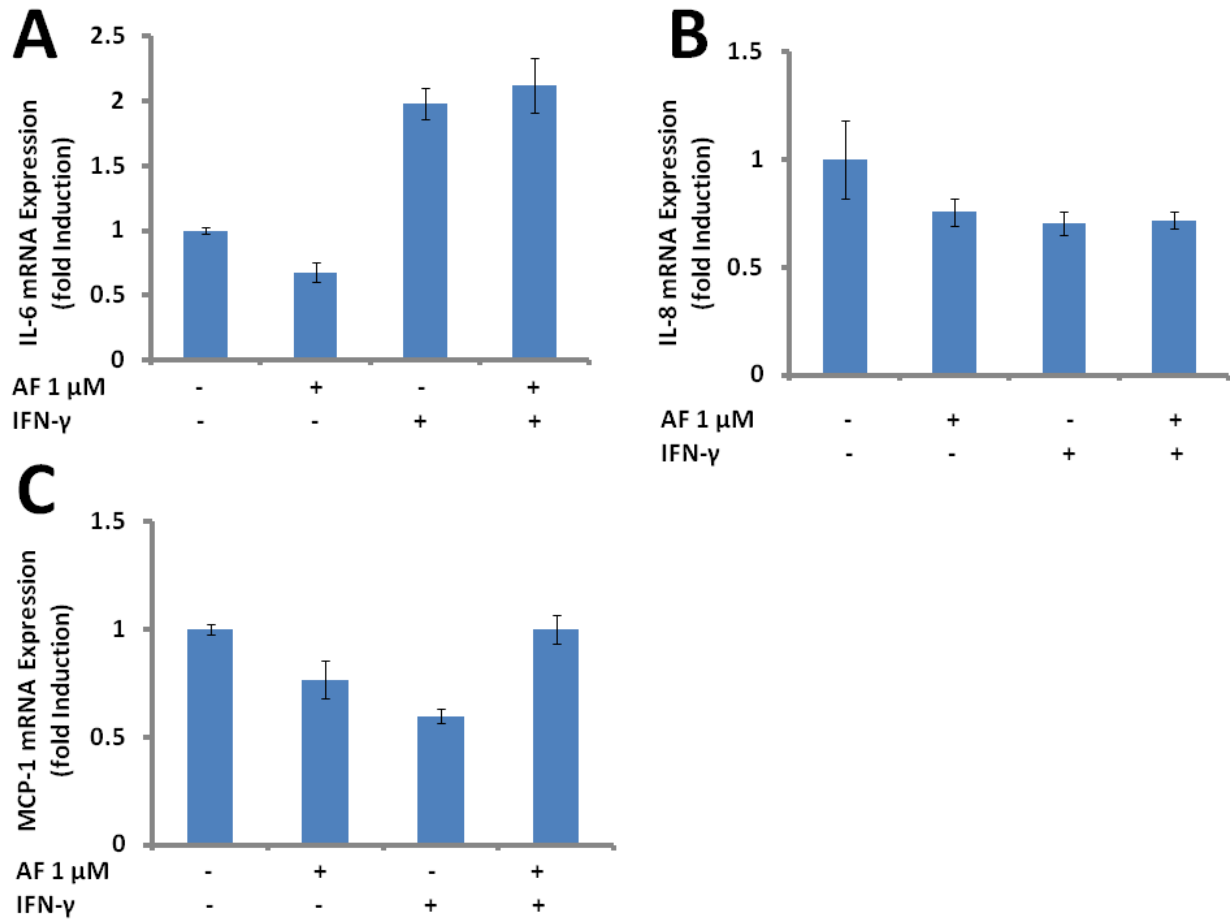


**Fig. 24:** AF does not change IL-6, IL-8 or MCP-1 expression in unstimulated or IFN- $\gamma$ -stimulated U-373 MG astrocytic cells. U-373 MG cells were treated with either 1  $\mu$ M AF or DMSO vehicle solutions and were either left unstimulated or were stimulated with IFN- $\gamma$  (150 U/ml). Total RNA was extracted 24 h later and IL-6 (**A**), IL-8 (**B**) and MCP-1 (**C**) mRNA expression was analyzed by using specific primers and RT-qPCR. Results were normalized to a reference gene  $\beta$ -actin and are presented as a fold increase compared to the HOX-1 mRNA level in control unstimulated cells not exposed to AF (expression level = 1). Data from 3 independent biological replicates are presented; the observed differences in expression levels were assessed by the randomized block design ANOVA, followed by Fishers LSD post-hoc test, no significance was found.

### 3.3.2.2. Effects of AF on the secretion of IL-6, IL-8, and MCP-1 by astrocytic cells

The effect of gold compounds on the secretion of IL-6, IL-8, and MCP-1 by stimulated U-373 MG and U-118 MG astrocytic cells was investigated using ELISA to measure the concentrations of cytokines in 24 h stimulated astrocytic cell supernatants. AF was tested at concentrations ranging from 0.1 – 5  $\mu$ M and results were compared to those obtained from samples treated with DMSO vehicle solution only. The baseline secretion of cytokines by unstimulated cells is indicated by dashed lines (Fig. 25 and 26). AF did not significantly change the secretion of IL-8 (Fig. 25A), IL-6 (Fig. 25B), or MCP-1 (Fig. 25C) by stimulated U-373 MG cells. Note that stimulation of U-373 MG cells by IFN- $\gamma$  did not upregulate secretion of the cytokines studied; therefore, experiments were repeated using U-118 MG cells. As shown in Fig. 26, stimulation of U-118 MG cells with a combination of IL-1 $\beta$  and IFN- $\gamma$  resulted in a significant increase in IL-6 (Fig. 26A) and IL-8 (Fig. 26B) secretion. However, AF did not affect the secretion of IL-6 (Fig. 26A) or IL-8 (Fig. 26B) by stimulated U-118 MG cells.

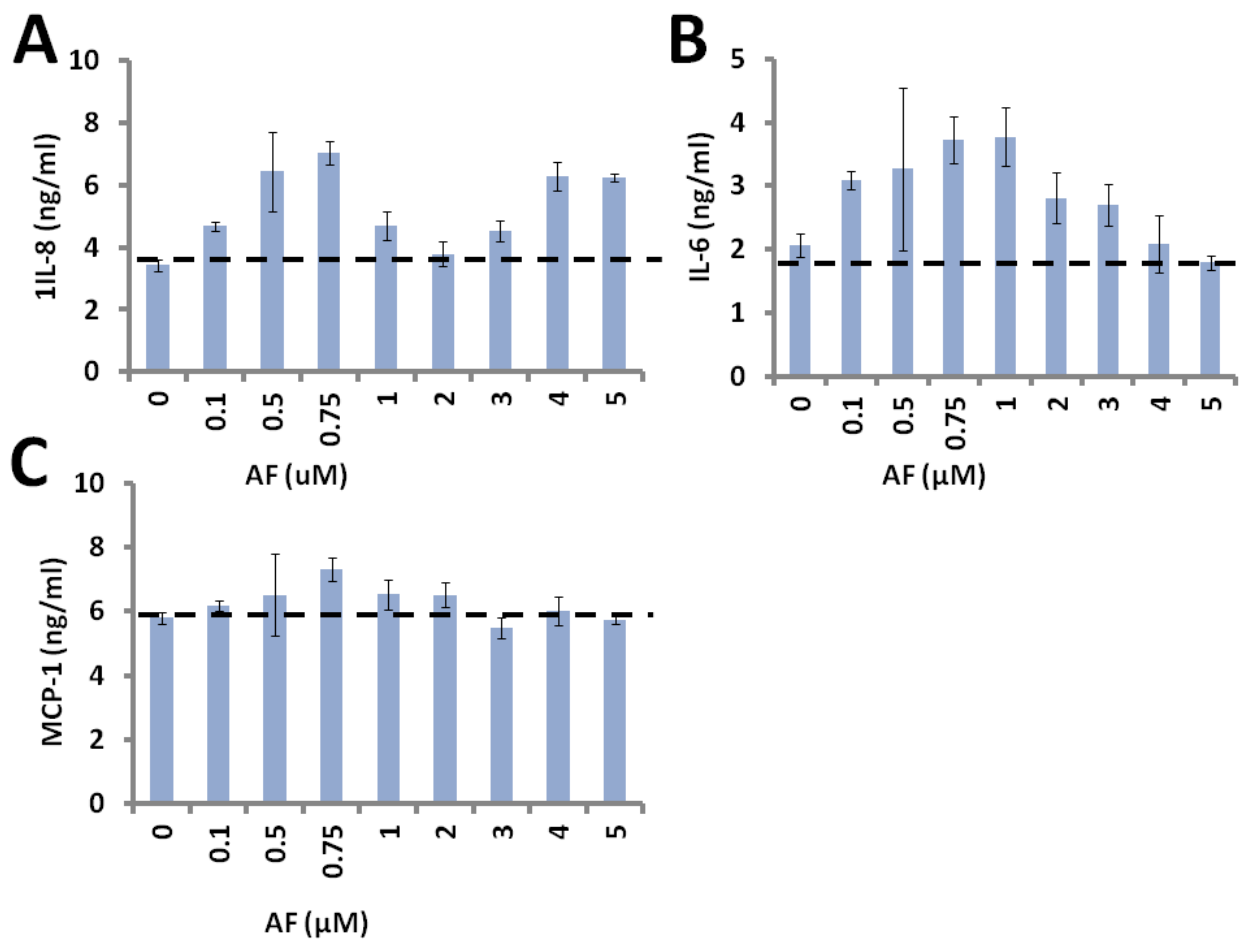


**Fig. 25:** AF has no significant effect on cytokine secretion by stimulated U-373 MG cells. U-373 MG cells were stimulated as described in the legend of Fig. 7. Following a 48 h incubation period, IL-8 (**A**), IL-6 (**B**) and MCP-1 (**C**) concentration in U-373 MG culture supernatants was measured by ELISA. Data from 3 independent experiments are presented. The horizontal dashed lines indicate cytokine concentrations in supernatants from unstimulated U-373 MG cells. The concentration-dependent effects of the compound were assessed by the randomized block design ANOVA, no significance was found.

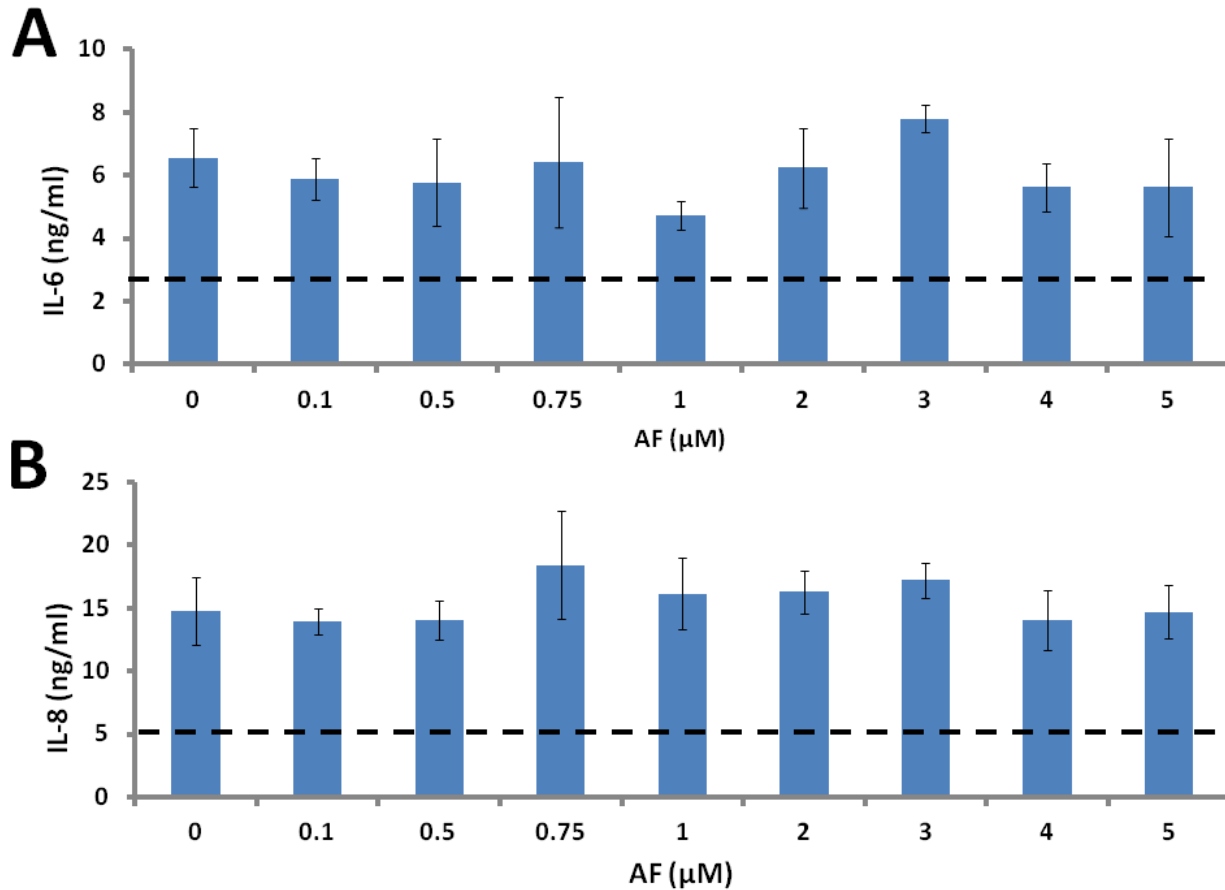


**Fig. 26:** AF has no significant effect on cytokine secretion by stimulated U-118 MG cells. U-118 MG cells were stimulated as described in the legend of Fig. 11. Following a 48 h incubation period, IL-6 (**A**) and IL-8 (**B**) concentration in U-118 MG culture supernatants was measured by ELISA. Data from 3 independent experiments are presented. The horizontal dashed lines indicate cytokine concentrations in supernatants from unstimulated U-373 MG cells. The concentration-dependent effects of the compound were assessed by the randomized block design ANOVA, no significance was found.

### 3.3.2.3. Effects of the calmodulin inhibitor TFP on the anti-neurotoxic activity of AF

The effect of inhibiting calmodulin signalling on the anti-neurotoxic activity of AF in astrocytic cells was investigated. U-118 MG cells were pre-treated for 15 min with 2  $\mu\text{M}$  TFP prior to treatment with 0.1 - 5  $\mu\text{M}$  AF and subsequent stimulation with the combination of IL-1 $\beta$

and IFN- $\gamma$ . 2  $\mu$ M TFP was used because at this concentration it was not toxic to U-118 MG cells and was within the IC<sub>50</sub> (1 - 10  $\mu$ M) values reported by Fisher Scientific. Following 48 h incubation, cell-free supernatants were transferred to SH-SY5Y neuronal cells. In agreement with previous results, treatment with AF decreased the toxicity of U-118 MG cells towards SH-SY5Y cells (Fig. 27A and 27B). Pre-treating the cells with TFP (indicated by white bars) did not abolish the anti-neurotoxic effects of AF.

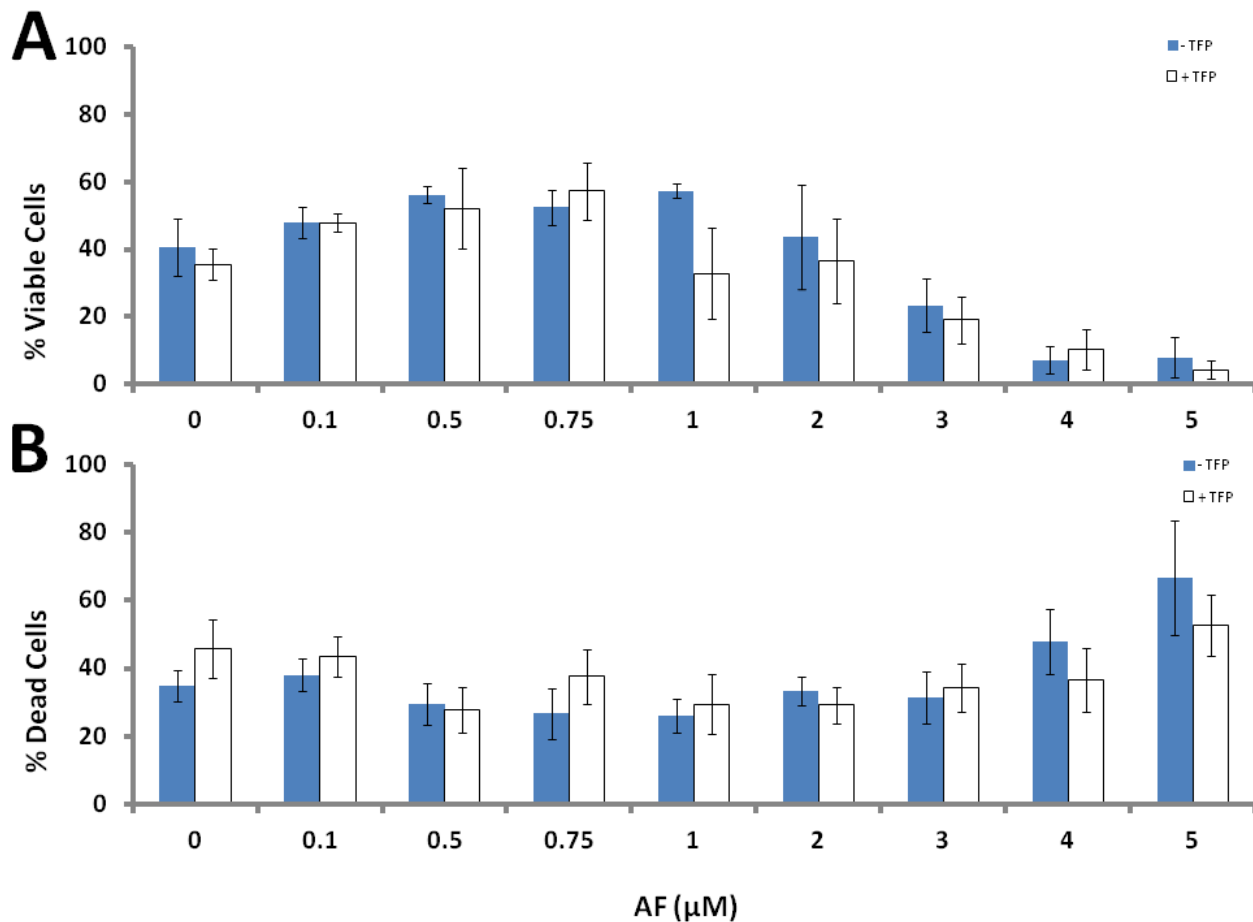


**Fig. 27:** Calmodulin inhibitor TFP does not affect the anti-neurotoxic activity of AF. U-118 MG cells were incubated with 2μM TFP and various concentrations of AF (white bars) or various concentrations of AF alone (grey bars). After 15 min incubation the U-118 MG cells were stimulated with a combination of IL-1β (100 U/ml) and IFN-γ (150 U/ml). Following 48 h incubation, 0.4 ml of supernatant was transferred onto SH-SY5Y cells. Following further 72 h incubation, SH-SY5Y viability was assessed by the MTT (**A**) and LDH (**B**) assays. Data from 4 independent experiments are presented. The effects of TFP were analyzed using two-way ANOVA, no significant difference between TFP treated and untreated cell viability was found.

#### 3.3.2.4. Effects of AF on the expression and secretion of IL-4 by human astrocytic cells

The effect of AF on the secretion and expression of IL-4 in U-373 MG cells and primary human astrocytes was investigated by RT-qPCR and ELISA. RT-qPCR was used to measure the

fold induction of IL-4 in stimulated and unstimulated U-373 MG cells treated with AF and ELISA was used to measure the concentration of IL-4 in stimulated human astrocyte supernatants. Fig. 28A shows that the detection limit of the assay was unable to determine if AF significantly affected the expression of IL-4 in either unstimulated or stimulated U-373 MG cells. The dashed line in Fig. 28B indicates the levels of IL-4 in F5 media. As the concentration of IL-4 in AF-treated, stimulated cells was below the detection limit of the assay which is the concentration in F5 media (see methods section 2.9 for procedures used to calculate the detection limit of ELISA used), no conclusions can be drawn from the data.

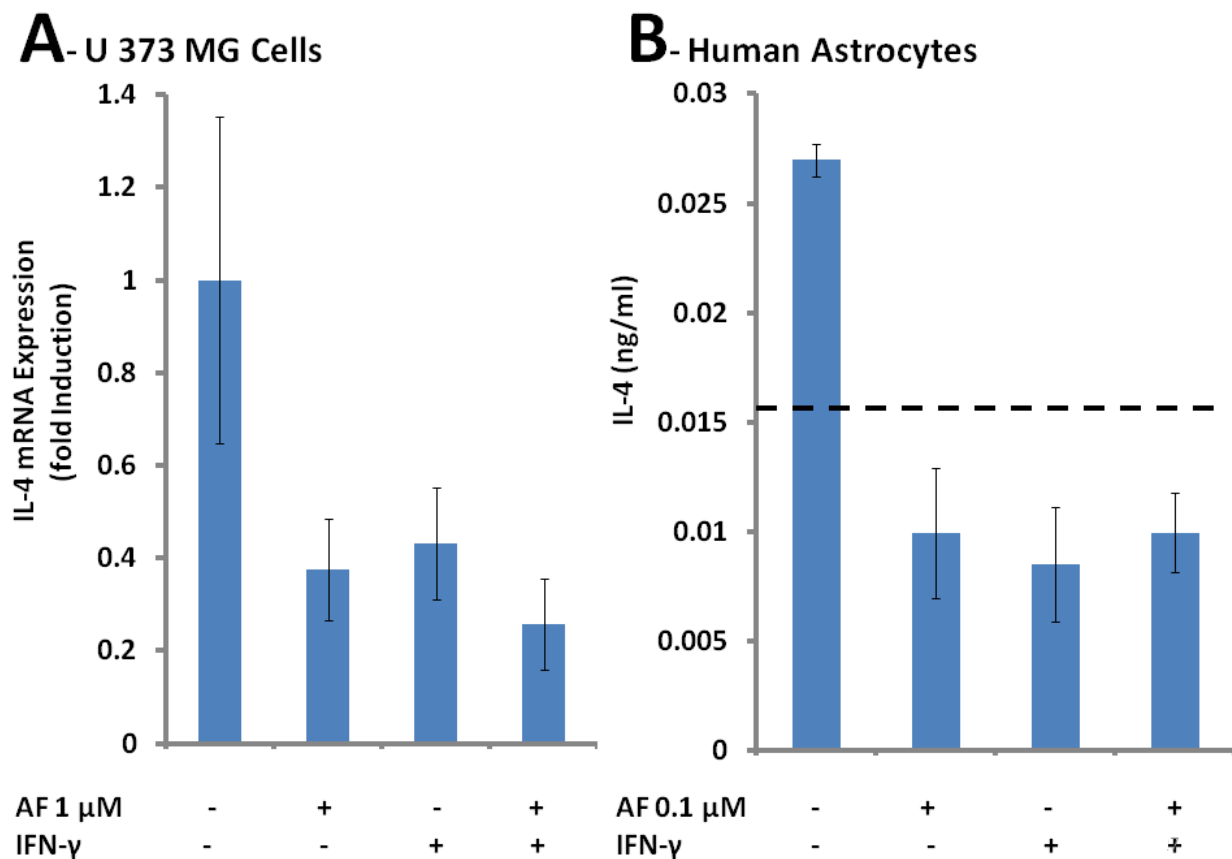


**Fig. 28:** AF has no effect on IL-4 expression in U-373 MG astrocytic cells; it also does not affect IL-4 secretion by primary human astrocytes. qPCR experiments were performed as described in Fig. 21. The relative expression of IL-4 in samples treated with AF was not significantly different from expression in cells treated with a vehicle control (DMSO) only (A). For IL-4 secretion experiments, human astrocytes were stimulated as described in the legend of Fig. 14. Following a 24 h incubation period, IL-4 concentration in human astrocyte culture supernatants was measured by ELISA (B). The horizontal dashed line indicates IL-4 concentration in F5 media. The effect of AF on IL-4 secretion was not assessed as concentrations of this cytokine in treated samples were below the detection limit of the assay (concentration in F5 media). Data from 3 independent experiments are presented.

### **3.3.3. Mechanisms of Action of AF in Neurons**

#### **3.3.3.1. Effect of AF on HOX-1 expression in neurons**

RT-qPCR was used to measure neuronal expression of the anti-inflammatory mediator HOX-1 in the presence or absence of AF. Figure 29 illustrates that exposing human neuronal SH-SY5Y cells to 0.5  $\mu$ M AF did not increase HOX-1 expression. However, when neuronal cells were exposed to 0.5  $\mu$ M AF in the presence of a partially cytotoxic (0.5 mM) concentration of H<sub>2</sub>O<sub>2</sub>, HOX-1 expression was increased 10 fold compared to H<sub>2</sub>O<sub>2</sub> stimulated cells treated with DMSO vehicle solution only (Fig. 29).

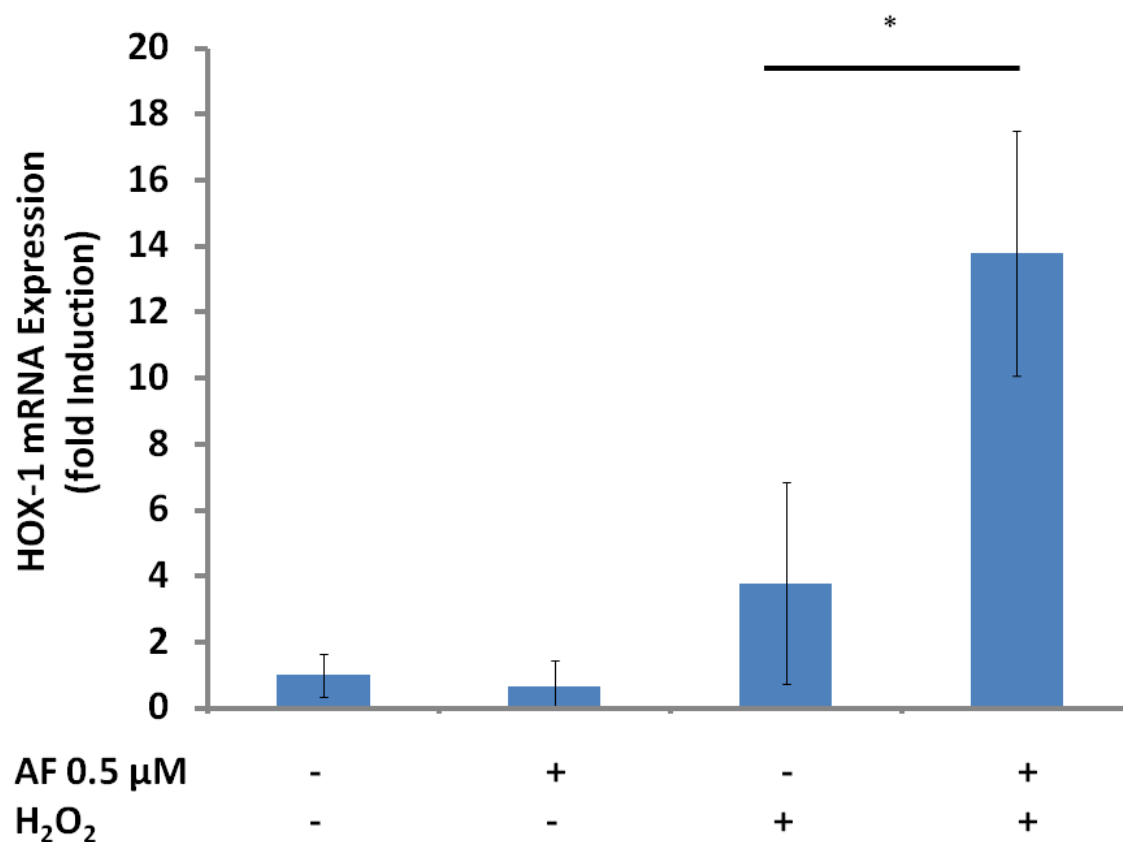


**Fig. 29:** AF upregulates heme oxygenase (HOX-1) mRNA expression in stimulated SH-SY5Y cells. Neuronal cells were treated with either AF or DMSO vehicle solutions. They were either left unstimulated or were treated with H<sub>2</sub>O<sub>2</sub> (0.5 mM). Total RNA was extracted 24 h later and the HOX-1 mRNA expression was analyzed by using specific primers and RT-qPCR. Data were normalized to a reference gene  $\beta$ -actin and are presented as a fold increase compared to the HOX-1 mRNA level in control unstimulated cells not exposed to AF (expression level = 1). Data from 3-4 independent experiments are presented; the observed differences in expression levels were assessed by two-way ANOVA, followed by Fishers LSD post-hoc test. \*  $p < 0.05$ , significantly different from samples treated with the vehicle solution only.

### 3.3.3.2. Effects of the calmodulin inhibitor TFP on the neuroprotective activity of AF

The effect of inhibiting calmodulin signalling on the direct neuroprotective activity of AF in neuronal cells was investigated. SH-SY5Y cells were pre-treated with 2  $\mu$ M TFP prior to treatment with 0.1 - 5  $\mu$ M AF and exposure to 0.5 mM H<sub>2</sub>O<sub>2</sub>. 2  $\mu$ M TFP was used as this concentration was non-toxic to neuronal cells and was within the IC<sub>50</sub> (1 - 10  $\mu$ M) values reported by Fisher Scientific. Following 24 h incubation, SH-SY5Y cell viability was assessed using MTT cell viability (Fig. 30A) and LDH cell death (Fig. 30B) assays. Similar to previous experiments, treatment with AF increased the viability of SH-SY5Y cells exposed to H<sub>2</sub>O<sub>2</sub> (Fig. 30A). Pre-treating the cells with TFP (indicated by white bars) did not abolish the neuroprotective effects of AF as shown in Fig. 30A and Fig. 30B.

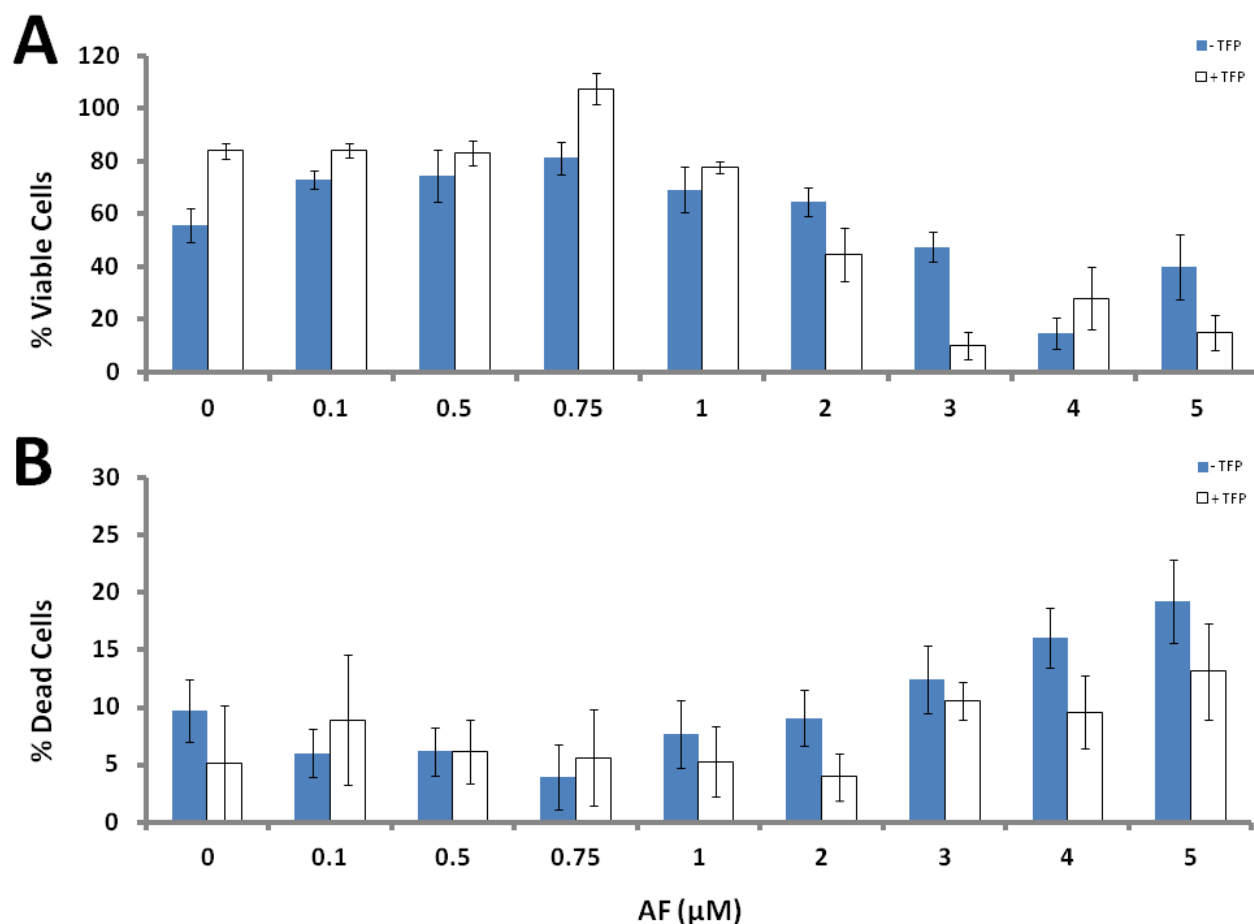


**Fig. 30:** Effects of calmodulin inhibitor, TFP, on the neuroprotective activity of AF. SH-SY5Y cells were incubated with 2μM TFP and various concentrations of AF (white bars) or various concentrations of AF alone (grey bars). After 15 min incubation, the SH-SY5Y cells were treated with 0.5 mM H<sub>2</sub>O<sub>2</sub>. Following additional 24 h incubation, SH-SY5Y viability was assessed by the MTT (A) and LDH (B) assays. Data from 4 independent experiments are presented. The effects of TFP were analyzed using two way ANOVA, no significant difference between viability of cells treated and not treated with TFP was found.

### 3.4. *In vivo* Distribution of AF after Oral Administration in Mice

The distribution of AF to the brain, liver, kidneys, lungs, gut, and spleen of mice that had been administered oral AF was quantified using LA-ICP-MS. Mice were monitored for morbidity throughout the 7 day AF treatment and none of the AF-treated mice showed any

symptoms different from control mice. Mice were weighed immediately prior to treatment each day throughout the 7 day treatment course and no differences in weight gain were observed in mice receiving the experimental treatment compared to control mice. Macroscopic examination of the gastrointestinal tract and liver post-treatment revealed no ulcers or any other visible pathology. Table 3 shows data obtained by LA-ICP-MS tissue analysis of tissues from three mice exposed to AF and three control mice, Table 3 compares gold concentrations measured using this technique in six different tissues with data obtained by Walz *et al.* (1983), who used radioactively labelled AF for studies with rats. The highest gold concentration was measured in kidneys (248  $\mu\text{M}$ ) while the lowest concentration was measured in the brain (4.8  $\mu\text{M}$ ).

**Table 3: Concentrations of gold in various organs of mice and rats after oral gavage of auranofin**

Tissue	LA-ICP-MS <sup>a</sup>	Radioactively Labelled <sup>195</sup> Au <sup>b</sup>
	( $\mu\text{M}$ , mean $\pm$ SD)	( $\mu\text{M}$ , mean $\pm$ SD)
Kidney	248.67 $\pm$ 58.02	104.81 $\pm$ 1.99
Liver	149.82 $\pm$ 39.34	2.82 $\pm$ 0.21
Lungs	83.81 $\pm$ 51.39	4.29 $\pm$ 1.11
Gut	7.12 $\pm$ 1.19	1.30 $\pm$ 0.10
Spleen	6.79 $\pm$ 3.58	5.33 $\pm$ 0.60
Brain	4.79 $\pm$ 1.07	0.16 $\pm$ 0.01

<sup>a</sup> Mice administered AF 2 mg kg<sup>-1</sup> per day for 7 days (n=3)

<sup>b</sup> Rats administered AF 1 mg kg<sup>-1</sup> per day for 5 days (n=9): data from Walz *et al.* (1983)

## **4.0. Discussion**

### **4.1. Anti-Neurotoxic Activity of Gold Compounds**

#### **4.1.1. Effect of Gold Compounds on Microglial Toxicity**

The gold compounds AF, ATM, ATG, and ATS were investigated for their potential to reduce neuroinflammation using an *in vitro* model relevant to the inflammatory processes that occur in degenerative conditions. I hypothesized that due to the potent anti-inflammatory activity of these compounds in the periphery, they could also be effective at inhibiting the inflammation in the CNS<sup>28,30,45</sup>. In answer to my first hypothesis, I found that at non-toxic, low micromolar concentrations (0.1 - 3  $\mu$ M) AF reduced the toxicity of both stimulated human THP-1 promonocytic cells and primary human microglia towards neurons, indicating a potential protective effect of AF. This effect was not observed with ATM, ATG or ATS.

The anti-neurotoxic effect of AF was observed at non-toxic concentrations: 0.1  $\mu$ M in primary human microglial cultures and between 0.5 - 3  $\mu$ M in human microglial-like THP-1 cell cultures. Previous research using a similar assay has shown that primary human cells could be more sensitive to anti-inflammatory drug treatment than cell lines, therefore the lower effective concentration in primary cells was not unexpected<sup>62,92</sup>. AF caused a significant decrease in THP-1 cell viability between 3 - 5  $\mu$ M, this is consistent with the previously reported anti-neoplastic activity of AF towards leukemia cell lines at 0.2 - 2  $\mu$ M concentrations<sup>58,72</sup>. Because of the toxicity of high concentration of AF towards glial cells used, only the non-toxic concentrations were considered to be anti-neurotoxic.

#### **4.1.2. Activity of Gold Compounds on Astrocyte Toxicity**

The gold compounds AF, ATM, ATG, and ATS were next investigated for their potential to reduce astrocyte-mediated toxicity towards SH-SY5Y neuroblastoma cells. In answer to my

first hypothesis, I found that at non-toxic, low micromolar concentrations AF reduced the toxicity of astrocytes towards neurons. The anti-neurotoxic effect of AF was observed at non-toxic concentrations: 0.1  $\mu\text{M}$  in primary human astrocyte cultures and between 1 - 3  $\mu\text{M}$  in human U-373 MG and U-118 astrocytoma cell cultures. This effect was not observed with ATM, ATG or ATS. Similar to THP-1 experiments, AF was significantly toxic towards U-118 MG cells at 3 - 5  $\mu\text{M}$ . This toxic activity was not seen towards the primary human cells and AF caused a significant increase in primary human astrocyte viability at 5  $\mu\text{M}$ . This is not surprising as AF has been taken by some human patients for years for RA and is considered by medical practitioners to have an acceptable safety profile in the management of some disease states <sup>93</sup>

The observation that AF, but not ATM, ATG nor ATS, inhibited toxic secretions by glial cells is similar to previous studies indicating AF has several biological activities distinct from the other gold compounds. Walz *et al.* (1983) demonstrated that AF and ATM, but not ATG, were able to reduce the secretion of lysosomal enzymes from polymorphonuclear cells. Furthermore, AF inhibited antibody-dependent cellular cytotoxicity of polymorphonuclear cells and release of reactive oxygen species from neutrophils, while ATM, ATG, and the ligands of auranofin showed no effect <sup>94</sup>. It has been previously demonstrated that AF has immunosuppressive activity, such as the ability to inhibit lymphoblastogenesis, an effect not observed with other gold compounds <sup>95</sup>.

Several anti-neurotoxic compounds affecting microglial toxicity have been identified over the past decade including: 9-methyl- $\beta$ -carboline, cannabinoid type 2 (CB2) receptor ligands, 5-LOX inhibitors and NSAIDs <sup>86,96-99</sup>. All of these anti-neurotoxic molecules inhibit inflammatory cascades through several different mechanisms. 9-methyl- $\beta$ -carboline is a monoamine oxidase inhibitor and has been shown to decrease the toxicity of  $\beta$ -carboline in PD

models by inhibiting the proliferation of microglia and decreasing microglial production of pro-inflammatory chemotactic cytokines<sup>97</sup>. The concentration of 9-methyl- $\beta$ -carboline required to induce protective effects (50 - 90  $\mu$ M), however, is much higher than pharmacologically relevant<sup>100</sup>. Endocannabinoids are known for their anti-inflammatory and hypothermic effects in the CNS<sup>86</sup>. CB2 receptor ligands have been shown to inhibit microglial toxicity towards neurons at concentrations between 5 – 10  $\mu$ M<sup>86</sup>. Other anti-neurotoxic molecules include 5-lipoxygenase (LOX) and COX inhibitors<sup>98</sup>. Leukotrienes are products of arachidonic acid metabolism; they are synthesized by LOX enzymes and contribute to inflammation, including the activation of microglia<sup>98</sup>. It has been shown previously that inhibition of 5-LOX activating protein (FLAP) reduces microglial toxicity towards neuronal cells at concentrations between 2 – 5  $\mu$ M; this range is similar to the effective concentrations of AF in our model<sup>98</sup>. In addition to 9-methyl- $\beta$ -carboline and FLAP inhibitor, NSAIDs have also shown anti-neurotoxic activity by inhibiting the pro-inflammatory COX enzymes<sup>96</sup>. The anti-neurotoxic activity of the NSAIDs is most likely mediated through inhibition of COX-1 as opposed to COX-2, as COX-1 is more predominant in the CNS and is the main isoform expressed by microglia<sup>101</sup>. Various COX inhibitors including indomethacin, aspirin and diclofenac have all been shown to have anti-neurotoxic activity, though at higher concentrations (10 – 100  $\mu$ M) than either FLAP inhibitor or AF<sup>96,98</sup>.

More recently the contribution of activated astrocytes to inflammation in the CNS has become recognized by researchers<sup>32</sup>. Because astrocytes comprise the most abundant glial cell type in the brain and are important in maintaining neuronal viability, compounds that inhibit astrocyte mediated neurotoxicity are now being investigated. Anti-neurotoxic compounds that target astrocytes include proton-pump inhibitors and STAT-3 inhibitors<sup>62,63</sup>. Investigations by

Hashioka *et al.* (2011) found that STAT-3 and JAK-1 inhibitors decrease the toxicity of IFN- $\gamma$  stimulated astrocytic cells towards neurons. It was later found that proton pump inhibitors attenuated astrocyte mediated neurotoxicity at concentrations between 1 – 10  $\mu$ M through the inhibition of the STAT-3 signalling pathway<sup>62</sup>. AF has been shown to decrease both JAK-1 and STAT-3 activation in macrophages by decreasing IL-6 production and expression<sup>47</sup>. Therefore, the anti-neurotoxic properties of AF in astrocytic cells could be due to inhibition of STAT-3 activity, but this hypothesis requires experimental confirmation. Due to the potent anti-neurotoxic activity of AF, subsequent experiments were performed to elucidate the mechanism of the protective activity of AF.

#### **4.2. Neuroprotective Activity of AF**

To determine whether the anti-neurotoxic effects observed were due to the activity of AF on glial cells directly, or whether the effects could be due to transfer of some of the compound with the supernatants and their direct action on neuronal cells, experiments were performed where AF was applied directly to neuronal cells, which were subsequently exposed to toxins. In answer to my second hypothesis, I found that only AF, and not the other three gold compounds tested, exhibited neuroprotective activity. Interestingly, treating SH-SY5Y neuronal cells with 0.5 - 1  $\mu$ M AF protected them from H<sub>2</sub>O<sub>2</sub>-induced toxicity as well as toxicity induced by supernatants from stimulated U-373 MG cells and toxicity induced by supernatants from stimulated THP-1 cells. A direct protective effect of AF on neurons or neuronal cells has not been reported previously and our observations may indicate that AF confers neuroprotection in addition to its better-known and accepted anti-inflammatory effects. The direct protective activity of AF could be partially responsible for its anti-neurotoxic effects on astrocytic cells when this drug is added before stimulation since some AF may be transferred onto neuronal cells

along with the supernatants. However, this was unlikely the sole reason for the anti-neurotoxic activity of AF since this drug effectively inhibited primary microglial and astrocyte toxicity at 0.1  $\mu\text{M}$ , a concentration that was ineffective at rescuing neuronal cells from the toxicity of microglial and astrocytic cell supernatants.

One of the proposed strategies for the treatment of neurodegenerative diseases is to modify neuronal viability, increasing tolerance of neurons to oxidative damage and inflammatory mediators released by activated glial cells. There are many endogenous neuroprotective molecules that are released by glial cells in the CNS, including insulin and pro-insulin, and these have received attention as potential therapeutic agents for preventing the neuronal death in AD and PD<sup>4,102</sup>. In addition to endogenous molecules, several drugs have been developed in an attempt to increase neuronal viability. Flavonoids such as quercetin have been recognized as neuroprotective molecules; Dajas *et al.* (2003) found that 25  $\mu\text{M}$  quercetin protected neuronal cells against hydrogen peroxide toxicity. This protective effect was thought to be due to the anti-oxidant activity of the flavonoids<sup>103</sup>. Alternatively, caffeoylquinic acid derivatives (10 – 50  $\mu\text{M}$ ), have been shown to protect neurons against damage from both hydrogen peroxide and A $\beta$  toxicity<sup>104,105</sup>. A potential mechanism of action of these compounds is the suppression of caspase-3 activation and maintaining high intracellular concentration of the anti-oxidant glutathione molecule<sup>105</sup>. AF has been shown to activate caspase-3 and disrupt redox balance within cells, so the protective mechanisms of the flavonoids and caffeoylquinic acid derivatives are likely different from those of AF<sup>47,58,103,105,106</sup>. Novel mechanisms responsible for the neuroprotective activity of AF were investigated.

### 4.3. Mechanisms of AF action

#### 4.3.1. Mechanisms of Action of AF on Microglia

Due to the protective and anti-neuroinflammatory activity of AF, several potential mechanisms of action of this drug were investigated in microglia-like THP-1 cells including effects on MCP-1 secretion. MCP-1 is a chemotactic agent and indicator of inflammation<sup>107</sup>, therefore the secretion of MCP-1 by THP-1 cells treated with AF was investigated, and no effect was found. Production of ROS was also investigated using the promyelocytic HL-60 cell line. HL-60 cells were used as a model possessing enzymatically active NADPH oxidase complexes to measure the effects of the gold compounds on the respiratory burst. The effect of treating HL-60 cells with the gold compounds for 30 minutes was investigated. Previous studies have shown that AF inhibits the neutrophil respiratory burst directly and does not scavenge free radicals<sup>108</sup>. In our experiments, 5  $\mu$ M AF inhibited production of ROS; however, this concentration was significantly toxic towards HL-60 cells, therefore the inhibitory effect at this concentration was most likely due to direct toxicity. It could be that previous reports of AF inhibiting the respiratory burst have just been measuring the toxicity of AF. These studies performed the LDH assay as a measure of cell viability, which in our studies was ineffective in measuring AF-induced toxicity<sup>45,94</sup>.

Inhibition of NADPH-oxidase priming is a good target for pharmacological intervention because it would interfere with a pathological increase in ROS production while maintaining the normal physiological NADPH-oxidase immune response<sup>37</sup>. HL-60 cells were primed with LPS, a known priming agent, or Tfam, a mitochondrial DAMP, and were either treated with AF at time of priming or acutely for 30 minutes prior to stimulation with fMLP. 24 h treatment with AF inhibited LPS and Tfam priming of the respiratory burst at the non-toxic 0.1 - 0.5  $\mu$ M range.

Treating HL-60 cells with AF for 30 min did not inhibit the increase in ROS production resulting from priming the cells with either LPS or Tfm. The long incubation time needed for the inhibitory effect of AF suggests that AF is regulating gene expression or slow acting cellular pathways as opposed to regulating the NADPH-oxidase enzyme directly. Previous research indicates that the majority of AF is taken up by cells within 20 min; therefore a 30 min treatment would give enough time for AF to enter cells and interact with NADPH-oxidase subunits if this was the mechanism of action <sup>109</sup>. Agents that inhibit the priming of NADPH-oxidase, but not the functioning of this enzymatic complex, are not common. IL-4 and lipid A analogues have both been shown to inhibit the priming response of neutrophils <sup>110,111</sup>. IL-4 inhibits NADPH-oxidase assembly by decreasing the expression of the gp91-*phox* subunit of NADPH-oxidase, effectively reducing the number of active enzyme complexes <sup>110,112</sup>. Lipid A analogues are structurally similar to LPS and it is thought that they inhibit NADPH-oxidase priming by antagonizing the LPS-binding regions on cell surfaces <sup>111</sup>. It is possible that AF inhibits priming of the respiratory burst through either of these mechanisms. Future investigations into the exact mechanism by which AF inhibits priming in response to LPS and Tfm should focus on expression of NADPH-oxidase subunits and potential antagonism of priming receptors.

#### **4.3.2. Mechanisms of Action of AF on Astrocytes**

Previous research has highlighted several molecular mechanisms potentially responsible for the protective effects of AF, including protecting against cocaine-induced hepatic injury both in mice and in cultured hepatocytes by up-regulating the protective enzyme HOX-1 <sup>78</sup>. HOX-1 induction was investigated as a potential mechanism for the protective activity of AF observed in our experiments. As stimulated astrocytes undergo oxidative stress, up-regulation of HOX-1 would protect them against associated damage. Additionally, HOX-1 has been reported to have

anti-inflammatory effects which could also contribute to the decreased toxicity of astrocytes towards neurons<sup>42,78,113</sup>. Our study demonstrated that AF, but not ATG, induced HOX-1 expression in both stimulated and unstimulated primary human astrocytes and U-373 MG cells. Therefore, up-regulation of HOX-1 could be at least partially responsible for the biological activity of AF observed in our study.

Several other potential anti-inflammatory mechanisms of action have been reported for AF, including modulation of the expression and release of pro-inflammatory cytokines such as IL-6 and IL-8 by human THP-1 monocytic cells and murine RAW 264.5 macrophages<sup>47,50,78</sup>. Inhibiting excessive IL-6, IL-8 and MCP-1 secretion could be beneficial in neuroinflammation as these cytokines perpetuate the chronic inflammatory state. However, treatment of U-373 MG and U-118 MG astrocytic cells with AF did not affect the expression or secretion of IL-6, IL-8 or MCP-1 as measured by qPCR and ELISA respectively. These observations indicate that the effects of AF on glial cell-mediated neuroinflammation are different from its effects on peripheral immune cells.

Two novel hypotheses on the mechanism of action of AF were also investigated. Previous studies have shown that AF has several  $\text{Ca}^{2+}$  dependent activities including induction of the release of  $\text{Ca}^{2+}$  from the intracellular stores while decreasing the influx of extracellular  $\text{Ca}^{2+}$  which leads to modified  $\text{Ca}^{2+}$  dependent activity such as neutrophil chemotaxis<sup>56,114</sup>. Calmodulin is a  $\text{Ca}^{2+}$  binding protein that regulates numerous intracellular processes including the release of  $\text{Ca}^{2+}$  from intracellular stores and also the microtubule assembly necessary for cell motility<sup>115</sup>. Because previous studies have shown that many of the effects of AF in neutrophils are  $\text{Ca}^{2+}$  dependent, it was hypothesized that activity of AF observed in our experiments could be mediated through calmodulin<sup>56,114</sup>. To test this hypothesis a calmodulin inhibitor, TFP, was

added to astrocytic cells to determine whether it would abolish the anti-neuroinflammatory activity of AF. It was found that inhibiting the activity of calmodulin in U-118 MG astrocytic cells by using TFP did not abolish the anti-neurotoxic activity of AF. Next it was hypothesized that the anti-neurotoxic activity of AF could be due to increased IL-4 stability. Curbo *et al.* (2009) found that AF was able to decrease the reduction of the disulphide bonds of IL-4 which increased its ability to bind to the IL-4R $\alpha$  receptor. IL-4 is recognized in the periphery for its ability to promote class switching of macrophages into a more anti-inflammatory M2 phenotype, and previous studies have shown that it reduces microglial and astrocyte activation<sup>43,116,117</sup>. It is unlikely that AF would affect the expression of IL-4 mRNA as AF has only been reported to stabilize the disulphide bonds within IL-4 molecules, thus stabilizing this cytokine and decreasing IL-4 degradation by cells<sup>118</sup>. AF may decrease the levels of IL-4 in cell culture supernatants as only intact IL-4 is taken up by cells when it interacts with the IL-4R $\alpha$  receptor<sup>118</sup>. Astrocytic IL-4 expression and secretion in response to treatment with AF were investigated. The expression of IL-4 was unchanged in AF-treated U-373 MG cells and the secretion of IL-4 by primary human astrocytes was below the detection limit of the assay. Therefore further studies will be needed to determine whether the anti-neurotoxic activity of AF is partially due to stabilization of IL-4.

#### **4.3.3. Mechanisms of Action of AF on Neurons**

The direct neuroprotective activity of AF has not been previously reported therefore, further experiments were performed to elucidate the mechanisms of this activity. Up-regulation of HOX-1 could be protective in neurons. Yamamoto *et al.* (2010) demonstrated that HOX-1 induction protected dopaminergic neurons in an *in vitro* model of Parkinson's disease<sup>33</sup>. We showed that AF was able to induce HOX-1 expression in SH-SY5Y neuronal cells exposed to a

toxic concentration of hydrogen peroxide. By up-regulating protective enzymes like HOX-1 AF could directly increase the ability of neurons to withstand toxic insults. As mentioned previously, some of the effects of AF are dependent on  $\text{Ca}^{2+}$  signalling. AF could affect glia, neurons, or both in a  $\text{Ca}^{2+}$  dependent manner, therefore the effect of the calmodulin inhibitor TFP was also investigated in experiments where neuronal cells were treated with TFP along with the gold compounds directly and then exposed to toxic mediators. Similar to results with astrocytic cells, inhibiting calmodulin signalling did not abolish the protective effects of AF in neurons exposed to hydrogen peroxide.

In answer to my third hypothesis I found that the anti-neurotoxic activity of AF was most likely mediated through inhibition of the priming response of the respiratory burst in microglia-like cells and through induction of the protective enzyme HOX-1 in astrocytes. Additionally, the neuroprotective activity of AF was most likely mediated through the induction of HOX-1 in neuronal cells.

#### **4.4. *In vivo* Distribution of AF after Oral Administration in Mice**

Lastly, the distribution of gold atoms (Au) in mice treated with AF was investigated to determine whether AF was able to penetrate the BBB. In answer to my fourth hypothesis, Au molecules from AF were detectable by LA-ICP-MS in the CNS of mice after oral administration of this gold compound for seven days. A study by Walz *et al.* (1983) demonstrated that in rats administered 1 mg/kg AF for 5 days, the level of Au was highest in the kidneys (104.81  $\mu\text{M}$ , see Table 3) while only a very small amount of Au entered the brain, reaching a concentration of 0.16  $\mu\text{M}$ <sup>45</sup>. These values were calculated from the  $\mu\text{g Au/g}$  of tissue values reported by Walz *et al.* (1983) using the assumption that 1 g of tissue was equivalent to 1 ml of solution and then

using the molecular weight of Au to calculate the molar concentration of gold in each sample. We performed experiments similar to those described by Walz *et al.* (1983) using mice instead of rats. AF was administered at 2 mg/kg to mice for 7 days. We were able to detect Au in all tissues studied (see Table 3) using LA-ICP-MS-based measurements which are similar to the previously described methods used by Zoriy *et al.* (2007) to measure cisplatin in mice. Similar to Walz *et al.* (1983), we found Au to be most concentrated in the kidneys, but our measurements indicated almost 1.5 times greater concentration (249 vs. 104  $\mu\text{M}$ ). Compared to the values reported by Walz *et al.* (1983), who used the radioactively labelled Au method, the concentrations of Au detected by LA-ICP-MS in our studies were greater for all tissues studied. This difference was especially pronounced in the brain, with our measurements indicating 5  $\mu\text{M}$  Au concentration while only 0.16  $\mu\text{M}$  Au was detected by Walz *et al.* (1983). In addition to concentration differences, the relative order of distribution of Au according to its concentration in the liver, lungs, gut, and spleen did not match that reported by Walz *et al.* (1983). These discrepancies could be due to the use of different animal species (rats vs. mice) and/or differences in the duration and the dose of AF treatment. AF has been reported to have a long half-life of approximately 17 days in humans<sup>119</sup>; therefore, there could be significant differences in tissue accumulation of AF between 5 and 7 day treatment regimens<sup>44,119</sup>.

Differences in the techniques used to detect Au could also have contributed to the discrepancies. LA-ICP-MS directly measures the total number of unlabeled Au atoms in a tissue sample by comparing the signals obtained from the experimental samples with those obtained from samples with known Au concentrations. On the other hand, the radioactively-labelled Au technique used by Walz *et al.* (1983) involves administration of a mixture of labelled and unlabeled AF and several steps of sample preparation before measurements can be performed;

thus, it is a less direct measurement of Au atoms compared to LA-ICP-MS. Both these techniques measure Au concentration as opposed to the concentration of intact AF molecules as neither of the techniques is able to distinguish between AF and its metabolites, including Au as a breakdown product of AF<sup>29,45</sup>. Therefore, further studies are required to establish whether intact AF crosses the BBB and enters brain tissue. Similar radioactively labelled atom techniques have been used to establish that the available circulating levels of Au in patients being treated with AF can reach approximately 0.4  $\mu\text{M}$ <sup>44</sup>, which exceeds the 0.1  $\mu\text{M}$  AF concentration required to reduce microglial and astrocyte toxicity in our model.

Since AF is known to accumulate in tissue over time and our study indicates that Au passes through the BBB, it is feasible that levels of AF in the brain could reach concentrations effective at reducing glial-mediated neurotoxicity. The relatively low  $\text{IC}_{50}$  of AF as well as the possibility that it is able to cross the BBB makes it a new candidate for treating inflammation in the CNS.

## 5.0. Conclusions and Future Work

### 5.1. Limitations of Research

There are several limitations of this thesis research including the use of cell lines, which are actually tumor cells derived from different cell types (e.g., astrocytoma U-373 MG cells in lieu of astrocytes). It is possible that these cell lines behave differently than their primary cell counterparts. To overcome this limitation all major experiments were repeated by using primary human microglia and astrocytes to confirm the obtained results.

Another potential limitation to this research is the cytotoxic properties of AF. At concentrations above 4  $\mu\text{M}$  AF is significantly toxic to THP-1 and HL-60 cells. At  $> 5 \mu\text{M}$  it is toxic to SH-SY5Y and U-118 astrocytoma cells. The death of the glial cells could confound the results obtained by measuring neuronal viability; instead of inhibiting secretion of toxins by glial cells, AF could be killing these cells thus reducing the number of cells producing toxic secretions. To overcome this limitation I only considered to be positive those data that showed decreases in neurotoxicity at concentrations of AF that did not affect glial viability. In addition, I used primary human glial cells which were less susceptible to the cytotoxic action of AF.

Lastly, measuring the concentration of Au atoms instead of intact AF molecules in the AF *in vivo* distribution studies does not provide information on whether the active moiety of AF is entering the CNS. The gold-triethylphosphine ligand of AF is responsible for its activity against thiol redox enzymes and would be a good target to assess for its CNS penetration, but our technique was not able to differentiate AF from its other potential metabolites<sup>120</sup>. However, we can conclude that Au from AF accumulates in tissues over time. Furthermore, because we measured a relatively high (5  $\mu\text{M}$ ) concentration of Au in the brain, it is likely that the active AF moiety is also accumulating in the CNS.

## 5.2. Future Work

This thesis work provides substantial evidence that AF could be beneficial as an inhibitor of neuroinflammation. Specifically, because of its dual anti-neurotoxic and neuroprotective properties, AF could be more effective than previous anti-inflammatory interventions that have been investigated for neuroinflammatory diseases<sup>21</sup>. Future research looking at the effects of AF in disease-specific animal models of multiple sclerosis, PD, and AD would be a natural extension of this study. Research into the outcomes of patients with RA who are taking AF with regard to the risk of developing different neurodegenerative diseases would be interesting additional studies. My literature searches failed to identify any epidemiological studies that investigated AF and neurodegenerative disorders.

Following up on the *in vivo* distribution studies with more specialized spectroscopy techniques to determine the exact molecules entering the CNS would also enhance my data. Determining the nature of AF metabolites entering the CNS, and then testing them in our assays would add robustness to our suggestion that active AF, or its bioactive metabolites, is entering the brain. Even though previous studies suggest that the gold containing ligand is important for the biological activity of AF, we cannot rule out the possibility that other metabolites are active in our model.

## 5.3. Significance of Findings

This thesis demonstrates that the gold compound AF is able to reduce human gliamediated toxicity and that it has neuroprotective properties. These novel *in vitro* properties of AF, as well as the *in vivo* data confirming earlier studies suggesting that AF is able to cross the BBB, warrant further testing of AF in animal models of neuroinflammation. Low micromolar concentrations of AF were effective at inhibiting both astrocyte and microglia mediated

neurotoxicity. In addition, AF was able to protect neurons against toxicity caused by hydrogen peroxide and toxic supernatants from stimulated glial cells. My data indicate that one of the potential mechanisms for this AF activity could be upregulation of the anti-inflammatory and protective enzyme HOX-1.

Anti-inflammatory intervention has the potential to slow neuronal loss in disorders such as PD and AD where neuroinflammation contributes to pathogenesis<sup>85,121</sup>. As AF has already been approved for use in humans in several countries and is considered by medical practitioners to have an acceptable safety profile in the management of some disease states<sup>93</sup>, it would be an excellent compound to investigate for the treatment of neuroinflammatory conditions as an alternative to steroidal and non-steroidal anti-inflammatory drugs which have been declared to be ineffective for treatment of AD<sup>23,101</sup>.

## References

1. Giasson BI, Ischiropoulos H, Lee VM, Trojanowski JQ. The relationship between oxidative/nitrative stress and pathological inclusions in Alzheimer's and Parkinson's diseases. *Free Rad Biol Med* 2002;32(12):1264-75.
2. Cummings JL, Cole G. Alzheimer disease. *JAMA* 2002;287(18):2335-8.
3. Heneka MT, O'Banion MK, Terwel D, Kummer MP. Neuroinflammatory processes in Alzheimer's disease. *J Neural Transm* 2010;117(8):919-47.
4. Block ML, Zecca L, Hong JS. Microglia-mediated neurotoxicity: uncovering the molecular mechanisms. *Nat Rev Immunol* 2007;8(1):57-69.
5. Rogers J, Strohmeyer R, Kovelowski CJ, Li R. Microglia and inflammatory mechanisms in the clearance of amyloid beta peptide. *Glia* 2002;40(2):260-9.
6. Hu J, Akama KT, Krafft GA, Chromy BA, Van Eldik LJ. Amyloid-beta peptide activates cultured astrocytes: morphological alterations, cytokine induction and nitric oxide release. *Brain Res* 1998;785(2):195-206.
7. Block ML, Zecca L, Hong JS. Microglia-mediated neurotoxicity: uncovering the molecular mechanisms. *Nat Rev Neurosci* 2007;8(1):57-69.
8. Jenner P. Oxidative stress in Parkinson's disease. *Ann Neurol* 2003;53 Suppl 3:S26-36; discussion S36-8.
9. Nguyen MD, Julien JP, Rivest S. Innate immunity: the missing link in neuroprotection and neurodegeneration? *Nat Rev Neurosci* 2002;3(3):216-27.
10. Boyadjieva NI, Sarkar DK. Role of microglia in ethanol's apoptotic action on hypothalamic neuronal cells in primary cultures. *Alcohol Clin Exp Res* 2011;34(11):1835-42.

11. McGeer PL, McGeer EG. Inflammation and neurodegeneration in Parkinson's disease. *Parkinsonism Relat Disord* 2004;10 Suppl 1:S3-7.
12. Marieb EN, editor. *Human Anatomy and Physiology*. 6 ed. San Francisco Pearson Cummings; 2003. 1242 p.
13. Hashioka S, Klegeris A, Schwab C, McGeer PL. Interferon-gamma-dependent cytotoxic activation of human astrocytes and astrocytoma cells. *Neurobiol Aging* 2009;30(12):1924-35.
14. Cameron B, Landreth GE. Inflammation, microglia, and Alzheimer's disease. *Neurobiol Dis* 2010;37(3):503-9.
15. Zhang W, Wang T, Pei Z, Miller DS, Wu X, Block ML, Wilson B, Zhou Y, Hong JS, Zhang J. Aggregated alpha-synuclein activates microglia: a process leading to disease progression in Parkinson's disease. *FASEB Journal* 2005;19(6):533-42.
16. Li C, Zhao R, Gao K, Wei Z, Yin MY, Lau LT, Chui D, Hoi Yu AC. Astrocytes: implications for neuroinflammatory pathogenesis of Alzheimer's disease. *Curr Alzheimer Res* 2011;8(1):67-80.
17. Gao HM, Zhou H, Zhang F, Wilson BC, Kam W, Hong JS. HMGB1 acts on microglia Mac1 to mediate chronic neuroinflammation that drives progressive neurodegeneration. *J Neurosci* 2011;31(3):1081-92.
18. Klegeris A, McGeer EG, McGeer PL. Therapeutic approaches to inflammation in neurodegenerative disease. *Curr Opin Neurol* 2007;20(3):351-7.
19. Lee M, Suk K, Kang Y, McGeer E, McGeer PL. Neurotoxic factors released by stimulated human monocytes and THP-1 cells. *Brain Res* 2011;1400:99-111.

20. Akiyama H, Barger S, Barnum S, Bradt B, Bauer J, Cole GM, Cooper NR, Eikelenboom P, Emmerling M, Fiebich BL and others. Inflammation and Alzheimer's disease. *Neurobiol Aging* 2000;21(3):383-421.
21. McGeer PL, McGeer EG. NSAIDs and Alzheimer disease: epidemiological, animal model and clinical studies. *Neurobiol Aging* 2007;28(5):639-47.
22. Leoutsakos JM, Muthen BO, Breitner JC, Lyketsos CG. Effects of non-steroidal anti-inflammatory drug treatments on cognitive decline vary by phase of pre-clinical Alzheimer disease: findings from the randomized controlled Alzheimer's Disease Anti-inflammatory Prevention Trial. *Int J Geriatr Psychiatry* 2011;27(4):364-74.
23. Aisen PS. Evaluation of selective COX-2 inhibitors for the treatment of Alzheimer's disease. *J Pain Symptom Manage* 2002;23(4 Suppl):S35-40.
24. de Jong D, Jansen R, Hoefnagels W, Jellesma-Eggenkamp M, Verbeek M, Borm G, Kremer B. No effect of one-year treatment with indomethacin on Alzheimer's disease progression: a randomized controlled trial. *PLoS One* 2008;3(1):e1475.
25. Scharf S, Mander A, Ugoni A, Vajda F, Christophidis N. A double-blind, placebo-controlled trial of diclofenac/misoprostol in Alzheimer's disease. *Neurology* 1999;53(1):197-201.
26. Fricker SP. Medicinal chemistry and pharmacology of gold compounds. *Transition Met Chem* 1996;21:377-383.
27. Kim KH, Kim DS. Juvenile idiopathic arthritis: Diagnosis and differential diagnosis. *Korean J Pediatr* 2010;53(11):931-5.
28. Kean WF, Kean IR. Clinical pharmacology of gold. *Inflammopharmacology* 2008;16(3):112-25.

29. Kean WF, Hart L, Buchanan WW. Auranofin. *Br J Rheumatol* 1997;36(5):560-72.
30. Papp KA, Shear NH. Systemic gold therapy. *Clin Dermatol* 1991;9(4):535-51.
31. Kean WF. Intramuscular versus oral gold therapy. *Baillieres Clin Rheumatol* 1990;4(2):219-46.
32. Ammon HV, Fowle SA, Cunningham JA, Komorowski RA, Loeffler RF. Effects of auranofin and myochrysin on intestinal transport and morphology in the rat. *Gut* 1987;28(7):829-34.
33. Hashioka S, Klegeris A, Schwab C, McGeer PL. Interferon-gamma-dependent cytotoxic activation of human astrocytes and astrocytoma cells. *Neurobiol Aging* 2009;30(12):1924-35.
34. Yamamoto N, Izumi Y, Matsuo T, Wakita S, Kume T, Takada-Takatori Y, Sawada H, Akaike A. Elevation of heme oxygenase-1 by proteasome inhibition affords dopaminergic neuroprotection. *J Neurosci Res* 2010;88(9):1934-42.
35. Szczepanik AM, Funes S, Petko W, Ringheim GE. IL-4, IL-10 and IL-13 modulate A beta(1--42)-induced cytokine and chemokine production in primary murine microglia and a human monocyte cell line. *J Neuroimmunol* 2001;113(1):49-62.
36. Klegeris A, McGeer PL. Interaction of various intracellular signaling mechanisms involved in mononuclear phagocyte toxicity toward neuronal cells. *J Leukoc Biol* 2000;67(1):127-33.
37. Muranaka S, Fujita H, Fujiwara T, Ogino T, Sato EF, Akiyama J, Imada I, Inoue M, Utsumi K. Mechanism and characteristics of stimuli-dependent ROS generation in undifferentiated HL-60 cells. *Antioxid Redox Signal* 2005;7(9-10):1367-76.

38. Forehand JR, Pabst MJ, Phillips WA, Johnston RB, Jr. Lipopolysaccharide priming of human neutrophils for an enhanced respiratory burst. Role of intracellular free calcium. *J Clin Invest* 1989;83(1):74-83.
39. Arnason BG. Immunologic therapy of multiple sclerosis. *Annu Rev Med* 1999;50:291-302.
40. Serhan CN, Drazen JM. Antiinflammatory potential of lipoxygenase-derived eicosanoids: a molecular switch at 5 and 15 positions? *J Clin Invest* 1997;99(6):1147-8.
41. Drummond GR, Selemidis S, Griendling KK, Sobey CG. Combating oxidative stress in vascular disease: NADPH oxidases as therapeutic targets. *Nat Rev Drug Discov* 2011;10(6):453-71.
42. Frohman EM, Racke MK, Raine CS. Multiple sclerosis--the plaque and its pathogenesis. *N Engl J Med* 2006;354(9):942-55.
43. Cuadrado A, Rojo AI. Heme oxygenase-1 as a therapeutic target in neurodegenerative diseases and brain infections. *Curr Pharm Des* 2008;14(5):429-42.
44. Chao CC, Molitor TW, Hu S. Neuroprotective role of IL-4 against activated microglia. *J Immunol* 1993;151(3):1473-81.
45. Finkelstein AE, Roisman FR, Batista V, de Nudelman FG, de Titto EH, Mizraji M, Walz DT. Oral chrysotherapy in rheumatoid arthritis: minimum effective dose. *J Rheumatol* 1980;7(2):160-8.
46. Walz DT, Dimartino MJ, Griswold DE, Intoccia AP, Flanagan TL. Biologic actions and pharmacokinetic studies of auranofin. *Am J Med* 1983;75(6A):90-108.
47. Zoriy M, Matuschb, A., Sprussc, T., Becker, J. S. Laser ablation inductively coupled plasma mass spectrometry for imaging of copper, zinc, and platinum in thin sections of a

- kidney from a mouse treated with cis-platin. *Int J Mass Spectrom* 2007;260(2-3):102-106.
48. Kim NH, Lee MY, Park SJ, Choi JS, Oh MK, Kim IS. Auranofin blocks interleukin-6 signalling by inhibiting phosphorylation of JAK1 and STAT3. *Immunology* 2007;122(4):607-14.
49. Kim NH, Oh MK, Park HJ, Kim IS. Auranofin, a gold(I)-containing antirheumatic compound, activates Keap1/Nrf2 signaling via Rac1/iNOS signal and mitogen-activated protein kinase activation. *J Pharmacol Sci* 2010;113(3):246-54.
50. Nakaya A, Sagawa M, Muto A, Uchida H, Ikeda Y, Kizaki M. The gold compound auranofin induces apoptosis of human multiple myeloma cells through both down-regulation of STAT3 and inhibition of NF-kappaB activity. *Leuk Res* 2011;35(2):243-9.
51. Stern I, Wataha JC, Lewis JB, Messer RL, Lockwood PE, Tseng WY. Anti-rheumatic gold compounds as sublethal modulators of monocytic LPS-induced cytokine secretion. *Toxicol In Vitro* 2005;19(3):365-71.
52. Yamashita M, Niki H, Yamada M, Watanabe-Kobayashi M, Mue S, Ohuchi K. Dual effects of auranofin on prostaglandin E2 production by rat peritoneal macrophages. *Eur J Pharmacol* 1997;325(2-3):221-7.
53. Danis VA, Kulesz AJ, Nelson DS, Brooks PM. The effect of gold sodium thiomalate and auranofin on lipopolysaccharide-induced interleukin-1 production by blood monocytes in vitro: variation in healthy subjects and patients with arthritis. *Clinical & Experimental Immunology* 1990;79(3):335-40.

54. Han S, Kim K, Kim H, Kwon J, Lee YH, Lee CK, Song Y, Lee SJ, Ha N. Auranofin inhibits overproduction of pro-inflammatory cytokines, cyclooxygenase expression and PGE2 production in macrophages. *Arch Pharm Res* 2008;31(1):67-74.
55. Dimartino MJ, Walz DT. Inhibition of lysosomal enzyme release from rat leukocytes by auranofin. A new chrysotherapeutic agent. *Inflammation* 1977;2(2):131-42.
56. Pham Huu T, Marquetty C, Amit N, Hakim J. Effect of degranulation on superoxide dismutase activity in human neutrophils. *J Free Radic Biol Med* 1986;2(3):213-7.
57. Elferink JG, de Koster BM. Potentiation and inhibition of migration of human neutrophils by auranofin. *Ann Rheum Dis* 1993;52(8):595-8.
58. Jeon KI, Jeong JY, Jue DM. Thiol-reactive metal compounds inhibit NF-kappa B activation by blocking I kappa B kinase. *J Immunol* 2000;164(11):5981-9.
59. Park SJ, Kim IS. The role of p38 MAPK activation in auranofin-induced apoptosis of human promyelocytic leukaemia HL-60 cells. *Br J Pharmacol* 2005;146(4):506-13.
60. Greten FR, Karin M. The IKK/NF-kappaB activation pathway-a target for prevention and treatment of cancer. *Cancer Lett* 2004;206(2):193-9.
61. Yamamoto Y, Gaynor RB. Therapeutic potential of inhibition of the NF-kappaB pathway in the treatment of inflammation and cancer. *J Clin Investig* 2001;107(2):135-42.
62. Yamada R, Sano H, Hla T, Hashiramoto A, Fukui W, Miyazaki S, Kohno M, Tsubouchi Y, Kusaka Y, Kondo M. Auranofin inhibits interleukin-1beta-induced transcript of cyclooxygenase-2 on cultured human synoviocytes. *Euro J Pharmacol* 1999;385(1):71-9.
63. Hashioka S, Klegeris A, McGeer PL. Proton pump inhibitors reduce interferon-gamma-induced neurotoxicity and STAT3 phosphorylation of human astrocytes. *Glia* 2011;59(5):833-40.

64. Hashioka S, Klegeris A, Qing H, McGeer PL. STAT3 inhibitors attenuate interferon-gamma-induced neurotoxicity and inflammatory molecule production by human astrocytes. *Neurobiol Dis* 2011;41(2):299-307.
65. Terai K, Matsuo A, McGeer PL. Enhancement of immunoreactivity for NF-kappa B in the hippocampal formation and cerebral cortex of Alzheimer's disease. *Brain Res* 1996;735(1):159-68.
66. Griffioen AW, Molema G. Angiogenesis: potentials for pharmacologic intervention in the treatment of cancer, cardiovascular diseases, and chronic inflammation. *Pharmacol Rev* 2000;52(2):237-68.
67. Vagnucci AH, Jr., Li WW. Alzheimer's disease and angiogenesis. *Lancet* 2003;361(9357):605-8.
68. Saura R, Matsubara T, Mizuno K. Inhibition of neovascularization in vivo by gold compounds. *Rheumatol Int* 1994;14(1):1-7.
69. Park SJ, Lee AN, Youn HS. TBK1-targeted suppression of TRIF-dependent signaling pathway of toll-like receptor 3 by auranofin. *Arch Pharm Res* 2010;33(6):939-45.
70. Korherr C, Gille H, Schafer R, Koenig-Hoffmann K, Dixelius J, Eglund KA, Pastan I, Brinkmann U. Identification of proangiogenic genes and pathways by high-throughput functional genomics: TBK1 and the IRF3 pathway. *Proc Natl Acad Sci USA* 2006;103(11):4240-5.
71. Youn HS, Lee JY, Saitoh SI, Miyake K, Hwang DH. Auranofin, as an anti-rheumatic gold compound, suppresses LPS-induced homodimerization of TLR4. *Bioch Biophys Res Comm* 2006;350(4):866-71.

72. van Oosten BW, Lai M, Barkhof F, Miller DH, Moseley IF, Thompson AJ, Hodgkinson S, Polman CH. A phase II trial of anti-CD4 antibodies in the treatment of multiple sclerosis. *Mult Scler* 1996;1(6):339-42.
73. Ashino T, Sugiuchi J, Uehara J, Naito-Yamamoto Y, Kenmotsu S, Iwakura Y, Shioda S, Numazawa S, Yoshida T. Auranofin protects against cocaine-induced hepatic injury through induction of heme oxygenase-1. *J Toxicol Sci* 2011;36(5):635-43.
74. Shabani F, McNeil J, Tippett L. The oxidative inactivation of tissue inhibitor of metalloproteinase-1 (TIMP-1) by hypochlorous acid (HOCl) is suppressed by anti-rheumatic drugs. *Free Radic Res* 1998;28(2):115-23.
75. Park CH, Lee MJ, Ahn J, Kim S, Kim HH, Kim KH, Eun HC, Chung JH. Heat shock-induced matrix metalloproteinase (MMP)-1 and MMP-3 are mediated through ERK and JNK activation and via an autocrine interleukin-6 loop. *J Invest Dermatol* 2004;123(6):1012-9.
76. Frears ER, Zhang Z, Blake DR, O'Connell JP, Winyard PG. Inactivation of tissue inhibitor of metalloproteinase-1 by peroxynitrite. *FEBS Lett* 1996;381(1-2):21-4.
77. Otterbein LE, Soares MP, Yamashita K, Bach FH. Heme oxygenase-1: unleashing the protective properties of heme. *Trends Immunol* 2003;24(8):449-55.
78. Zakhary R, Poss KD, Jaffrey SR, Ferris CD, Tonegawa S, Snyder SH. Targeted gene deletion of heme oxygenase 2 reveals neural role for carbon monoxide. *Proc Natl Acad Sci U S A* 1997;94(26):14848-53.
79. Yachie A, Niida Y, Wada T, Igarashi N, Kaneda H, Toma T, Ohta K, Kasahara Y, Koizumi S. Oxidative stress causes enhanced endothelial cell injury in human heme oxygenase-1 deficiency. *J Clin Invest* 1999;103(1):129-35.

80. Lee YJ, Han SB, Nam SY, Oh KW, Hong JT. Inflammation and Alzheimer's disease. *Arch Pharm Res* 2010;33(10):1539-56.
81. Klegeris A, Bissonnette CJ, McGeer PL. Reduction of human monocytic cell neurotoxicity and cytokine secretion by ligands of the cannabinoid-type CB2 receptor. *Br J Pharmacol* 2003;139(4):775-86.
82. Klegeris A, McGeer PL. Toxicity of human monocytic THP-1 cells and microglia toward SH-SY5Y neuroblastoma cells is reduced by inhibitors of 5-lipoxygenase and its activating protein FLAP. *J Leukoc Biol* 2003;73(3):369-78.
83. Rieu I, Powers SJ. Real-time quantitative RT-PCR: design, calculations, and statistics. *Plant Cell* 2009;21(4):1031-3.
84. Glass GV, Peckham PD, Sanders JR. Consequences of Failure to Meet Assumptions Underlying Fixed Effects Analyses of Variance and Covariance. *Rev Educ Res* 1972;42(3):237-288.
85. Klegeris A, Bissonnette CJ, McGeer PL. Modulation of human microglia and THP-1 cell toxicity by cytokines endogenous to the nervous system. *Neurobiol Aging* 2005;26(5):673-82.
86. Hashioka S, Klegeris A, McGeer PL. Proton pump inhibitors exert anti-inflammatory effects and decrease human microglial and monocytic THP-1 cell neurotoxicity. *Exp Neurol* 2009;217(1):177-83.
87. Kim IS, Jin JY, Lee IH, Park SJ. Auranofin induces apoptosis and when combined with retinoic acid enhances differentiation of acute promyelocytic leukaemia cells in vitro. *Br J Pharmacol* 2004;142(4):749-55.

88. Glennas A, Kvien TK, Andrup O, Clarke-Jenssen O, Karstensen B, Brodin U. Auranofin is safe and superior to placebo in elderly-onset rheumatoid arthritis. *Br J Rheumatol* 1997;36(8):870-7.
89. Roisman FR, Walz DT, Finkelstein AE. Superoxide radical production by human leukocytes exposed to immune complexes: inhibitory action of gold compounds. *Inflammation* 1983;7(4):355-62.
90. Crooke ST. A comparison of the molecular pharmacology of gold and platinum complexes. *J Rheumatol* 1982;9(SUPPL. 8):61-70.
91. Lee M, Sparatore A, Del Soldato P, McGeer E, McGeer PL. Hydrogen sulfide-releasing NSAIDs attenuate neuroinflammation induced by microglial and astrocytic activation. *Glia* 2010;58(1):103-13.
92. Polanski W, Reichmann H, Gille G. Stimulation, protection and regeneration of dopaminergic neurons by 9-methyl-beta-carboline: a new anti-Parkinson drug? *Expert Rev Neurother* 2011;11(6):845-60.
93. Klegeris A, McGeer PL. Cyclooxygenase and 5-lipoxygenase inhibitors protect against mononuclear phagocyte neurotoxicity. *Neurobiol Aging* 2002;23(5):787-94.
94. Klusa V, Klimaviciusa L, Duburs G, Poikans J, Zharkovsky A. Anti-neurotoxic effects of tauropyrone, a taurine analogue. *Adv Exp Med Biol* 2006;583:499-508.
95. Polanski W, Enzensperger C, Reichmann H, Gille G. The exceptional properties of 9-methyl-beta-carboline: stimulation, protection and regeneration of dopaminergic neurons coupled with anti-inflammatory effects. *J Neurochem* 2010;113(6):1659-75.

96. Klegeris A, McGeer PL. Non-steroidal anti-inflammatory drugs (NSAIDs) and other anti-inflammatory agents in the treatment of neurodegenerative disease. *Curr Alzheimer Res* 2005;2(3):355-65.
97. de la Rosa EJ, de Pablo F. Proinsulin: from hormonal precursor to neuroprotective factor. *Front Mol Neurosci* 2011;4:20.
98. Hur JY, Soh Y, Kim BH, Suk K, Sohn NW, Kim HC, Kwon HC, Lee KR, Kim SY. Neuroprotective and neurotrophic effects of quinic acids from *Aster scaber* in PC12 cells. *Biol Pharm Bull* 2001;24(8):921-4.
99. Kim SS, Park RY, Jeon HJ, Kwon YS, Chun W. Neuroprotective effects of 3,5-dicaffeoylquinic acid on hydrogen peroxide-induced cell death in SH-SY5Y cells. *Phytother Res* 2005;19(3):243-5.
100. Angelucci F, Sayed AA, Williams DL, Boumis G, Brunori M, Dimastrogiovanni D, Miele AE, Pauly F, Bellelli A. Inhibition of *Schistosoma mansoni* thioredoxin-glutathione reductase by auranofin: structural and kinetic aspects. *J Biol Chem* 2009;284(42):28977-85.
101. Dajas F, Rivera F, Blasina F, Arredondo F, Echeverry C, Lafon L, Morquio A, Heizen H. Cell culture protection and in vivo neuroprotective capacity of flavonoids. *Neurotox Res* 2003;5(6):425-32.
102. Ellingsen T, Buus A, Stengaard-Pedersen K. Plasma monocyte chemoattractant protein 1 is a marker for joint inflammation in rheumatoid arthritis. *J Rheumatol* 2001;28(1):41-6.
103. Miyachi Y, Yoshioka A, Imamura S, Niwa Y. Anti-oxidant effects of gold compounds. *Br J Dermatol* 1987;116(1):39-46.

104. Mirabelli CK, Johnson RK, Sung CM, Faucette L, Muirhead K, Crooke ST. Evaluation of the in vivo antitumor activity and in vitro cytotoxic properties of auranofin, a coordinated gold compound, in murine tumor models. *Cancer Res* 1985;45(1):32-9.
105. Moulton PJ, Hiran TS, Goldring MB, Hancock JT. Detection of protein and mRNA of various components of the NADPH oxidase complex in an immortalized human chondrocyte line. *Br J Rheumatol* 1997;36(5):522-9.
106. Van Dervort AL, Doerfler ME, Stuetz P, Danner RL. Antagonism of lipopolysaccharide-induced priming of human neutrophils by lipid A analogs. *J Immunol* 1992;149(1):359-66.
107. Abramson SL, Gallin JI. IL-4 inhibits superoxide production by human mononuclear phagocytes. *J Immunol* 1990;144(2):625-30.
108. Krause D, Suh HS, Tarassishin L, Cui QL, Durafourt BA, Choi N, Bauman A, Cosenza-Nashat M, Antel JP, Zhao ML and others. The tryptophan metabolite 3-hydroxyanthranilic acid plays anti-inflammatory and neuroprotective roles during inflammation: role of hemeoxygenase-1. *Am J Pathol* 2011;179(3):1360-72.
109. Wong K, Parente J, Prasad KV, Ng D. Auranofin modulated cytoplasmic free calcium in neutrophils by mobilizing intracellular calcium and inhibiting protein kinase. *J Biol Chem* 1990;265(35):21454-61.
110. Means AR, Dedman JR. Calmodulin--an intracellular calcium receptor. *Nature* 1980;285(5760):73-7.
111. Chomarat P, Banchereau J. Interleukin-4 and interleukin-13: their similarities and discrepancies. *Int Rev Immunol* 1998;17(1-4):1-52.

112. Brodie C, Goldreich N, Haiman T, Kazimirsky G. Functional IL-4 receptors on mouse astrocytes: IL-4 inhibits astrocyte activation and induces NGF secretion. *J Neuroimmunol* 1998;81(1-2):20-30.
113. Curbo S, Gaudin R, Carlsten M, Malmberg KJ, Troye-Blomberg M, Ahlborg N, Karlsson A, Johansson M, Lundberg M. Regulation of interleukin-4 signaling by extracellular reduction of intramolecular disulfides. *Biochem Biophys Res Commun* 2009;390(4):1272-7.
114. Blocka K. Auranofin versus injectable gold. Comparison of pharmacokinetic properties. *Am J Med* 1983;75(6A):114-22.
115. Bonilla M, Denicola A, Novoselov SV, Turanov AA, Protasio A, Izemendi D, Gladyshev VN, Salinas G. Platyhelminth mitochondrial and cytosolic redox homeostasis is controlled by a single thioredoxin glutathione reductase and dependent on selenium and glutathione. *J Biol Chem* 2008;283(26):17898-907.
116. Saijo K, Glass CK. Microglial cell origin and phenotypes in health and disease. *Nat Rev Immunol* 2011;11(11):775-87.

## Appendices

### Appendix A: ELISA Assay Reagents

A. Phosphate Stock (200mM) –3.7g monobasic sodium phosphate, and 40.3g dibasic sodium phosphate were dissolved in 500mL dH<sub>2</sub>O and stored at room temperature in airtight bottle.

B. PBS-Tween – Dissolved 9g NaCl in 950mL dH<sub>2</sub>O (9g NaCl in 1L=0.09%); added 50ml Phosphate Buffer and 0.5ml Tween-20 --- please check which tween.... Final concentration of Tween 0.05% v/v. Stored at room temperature in airtight bottle.

C. Blocking Solution – Dissolve 1% (w/v) skim milk powder and 1% (w/v) bovine serum albumin (BSA) in PBS.. Cover with adhesive tape and store at 4°C for up to 1 week.

D. Coating Buffer (0.1 M sodium bicarbonate (NaHCO<sub>3</sub>) buffer) –Dissolved 0.159g/100mL Na<sub>2</sub>HCO<sub>3</sub> and 0.293g NaHCO<sub>3</sub> in sterile water (pH corrected to 9.6). Stored at room temperature in airtight bottle.

E. Substrate Buffer – Dissolved 101mg MgCl<sub>2</sub>x5H<sub>2</sub>O (50mM) or 111mg of MgCl<sub>2</sub>x6H<sub>2</sub>O in 800mL dH<sub>2</sub>O. When dissolved added 97mL diethanolamine and mixed thoroughly. Adjusted pH to 9.8 with concentrated HCl. Added H<sub>2</sub>O to 1L, and stored in the dark at 4°C.

Appendix B: This article has been accepted for publication by Immunopharmacology

The Biological Activity of Auranofin: Implications for Novel Treatment of Diseases

Madeira, J.M.,<sup>1</sup> Gibson, D.L.,<sup>1</sup> Kean, W.F.,<sup>2</sup> Klegeris, A.<sup>1\*</sup>

<sup>1</sup> Department of Biology, Irving K. Barber School of Arts and Sciences, University of British Columbia Okanagan Campus, Kelowna, BC, Canada.

<sup>2</sup> Department of Medicine (Rheumatology), McMaster University, Hamilton, ON, Canada.

\* address correspondence at: Department of Biology, I.K. Barber School of Arts and Sciences, University of British Columbia Okanagan Campus, 3333 University Way, Kelowna, BC, V1V 1V7, Canada. E-mail: [andis.klegeris@ubc.ca](mailto:andis.klegeris@ubc.ca); Tel. (250) 807 9557; Fax. (250) 807 8830.

Short Title: Novel Clinical Applications of Auranofin

Abstract

More than 30 years ago, auranofin was developed for the treatment of rheumatoid arthritis as a substitution for the injectable gold compounds aurothiomalate and aurothioglucose. Both the ease of oral administration over intramuscular injections and more potent anti-inflammatory effects *in vitro* made auranofin seem like an excellent substitute for the traditional injectable gold compounds. Despite efficacy in the treatment of both rheumatoid arthritis and psoriasis, currently, auranofin is seldom used as a treatment for patients with rheumatoid arthritis

as more novel anti-rheumatic medications have become available. Despite the decline in its clinical applications, research on auranofin has continued as it shows promise in the treatment of several different diseases. In recent years, advances in technology have allowed researchers to use molecular techniques to identify novel mechanisms of action of auranofin. Additionally, researchers are discovering potential new applications of auranofin. Dual inhibition of inflammatory pathways and thiol redox enzymes by auranofin makes it a new candidate for cancer therapy and treating microbial infections. This review will summarize recently obtained data on the mechanisms of action of auranofin, and potential new applications of auranofin in the treatment of various diseases, including several types of leukemia, carcinomas, and parasitic, bacterial, and viral infections.

Keywords: Auranofin, anti-inflammatory, anti-tumor, anti-parasitic, anti-microbial

## 1. Introduction

Gold compounds have been used for medicinal purposes for centuries and records indicate their use in China as early as 2500 B.C.E.<sup>30</sup>. More recently, in the early 20<sup>th</sup> century, gold compounds were used to treat human and bovine tuberculosis after *in vitro* anti-tubercle activity of gold cyanide was observed by bacteriologist Dr. Koch<sup>122</sup>. While gold compounds were used to treat tuberculosis for several years, they were eventually discontinued as doctors found that the gold compounds did not stop either bacterial growth or disease progression in tuberculosis patients, but that instead they were effective at slowing the progression of rheumatoid arthritis (RA)<sup>30,31</sup>. This observation led to the development of the current gold treatments used in RA, including intramuscular injections of aurothiomalate and aurothioglucose. The oral gold compound 2,3,4,6-tetra-o-acetyl-1-thio-β-D-glucopyrano-sato-S-(triethyl-

phosphine) gold manufactured as auranofin (AF) was developed in the 1980s and quickly gained popularity among researchers<sup>28,31,123</sup>. Though AF initially showed promise as a treatment for RA, it was eventually concluded that the intramuscular injections of gold drugs aurothiomalate and aurothioglucose were more effective at treating RA symptoms<sup>28</sup>.

While the biological activity, especially the anti-inflammatory effect, of AF has been studied in great detail, its *in vivo* metabolism and the potential role of active metabolites of this gold drug still remain poorly understood. Figure 1A shows the structures of AF, which is used in most *in vivo* and *in vitro* studies, however two of its metabolites could be responsible for at least some of the *in vivo* effects of AF. Triethylphosphine gold (TP-gold) (Fig. 1B) is the metabolite responsible for several of the reduction-oxidation (redox)-dependent effects of AF (Caroli *et al.* , 2012). Deacetylated AF (Fig. 1C) is another metabolite formed in the gastro-intestinal tract<sup>124,125</sup> and many *in vitro* studies do not take into account this first-pass metabolite, which is more lipophilic than AF and could have biological activity that is different from the parent compound<sup>126</sup>.

Experimental evidence also indicates that the Au-S and Au-P bonds could break when AF passes through the intestine during the absorption. However, this has not been established conclusively since contrary to observations made by Walz *et al.* (1983), which showed a complete dissociation of Au-S and Au-P in the intestine, Tepperman *et al.* (1984) suggested that intact deacetylated AF passes through the intestine. Even though the metabolic fate of AF has not been established conclusively, it is clear that the gold atom is necessary for the biological activity of AF (McKeage *et al.* , 2000; Walz *et al.* , 1983). Establishing the exact nature of the bioactive metabolite(s) of AF is important for designing *in vitro* assay systems that are representative of *in vivo* conditions.

While the precise mechanism of AF's anti-inflammatory activity has not been established, a range of effects of AF on peripheral inflammatory pathways have been well documented<sup>47-51</sup>. AF affects the secretion of several cytokines, and there have been reports of AF modulating the secretion of interleukin (IL)-8 and IL-6 from lipopolysaccharide (LPS)-stimulated monocytes and macrophages<sup>48,50</sup>. AF also modulates intracellular signaling pathways, including activating mitogen activated protein kinases (MAPK), preventing nuclear factor *kappa*-light-chain-enhancer of activated-B-cells (NF- $\kappa$ B) activation, and preventing the induction of pro-inflammatory cytokines<sup>53,57,58</sup>. Several excellent reviews summarizing mechanisms of action of AF in RA are available<sup>29,30,123</sup>.

More recently, AF has been investigated for treatment of disorders other than RA<sup>73,127,128</sup>. AF is toxic towards parasites, leukemia cells, and carcinoma cells by inhibiting thiol-redox enzymes such as thioredoxin reductase (TrxR) and glutathione thioredoxin reductase (TGR)<sup>73,128</sup>. The inhibition of redox enzymes by AF has also been implicated in disrupting selenium (Se) synthesis in bacteria, accounting for the bactericidal activity of AF<sup>127</sup>. Recently, AF has shown promise in the treatment of human immunodeficiency virus (HIV) infection by reducing viral load in infected memory T-cells<sup>129</sup>. In addition to these effects, and perhaps more interestingly, cytoprotective activities of AF have been observed including induction of heme-oxygenase (HOX)-1 in cocaine-induced hepatic injury<sup>78</sup>. This review will summarize current research on the gold drug AF and its mechanisms of action in diseases other than RA.

## 2. Anti-Neoplastic Properties

### 2.1 Inflammation-associated anti-neoplastic activity

AF inhibits several pro-inflammatory pathways and is therefore a potential candidate for the treatment of cancer, or neoplasms<sup>47,53,57</sup>. The balance between the anti-inflammatory and cytotoxic activities of a compound can involve identical molecular pathways but with varying degrees of induction<sup>60</sup>. AF inhibits several distinct inflammatory pathways which could make it an effective drug for cancer therapy. For example, AF inhibits NF- $\kappa$ B activation, decreases tumor necrosis factor (TNF)- $\alpha$  production and secretion, reduces signal transducer and activator of transcription (STAT)-3 activation, suppresses toll like receptor (TLR) signalling, and inhibits angiogenesis<sup>47,50,53,57</sup>. The aforementioned pathways have been implicated in tumor growth and development as well as in the cytotoxicity of AF<sup>59,60</sup>.

TNF- $\alpha$ -induced activation of NF- $\kappa$ B and subsequent activation of NF- $\kappa$ B-dependent pathways have been linked to neoplasm growth and development, or clonal evolution, via their induction of several anti-apoptotic factors<sup>59,60</sup>. Cyclosporin A and tacrolimus, drugs currently used in cancer therapy, block NF- $\kappa$ B activation by preventing NF- $\kappa$ B inhibitor (I $\kappa$ B)- $\alpha$  degradation and blocking the translocation of c-Rel from the cytoplasm to the nucleus<sup>60</sup>. Similarly, AF inhibits activation of NF- $\kappa$ B by preventing the breakdown of I $\kappa$ B- $\alpha$  and I $\kappa$ B- $\beta$  in macrophages stimulated with LPS<sup>57</sup>. Additionally, AF prevents nuclear translocation of NF- $\kappa$ B in macrophages by inhibiting I $\kappa$ B kinase (IKK) activation<sup>51,57</sup>. This inhibitory activity may be through the suppression of TNF- $\alpha$ <sup>57</sup>. However, it appears that the activity of AF may be specific to cell type, particularly with respect to TNF- $\alpha$  induction. Han *et al.* (2008) found that treating LPS-stimulated RAW 264.7 macrophages with AF decreased expression and production of TNF- $\alpha$  whereas Stern *et al.* (2005) found that treating LPS-stimulated human THP-1 promonocytic cells with AF had no effect on TNF- $\alpha$  production<sup>50,53</sup>. Because NF- $\kappa$ B activates oncogenes, suppressing NF- $\kappa$ B activation is one strategy for the suppression of neoplasm clonal evolution<sup>59</sup>.

While the inhibition of TNF- $\alpha$ -dependent NF- $\kappa$ B activation by AF may be cell and stimulus specific, AF blocks other pathways that activate NF- $\kappa$ B, including inhibiting IL-1 $\beta$  and IL-6 release and expression.

In cultured human monocytes and synoviocytes, AF inhibits release of IL-1 $\beta$  and prevents NF- $\kappa$ B nuclear translocation<sup>61</sup>. AF has been shown to reduce IL-6 release and inhibit IL-6-dependent activation of janus kinase (JAK)-1 and -2<sup>47,49</sup>. Inhibiting JAK-1 and -2 prevents phosphorylation of STAT-3 in multiple myeloma cell lines and AF-induced reduction in STAT-3 activity leads to decreased NF- $\kappa$ B activation<sup>47,49</sup>. The combination of inhibition of STAT-3 signalling and inhibition of cellular release of TNF- $\alpha$  and IL-1 $\beta$  may contribute to the molecular mechanisms responsible for the cytotoxicity of AF towards neoplasms<sup>49</sup>. As NF- $\kappa$ B activation occurs through many different pathways; including intrinsic activation via cytokines and extrinsic activation through TLRs, targeting more than one pathway may yield more effective inhibition of the development and clonal evolution of neoplasms<sup>59,130</sup>.

Not only do cancer and inflammation involve similar cytokines and pathways, they are also linked in causation<sup>130</sup>. Several types of carcinomas; including ovarian, bladder and colorectal, are associated with an inflammatory response, usually caused by an infection<sup>130</sup>. For example, bacteria and viruses can activate tumorigenic pathways in carcinomas<sup>59,130</sup>. One such pathway involves TLRs which detect various pathogens. Specifically, TLR-4 signalling through myeloid differentiation primary response gene 88 (MyD88) has been shown to increase the growth of primary human ovarian carcinoma cells *in vitro*<sup>131</sup>. AF has been shown to inhibit both MyD88 and Toll/interleukin-1 receptor (TIR)-domain-containing adapter-inducing interferon- $\beta$  (TRIF) pathways of TLR-4 activation<sup>70,71</sup>. The thiol moiety on AF binds the MD-2 region of TLR-4, preventing its activation<sup>71</sup>. By blocking both the TRIF and MyD88 pathways that lead to

activation of NF- $\kappa$ B, AF could prevent the clonal evolution of neoplasms caused by TLR-4 activation. Recently, the activation of TLRs has been implicated in not only NF- $\kappa$ B driven clonal evolution, but also in the angiogenesis associated with solid tumors <sup>69</sup>.

Angiogenesis is a key factor in the clonal evolution of solid tumors as proliferating neoplastic cells typically require a direct blood supply <sup>65</sup>. AF has been shown to directly inhibit neovascularization, which would result in decreased blood supply to neoplasms <sup>67</sup>. A molecular basis for this activity could be inhibition of TLR-3 activation and signalling <sup>68</sup>. Viral TLR-3 signalling through a TRIF-dependent pathway has been linked with the angiogenesis induced by neoplastic cells <sup>69</sup>. AF inhibits the phosphorylation and transcription of interferon regulatory factor (IRF)-3 and prevents TRIF activation which would inhibit angiogenesis <sup>68,70</sup>. Therefore, by inhibiting TLR-3 signalling and preventing angiogenesis, AF may be able to decrease the clonal evolution of neoplasms.

The development and potentiation of neoplasms are linked with a number of inflammatory pathways <sup>130</sup>. By blocking several independent inflammatory pathways implicated in neoplasm clonal evolution, AF shows promise as a candidate for cancer therapy including the treatment of leukemia and ovarian carcinomas <sup>47,131</sup>. In addition to its anti-inflammatory activity, AF affects the redox status of cells which is another potential target in cancer therapy <sup>72</sup>.

## *2.2. Anti-neoplastic activity and oxidative stress*

Reactive oxygen species (ROS) have dual effects in cells: at low levels they act as messengers turning signalling cascades on and off whereas at high levels they can induce damage and apoptosis <sup>132</sup>. ROS are known to induce changes and damage to DNA, such as strand breaks and increased susceptibility to radiation, both of which can lead to the development of

neoplastic cells<sup>132,133</sup>. While low levels of ROS can lead to damage without inducing apoptosis, thereby increasing the risk of developing neoplasms, high levels of ROS can lead to apoptosis of aberrant cells and neoplastic cells in particular, as many types of neoplasms are susceptible to oxidative damage<sup>74</sup>. AF has been shown to induce apoptosis in several neoplastic cell lines through oxidative damage and modifications of cellular redox status<sup>58,72,74</sup>.

AF increases the production of ROS in both neoplastic cell lines and cultured human carcinomas; AF-induced production of ROS has been linked to its cytotoxic effects as several types of leukemia and carcinoma are more susceptible to oxidative damage than normal cells<sup>58,72,78,134-136</sup>. In acute promyelocytic leukemia (APL) NB4 cells, low concentrations of AF have been shown to induce caspase-3-dependent apoptosis, which can be reversed by the addition of an antioxidant<sup>72</sup>. In another APL model, HL-60 cells, AF causes the activation of caspase-3, caspase-8 and caspase-9, and causes the release of cytochrome c, leading to apoptosis<sup>58</sup>. The same study found that p38 MAPK was activated in HL-60 cells treated with AF and that treatment with an antioxidant rescued these cells from AF-induced apoptosis<sup>58</sup>. While these results initially seemed promising, conflicting data obtained by Omata *et al.* (2006) demonstrated that the cytotoxic activity of AF was not dependent upon ROS. AF-induced production of ROS in THP-1 leukemia cells did not correlate with the timing of cell death and it was concluded that the inhibition of mitochondrial enzymes was responsible for the pro-apoptotic activity of AF<sup>137</sup>.

One effect shared by several of the gold compounds used in the treatment of RA is the inhibition of the thioredoxin reductase (TrxR) enzyme in mitochondria and in the cytosol<sup>75</sup>. Gold-induced inhibition of TrxR in Jurkat T lymphoma and U937 leukemia cells causes oxidative stress including peroxiredoxin (Per) 3 oxidation<sup>73,74</sup>. Per3 oxidation prevents the

breakdown of H<sub>2</sub>O<sub>2</sub> in the mitochondria, resulting in oxidative damage as H<sub>2</sub>O<sub>2</sub> accumulates in cells<sup>138</sup>. The inhibition of TrxR and Per3 oxidation is followed by Bax/Bak-dependent apoptosis in both Jurkat T lymphoma and U937 leukemia cells<sup>74</sup>. An additional effect of TrxR inhibition is disruption of selenoprotein synthesis, as TrxR is essential for Se metabolism<sup>76</sup>. AF inhibits both Se metabolism and selenoprotein synthesis, and this effect is thought to be responsible for some of the cytotoxic properties of AF as neoplastic cells are susceptible to oxidative stress and disruption of DNA synthesis<sup>76</sup>. The downstream effects of the inhibition of TrxR by AF are outlined in Figure 2. In addition to the inhibition of TrxR, AF reduces the expression of glutathione peroxidase (Gtx)-3, another selenoenzyme. This dual inhibition of TrxR and Gtx3 could significantly reduce the ability of malignant cells to withstand oxidative stress and replicate their genetic material<sup>139</sup>.

In summary, AF inhibits many pathways that are critical to the development and progression of neoplasms, and these molecular effects are summarized in Table 1. By targeting several independent pathways; including NF-κB activation, ROS induction of apoptosis, and Se-dependent DNA synthesis, AF could be effective in inhibiting the clonal evolution of a broad range of neoplasms including ovarian carcinomas and several types of leukemia<sup>57,76</sup>. It has been shown that AF is cytotoxic towards several different types of neoplastic cells *in vitro*, including ovarian, multiple myeloma, and promyelocytic leukemia cells<sup>49,58,134</sup>. The cytotoxic activity of AF along with its relatively safe profile in patients<sup>93</sup> warrant further investigations into AF as a drug that could potentially be used in cancer therapy. To date, a phase 2 clinical trial investigating AF for the treatment of chronic lymphocytic leukemia is recruiting patients (clinicaltrials.gov).

### 3. Anti-Parasitic Activity of AF

Anti-parasitic activity of AF has been demonstrated and much of the current research on AF is investigating the potential mechanisms of this activity<sup>128,140</sup>. This research is important as many parasitic infections have limited treatment options and the treatments that are available are often expensive and have unpleasant side effects<sup>141-143</sup>. Parasitic infections are rampant in developing countries, and despite having serious adverse effects on human populations they remain poorly understood and under-researched<sup>142</sup>. Therefore, the development of therapeutics such as AF which are both affordable and safe is necessary.

Several human parasites spend a portion of their lives in the blood stream and are therefore exposed to high levels of ROS<sup>140,143</sup>. As such, parasites have evolved specific enzymes that enable them to maintain redox balance; these enzymes are good targets for the treatment of parasitic infections as they are necessary for parasite survival and are often organism specific<sup>106,124</sup>. Additionally, parasites usually have either TrxR or thioredoxin glutathione reductase (TGR) alone to maintain thiol redox balance whereas mammals have two independent pathways involving TrxR or glutathione reductase (GR)<sup>106</sup>. As mentioned previously, AF inhibits thiol redox enzymes and increases intracellular H<sub>2</sub>O<sub>2</sub> (as shown in Figure 2); this activity could potentially make AF an effective treatment for parasitic infections.

Infection with *Plasmodium falciparum* causes a severe form of malaria often resulting in neurological damage or death in infected children<sup>143</sup>. Sannella *et al.* (2008) investigated AF for its toxicity towards *P. falciparum in vitro* and found that 1-10 µM AF killed adult and larval parasites. This toxicity was attributed to inhibition of the TrxR enzyme, although this was not confirmed experimentally<sup>128</sup>. A recent study by Caroli *et al.* (2012) demonstrated that a ligand of AF, TP-gold, bound to and inhibited the TrxR enzyme of *P. falciparum*, and it was this action that was likely responsible for the toxicity of AF towards these parasites. The inhibition of TrxR

is also thought to be the mechanism responsible for the toxicity of AF towards *Entamoeba histolytica*<sup>140</sup>. *E. histolytica* causes amoebiasis and is a leading cause of death worldwide<sup>141</sup>. AF has been shown to kill *E. histolytica in vitro*. In fact, in comparison to metronidazole, the drug currently used to treat amoebiasis, AF was found to be ten times more effective at killing the parasites<sup>140</sup>. AF decreased not only the host parasite load, but also the damaging host inflammatory response, and the liver injury caused by *E. histolytica* infection. This activity was confirmed *in vivo* using a mouse model of amoebic colitis and a hamster model of amoebic liver abscess<sup>140</sup>. Similarly, AF has shown promise in the treatment of *Schistosoma mansoni*, the platyhelminth responsible for schistosomiasis. Kuntz *et al.* (2007) demonstrated that 5  $\mu$ M AF kills 100% of *S. mansoni* parasites *in vitro* and that treating mice with AF kills 60% of adult schistosomes. Angelucci *et al.* (2008) confirmed that the TP-gold ligand of AF inhibits TGR, the sole enzyme responsible for thiol redox balance in *S. mansoni*. Additionally, other platyhelminths possessing the TGR enzyme are susceptible to AF. *In vitro* studies investigating *Echinococcus granulosus*<sup>120</sup> and *Taenia crassiceps*<sup>144</sup> found that treating larvae with 5 and 10  $\mu$ M AF, respectively, results in 100% mortality of parasites.

Developing novel drugs is an expensive and lengthy process; therefore, utilizing medications that are currently clinically available, such as AF, and which have their patents released, is an effective way to keep the cost of treatments low. This has been seen with the food and drug administration recently giving AF orphan-drug status; the low cost of manufacturing and the potential of treating amoebiasis with AF makes it a priority for research despite minimal financial gains for pharmaceutical companies<sup>140</sup>. In the future, AF may become a mainstream defense against human parasites and could help alleviate some of the economic burden of these diseases in developing countries.

#### 4. Anti-bacterial activity of AF

Gold complexes became popular in western medicine in the early 1900's due to observations by bacteriologist Dr. Robert Koch that gold cyanide was bactericidal against the tubercle bacilli *in vitro*. These observations led scientists to study various gold compounds as agents for the treatment of tuberculosis<sup>31</sup>. The anti-tuberculoid activity of the injectable gold compounds was eventually ruled out as patients with tuberculosis receiving gold therapy did not respond to treatment; however, current research indicates that AF may be active against other bacteria such as *Clostridium difficile* and *Treponema denticola*<sup>127,145,146</sup>.

*C. difficile* is a human pathogen and is recognized as the leading cause of diarrhea in health care settings<sup>147</sup>. Virulent strains of *C. difficile* are becoming more common and leading to more severe symptoms such as toxic mega colon, septic shock, higher fatality rates, and poor responses to metronidazole<sup>147</sup>. As *C. difficile* is becoming more common, less treatable, and more virulent, novel therapeutic approaches are needed<sup>145,147</sup>. *C. difficile* utilizes selenoproteins for energy; therefore AF, which is known to inhibit Se processing, completely inhibits the growth of *C. difficile in vitro*<sup>145</sup>. Similarly, AF inhibits the growth of *T. denticola*, the bacteria responsible for periodontitis, in a Se-dependent manner<sup>146,148</sup>. By inhibiting selenoprotein synthesis in certain strains of pathological bacteria, AF shows promise as a novel antibacterial agent.

In addition to the bactericidal activity of AF, it has also been shown to have anti-toxin activity<sup>127</sup>. AF decreases the toxicity of the anthrax lethal-toxin produced by *Bacillus anthracis* which is responsible for the anthrax disease<sup>127,149</sup>. Newman *et al.* (2011) demonstrated that treatment with AF prevented the toxicity of anthrax lethal-toxin in murine macrophages and rats by inhibiting caspase-1 enzymatic activity. In addition to this anti-toxic effect, AF inhibited the

nucleotide-binding oligomerization domain containing proteins (NOD)-like receptor protein (NLRP) 1B and NLRP3 inflammasomes which contribute to the negative host inflammatory response to anthrax lethal-toxin <sup>127</sup>. This suggests that AF may be anti-toxic through modulating inflammasomes. Due to its bactericidal and anti-toxic effects AF may be effective across a wide range of organisms and diseases separate from RA.

#### 5. Anti-Viral activity of AF

AF has been shown to decrease the viral load in HIV-infected cells and increase the memory T cell count in patients infected with human immunodeficiency virus (HIV)-1. Due to these activities, AF is being studied as a novel therapeutic approach for the treatment of acquired immune deficiency syndrome (AIDS) <sup>129,150</sup>. In 2009, 33.3 million people worldwide were infected with HIV and 1.8 million people died from AIDS <sup>151</sup>. HIV infects both immune cells and lymphoid organs, ultimately leading to deterioration of the host immune system <sup>152</sup>. The current treatment for HIV involves anti-retroviral therapy which prevents replication of the virus and has led to a significant decline in HIV-associated mortality <sup>151</sup>. Unfortunately, anti-retroviral therapy often has severe side effects and does nothing to eliminate the viral reservoir in patients. Thus, the key to curing HIV would need to include eradicating the virus from the body <sup>153</sup>. The persistence of HIV in treated patients is partially due to the infection of short-term memory CD4<sup>+</sup> T cells with pro-viruses capable of replication <sup>154</sup>. AF has been shown to reduce the viral reservoir in HIV- infected human CD4<sup>+</sup> T cells *ex vivo* and to decrease the viral load in simian immunodeficiency virus (SIV)-infected rhesus monkeys <sup>129</sup>. This study also demonstrated that, in combination with anti-retroviral therapy, AF significantly decreased the amount of viral DNA by promoting differentiation and death of CD4<sup>+</sup> T cells. This effect was not due to general immune suppression as CD8<sup>+</sup> T cell count actually increased during AF therapy <sup>129</sup>. In HIV-infected

human CD4<sup>+</sup> T cells, treatment with AF resulted in cell differentiation from long-lived to short-lived phenotype and eventual apoptosis which would help in the eradication of HIV proviruses from the body <sup>129</sup>.

In untreated patients, HIV causes a decrease in the number of CD4<sup>+</sup> T cells by inhibiting lymphoblastogenesis, and this low CD4<sup>+</sup> T cell count is often an indication of the severity of the disease and is correlated with poor survival outcomes <sup>150,153</sup>. The first report indicating that AF may be useful in the treatment of HIV was by Shapiro and Masci (1996), who reported that in an HIV- infected patient treated with AF for psoriatic arthritis, the psoriatic arthritis symptoms improved but remarkably the patient's CD4<sup>+</sup> T cell count increased as well. As the natural progression of HIV results in decreased CD4<sup>+</sup> T cells, it was assumed that AF had caused the HIV virus to go into remission <sup>150</sup>. These data indicate that AF may be helpful in the treatment of HIV in combination with current anti-retroviral agents by reducing the HIV reservoir in infected patients and possibly by causing the virus to go into remission.

## 6. Cytoprotective effects of AF

It has been well documented that AF is toxic towards a wide variety of cell types and organisms, but its other effects of interest include the cytoprotective mechanism of action of AF observed in a number of different cells and model systems. Under inflammatory conditions, such as RA, an ideal treatment would involve stopping or slowing deleterious pro-inflammatory responses while stimulating innate protective mechanisms <sup>39</sup>. Inflammation can be beneficial, and treatments designed to decrease all inflammatory responses without stimulating protective mechanisms have yielded suboptimal results. For example, negative outcomes were observed

when multiple sclerosis patients were treated with TNF- $\alpha$  inhibitors as some inflammatory mechanisms are involved in the healing process<sup>38,77</sup>. Along with inhibiting pro-inflammatory pathways, AF induces several protective molecules, which may make AF a good candidate for the treatment of inflammatory conditions<sup>78,79</sup>.

Matrix metalloproteinase (MMP)-1 is an enzyme that helps in wound repair by degrading collagen<sup>80</sup>. MMP-1 has been shown to contribute to inflammation by augmenting monocyte chemoattractant protein (MCP)-1 signalling, inducing the processing of stromal cell derived factor (SDF)-1 into a potentially neurotoxic form, and enhancing the processing of pro-TNF- $\alpha$  into active TNF- $\alpha$ <sup>80</sup>. Due to its activity on collagen, MMP-1 has been implicated in the tissue destruction common in RA<sup>79</sup>. Tissue inhibitor of matrix metalloproteinase (TIMP)-1 is responsible for controlling MMP-1 enzymatic activity; TIMP-1 binds to and inactivates MMP-1<sup>79</sup>. Upregulation or stabilization of TIMP-1 could be protective in MMP-1-associated destructive inflammation. TIMP-1 is susceptible to oxidative inactivation by hypochlorous acid (HOCl), a by-product of the neutrophil respiratory burst; therefore, during chronic inflammation the protective activity of TIMP-1 may be lost<sup>81</sup>. Shabani *et al.* (1998) demonstrated that AF, aurothiomalate, and aurothioglucose prevented the oxidative inactivation of TIMP-1. In this way, by preserving the protective activity of TIMP-1, AF may prevent tissue destruction by MMP-1 without impairing inflammatory processes.

Another cytoprotective molecule induced by AF is HOX-1<sup>78</sup>. HOX-1 catabolizes the heme molecule into carbon monoxide (CO), biliverdin, and free iron<sup>82</sup>. Additionally, HOX-1 has anti-inflammatory activity, as evidenced by observations that transgenic mice without HOX-1 develop chronic inflammation and the only human known to be born without HOX-1 enzymatic activity died of inflammation-related processes<sup>82-84</sup>. Induction of HOX-1 has been implicated in

the protective activities of several molecules including IL-10, rapamycin, and heat shock proteins, and in the anti-inflammatory activity of alcohol<sup>82</sup>. AF induces HOX-1 expression by increasing levels of nuclear factor erythroid 2-related factor 2 (Nrf2) through the activation of Ras-related C3 botulinum toxin substrate 1 (Rac1)<sup>48</sup>. The induction of HOX-1 has been linked with the beneficial effects of AF, including its ability to protect against cocaine-induced hepatic injury *in vivo* and to protect neurons from damage caused by toxic glial supernatants and hydrogen peroxide (Ashino *et al.* , 2011; Madeira *et al.* , unpublished observations).

Ashino *et al.* (2011) found that AF was able to induce HOX-1 expression in mouse and human hepatocytes *in vitro*. Additionally, treating mice with AF before exposure to cocaine significantly upregulated HOX-1 in the liver and protected mice from liver damage<sup>78</sup>. Research in our laboratory showed that AF induced HOX-1 expression in the human SH-SY5Y neuroblastoma cells and that treating these cells with AF protected them from the otherwise detrimental effects of exposure to toxic supernatants from stimulated glial cells as well as hydrogen peroxide (unpublished data). The effects of AF on the central nervous system cells have not been explored in detail yet, but our data suggest that AF may have potential in treating degenerative diseases associated with neuroinflammation and neuronal loss.

The balance between anti-inflammatory and protective activities of AF makes it a good candidate for the treatment of several diseases associated with inflammation and tissue damage<sup>78,79</sup>. The potential cytoprotective effects of AF are particularly exciting as many of the currently available anti-inflammatory treatments stop inflammation without inducing protective mechanisms that enhance recovery<sup>39</sup>. By inducing several protective pathways, AF has the potential to be part of a new therapeutic approach aimed at achieving a balanced inflammatory response<sup>39</sup>.

## 7. Conclusion

Though it has been studied for over 30 years, researchers continue to find novel applications for, and mechanisms of action of, AF. Studies on the anti-tumor, anti-parasitic and anti-microbial activities of AF have led to a phase II clinical trial for AF in the treatment of chronic lymphocytic leukemia and reclassification of AF as an ‘orphan drug’ to promote its use as a treatment for parasitic infections (clinicaltrials.gov; Debnath *et al.* , 2012). Recent identification of novel mechanisms of action combined with an acceptable clinical safety profile of AF, may lead to renaissance of this gold compound in the treatment of inflammatory arthritis<sup>155</sup>. AF is an interesting compound with many complex activities and a variety of known and as-of-yet unknown applications. AF and its ligands’ selective biological actions demonstrate that this gold complex is an excellent tool in the broad spectrum of inflammation and tumour research. As described, AF may have a variety of potentially very useful clinical applications in disease states which to date have been extremely difficult to manage.

## Acknowledgements

This work was supported by grants from the Natural Sciences and Engineering Research Council of Canada and the Jack Brown and Family Alzheimer’s Disease Research Foundation. We would like to thank Ms. N. Gill for help with preparation of the manuscript.

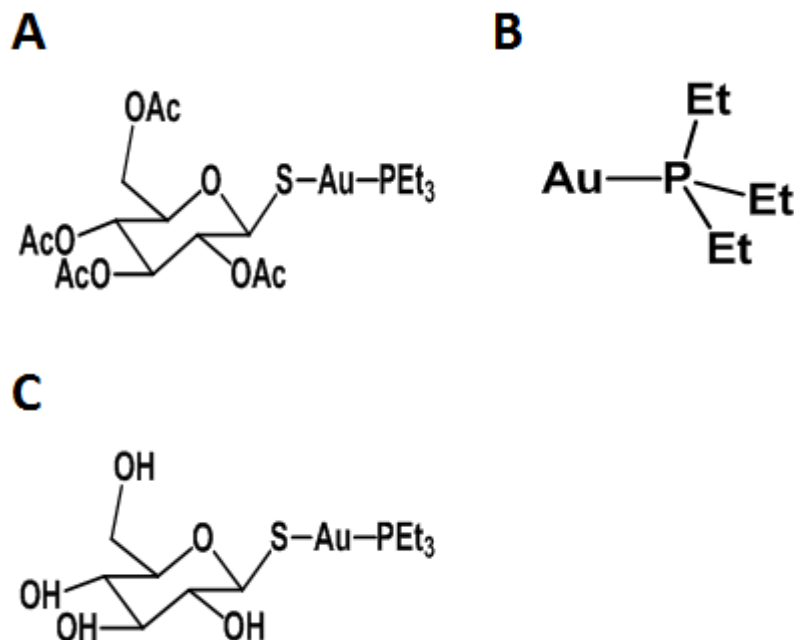


Fig. 1. The chemical structures of AF (A), triethylphosphine-gold (B), an active metabolite of AF, and deacetylated AF (C), the first-pass metabolite of AF. Ac, acetyl group; Et, ethyl group.

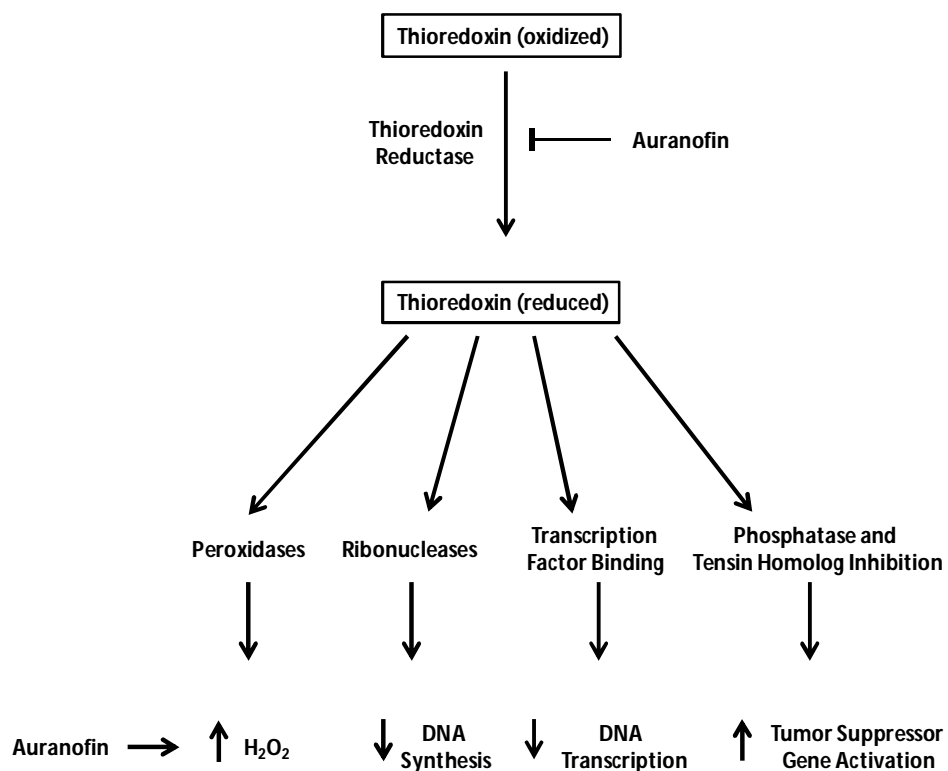


Fig. 2. The molecular pathways affected by AF through inhibition of thioredoxin reductase. AF prevents the conversion of oxidized thioredoxin to reduced thioredoxin by inhibiting the enzyme that catalyzes this reaction, thioredoxin reductase. Reduced thioredoxin affects several cellular pathways including: acting as a substrate for redox enzymes such as peroxidases and ribonucleases, and acting as a regulatory factor for DNA transcription and gene activation. The thioredoxin-dependent effects implicated in the cytotoxicity of AF are outlined in the text.

## References

- Angelucci, F., Sayed, A. A., Williams, D. L., Boumis, G., Brunori, M., Dimastrogiovanni, D., Miele, A. E., Pauly, F. & Bellelli, A. (2009) Inhibition of *Schistosoma mansoni* thioredoxin-glutathione reductase by auranofin: structural and kinetic aspects. *J Biol Chem*, 284, 28977-85.
- Arnason, B. G. (1999) Immunologic therapy of multiple sclerosis. *Annu Rev Med*, 50, 291-302.
- Ashino, T., Sugiuchi, J., Uehara, J., Naito-Yamamoto, Y., Kenmotsu, S., Iwakura, Y., Shioda, S., Numazawa, S. & Yoshida, T. (2011) Auranofin protects against cocaine-induced hepatic injury through induction of heme oxygenase-1. *J Toxicol Sci*, 36, 635-43.
- Balkwill, F. & Mantovani, A. (2001) Inflammation and cancer: back to Virchow? *Lancet*, 357, 539-45.
- Berners-Price, S. J. & Filipovska, A. (2011) Gold compounds as therapeutic agents for human diseases. *Metallomics*, 3, 863-873.
- Bonilla, M., Denicola, A., Novoselov, S. V., Turanov, A. A., Protasio, A., Izmendi, D., Gladyshev, V. N. & Salinas, G. (2008) Platyhelminth mitochondrial and cytosolic redox homeostasis is controlled by a single thioredoxin glutathione reductase and dependent on selenium and glutathione. *J Biol Chem*, 283, 17898-907.
- Brown, K. K., Cox, A. G. & Hampton, M. B. (2010) Mitochondrial respiratory chain involvement in peroxiredoxin 3 oxidation by phenethyl isothiocyanate and auranofin. *FEBS Lett*, 584, 1257-62.

- Brown, N. S. & Bicknell, R. (2001) Hypoxia and oxidative stress in breast cancer. Oxidative stress: its effects on the growth, metastatic potential and response to therapy of breast cancer. *Breast Cancer Res*, 3, 323-7.
- Caroli, A., Simeoni, S., Lepore, R., Tramontano, A. & Via, A. (2012) Investigation of a potential mechanism for the inhibition of SmtGR by Auranofin and its implications for Plasmodium falciparum inhibition. *Biochem Biophys Res Commun*, 417, 576-81.
- Champion, G. D., Graham, G. G. & Ziegler, J. B. (1990) The gold complexes. *Baillieres Clin Rheumatol*, 4, 491-534.
- Chiellini, C., Casini, A., Cochet, O., Gabbiani, C., Ailhaud, G., Dani, C., Messori, L. & Amri, E. Z. (2008) The influence of auranofin, a clinically established antiarthritic gold drug, on bone metabolism: analysis of its effects on human multipotent adipose-derived stem cells, taken as a model. *Chem Biodivers*, 5, 1513-20.
- Chomont, N., El-Far, M., Ancuta, P., Trautmann, L., Procopio, F. A., Yassine-Diab, B., Boucher, G., Boulassel, M. R., Ghattas, G., Brenchley, J. M., Schacker, T. W., Hill, B. J., Douek, D. C., Routy, J. P., Haddad, E. K. & Sekaly, R. P. (2009) HIV reservoir size and persistence are driven by T cell survival and homeostatic proliferation. *Nat Med*, 15, 893-900.
- Cox, A. G., Brown, K. K., Arner, E. S. & Hampton, M. B. (2008) The thioredoxin reductase inhibitor auranofin triggers apoptosis through a Bax/Bak-dependent process that involves peroxiredoxin 3 oxidation. *Biochem Pharmacol*, 76, 1097-109.
- Debnath, A., Parsonage, D., Andrade, R. M., He, C., Cobo, E. R., Hirata, K., Chen, S., Garcia-Rivera, G., Orozco, E., Martinez, M. B., Gunatilleke, S. S., Barrios, A. M., Arkin, M. R., Poole, L. B., Mckerrow, J. H. & Reed, S. L. (2012) A high-throughput drug screen for Entamoeba histolytica identifies a new lead and target. *Nat Med.*, 18, 956-960.
- Fauci, A. S. (1996) Host factors and the pathogenesis of HIV-induced disease. *Nature*, 384, 529-34.
- Fonteh, P. N., Keter, F. K. & Meyer, D. (2010) HIV therapeutic possibilities of gold compounds. *Biometals*, 23, 185-96.
- Frears, E. R., Zhang, Z., Blake, D. R., O'connell, J. P. & Winyard, P. G. (1996) Inactivation of tissue inhibitor of metalloproteinase-1 by peroxynitrite. *FEBS Lett*, 381, 21-4.

- Glennas, A., Kvien, T. K., Andrup, O., Clarke-Jenssen, O., Karstensen, B. & Brodin, U. (1997) Auranofin is safe and superior to placebo in elderly-onset rheumatoid arthritis. *Br J Rheumatol*, 36, 870-7.
- Greten, F. R. & Karin, M. (2004) The IKK/NF-kappaB activation pathway-a target for prevention and treatment of cancer. *Cancer Lett*, 206, 193-9.
- Griffioen, A. W. & Molema, G. (2000) Angiogenesis: potentials for pharmacologic intervention in the treatment of cancer, cardiovascular diseases, and chronic inflammation. *Pharmacol Rev*, 52, 237-68.
- Han, S., Kim, K., Kim, H., Kwon, J., Lee, Y. H., Lee, C. K., Song, Y., Lee, S. J. & Ha, N. (2008) Auranofin inhibits overproduction of pro-inflammatory cytokines, cyclooxygenase expression and PGE2 production in macrophages. *Arch Pharm Res*, 31, 67-74.
- Hileman, E. O., Liu, J., Albitar, M., Keating, M. J. & Huang, P. (2004) Intrinsic oxidative stress in cancer cells: a biochemical basis for therapeutic selectivity. *Cancer Chemother Pharmacol*, 53, 209-19.
- Hill, K. E., Mccollum, G. W., Boeglin, M. E. & Burk, R. F. (1997) Thioredoxin reductase activity is decreased by selenium deficiency. *Biochem Biophys Res Commun*, 234, 293-5.
- Ichimura, K., Pearson, D. M., Kocialkowski, S., Backlund, L. M., Chan, R., Jones, D. T. & Collins, V. P. (2009) IDH1 mutations are present in the majority of common adult gliomas but rare in primary glioblastomas. *Neuro-Oncology*, 11, 341-7.
- Jackson-Rosario, S., Cowart, D., Myers, A., Tarrien, R., Levine, R. L., Scott, R. A. & Self, W. T. (2009) Auranofin disrupts selenium metabolism in *Clostridium difficile* by forming a stable Au-Se adduct. *J Biol Inorg Chem*, 14, 507-19.
- Jackson-Rosario, S. & Self, W. T. (2009) Inhibition of selenium metabolism in the oral pathogen *Treponema denticola*. *J Bacteriol*, 191, 4035-40.
- Jeon, K. I., Jeong, J. Y. & Jue, D. M. (2000) Thiol-reactive metal compounds inhibit NF-kappa B activation by blocking I kappa B kinase. *J Immunol*, 164, 5981-9.
- Jones, J. S. (1998) Life in the 21st century - a vision for all. *S Afr Med J*, 88, 674.
- Kean, W. F. (1990) Intramuscular versus oral gold therapy. *Baillieres Clin Rheumatol*, 4, 219-46.
- Kean, W. F., Forestier, F., Kassam, Y., Buchanan, W. W. & Rooney, P. J. (1985) The history of gold therapy in rheumatoid disease. *Semin Arthritis Rheu*, 14, 180-6.
- Kean, W. F., Hart, L. & Buchanan, W. W. (1997) Auranofin. *Br J Rheumatol*, 36, 560-72.

- Kean, W. F. & Kean, I. R. (2008) Clinical pharmacology of gold. *Inflammopharmacology*, 16, 112-25.
- Kelly, M. G., Alvero, A. B., Chen, R., Silasi, D. A., Abrahams, V. M., Chan, S., Visintin, I., Rutherford, T. & Mor, G. (2006) TLR-4 signaling promotes tumor growth and paclitaxel chemoresistance in ovarian cancer. *Cancer Res*, 66, 3859-68.
- Kim, I. S., Jin, J. Y., Lee, I. H. & Park, S. J. (2004) Auranofin induces apoptosis and when combined with retinoic acid enhances differentiation of acute promyelocytic leukaemia cells in vitro. *Br J Pharmacol*, 142, 749-55.
- Kim, N. H., Lee, M. Y., Park, S. J., Choi, J. S., Oh, M. K. & Kim, I. S. (2007) Auranofin blocks interleukin-6 signalling by inhibiting phosphorylation of JAK1 and STAT3. *Immunology*, 122, 607-14.
- Kim, N. H., Oh, M. K., Park, H. J. & Kim, I. S. (2010) Auranofin, a gold(I)-containing antirheumatic compound, activates Keap1/Nrf2 signaling via Rac1/iNOS signal and mitogen-activated protein kinase activation. *J Pharmacol Sci*, 113, 246-54.
- Korherr, C., Gille, H., Schafer, R., Koenig-Hoffmann, K., Dixelius, J., Eglund, K. A., Pastan, I. & Brinkmann, U. (2006) Identification of proangiogenic genes and pathways by high-throughput functional genomics: TBK1 and the IRF3 pathway. *Proc Natl Acad Sci USA*, 103, 4240-5.
- Lewis, M. G., Dafonseca, S., Chomont, N., Palamara, A. T., Tardugno, M., Mai, A., Collins, M., Wagner, W. L., Yalley-Ogunro, J., Greenhouse, J., Chirullo, B., Norelli, S., Garaci, E. & Savarino, A. (2011) Gold drug auranofin restricts the viral reservoir in the monkey AIDS model and induces containment of viral load following ART suspension. *AIDS*, 25, 1347-56.
- Lo Vecchio, A. & Zacur, G. M. (2012) Clostridium difficile infection: an update on epidemiology, risk factors, and therapeutic options. *Curr Opin Gastroenterol*, 28, 1-9.
- Mancek-Keber, M., Gradisar, H., Inigo Pestana, M., Martinez De Tejada, G. & Jerala, R. (2009) Free thiol group of MD-2 as the target for inhibition of the lipopolysaccharide-induced cell activation. *J Biol Chem*, 284, 19493-500.
- Martinez-Gonzalez, J. J., Guevara-Flores, A., Alvarez, G., Rendon-Gomez, J. L. & Del Arenal, I. P. (2010) In vitro killing action of auranofin on Taenia crassiceps metacestode

- (cysticerci) and inactivation of thioredoxin-glutathione reductase (TGR). *Parasitol Res*, 107, 227-31.
- Marzano, C., Gandin, V., Folda, A., Scutari, G., Bindoli, A. & Rigobello, M. P. (2007) Inhibition of thioredoxin reductase by auranofin induces apoptosis in cisplatin-resistant human ovarian cancer cells. *Free Rad Biol Med*, 42, 872-81.
- Mckeage, M. J., Berners-Price, S. J., Galettis, P., Bowen, R. J., Brouwer, W., Ding, L., Zhuang, L. & Baguley, B. C. (2000) Role of lipophilicity in determining cellular uptake and antitumour activity of gold phosphine complexes. *Cancer Chemother Pharmacol*, 46, 343-50.
- Moayeri, M., Crown, D., Dorward, D. W., Gardner, D., Ward, J. M., Li, Y., Cui, X., Eichacker, P. & Leppla, S. H. (2009) The heart is an early target of anthrax lethal toxin in mice: a protective role for neuronal nitric oxide synthase (nNOS). *PLoS Pathog*, 5, e1000456.
- Nakaya, A., Sagawa, M., Muto, A., Uchida, H., Ikeda, Y. & Kizaki, M. (2011) The gold compound auranofin induces apoptosis of human multiple myeloma cells through both down-regulation of STAT3 and inhibition of NF-kappaB activity. *Leuk Res*, 35, 243-9.
- Newman, Z. L., Sirianni, N., Mawhinney, C., Lee, M. S., Leppla, S. H., Moayeri, M. & Johansen, L. M. (2011) Auranofin protects against anthrax lethal toxin-induced activation of the Nlrp1b inflammasome. *Antimicrob Agents Chemother*, 55, 1028-35.
- Omata, Y., Lewis, J. B., Lockwood, P. E., Tseng, W. Y., Messer, R. L., Bouillaguet, S. & Wataha, J. C. (2006) Gold-induced reactive oxygen species (ROS) do not mediate suppression of monocytic mitochondrial or secretory function. *Toxicol in Vitro*, 20, 625-33.
- Otterbein, L. E., Soares, M. P., Yamashita, K. & Bach, F. H. (2003) Heme oxygenase-1: unleashing the protective properties of heme. *Trends Immunol*, 24, 449-55.
- Papp, K. A. & Shear, N. H. (1991) Systemic gold therapy. *Clin Dermatol*, 9, 535-51.
- Park, C. H., Lee, M. J., Ahn, J., Kim, S., Kim, H. H., Kim, K. H., Eun, H. C. & Chung, J. H. (2004) Heat shock-induced matrix metalloproteinase (MMP)-1 and MMP-3 are mediated through ERK and JNK activation and via an autocrine interleukin-6 loop. *J Invest Dermatol*, 123, 1012-9.
- Park, S. J. & Kim, I. S. (2005) The role of p38 MAPK activation in auranofin-induced apoptosis of human promyelocytic leukaemia HL-60 cells. *Br J Pharmacol*, 146, 506-13.

- Park, S. J., Lee, A. N. & Youn, H. S. (2010) TBK1-targeted suppression of TRIF-dependent signaling pathway of toll-like receptor 3 by auranofin. *Arch Pharm Res*, 33, 939-45.
- Rabasseda, X. (2011) A report from the XVIII International AIDS Conference. (July 18-23, 2010-Vienna, Austria). *Drugs Today (Barc)*, 46, 945-57.
- Sannella, A. R., Casini, A., Gabbiani, C., Messori, L., Bilia, A. R., Vincieri, F. F., Majori, G. & Severini, C. (2008) New uses for old drugs. Auranofin, a clinically established antiarthritic metallodrug, exhibits potent antimalarial effects in vitro: Mechanistic and pharmacological implications. *FEBS Lett*, 582, 844-7.
- Saura, R., Matsubara, T. & Mizuno, K. (1994) Inhibition of neovascularization in vivo by gold compounds. *Rheumatol Int*, 14, 1-7.
- Savioli, L., Smith, H. & Thompson, A. (2006) Giardia and Cryptosporidium join the 'Neglected Diseases Initiative'. *Trends Parasitol*, 22, 203-8.
- Serhan, C. N. & Drazen, J. M. (1997) Antiinflammatory potential of lipoxygenase-derived eicosanoids: a molecular switch at 5 and 15 positions? *J Clin Invest*, 99, 1147-8.
- Shabani, F., Mcneil, J. & Tippett, L. (1998) The oxidative inactivation of tissue inhibitor of metalloproteinase-1 (TIMP-1) by hypochlorous acid (HOCl) is suppressed by anti-rheumatic drugs. *Free Radic Res*, 28, 115-23.
- Shapiro, D. L. & Masci, J. R. (1996) Treatment of HIV associated psoriatic arthritis with oral gold. *J Rheumatol*, 23, 1818-20.
- Simonson, L. G., Goodman, C. H., Bial, J. J. & Morton, H. E. (1988) Quantitative relationship of Treponema denticola to severity of periodontal disease. *Infect Immun*, 56, 726-8.
- Stanley, B. A., Sivakumaran, V., Shi, S., Mcdonald, I., Lloyd, D., Watson, W. H., Aon, M. A. & Paolucci, N. (2011) Thioredoxin reductase-2 is essential for keeping low levels of H<sub>2</sub>O<sub>2</sub> emission from isolated heart mitochondria. *J Biol Chem*, 286, 33669-77.
- Stern, I., Wataha, J. C., Lewis, J. B., Messer, R. L., Lockwood, P. E. & Tseng, W. Y. (2005) Anti-rheumatic gold compounds as sublethal modulators of monocytic LPS-induced cytokine secretion. *Toxicol In Vitro*, 19, 365-71.
- Talbot, S., Nelson, R. & Self, W. T. (2008) Arsenic trioxide and auranofin inhibit selenoprotein synthesis: implications for chemotherapy for acute promyelocytic leukaemia. *Br J Pharmacol*, 154, 940-8.

- Tepperman, K., Finer, R., Donovan, S., Elder, R. C., Doi, J., Ratliff, D. & Ng, K. (1984) Intestinal uptake and metabolism of auranofin, a new oral gold-based antiarthritis drug. *Science*, 225, 430-2.
- Valko, M., Rhodes, C. J., Moncol, J., Izakovic, M. & Mazur, M. (2006) Free radicals, metals and antioxidants in oxidative stress-induced cancer. *Chem Biol Interact*, 160, 1-40.
- Van Oosten, B. W., Lai, M., Barkhof, F., Miller, D. H., Moseley, I. F., Thompson, A. J., Hodgkinson, S. & Polman, C. H. (1996) A phase II trial of anti-CD4 antibodies in the treatment of multiple sclerosis. *Mult Scler*, 1, 339-42.
- Winzeler, E. A. (2008) Malaria research in the post-genomic era. *Nature*, 455, 751-6.
- Yachie, A., Niida, Y., Wada, T., Igarashi, N., Kaneda, H., Toma, T., Ohta, K., Kasahara, Y. & Koizumi, S. (1999) Oxidative stress causes enhanced endothelial cell injury in human heme oxygenase-1 deficiency. *J Clin Invest*, 103, 129-35.
- Yamada, R., Sano, H., Hla, T., Hashiramoto, A., Fukui, W., Miyazaki, S., Kohno, M., Tsubouchi, Y., Kusaka, Y. & Kondo, M. (1999) Auranofin inhibits interleukin-1beta-induced transcript of cyclooxygenase-2 on cultured human synoviocytes. *Eur J Pharmacol*, 385, 71-9.
- Yamamoto, Y. & Gaynor, R. B. (2001) Therapeutic potential of inhibition of the NF-kappaB pathway in the treatment of inflammation and cancer. *J Clin Invest*, 107, 135-42.
- Yamashita, M., Niki, H., Yamada, M., Watanabe-Kobayashi, M., Mue, S. & Ohuchi, K. (1997) Dual effects of auranofin on prostaglandin E2 production by rat peritoneal macrophages. *Eur J Pharmacol*, 325, 221-7.
- Youn, H. S., Lee, J. Y., Saitoh, S. I., Miyake, K. & Hwang, D. H. (2006) Auranofin, as an anti-rheumatic gold compound, suppresses LPS-induced homodimerization of TLR4. *Bioch Biophys Res Comm*, 350, 866-71.
- Zakhary, R., Poss, K. D., Jaffrey, S. R., Ferris, C. D., Tonegawa, S. & Snyder, S. H. (1997) Targeted gene deletion of heme oxygenase 2 reveals neural role for carbon monoxide. *Proc Natl Acad Sci U S A*, 94, 14848-53.

Appendix C: This article has been submitted to J. Neuroimmunol.

Auranofin inhibits astrocyte-mediated neuroinflammation *in vitro* and is directly neuroprotective

J.M. Madeira,<sup>1</sup> C.J. Renschler,<sup>1</sup> B. Mueller,<sup>2</sup> S. Hashioka,<sup>3</sup> D.L. Gibson,<sup>1</sup> A. Klegeris<sup>1,\*</sup>

<sup>1</sup> Department of Biology and <sup>2</sup>Fipke Laboratory for Trace Element Research, Irving K. Barber School of Arts and Sciences, University of British Columbia Okanagan Campus, Kelowna, BC, Canada.

<sup>3</sup> Kinsmen Laboratory of Neurological Research, Department of Psychiatry, the University of British Columbia, 2255 Wesbrook Mall, Vancouver, B.C., V6T 1Z3 Canada.

\* address correspondence at: Department of Biology, I.K. Barber School of Arts and Sciences, University of British Columbia Okanagan Campus, 3333 University Way, Kelowna, BC, V1V 1V7, Canada. E-mail: [andis.klegeris@ubc.ca](mailto:andis.klegeris@ubc.ca); Tel. (250) 807 9557; Fax. (250) 807 8830.

## Abstract

Degenerative diseases of the central nervous system are characterized by chronic inflammation; reducing neuroinflammation may diminish the observed neuronal loss. Gold thiol compounds, including aurothiomalate, aurothioglucose and auranofin reduce peripheral inflammation in rheumatoid arthritis patients, but their effects on neuroinflammation are unknown. We demonstrate that auranofin (0.1 – 5  $\mu$ M) unlike other gold compounds inhibits human astrocytic cell toxicity towards neuronal cells. In addition, it directly protects neuronal cells from toxicity induced by hydrogen peroxide or toxic astrocyte supernatants through the upregulation of heme-oxygenase (HOX)-1. Mass spectrometry indicates that auranofin may reach low micromolar concentrations in mouse brain following oral administration.

## Key Words

Brain, anti-inflammatory, neuroinflammation, heme oxygenase, neurotoxicity, neurodegenerative diseases

## Introduction

Accumulating data indicate that inflammation in the central nervous system (CNS) contributes to several neurological impairments including Alzheimer's and Parkinson's diseases<sup>41,85</sup>. As there are currently no effective treatments directed at preventing or stopping this inflammation, research into novel therapeutics is warranted. Neuroinflammation is driven by two glial cell types: microglia and astrocytes<sup>16,156</sup>; therefore, these cells could be targets in the treatment of neuroinflammation<sup>4</sup>. In an inflammatory state, the increased secretion of toxins and inflammatory mediators as well as the deficiency in neurotrophic factors could harm neurons surrounding glial cells<sup>14</sup>. By decreasing the release of neurotoxins from glia or increasing their release of neurotrophic factors, some of the neuronal loss caused by neuroinflammation could potentially be reduced.

For hundreds of years, humans have used gold compounds for medicinal purposes<sup>30</sup>. In the early 20<sup>th</sup> century, gold compounds including gold sodium thiomalate and gold cyanide were used in the treatment of tuberculosis due to their anti-tuberculoid activity *in vitro*<sup>31</sup>. It was later

noted that gold compounds effectively slowed rheumatoid arthritis (RA) in some patients. This led to the development of the current gold treatments used in RA, including intramuscular injections of aurothiomalate (ATM) and aurothioglucose (ATG) as well as the oral gold compound 2,3,4,6-tetra-*o*-acetyl-1-thio- $\beta$ -D-glucopyrano-sato-S-(triethyl-phosphine) gold manufactured as auranofin (AF)<sup>29,31,123</sup>.

While the exact mechanisms of AF's anti-inflammatory activity have not been established conclusively, a range of different effects of AF on peripheral immune cell functions has been documented<sup>47-51</sup>. AF affects the secretion of several cytokines including increasing the secretion of interleukin (IL)-8 from lipopolysaccharide (LPS) stimulated human promonocytic THP-1 cells while selectively reducing IL-6 secretion. AF also reduces IL-6 dependent activation of janus kinase (JAK1 and JAK2) and subsequent phosphorylation of signal transducer and activator of transcription 3 (STAT-3)<sup>47,49,50</sup>. The anti-inflammatory activity of AF has been partially attributed to its effects on cyclooxygenase (COX) dependent prostaglandin (PGE<sub>2</sub>) production<sup>51</sup>. AF has been shown to differentially affect PGE<sub>2</sub> production by stimulating COX-1 dependent PGE<sub>2</sub> production while reducing COX-2 dependent PGE<sub>2</sub> production<sup>51</sup>. AF has also been shown to induce the anti-inflammatory enzyme heme-oxygenase (HOX)-1 in THP-1 cells<sup>48</sup>. Several other inflammatory pathways are modulated by AF and could contribute to its anti-inflammatory activity, including activation of mitogen activated protein kinases (MAPK), prevention of nuclear factor NF $\kappa$ B activation, and prevention of the induction of IL-1 $\beta$ <sup>53,57,58</sup>. Although their anti-inflammatory effects in the periphery are well known, the effects of gold compounds on neuroinflammation and in the CNS in general have yet to be determined. The lack of research in this area may be due to previous studies showing that gold compounds do not distribute well into the brain<sup>45</sup>.

Our current study investigated the effects of the gold compounds as inhibitors of human astrocyte-mediated neuroinflammation<sup>32</sup>. We investigated three of the clinically available gold compounds: ATM, ATG and AF, along with aurothiosulphate (ATS), a monovalent gold thiol compound similar to the other gold compounds tested<sup>157</sup> and shown to be ineffective as an anti-inflammatory drug. All compounds were tested for their direct toxicity and for their ability to reduce the cytotoxic secretions produced by activated human astrocytic cells. We also investigated the ability of the gold compounds to protect neurons from the toxicity induced by

supernatants from stimulated astrocytic cells as well as from the oxidative damage induced by hydrogen peroxide. Of the four gold compounds tested, only AF exhibited neuroprotective and also anti-neurotoxic activity by inhibiting secretion of toxins by astrocytic cells. Effects of AF on the secretion and expression of several cytokines including IL-6, IL-8, and monocyte chemotactic protein (MCP)-1 along with the expression of heme-oxygenase (HOX)-1 were also studied. The *in vivo* distribution of AF after its oral administration in mice was investigated using laser ablation inductively coupled plasma mass spectrometry (LA-ICP-MS) to assess the gold concentration achieved in the brain and several other tissues. This technique has previously been used to detect platinum-containing drugs in animal tissues <sup>46</sup>.

## Materials and methods

### 2.1. Reagents

AF was obtained from Cedarlane Canada (Burlington, ON, Canada) and the control salt ATS was obtained from VWR International (Mississauga, ON, Canada). The following substances were used in the various assays and were obtained from Sigma-Aldrich (Oakville, ON, Canada): ATM, ATG, dimethyl sulfoxide (DMSO), sulforhodamine B (SRB), Triton X-100, and MTT (3-(4,5-dimethylthiazol-2-yl)-2,5-diphenyl tetrazolium bromide). Human recombinant interferon (IFN)- $\alpha$ , human recombinant IL-1 $\beta$ , and anti-human IL-6 and IL-8 antibodies and recombinant protein standards used in the IL-6 and IL-8 enzyme linked immunoabsorbent assays (ELISA) were purchased from Peprotech (Rocky Hill, NJ, USA).

### 2.2. Cell culture

The human astrocytic U-118 MG and U-373 MG cells were obtained from the American Type Culture Collection (ATCC, Manassas, VA, USA). The human neuroblastoma SH-SY5Y cell line was a gift from Dr. R. Ross, Fordham University, NY. Human primary astrocytes were obtained from epileptic patients undergoing temporal lobe surgery. The specimens were from normal tissue overlying the epileptic foci. The use of human brain materials was approved by the Clinical Screening Committee for Human Subjects of the University of British Columbia (UBC). Astrocytes were isolated following protocols described by Hashioka *et al* .<sup>32</sup>. All cells were grown in Dulbecco's modified Eagle's medium-nutrient mixture F12 ham (DMEM-F12) supplemented with 10% fetal bovine serum (FBS) and an antibiotic solution (100 U/ml

penicillin, 100 µg/ml streptomycin) supplied by Thermo Scientific HyClone (Logan, UT, USA). The cell lines were used without differentiation.

### *2.3. Effects of gold compounds on U-118 MG, U-373 MG cell and human astrocyte viability and on IL-6 and IL-8 secretion by U-118 MG astrocytoma cells.*

Human astrocytic U-118 MG and U-373 MG cells were seeded onto 24-well plates at a concentration of  $2 \times 10^5$  cells/ml in 0.9 ml of DMEM-F12 containing 5% FBS and were incubated for 24 h before use in experiments to allow the cells to adhere. Human astrocytes were plated onto 6-well plates at  $2.5 \times 10^5$  cells/ml in 2 ml DMEM-F12 containing 5% FBS. The media was replaced following 24 h incubation. Cells were incubated in the presence or absence of various compounds or their vehicle solution (DMSO) for 15 min prior to addition of the activating stimulus (150 U/ml IFN- $\gamma$  for U-373 MG cells and human astrocytes or 150 U/ml IFN-  $\gamma$  plus 100 U/ml IL-1 $\beta$  for U-118 MG cells). The final concentration of DMSO in cell culture medium did not exceed 0.13%; at this concentration DMSO did not affect cell viability or function. Evaluation of the surviving cells after 48 h incubation was performed using the MTT assay. The concentrations of IL-6 and IL-8 (ng/ml) in 0.1 ml of U-118 MG cell supernatants were measured by ELISA according to the protocol provided by the supplier of the antibodies (Peprotech).

### *2.4. Cytotoxicity of supernatants from U-118 MG, U-373 MG cells and human astrocytes toward SH-SY5Y neuronal cells*

The experiments were performed as previously described<sup>13 86</sup>. Briefly, U-118 MG, U-373 MG and human astrocytes were seeded into 24- or 6-well plates and stimulated in the presence or absence of various compounds as described above. After 24 h or 48 h incubation, 0.4 ml of cell-free supernatant was transferred to each well containing SH-SY5Y cells that had been plated 24 h earlier at a concentration of  $2 \times 10^5$  cells/ml in 0.4 ml of DMEM-F12 medium containing 5% FBS. After 72 h incubation, neuronal cell viability was assessed by the MTT and SRB assays. SH-SY5Y cells in culture were also observed with an inverted phase contrast microscope (Motic, Richmond, BC, Canada) and photographed using Motic 3000 digital camera.

## 2.5. Protective activity of gold compounds on SH-SY5Y neuronal cells

SH-SY5Y cells were plated at  $2 \times 10^5$  cells/ml in 0.4 ml of DMEM-F12 medium containing 5% FBS. Following 24 h incubation, media was removed and replaced with fresh. Cells were treated with AF or its vehicle solution (DMSO) for 15 min prior to addition of 0.5 mM hydrogen peroxide. After additional 24 h incubation, the survival of neuronal cells was evaluated by the MTT assay.

In another series of experiments, supernatants from stimulated U-373 MG cells were used to induce neuronal cell death. U-373 MG cells were first plated at  $2 \times 10^5$  cells/ml in 15 ml of DMEM-F12 containing 5% FBS. Following 24 h incubation, media was removed and replaced with fresh media prior to the addition of the activating stimulus (150 U/ml IFN- $\gamma$ ). Following an additional 48 h incubation, 0.2 ml of cell-free supernatant and 0.2 ml of fresh media was transferred to each well containing SH-SY5Y cells. Immediately after transfer of supernatants, SH-SY5Y cells were treated with the various gold compounds or their vehicle solution (DMSO). Following 72 h incubation, the survival of neuronal cells was measured by the MTT assay. Direct effects of AF on neuronal cell viability were assessed by treating SH-SY5Y cells with AF or its vehicle solution (DMSO) for 72 h and evaluating survival of neuronal cells by the MTT assay.

## 2.6. Cell viability assay: Reduction of formazan dye (MTT)

The MTT assay was performed as previously described<sup>158,159</sup>. This assay is based on the ability of viable, but not dead, cells to convert the tetrazolium salt MTT to coloured formazan. The viability of cell cultures was determined by adding MTT to reach a final concentration of 0.5 mg/ml. Following a 1-2 h incubation at 37°C, the dark crystals which had formed were dissolved by adding an equal volume of SDS/DMF (20% sodium dodecyl sulphate, 50% N,N-dimethyl formamide, pH 4.7) to each well. The plates were then incubated at 37°C for 3 h. Optical densities were measured at 570 nm using a microplate reader after transferring 0.1 ml aliquots to 96-well plates. The viable cell value was calculated as a percent of the value obtained from cells incubated with fresh medium only.

## 2.7. Cell viability assay: Sulforhodamine B (SRB) Colorimetric Assay

The SRB assay was performed as previously described by Skehan *et al* .<sup>160</sup>. This assay is based on measuring total cellular protein. Briefly, supernatants from cell cultures were aspirated and 0.25 ml of 10% trichloroacetic acid: phosphate buffered saline (PBS) solution was added to each well followed by 1 h incubation at 4°C. Wells were aspirated and washed 4 times with H<sub>2</sub>O. 0.2 ml of 0.4% (w/v) SRB in 1% acetic acid was added to each well and plates were incubated for 10 min at room temperature. Plates were aspirated and washed 4 times with 1% acetic acid followed by addition of 0.2 ml of 10 mM Tris base solution (pH 10.5) to each well and plates were incubated for 30 min at room temperature. Optical densities were measured at 492 nm and 620nm using a microplate reader after transferring 0.1 ml aliquots to 96-well plates. The cell viability was calculated as a percent of the value obtained from cells incubated with fresh medium only.

## 2.8. RT-qPCR

U-373 MG cells were plated at  $2 \times 10^6$  cells/ml in 2 ml in 6-well plates and were either left unstimulated (DMSO vehicle control), treated with 1  $\mu$ M AF, stimulated with 150 U/ml IFN- $\gamma$  in the presence of DMSO vehicle control, or treated with 1  $\mu$ M AF before stimulation with IFN- $\gamma$ . Primary human astrocytes were plated at  $2.5 \times 10^5$  cells/ml and were treated as described for U-373 MG cells above with the exception that AF was added at 0.1  $\mu$ M. SH-SY5Y cells were plated at  $2 \times 10^6$  cells/ml in 2 ml in 6-well plates and were either left unstimulated (DMSO vehicle control), treated with 0.5  $\mu$ M AF, stimulated with 0.5 mM H<sub>2</sub>O<sub>2</sub> in the presence of DMSO vehicle control, or treated with 0.5  $\mu$ M AF before stimulation with 0.5 mM H<sub>2</sub>O<sub>2</sub>. mRNA was isolated from cells following 24 h incubation using the Aurum RNA extraction kit according to the manufacturer's instructions (Bio-Rad laboratories, Ltd., Mississauga, ON, Canada). The RNA was quantified by spectrophotometric analysis at 260/280nm using a NanoDrop 1000 (Thermo Scientific, Wilmington, DE) and converted to template cDNA using the qScript cDNA synthesis kit according to the manufacturer's protocols (Quanta Biosciences, Gaithersburg, MD). Primers with previously published sequences for IL-6, IL-8, MCP-1, HOX-1 and  $\beta$ -actin<sup>161,162</sup> were obtained from Integrated DNA Technologies (Vancouver, BC, Canada). The primers were checked for specificity using National Center for Biotechnology Information (NCBI) primer Basic Local Alignment Search Tool (BLAST) and were tested for optimal annealing

temperatures, primer dimer formation, and efficiency before being used in experiments as per minimum information for publication of quantitative real-time PCR experiments (MIQE) guidelines<sup>88</sup>. Quantitative PCR reactions were performed as previously described<sup>163</sup>. Expression of IL-6, IL-8, MCP-1 and HOX-1 in stimulated and AF-treated cells was normalized to the reference gene beta-actin and then compared to the mRNA found in unstimulated, DMSO vehicle-treated control cells, which were set to a value of one. Relative expression values were calculated using GeneExMacro OM 3.0 software (Bio-Rad) and the results shown as means  $\pm$  standard error of the mean (SEM).

## 2.9. Treatment of mice with AF and tissue preparation for LA-ICP-MS

Eight-week-old female C57BL/6 mice obtained from Jackson Laboratories (Bar Harbor, ME) were maintained at the UBC Center for Disease Modelling, Vancouver in sterilized, filter-topped cages in a temperature-controlled ( $22 \pm 2$  °C) facility with a 12 h light-dark cycle. Mice were maintained under pathogen-free conditions and fed a standard sterile chow (Laboratory Rodent Diet 5001, Purina Mills, St. Louis, MO) with access to tap water *ad libitum* throughout the experiments. All procedures involving the care and handling of mice were approved by the UBC Committee on Animal Care Ethics under the guidelines of the Canadian Council on the Use of Laboratory Animals. Three mice were administered 0.1 ml of 2 mg/kg AF dissolved in 10% ethanol once daily for 7 days by oral gavage while control mice were administered 10% ethanol solution only. Mice were euthanized at day 7 and the liver, spleen, kidneys, duodenum, lungs, and brain of each mouse were harvested, rinsed in PBS and stored frozen at -20°C. Small sections of frozen tissue were placed on a glass slide then homogenized by cutting repeatedly with a razor blade. The mass of the homogenized tissue was measured and 5 ppm platinum in 5% HNO<sub>2</sub> in PBS was added 1:1 (w/v). Each tissue/platinum sample was then vortexed and sonicated for 30 s. One  $\mu$ l of fully homogenized tissue/platinum suspension was pipetted on a glass slide with three replicate spots per tissue per experimental animal. Standards with known AF concentrations were also prepared by adding aliquots of serial dilutions of AF solutions to homogenized control tissues. The spots were allowed to dry for 24 h before being analyzed via LA-ICP-MS. The calibration curves for gold measured with the standards yielded correlation factors R<sup>2</sup> between 0.9662 - 0.9995.

## 2.10. LA-ICP-MS

A procedure similar to the previously described method used to measure distribution of platinum drug cisplatin in kidneys<sup>46</sup> was developed for use with AF. Murine tissues were ablated using an Analyte 193 argon-fluoride laser (Photon Machines Inc., Redmond, WA). Aerosols generated were transported by 600 ml/min He flow to an Element XR sector field ICP-MS (Thermo Scientific) for gold analysis. The wavelength of the laser was 193 nm (deep UV) and it was fired at 10 pulses/s focused to 148  $\mu\text{m}$  spot diameter, 50% power equivalent to 3.63 joules  $\text{cm}^{-2}$  and scanned across samples at a speed of 370  $\mu\text{m/s}$ . Counts for isotopes <sup>194</sup>Pt, <sup>195</sup>Pt and <sup>197</sup>Au were acquired for 18 s in low mass resolution, 1 sample per peak, 0.01 s dwell time, in speed mode. Blank data were acquired before sampling each standard or sample in the manner described above, except that the laser was not fired. Signal counts for <sup>197</sup>Au were normalized to the <sup>194</sup>Pt counts before blank subtraction.

## 2.11. Statistical analysis

Due to considerable variability in the absolute values obtained from independent experiments performed on different days, randomized block design Analysis of Variance (ANOVA) was used, followed by Fisher's least significant difference (LSD) post hoc test. For RT-qPCR experiments, a one-way ANOVA was performed on Ct values with Fisher's LSD as a post hoc test. Data are presented as means  $\pm$  SEM or standard deviation (SD). A P value less than 0.05 was considered statistically significant.

## Results

### 3.1. Effects of gold compounds on U-373 MG and U-118 MG astrocytic cell viability, cytotoxicity and cytokine secretion

Four gold compounds were tested for their ability to inhibit human astrocytic cell toxicity towards human neuronal SH-SY5Y cells. Compounds were tested at concentrations ranging from 0.5–5  $\mu\text{M}$  and results were compared to those obtained from samples treated with DMSO vehicle solution only. At the concentrations used (<0.13%, v/v), DMSO alone had no detectable effects in the assays used (data not shown). The compounds were added to U-373 MG cells 15 min before stimulation with IFN- $\gamma$ . Following 48 h incubation, viability of U-373 cells was assessed

by the MTT assay (Fig.1A). ATS was moderately toxic to U-373 MG cells at 0.5  $\mu$ M. AF, ATM, and ATG were not toxic to stimulated U-373 MG cells at the concentrations tested.

Cell-free supernatants from the U-373 MG astrocytic cell cultures were transferred to SH-SY5Y neuroblastoma cells to assess their cytotoxicity. Following a 72 h incubation period, the viability of neuronal cells was measured using the MTT assay (Fig. 1B). Supernatants from unstimulated U-373 MG cells did not significantly affect the viability of SH-SY5Y cells (see dashed line on Fig. 1B). As reported previously<sup>32</sup>, transfer of cell-free supernatants from stimulated U-373 MG cells to SH-SY5Y cells resulted in significantly reduced neuronal cell viability (Fig. 1B). IFN- $\gamma$  was used to achieve maximal stimulation of cells<sup>32</sup>. Fig. 1B illustrates that ATM, ATG, and ATS did not have any anti-neurotoxic activity while AF inhibited the toxicity of stimulated U-373 MG supernatants at the 1 – 5  $\mu$ M range ( $IC_{50}$  = 1  $\mu$ M). The anti-neurotoxic activity of AF was not due to its toxicity towards astrocytic cells but was most likely due to specific inhibition of the U-373MG cytotoxic secretions. SRB assay was used to confirm SH-SY5Y and U-373 MG cell viability data obtained by the MTT assay and it yielded similar results (data not shown).

Phase contrast microscopy images were also taken of SH-SY5Y cells after incubation with U-373 MG cell supernatants. Fig. 2B illustrates the density and morphology of SH-SY5Y cells incubated with unstimulated supernatant, Fig. 2C illustrates SH-SY5Y cells after incubation with stimulated supernatant and DMSO vehicle control, and Fig. 2D illustrates SH-SY5Y cells after incubation with stimulated supernatant and 2  $\mu$ M AF. The morphology and density of SH-SY5Y cells treated with AF and stimulated supernatant appears more similar to unstimulated SH-SY5Y cells than to those exposed to stimulated U-373 MG cell supernatants. The anti-neurotoxic effect of AF was confirmed using a different human astrocytoma cell line (U-118 MG) stimulated with a combination of IFN- $\gamma$  and IL-1 $\beta$ . Similar to its effects on U-373 MG cells, AF was able to reduce the toxicity of U-118 MG cells towards the SH-SY5Y cells at non-toxic concentrations of 1 - 2  $\mu$ M ( $IC_{50}$  = 0.5 - 1  $\mu$ M , data not shown).

ELISA was used to measure concentrations of IL-6 and IL-8 in supernatants of U-373 MG and U-118 MG cells after 48 h stimulation with IFN- $\gamma$  or IFN- $\gamma$  plus IL-1 $\beta$  respectively. AF did not significantly affect the secretions of either of these cytokines by stimulated U-118 MG and U-373 MG cells (data not shown).

### *3.2. AF reduces cytotoxic secretions of primary human astrocytes*

The anti-neurotoxic effect of AF was confirmed using primary human astrocytes prepared from surgical brain tissue samples. AF was applied at 0.1  $\mu\text{M}$  since our previous studies have shown that primary glial cells are more sensitive to lower drug concentrations than human cell lines used as their surrogates<sup>62,92</sup>. Furthermore, previous pharmacokinetic studies have shown low AF concentrations in the brain following oral administration (see Table 1 and Walz *et al.* 1983<sup>45</sup>). The MTT assay was used to confirm that at 0.1  $\mu\text{M}$  AF did not reduce viability of human astrocytes (data not shown), but it significantly reduced the toxicity of supernatants from stimulated human astrocytes towards SH-SY5Y cells (Fig. 2A).

### *3.3. AF protects SH-SY5Y neuronal cells against toxicity induced by hydrogen peroxide and supernatants from stimulated U-373 MG cells*

The direct neuroprotective effect of AF on cultured SH-SY5Y cells was assessed by exposing neuronal cells to hydrogen peroxide in the presence of 0.1 – 1  $\mu\text{M}$  AF (Fig. 3A) and by adding AF to supernatants from stimulated U-373 MG cells at the time of their transfer to SH-SY5Y cells (Fig. 3B). In both cases, AF at 0.5 and 1  $\mu\text{M}$  significantly increased viability of SH-SY5Y cells (Fig. 3B). Figure 3C demonstrates that at the concentrations studied AF had no direct effect on SH-SY5Y cell viability in the absence of hydrogen peroxide or astrocyte-derived toxins.

### *3.4. AF upregulates HOX-1 mRNA expression in U-373 MG cells, human astrocytes and SH-SY5Y neuronal cells*

Figure 4 illustrates that 24 h incubation of U-373 MG cells and human astrocytes in the presence of AF significantly upregulated HOX-1 mRNA expression. RT-qPCR analysis indicated that 1  $\mu\text{M}$  AF upregulated HOX-1 expression in unstimulated U-373 MG cells more than 75 fold, compared to DMSO solvent-treated cells (Fig. 4A). Similarly, treatment of human astrocytes with 0.1  $\mu\text{M}$  AF resulted in more than 2 fold upregulation of HOX-1 in human astrocytes (Fig. 4B). Stimulation of U-373 MG cells or human astrocytes with IFN- $\gamma$  alone did not induce a significant increase in HOX-1 expression. However, combining AF and IFN- $\gamma$  treatments resulted in further doubling of HOX-1 mRNA levels compared to treatment with AF alone, which resulted in nearly 150 fold increase in HOX-1 expression in U-373 MG cells and a

more than 7 fold increase in HOX-1 expression in human astrocytes compared to unstimulated cells (Fig. 4A,B).

Exposure of human neuronal SH-SY5Y cells to 0.5  $\mu$ M AF did not cause increase in HOX-1 expression. However, when neuronal cells were exposed to 0.5  $\mu$ M AF in the presence of partially toxic (0.5 mM) concentration of H<sub>2</sub>O<sub>2</sub>, HOX-1 expression was increased 10 fold compared to H<sub>2</sub>O<sub>2</sub> stimulated cells treated with DMSO vehicle solution only (Fig. 4C). RT-qPCR analysis showed that there were no significant changes in the expression of MCP-1, IL-6, or IL-8 in U-373 MG cells following 24 h treatment with 1  $\mu$ M AF (data not shown).

### 3.5. *In vivo* distribution of AF after its oral administration in mice

Mice were monitored for morbidity throughout the 7 day treatment with AF and none showed any symptoms compared to control mice. Mice were weighed immediately prior to treatment each day throughout the 7 day treatment and none showed any differences in weight gain compared to control mice. Macroscopic examination of gastrointestinal tract and liver at the end of the treatment revealed no ulcers or any other visible pathology. Table 1 shows data obtained by LA-ICP-MS from three mice and compares concentrations measured by this technique in six different tissues with data obtained by Walz *et al* . who used radioactively labelled AF for their studies with rats<sup>45</sup>. The highest gold concentration was measured in kidneys (248  $\mu$ M) and the lowest concentration (4.8  $\mu$ M) in the brain.

## Discussion

Several gold compounds used in the treatment of RA were investigated for their potential to reduce neuroinflammation using an *in vitro* model relevant to the inflammatory processes that occur in degenerative conditions. We found that at non-toxic, low micromolar concentrations (1-5  $\mu$ M) AF reduced the toxicity of both stimulated U-373 MG and U-118 MG astrocytic cells towards neurons, indicating a potential protective effect of AF. This effect was not observed with ATM, ATG or ATS. At a lower concentration of 0.1  $\mu$ M, AF effectively inhibited the toxicity of stimulated primary human astrocytes towards neuronal cells.

The anti-inflammatory activities of AF and other gold compounds have been well studied using several different assays relevant to the peripheral immune response and are summarized in several excellent reviews<sup>28,30,45</sup>. Here we demonstrate for the first time that due to its ability to selectively inhibit the release of toxins from stimulated human astrocytic cells and primary astrocytes, AF has the potential to reduce the neurotoxicity associated with neuroinflammatory responses observed in degenerative disorders of the CNS.

Our observation that of the gold compounds studied, only AF inhibited toxic secretions agrees with the previous research showing that AF may have biological activities different from other clinically used gold compounds. For example, Walz *et al* . demonstrated that AF and ATM, but not ATG, were able to reduce the secretion of lysosomal enzymes from polymorphonuclear cells<sup>45</sup>. Furthermore, AF inhibited antibody-dependent cellular cytotoxicity of polymorphonuclear cells and release of reactive oxygen species from neutrophils while ATM, ATG, and the ligands of auranofin showed no effect<sup>94</sup>. It has been previously demonstrated that AF has immunosuppressive activity, such as the ability to inhibit lymphoblastogenesis, an effect not observed with other gold compounds<sup>95</sup>. Thus the difference in activities between the gold compounds was not unexpected, and subsequent experiments were performed to elucidate the mechanism of the protective activity of AF.

The anti-neurotoxic effect of AF was observed at 0.1  $\mu\text{M}$  in primary human astrocytes and at 1-5  $\mu\text{M}$  in human astrocytic cells. Our previous research using a similar assay has shown that primary astrocytes could be more sensitive to anti-inflammatory drug treatment than cell lines<sup>62,92</sup>. The effect of AF at low micromolar concentrations has been demonstrated in several different assays. For example, Kim *et al* . showed that 0.2  $\mu\text{M}$  AF effectively blocked STAT-3 signalling in rat astrocytes<sup>48</sup>. Stern *et al* . showed that at 0.1  $\mu\text{M}$ , AF was able to increase the secretion of IL-6 in lipopolysaccharide stimulated THP-1 cells, while a higher concentration range (5 - 25  $\mu\text{M}$ ) was required to achieve similar effects using ATM<sup>50</sup>.

Interestingly, treating SH-SY5Y neuronal cells with 0.5 - 1  $\mu\text{M}$  AF protected them from hydrogen peroxide-induced toxicity with similar doses of AF being protective against toxicity induced by supernatants from stimulated U-373 MG cells. Such direct protective effect of AF on neurons or neuronal cells has not been reported previously and our observations may indicate that AF confers neuroprotective activity in addition to its better-known and accepted anti-

inflammatory effects. The direct protective activity of AF could be partially responsible for its anti-neurotoxic effects on astrocytic cells since some AF may be transferred onto neuronal cells along with the supernatants. However, this is unlikely the sole reason for the anti-neurotoxic activity of AF since this drug effectively inhibited primary astrocyte toxicity at 0.1  $\mu$ M, a concentration that was ineffective at rescuing neuronal cells from the toxicity of astrocytic cell supernatants.

Previous research has highlighted several molecular mechanisms responsible for the protective effects of AF, including preventing the oxidative inactivation of tissue inhibitor of metalloproteinase 1 (TIMP-1). By maintaining TIMP-1 integrity, AF could prevent the damage induced by matrix metalloproteinases (MMP) such as the neurotoxic MMP-1 released by stimulated astrocytes<sup>79,164</sup>. In addition, Ashino *et al* . demonstrated that AF was able to protect against cocaine-induced hepatic injury both in mice and in cultured hepatocytes by upregulating the protective enzyme HOX-1<sup>78</sup>. We therefore investigated HOX-1 induction as a potential mechanism for the protective activity of AF observed in our experiments. As stimulated astrocytes undergo oxidative stress, upregulation of HOX-1 would protect them against associated damage. In addition, HOX-1 has been reported to have anti-inflammatory effects which could also contribute to the decreased toxicity of astrocytes towards neurons<sup>42,78,113</sup>. In addition to decreasing the toxicity of astrocytes, upregulation of HOX-1 could be protective in neurons. Yamamoto *et al* . demonstrated that HOX-1 induction protected dopaminergic neurons in an *in vitro* model of Parkinson's disease<sup>33</sup>. Our study demonstrated that AF induced HOX-1 expression in both stimulated and unstimulated primary human astrocytes and U-373 MG cells. We also showed that AF was able to induce HOX-1 expression above a vehicle control in SH-SY5Y neuronal cells exposed to a toxic concentration of hydrogen peroxide. Therefore, upregulation of HOX-1 could be at least partially responsible for the biological activity of AF observed in our study.

Apart from HOX-1 induction, several other cellular mechanisms of action have been reported for AF, including modulation of the expression and release of inflammatory cytokines such as IL-6 and IL-8 by human THP-1 monocytic cells and murine RAW 264.5 macrophages<sup>47,50,78</sup>. However, treatment of U-373 MG astrocytic cells with AF did not affect the expression or secretion of several pro-inflammatory cytokines, including MCP-1, IL-6 and IL-8 (data not

shown). This indicates that the anti-neurotoxic effects of AF on astrocytes were selective and also rules out direct toxicity of AF as the cause for this effect. Furthermore, these observations may suggest that the effects of AF on glial cells and neuroinflammation are different from its effects on peripheral immune cells.

Finally, we studied the distribution of gold (Au) in mice treated with AF to determine whether AF is able to penetrate the blood brain barrier. Previous studies by Walz *et al.* indicated that following daily oral administration of 1 mg/kg AF in rats for 5 days, the level of Au was highest in the kidneys (30  $\mu\text{M}$ , see Table 1) while only a very small amount of Au entered the brain, reaching a concentration of 0.05  $\mu\text{M}$ <sup>45</sup>. We performed similar experiments administering AF at 2 mg/kg to mice for 7 days and were able to detect Au in all tissues studied (Table 1) using LA-ICP-MS-based measurements<sup>46</sup>. Similar to Walz *et al.*, we found Au to be the most concentrated in the kidneys, but we measured a concentration almost 10 times greater (249 vs. 30  $\mu\text{M}$ )<sup>45</sup>. Compared to the values reported by Walz *et al.*, the concentrations of Au detected by LA-ICP-MS in our studies were greater for all tissues studied<sup>45</sup>. This difference was especially pronounced in the brain, with our measurements indicating Au levels at 5  $\mu\text{M}$  while 0.05  $\mu\text{M}$  Au was detected by Walz *et al.*<sup>45</sup>. In addition to concentration differences, the relative order of distribution of Au according to concentration in the liver, lungs, gut, and spleen did not match that reported by Walz *et al.*<sup>45</sup>. These discrepancies could be due to the use of different animal species (rats vs. mice) and/or differences in the duration and dose of AF treatment. AF has been reported to have a long half-life of approximately 17 days in humans<sup>119</sup>; therefore, there could be significant differences in tissue accumulation of AF between 5 and 7 day treatment regimens<sup>44,119</sup>.

Differences in the techniques used to detect Au could also have contributed to the discrepancies. LA-ICP-MS directly measures the total number of unlabeled Au atoms in a tissue sample by comparing the signals obtained from experimental tissue samples with those obtained from preparations with known Au concentrations. On the other hand, the radioactively-labeled AF technique used by Walz *et al.* involves administration of a mixture of labeled and unlabeled AF and several steps of sample preparation before measurements can be performed, thus it is a less direct measurement of Au than LA-ICP-MS<sup>45</sup>. Both techniques measure Au concentration as opposed to concentration of intact AF molecules as neither of the techniques is able to

distinguish between AF and its metabolites, including Au as a breakdown product of AF<sup>29,45</sup>. Therefore, further studies are required to establish whether intact AF can enter brain tissue. Similar techniques have been used to establish that the available circulating levels of Au in patients being treated with AF can reach approximately 0.4  $\mu\text{M}$ <sup>44</sup>, which exceeds the 0.1  $\mu\text{M}$  AF concentration required to reduce astrocyte toxicity in our model.

As AF is known to accumulate in tissue over time and our study indicates that Au passes through the blood brain barrier, it is feasible that levels of AF in the brain could reach concentrations effective at reducing astrocyte-mediated toxicity. The relatively low  $\text{IC}_{50}$  of AF as well as the possibility that it is able to cross the blood brain barrier makes it a good candidate for treating inflammation in the CNS.

The present study demonstrates that the gold compound AF is able to reduce human astrocyte-mediated toxicity and that it has neuroprotective properties *in vitro*. These novel *in vitro* properties of AF, as well as the *in vivo* data confirming earlier studies suggesting that AF is able to cross the blood brain barrier, warrant further testing of AF in an animal model of neuroinflammation. Anti-inflammatory intervention has the potential to slow neuronal loss in disorders such as Parkinson's and Alzheimer's diseases where neuroinflammation contributes to pathogenesis<sup>85,121</sup>. As AF has already been approved for use in humans in several countries and is considered by medical practitioners to have an acceptable safety profile in the management of some disease states<sup>93</sup>, it would be an excellent compound to investigate for the treatment of neuroinflammatory conditions as an alternative to steroidal and non-steroidal anti-inflammatory drugs.

#### Acknowledgments

This work was supported by grants from the Natural Sciences and Engineering Research Council of Canada and the Jack Brown and Family Alzheimer's Disease Research Foundation. We would like to thank Ms. J. Lamothe for technical assistance, Ms. N. Gill for help with preparation of the manuscript, Dr. M. Rheault for advice with quantitative PCR, and Dr. W.F. Kean for helpful comments on the manuscript.

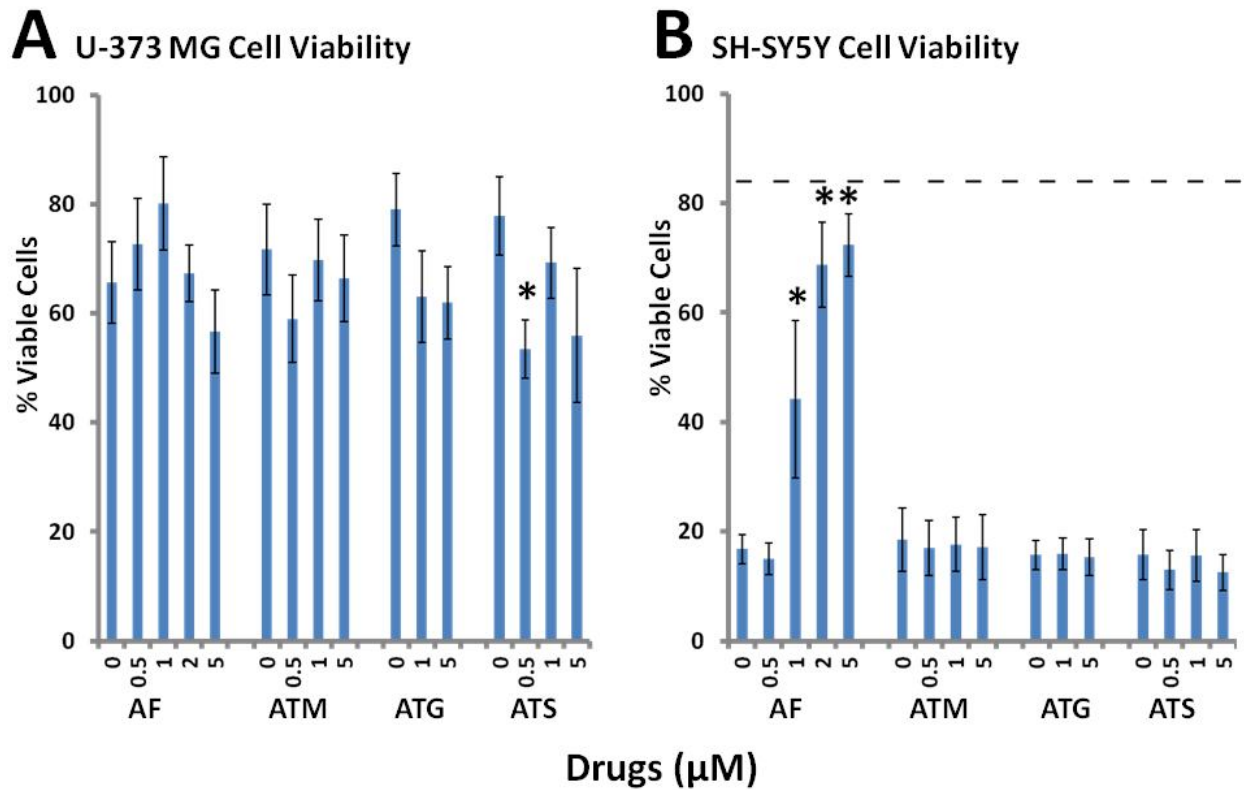


Fig. 1. AF is non-toxic to human U-373 MG astrocytoma cells and reduces toxicity of secretions from U-373 MG cells towards SH-SY5Y neuronal cells. Adherent astrocytoma cells were pre-treated with various concentrations of the gold compounds or their vehicle solution (DMSO) for 15 min before stimulation with IFN- $\gamma$  (150 U/ml). After 48 h incubation, the U-373 MG cell viability was assessed by the MTT assay (A) and 0.4 ml of cell-free supernatants was applied to SH-SY5Y cells. Survival of neuronal cells was assessed 72 h later by the MTT assay (B). Data from 4 independent experiments are presented. The horizontal dashed line indicates viability of SH-SY5Y cells exposed to supernatants from unstimulated U-373 MG cells (B). The concentration-dependent effects of the compound were assessed by the randomized block design ANOVA, followed by Fisher's LSD post hoc test. \*  $P < 0.05$ , significantly different from samples treated with the vehicle solution only.

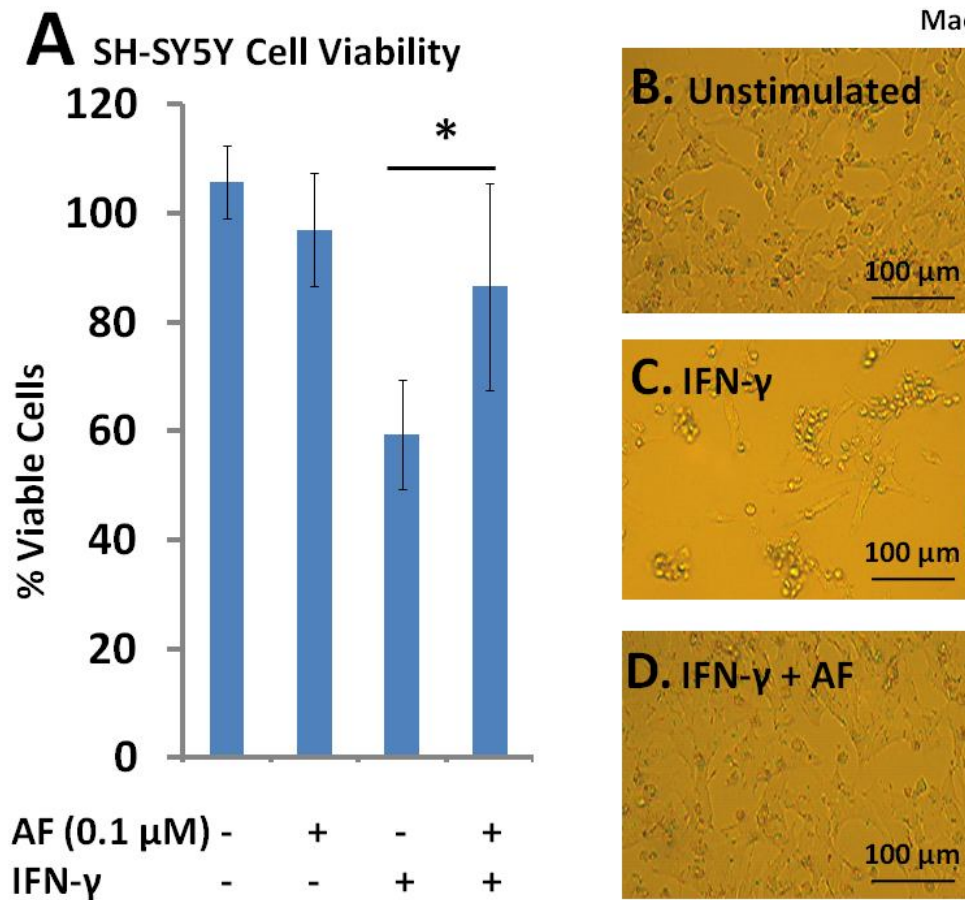
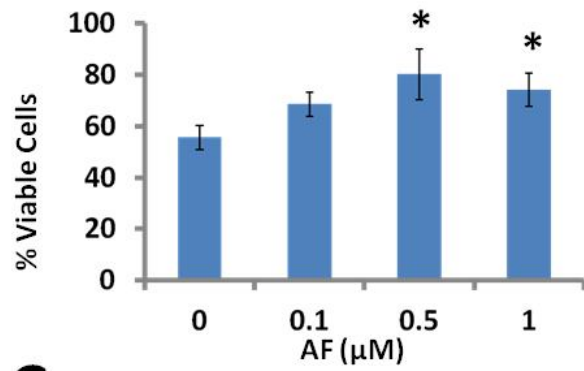
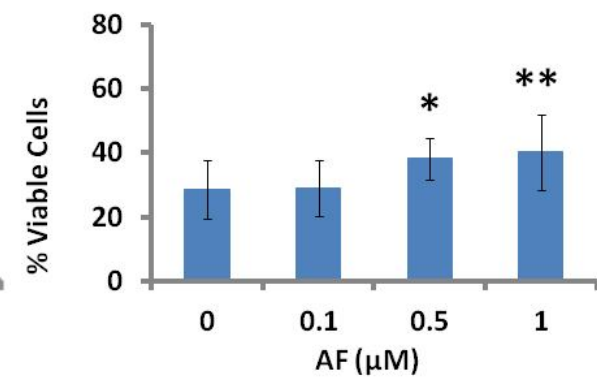


Fig. 2. AF reduces cytotoxic secretions of primary human astrocytes and restores SH-SY5Y morphology after treatment with stimulated U-373 MG cell supernatants. The effects of AF on the viability of SH-SY5Y neuronal cells exposed to supernatants from primary human astrocytes stimulated with IFN- $\gamma$  in the presence or absence of 0.1  $\mu\text{M}$  AF was examined (A). Data from 5 independent experiments with cells obtained from two different surgical cases are presented. The effects of AF were assessed by the randomized block design ANOVA, followed by Fishers LSD post-hoc test \*  $P < 0.05$ , significantly different from stimulated samples treated with the vehicle solution only. Phase contrast microscopy of SH-SY5Y cell cultures after incubation with unstimulated U-373 MG supernatant (B) IFN- $\gamma$  stimulated U-373 MG supernatant (C) and IFN- $\gamma$  stimulated with 2  $\mu\text{M}$  AF U-373 MG supernatant (D). Experiments were performed as described in Fig. 1. Photos are representative of 3 independent experiments. Magnification bars in B-D = 100  $\mu\text{m}$ .

**A** Hydrogen Peroxide



**B** Supernatant from Stimulated U-373 MG



**C** Untreated SH-SY5Y Cells

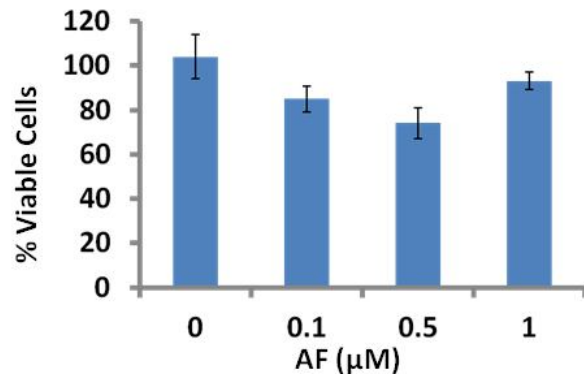


Fig. 3. AF protects SH-SY5Y neuronal cells against toxicity induced by hydrogen peroxide and supernatants from stimulated U-373 MG cells. The effects of gold compounds on viability of SH-SY5Y neuronal cells exposed to hydrogen peroxide, stimulated U-373 MG astrocytoma supernatants, or untreated neuronal cells were examined. A – AF (0.1 - 1  $\mu$ M), or its vehicle solution (DMSO), was added 15 min prior to the addition of 0.5 mM hydrogen peroxide. B - AF (0.1 - 1  $\mu$ M) or its vehicle solution (DMSO) were added to supernatants from stimulated U-373 MG cells at the time of their transfer to SH-SY5Y cell cultures. C - AF (0.1 - 1  $\mu$ M), or its vehicle solution (DMSO), was added to unstimulated SH-SY5Y cells. Viability of neuronal cells was assessed by the MTT assay 24 h (A) or 72 h (B, C) later. Data from 3-5 independent experiments are presented; the concentration-dependent effects of the compounds were assessed by the randomized block design ANOVA, followed by Fishers LSD post-hoc test. \*  $P < 0.05$ , \*\* $P < 0.01$  significantly different from samples treated with the vehicle solution only.

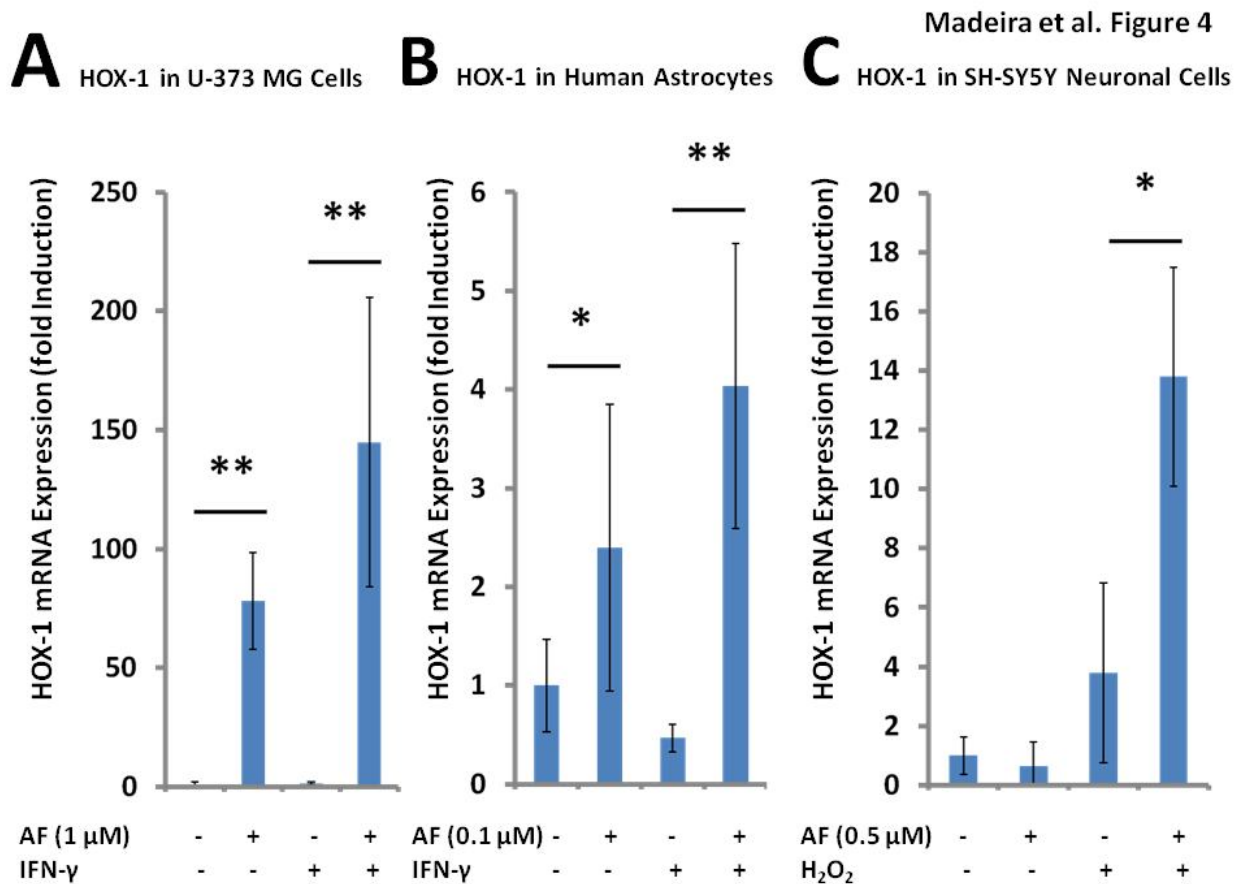


Fig. 4. AF upregulates heme oxygenase (HOX-1) mRNA expression in unstimulated and stimulated U-373 MG astrocytic cells and primary human astrocytes as well as in hydrogen peroxide stimulated SH-SY5Y neuronal cells. U-373 MG cells (A), human astrocytes (B), and SH-SY5Y neuronal cells (C) were treated with either AF or DMSO vehicle solutions. Astrocytic cells were either left unstimulated or were stimulated with IFN- $\gamma$  (150 U ml<sup>-1</sup>). Neuronal cells were treated with 0.5 mM hydrogen peroxide. Total RNA was extracted 24 h later and the HOX-1 mRNA expression was analyzed by using specific primers and RT-qPCR. Results were normalized to a reference gene  $\beta$ -actin and are presented as a fold increase compared to the HOX-1 mRNA level in control unstimulated cells not exposed to AF (expression level = 1). Data from 3-5 independent experiments are presented; the observed differences in expression levels were assessed by the randomized block design ANOVA, followed by Fishers LSD post-hoc test \* P<0.05; \*\* P<0.01, significantly different from samples treated with the vehicle solution only.

## References

- Ashino, T., Sugiuchi, J., Uehara, J., Naito-Yamamoto, Y., Kenmotsu, S., Iwakura, Y., Shioda, S., Numazawa, S., Yoshida, T., 2011. Auranofin protects against cocaine-induced hepatic injury through induction of heme oxygenase-1. *J Toxicol Sci* 36, 635-643.
- Block, M.L., Zecca, L., Hong, J.S., 2007. Microglia-mediated neurotoxicity: uncovering the molecular mechanisms. *Nat Rev Immunol* 8, 57-69.
- Blocka, K., 1983. Auranofin versus injectable gold. Comparison of pharmacokinetic properties. *Am J Med* 75, 114-122.
- Bruze, M., Bjorkner, B., Moller, H., 1995. Skin testing with gold sodium thiomalate and gold sodium thiosulfate. *Contact Dermatitis* 32, 5-8.
- Bustin, S.A., Benes, V., Garson, J.A., Hellems, J., Huggett, J., Kubista, M., Mueller, R., Nolan, T., Pfaffl, M.W., Shipley, G.L., Vandesompele, J., Wittwer, C.T., 2009. The MIQE guidelines: minimum information for publication of quantitative real-time PCR experiments. *Clin Chem* 55, 611-622.
- Cameron, B., Landreth, G.E., 2010. Inflammation, microglia, and Alzheimer's disease. *Neurobiol Dis* 37, 503-509.
- Champion, G.D., Graham, G.G., Ziegler, J.B., 1990. The gold complexes. *Baillieres Clin Rheumatol* 4, 491-534.
- Chien, W.L., Lee, T.R., Hung, S.Y., Kang, K.H., Lee, M.J., Fu, W.M., 2011. Impairment of oxidative stress-induced heme oxygenase-1 expression by the defect of Parkinson-related gene of PINK1. *J Neurochem* 117, 643-653.
- Crooke, S.T., 1982. A comparison of the molecular pharmacology of gold and platinum complexes. *J Rheumatol* 9, 61-70.
- Cuadrado, A., Rojo, A.I., 2008. Heme oxygenase-1 as a therapeutic target in neurodegenerative diseases and brain infections. *Curr Pharm Des* 14, 429-442.

- Finkelstein, A.E., Roisman, F.R., Batista, V., de Nudelman, F.G., de Titto, E.H., Mizraji, M., Walz, D.T., 1980. Oral chrysotherapy in rheumatoid arthritis: minimum effective dose. *J Rheumatol* 7, 160-168.
- Frohman, E.M., Racke, M.K., Raine, C.S., 2006. Multiple sclerosis--the plaque and its pathogenesis. *N Engl J Med* 354, 942-955.
- Glennas, A., Kvien, T.K., Andrup, O., Clarke-Jenssen, O., Karstensen, B., Brodin, U., 1997. Auranofin is safe and superior to placebo in elderly-onset rheumatoid arthritis. *Br J Rheumatol* 36, 870-877.
- Han, S., Kim, K., Kim, H., Kwon, J., Lee, Y.H., Lee, C.K., Song, Y., Lee, S.J., Ha, N., 2008. Auranofin inhibits overproduction of pro-inflammatory cytokines, cyclooxygenase expression and PGE2 production in macrophages. *Arch Pharm Res* 31, 67-74.
- Hansen, M.B., Nielsen, S.E., Berg, K., 1989. Re-examination and further development of a precise and rapid dye method for measuring cell growth/cell kill. *Journal of Immunological Methods* 119, 203-210.
- Hashioka, S., Klegeris, A., McGeer, P.L., 2009a. Proton pump inhibitors exert anti-inflammatory effects and decrease human microglial and monocytic THP-1 cell neurotoxicity. *Exp Neurol* 217, 177-183.
- Hashioka, S., Klegeris, A., McGeer, P.L., 2011. Proton pump inhibitors reduce interferon-gamma-induced neurotoxicity and STAT3 phosphorylation of human astrocytes. *GLIA* 59, 833-840.
- Hashioka, S., Klegeris, A., Schwab, C., McGeer, P.L., 2009b. Interferon-gamma-dependent cytotoxic activation of human astrocytes and astrocytoma cells. *Neurobiol Aging* 30, 1924-1935.
- Hayashi, F., Means, T.K., Luster, A.D., 2003. Toll-like receptors stimulate human neutrophil function. *Blood* 102, 2660-2669.
- Jeon, K.I., Jeong, J.Y., Jue, D.M., 2000. Thiol-reactive metal compounds inhibit NF-kappa B activation by blocking I kappa B kinase. *J Immunol* 164, 5981-5989.

- Kean, W.F., 1990. Intramuscular versus oral gold therapy. *Baillieres Clin Rheumatol* 4, 219-246.
- Kean, W.F., Hart, L., Buchanan, W.W., 1997. Auranofin. *Br J Rheumatol* 36, 560-572.
- Kean, W.F., Kean, I.R., 2008. Clinical pharmacology of gold. *Inflammopharmacology* 16, 112-125.
- Kim, N.H., Lee, M.Y., Park, S.J., Choi, J.S., Oh, M.K., Kim, I.S., 2007. Auranofin blocks interleukin-6 signalling by inhibiting phosphorylation of JAK1 and STAT3. *Immunology* 122, 607-614.
- Kim, N.H., Oh, M.K., Park, H.J., Kim, I.S., 2010. Auranofin, a gold(I)-containing antirheumatic compound, activates Keap1/Nrf2 signaling via Rac1/iNOS signal and mitogen-activated protein kinase activation. *J Pharmacol Sci* 113, 246-254.
- Klegeris, A., Bissonnette, C.J., McGeer, P.L., 2003. Reduction of human monocytic cell neurotoxicity and cytokine secretion by ligands of the cannabinoid-type CB2 receptor. *British Journal of Pharmacology* 139, 775-786.
- Krause, D., Suh, H.S., Tarassishin, L., Cui, Q.L., Durafourt, B.A., Choi, N., Bauman, A., Cosenza-Nashat, M., Antel, J.P., Zhao, M.L., Lee, S.C., 2011. The tryptophan metabolite 3-hydroxyanthranilic acid plays anti-inflammatory and neuroprotective roles during inflammation: role of hemeoxygenase-1. *Am J Pathol* 179, 1360-1372.
- Lee, Y.J., Han, S.B., Nam, S.Y., Oh, K.W., Hong, J.T., 2010. Inflammation and Alzheimer's disease. *Arch Pharm Res* 33, 1539-1556.
- Li, C., Zhao, R., Gao, K., Wei, Z., Yin, M.Y., Lau, L.T., Chui, D., Hoi Yu, A.C., 2011. Astrocytes: implications for neuroinflammatory pathogenesis of Alzheimer's disease. *Curr Alzheimer Res* 8, 67-80.
- Madeira, J.M., Beloukhina, N., Boudreau, K., Boettcher, T.A., Gurley, L., Walker, D.G., McNeil, W.S., Klegeris, A., 2012. Cobalt(II) beta-ketoamino complexes as novel inhibitors of neuroinflammation. *Eur J Pharmacol* 676, 81-88.

- Mosmann, T., 1983. Rapid colorimetric assay for cellular growth and survival: application to proliferation and cytotoxicity assays. *Journal of Immunological Methods* 65, 55-63.
- Nakaya, A., Sagawa, M., Muto, A., Uchida, H., Ikeda, Y., Kizaki, M., 2011. The gold compound auranofin induces apoptosis of human multiple myeloma cells through both down-regulation of STAT3 and inhibition of NF-kappaB activity. *Leuk Res* 35, 243-249.
- Papp, K.A., Shear, N.H., 1991. Systemic gold therapy. *Clin Dermatol* 9, 535-551.
- Park, S.J., Kim, I.S., 2005. The role of p38 MAPK activation in auranofin-induced apoptosis of human promyelocytic leukaemia HL-60 cells. *Brit J Pharmacol* 146, 506-513.
- Roisman, F.R., Walz, D.T., Finkelstein, A.E., 1983. Superoxide radical production by human leukocytes exposed to immune complexes: inhibitory action of gold compounds. *Inflammation* 7, 355-362.
- Saijo, K., Glass, C.K., 2011. Microglial cell origin and phenotypes in health and disease. *Nat Rev Immunol* 11, 775-787.
- Shabani, F., McNeil, J., Tippett, L., 1998. The oxidative inactivation of tissue inhibitor of metalloproteinase-1 (TIMP-1) by hypochlorous acid (HOCl) is suppressed by anti-rheumatic drugs. *Free Radic Res* 28, 115-123.
- Skehan, P., Storeng, R., Scudiero, D., Monks, A., McMahon, J., Vistica, D., Warren, J.T., Bokesch, H., Kenney, S., Boyd, M.R., 1990. New colorimetric cytotoxicity assay for anticancer-drug screening. *J Natl Cancer Inst* 82, 1107-1112.
- Stern, I., Wataha, J.C., Lewis, J.B., Messer, R.L., Lockwood, P.E., Tseng, W.Y., 2005. Anti-rheumatic gold compounds as sublethal modulators of monocytic LPS-induced cytokine secretion. *Toxicol In Vitro* 19, 365-371.
- Vos, C.M., Sjulson, L., Nath, A., McArthur, J.C., Pardo, C.A., Rothstein, J., Conant, K., 2000. Cytotoxicity by matrix metalloprotease-1 in organotypic spinal cord and dissociated neuronal cultures. *Exp Neurol* 163, 324-330.

- Walz, D.T., Dimartino, M.J., Griswold, D.E., Intoccia, A.P., Flanagan, T.L., 1983. Biologic actions and pharmacokinetic studies of auranofin. *Am J Med* 75, 90-108.
- Yamamoto, N., Izumi, Y., Matsuo, T., Wakita, S., Kume, T., Takada-Takatori, Y., Sawada, H., Akaike, A., 2010. Elevation of heme oxygenase-1 by proteasome inhibition affords dopaminergic neuroprotection. *J Neurosci Res* 88, 1934-1942.
- Yamashita, M., Niki, H., Yamada, M., Watanabe-Kobayashi, M., Mue, S., Ohuchi, K., 1997. Dual effects of auranofin on prostaglandin E2 production by rat peritoneal macrophages. *Eur J Pharmacol* 325, 221-227.
- Zilka, N., Kazmerova, Z., Jadhav, S., Neradil, P., Madari, A., Obetkova, D., Bugos, O., Novak, M., 2012. Who fans the flames of Alzheimer's disease brains? Misfolded tau on the crossroad of neurodegenerative and inflammatory pathways. *J Neuroinflammation* 9, 47.
- Zoriy, M., Matuschb, A., Sprussc, T., Becker, J. S., 2007. Laser ablation inductively coupled plasma mass spectrometry for imaging of copper, zinc, and platinum in thin sections of a kidney from a mouse treated with cis-platin. *Int J Mass Spectrom* 260, 102-106.

**Appendix D:** Article published in J. Alzheim. Dis. (2012) 30, Suppl. 2: S179-S183

The saturated fatty acid palmitate induces human monocytic cell toxicity towards neuronal cells:  
exploring a possible link between obesity-related metabolic impairments and neuroinflammation

Jonathan P. Little<sup>a\*</sup>, Jocelyn M. Madeira<sup>a</sup>, Andis Klegeris<sup>a</sup>

<sup>a</sup>Department of Biology, I.K. Barber School of Arts and Sciences, University of British  
Columbia Okanagan, Kelowna, BC, CANADA

*Running Title:* Palmitate-induced neurotoxicity

\*Corresponding Author Address:

Jonathan Little, PhD

Department of Biology

3333 University Way

Kelowna, BC V1V 1V7

CANADA

Telephone: 250-878-6893

Fax: 250-807-8005

[jonathan.little@ubc.ca](mailto:jonathan.little@ubc.ca)

## **Abstract**

Obesity is linked to increased risk of Alzheimer's disease and cognitive impairment. Microglia-mediated neuroinflammation is implicated in neuronal loss. Elevated levels of fatty acids seen in obesity induce inflammation in peripheral tissues. Whether fatty acids promote neuroinflammation is unknown. Using an established neuroinflammation model involving human microglia-like THP-1 cells and SH-SY5Y neuroblastoma cells we show that the saturated fatty acid palmitate, but not the unsaturated fatty acids oleate or linoleate, induces THP-1 cell pro-inflammatory cytokine secretion and neurotoxicity. Inhibition of c-Jun NH2-terminal kinase (JNK) reduces this neurotoxicity. Therefore, elevated saturated fatty acids may induce neuroinflammation through pathways involving JNK activation.

**Keywords:** Neurodegeneration, palmitic acid, metabolic syndrome X, Alzheimer's disease, microglia

## **Introduction**

Metabolic syndrome, a constellation of vascular and metabolic disorders of which visceral obesity is a principal feature, is a risk factor for cognitive impairment and neurodegeneration, including Alzheimer's disease (AD)<sup>165-168</sup>. The mechanisms linking adiposity to neurodegeneration have not been elucidated.

Neuroinflammation mediated by activated microglia is present in several neurodegenerative diseases, including AD<sup>85,169</sup>. Microglia belong to the mononuclear phagocyte

system and orchestrate brain innate immune responses. Sustained or uncontrolled microglia activation results in chronic inflammation that can lead to collateral neuronal damage<sup>169,170</sup>.

Elevated levels of the saturated fatty acid palmitate contribute to several pathological features in obesity<sup>171-173</sup>. In monocytes, palmitate activates inflammatory signaling and induces the secretion of pro-inflammatory cytokines<sup>174-176</sup>. Recent *in vivo* data indicate that brain palmitate uptake is increased in obese patients with metabolic syndrome<sup>177</sup>. Whether palmitate activates microglia and promotes brain inflammation is unknown.

The purpose of this study was to determine if palmitate activated neuroinflammation. We used an established cell culture system involving transfer of conditioned media from stimulated human microglia-like THP-1 monocytic cells to SH-SY5Y neuroblastoma cells to explore whether palmitate promoted neurotoxicity. THP-1 monocytic cells were used to model microglia because human microglia have limited availability and previous research demonstrates these cell types behave similarly in neurotoxicity experiments<sup>87,178-183</sup>.

## **Materials and Methods**

### *Preparation of fatty acids*

Analytical reagents used were from Sigma-Aldrich (Oakville, ON, Canada) unless stated otherwise. Fatty acid stock solutions (100 mM) were made by dissolving their sodium salts in 70% ethanol with gradual heating to 55°C. 8% fatty acid-free low-endotoxin bovine serum albumin (BSA) dissolved in serum-free DMEM-F12 was prepared fresh and sterile-filtered (0.2 µm) before each experiment. Fatty acids were complexed to BSA for 1 h at 37°C to achieve a fatty acid:albumin molar ratio of ~2:1 and the solution sterile-filtered before being added to cells

<sup>184</sup>. It is unlikely that endotoxin contamination of reagents influenced our results because up to 500 ng/ml of bacterial lipopolysaccharide does not induce THP-1 cell neurotoxicity <sup>178</sup>.

### *Cell Culture*

THP-1 cells were obtained from ATCC (Manassas, VA, USA) and SH-SY5Y cells were a gift from Dr. R. Ross (Fordham University, NY, USA). Cells were grown in DMEM-F12 supplemented with 10% fetal bovine serum (FBS) and 100 U/mL penicillin/100 µg/mL streptomycin (all from Fisher Scientific, Ottawa, ON, Canada) in a humidified 5% CO<sub>2</sub> incubator at 37°C. Neurotoxicity experiments were performed using previously described procedures <sup>87,92</sup>. THP-1 cells were seeded into 24-well plates (5 x 10<sup>5</sup> cells per mL in 0.9 mL) and serum-starved for 24 h prior to addition of fatty acid-BSA complexes. Palmitate was added at a final concentration of 125 µM and 250 µM, which represent moderate and high physiological levels of circulating palmitate, respectively <sup>171,172</sup>. DMEM-F12 containing BSA and ethanol equivalent to 250 µM palmitate served as a control. To determine whether the response was specific to palmitate, the monounsaturated fatty acid, oleate, and the polyunsaturated fatty acid, linoleate, were tested at equal concentrations. After 48 h incubation, MCP-1 and IL-8 concentrations were measured in cell-free culture media by enzyme-linked immunosorbent assay (ELISA) (Peprotech, Rocky Hill, NJ, USA). 0.4 mL of conditioned media was mixed at a 2:1 ratio with fresh DMEM-F12 5% FBS for transfer to SH-SY5Y cells which had been plated 24 h earlier (2 x 10<sup>5</sup> cells per mL in DMEM-F12 5% FBS). After 72 h, lactate dehydrogenase (LDH) activity was measured in cell-free supernatants to determine cell death as previously described <sup>179,185</sup>. LDH release was expressed as a fraction of the value obtained in comparative wells where cells were completely lysed with 1% Triton X-100. For c-Jun NH<sub>2</sub>-terminal kinase (JNK) inhibition

experiments, the specific inhibitor SP600125<sup>186</sup> (0.5-10  $\mu\text{M}$ ) or an equivalent volume of DMSO solvent was added 1 h prior to stimulation of THP-1 cells with palmitate.

### *Statistics*

Due to variability in experimental values obtained on different days, a randomized-block design Analysis of Variance (ANOVA) was used, followed by Dunnett's post-hoc test. Data are presented as means  $\pm$  standard error of the mean (SEM) and are based on 3-5 independent experiments. Significance was established at  $p < 0.05$ .

## **Results**

### *THP-1 cytokine secretion*

Palmitate at both 125 and 250  $\mu\text{M}$  ( $p < 0.001$ , Fig. 1) induced MCP-1 and IL-8 secretion from THP-1 cells. BSA alone was ineffective, indicating that cytokine secretion was induced by palmitate. LDH assay confirmed that palmitate was not toxic to THP-1 cells ( $< 10\%$  cell lysis,  $p > 0.05$ , data not shown).

### *THP-1 cell neurotoxicity*

Transfer of conditioned media from THP-1 cells stimulated with palmitate caused a significant increase in SH-SY5Y neuroblastoma cell death assessed by the LDH assay ( $p < 0.001$ , Fig. 2A). Conditioned media from THP-1 cells incubated with BSA alone, oleate, or linoleate had no effect on SH-SY5Y cell viability. To exclude direct neurotoxicity, SH-SY5Y cells were treated directly with palmitate for 72 h and cell lysis was measured by the LDH assay. Cell lysis was not different in palmitate treated (125  $\mu\text{M}$ =14 $\pm$ 1%, 250  $\mu\text{M}$ =15 $\pm$ 2%) compared to untreated control cell cultures (14 $\pm$ 2%,  $p > 0.05$ ). Treatment of THP-1 cells with the JNK inhibitor

SP600125 at 5 and 10  $\mu\text{M}$  abolished the neurotoxicity of palmitate-stimulated THP-1 cells ( $p=0.004$ , Fig. 2B), while 1 and 0.5  $\mu\text{M}$  had no effects ( $p>0.05$ ). SP600125 did not affect THP-1 cell viability at any concentration (LDH assay,  $<10\%$  lysis,  $p>0.05$ , data not shown).

## Discussion

The saturated fatty acid palmitate, which is implicated as a mediator of inflammation in obesity<sup>173,176,187</sup>, increased pro-inflammatory cytokine secretion by THP-1 monocytes and promoted THP-1 toxicity towards SH-SY5Y neuroblastoma cells. Our findings may provide mechanistic insight in the wide pathological scenario linking obesity to neurodegeneration; elevated levels of palmitate may induce neuronal death through inflammatory processes mediated by monocytes and/or microglia.

Previous research has shown that saturated fatty acids play an important role in obesity-related inflammation in several cell types<sup>173</sup>. Our results indicate that physiologically relevant concentrations of palmitate are not directly toxic towards SH-SY5Y neuronal cells. In contrast, palmitate significantly induced THP-1 cell-mediated neurotoxicity, suggesting that the metabolic environment present in obesity could indirectly promote neuronal death, possibly through activation of microglia or infiltrating monocytes. Treatment of THP-1 cells with the monounsaturated fatty acid, oleate, or polyunsaturated fatty acid, linoleate, did not induce a neurotoxic response, which is in agreement with several previous studies demonstrating that pro-inflammatory reactions are limited to saturated fatty acids<sup>174,175,187</sup>.

Palmitate is thought to promote inflammation through increased ceramide accumulation<sup>175,187</sup>. This effect of palmitate may be mediated by increased expression of dihydroceramide desaturase, which regulates ceramide synthesis<sup>188,189</sup>. In agreement with a role for ceramides, the

synthetic analog C2 ceramide (10-50  $\mu$ M) induced THP-1 neurotoxicity in a similar manner to palmitate (data not shown). Interestingly, longitudinal studies in humans report that elevated saturated fatty acid intake is associated with greater cognitive decline<sup>190</sup> and increased risk of AD<sup>191</sup>. Conversely, higher intake of anti-inflammatory n-3 polyunsaturated fatty acids may reduce the risk of AD<sup>192</sup>. Future research is needed to examine how specific fatty acid combinations influence neuroinflammation.

Activation of JNK may mediate inflammation in obesity<sup>193</sup>. Deletion of JNK1 in cells of myeloid lineage, which includes macrophages, reduces inflammation and prevents insulin resistance in mice fed a high-fat diet<sup>194</sup>. Since palmitate has been shown to activate JNK in THP-1 cells<sup>175,187</sup>, we assessed whether the JNK inhibitor SP600125 reduces palmitate-induced THP-1 neurotoxicity. SP600125 prevented neurotoxicity, suggesting that this pathway is involved. Whether JNK contributes to obesity-related cognitive decline remains to be determined and further research is required to decipher whether JNK inhibition can reduce neuroinflammation *in vivo*.

Accumulating evidence indicates that palmitate promotes inflammation in peripheral immune cells<sup>175,176,187,195</sup>. Palmitate has been shown to activate inflammatory pathways and induce cytokine secretion in THP-1 monocytes<sup>174,175,187</sup>; our findings indicate that palmitate can also induce THP-1 neurotoxicity. The pro-inflammatory effects of palmitate in monocytes are mediated by ceramide synthesis<sup>175,187</sup>, activation of JNK<sup>175</sup>, and/or activation of NF $\kappa$ B<sup>174</sup>. We demonstrate that palmitate may also promote neuroinflammation in the central nervous system, which is of relevance to obesity-related cognitive impairment given that brain palmitate uptake is increased in humans with metabolic syndrome<sup>177</sup>. *In vivo* confirmation of our observations that palmitate causes neurotoxicity through activation of glial cells is needed, although two recent

reports highlight involvement of microglia in obesity-related neuronal damage. Bilbo and Tsang<sup>196</sup> demonstrated that rat pups born to dams fed high saturated fatty acid diets during pregnancy and lactation had increased markers of hippocampal microglia activation accompanied by impaired learning and memory. Similarly, neonatal overnutrition induced symptoms of metabolic syndrome and increased microglia activation in young rats<sup>197</sup>. Together with our current study, these findings provide evidence that saturated fatty acids may activate microglia to promote neuroinflammation in obesity. This could perpetuate and/or enhance microglia activation in response to other triggers, such as amyloid  $\beta$  peptide in AD, to exacerbate neurodegeneration. Further studies are warranted to examine the influence of palmitate and other obesity-related metabolic abnormalities on microglia activation and neuroinflammation.

### **Acknowledgements**

This work was supported by grants from the Natural Sciences and Engineering Research Council of Canada (NSERC) and the Jack Brown and Family Alzheimer's Disease Research Foundation to AK. JPL is supported by an NSERC post-doctoral fellowship

### **References**

1. Giasson BI, Ischiropoulos H, Lee VM, Trojanowski JQ. The relationship between oxidative/nitrative stress and pathological inclusions in Alzheimer's and Parkinson's diseases. *Free Radical Biology & Medicine* 2002;32(12):1264-75.
2. Cummings JL, Cole G. Alzheimer disease. *JAMA* 2002;287(18):2335-8.
3. Heneka MT, O'Banion MK, Terwel D, Kummer MP. Neuroinflammatory processes in Alzheimer's disease. *Journal of Neural Transmission* 2010;117(8):919-47.
4. Block ML, Zecca L, Hong JS. Microglia-mediated neurotoxicity: uncovering the molecular mechanisms. *Nat Rev Immunol* 2007;8(1):57-69.
5. Rogers J, Strohmeier R, Kovelowski CJ, Li R. Microglia and inflammatory mechanisms in the clearance of amyloid beta peptide. *Glia* 2002;40(2):260-9.
6. Hu J, Akama KT, Krafft GA, Chromy BA, Van Eldik LJ. Amyloid-beta peptide activates cultured astrocytes: morphological alterations, cytokine induction and nitric oxide release. *Brain Res* 1998;785(2):195-206.
7. Block ML, Zecca L, Hong JS. Microglia-mediated neurotoxicity: uncovering the molecular mechanisms. *Nature Reviews Neuroscience* 2007;8(1):57-69.

8. Jenner P. Oxidative stress in Parkinson's disease. *Annals of Neurology* 2003;53 Suppl 3:S26-36; discussion S36-8.
9. Nguyen MD, Julien JP, Rivest S. Innate immunity: the missing link in neuroprotection and neurodegeneration? *Nature Reviews Neuroscience* 2002;3(3):216-27.
10. Boyadjieva NI, Sarkar DK. Role of microglia in ethanol's apoptotic action on hypothalamic neuronal cells in primary cultures. *Alcoholism: Clinical & Experimental Research* 2011;34(11):1835-42.
11. McGeer PL, McGeer EG. Inflammation and neurodegeneration in Parkinson's disease. *Parkinsonism & Related Disorders* 2004;10 Suppl 1:S3-7.
12. Marieb EN, editor. *Human Anatomy and Physiology*. 6 ed. San Francisco Pearson Cummings; 2003. 1242 p.
13. Hashioka S, Klegeris A, Schwab C, McGeer PL. Interferon-gamma-dependent cytotoxic activation of human astrocytes and astrocytoma cells. *Neurobiology of Aging* 2009;30(12):1924-35.
14. Cameron B, Landreth GE. Inflammation, microglia, and Alzheimer's disease. *Neurobiol Dis* 2010;37(3):503-9.
15. Zhang W, Wang T, Pei Z, Miller DS, Wu X, Block ML, Wilson B, Zhou Y, Hong JS, Zhang J. Aggregated alpha-synuclein activates microglia: a process leading to disease progression in Parkinson's disease. *FASEB Journal* 2005;19(6):533-42.
16. Li C, Zhao R, Gao K, Wei Z, Yin MY, Lau LT, Chui D, Hoi Yu AC. Astrocytes: implications for neuroinflammatory pathogenesis of Alzheimer's disease. *Curr Alzheimer Res* 2011;8(1):67-80.
17. Gao HM, Zhou H, Zhang F, Wilson BC, Kam W, Hong JS. HMGB1 acts on microglia Mac1 to mediate chronic neuroinflammation that drives progressive neurodegeneration. *Journal of Neuroscience* 2011;31(3):1081-92.
18. Klegeris A, McGeer EG, McGeer PL. Therapeutic approaches to inflammation in neurodegenerative disease. *Current Opinion in Neurology* 2007;20(3):351-7.
19. Lee M, Suk K, Kang Y, McGeer E, McGeer PL. Neurotoxic factors released by stimulated human monocytes and THP-1 cells. *Brain Res* 2011;1400:99-111.
20. Akiyama H, Barger S, Barnum S, Bradt B, Bauer J, Cole GM, Cooper NR, Eikelenboom P, Emmerling M, Fiebich BL and others. Inflammation and Alzheimer's disease. *Neurobiology of Aging* 2000;21(3):383-421.
21. McGeer PL, McGeer EG. NSAIDs and Alzheimer disease: epidemiological, animal model and clinical studies. *Neurobiology of Aging* 2007;28(5):639-47.
22. Leoutsakos JM, Muthen BO, Breitner JC, Lyketsos CG. Effects of non-steroidal anti-inflammatory drug treatments on cognitive decline vary by phase of pre-clinical Alzheimer disease: findings from the randomized controlled Alzheimer's Disease Anti-inflammatory Prevention Trial. *Int J Geriatr Psychiatry* 2011;27(4):364-74.
23. Aisen PS. Evaluation of selective COX-2 inhibitors for the treatment of Alzheimer's disease. *J Pain Symptom Manage* 2002;23(4 Suppl):S35-40.
24. de Jong D, Jansen R, Hoefnagels W, Jellesma-Eggenkamp M, Verbeek M, Borm G, Kremer B. No effect of one-year treatment with indomethacin on Alzheimer's disease progression: a randomized controlled trial. *PLoS One* 2008;3(1):e1475.
25. Scharf S, Mander A, Ugoni A, Vajda F, Christophidis N. A double-blind, placebo-controlled trial of diclofenac/misoprostol in Alzheimer's disease. *Neurology* 1999;53(1):197-201.
26. Fricker SP. Medicinal chemistry and pharmacology of gold compounds. *Transition Met. Chem.* 1996;21:377-383.
27. Kim KH, Kim DS. Juvenile idiopathic arthritis: Diagnosis and differential diagnosis. *Korean J Pediatr* 2010;53(11):931-5.
28. Kean WF, Kean IR. Clinical pharmacology of gold. *Inflammopharmacology* 2008;16(3):112-25.
29. Kean WF, Hart L, Buchanan WW. Auranofin. *Br J Rheumatol* 1997;36(5):560-72.
30. Papp KA, Shear NH. Systemic gold therapy. *Clin Dermatol* 1991;9(4):535-51.

31. Kean WF. Intramuscular versus oral gold therapy. *Baillieres Clin Rheumatol* 1990;4(2):219-46.
32. Hashioka S, Klegeris A, Schwab C, McGeer PL. Interferon-gamma-dependent cytotoxic activation of human astrocytes and astrocytoma cells. *Neurobiol Aging* 2009;30(12):1924-35.
33. Yamamoto N, Izumi Y, Matsuo T, Wakita S, Kume T, Takada-Takatori Y, Sawada H, Akaike A. Elevation of heme oxygenase-1 by proteasome inhibition affords dopaminergic neuroprotection. *J Neurosci Res* 2010;88(9):1934-42.
34. Szczepanik AM, Funes S, Petko W, Ringheim GE. IL-4, IL-10 and IL-13 modulate A beta(1--42)-induced cytokine and chemokine production in primary murine microglia and a human monocyte cell line. *J Neuroimmunol* 2001;113(1):49-62.
35. Klegeris A, McGeer PL. Interaction of various intracellular signaling mechanisms involved in mononuclear phagocyte toxicity toward neuronal cells. *J Leukoc Biol* 2000;67(1):127-33.
36. Muranaka S, Fujita H, Fujiwara T, Ogino T, Sato EF, Akiyama J, Imada I, Inoue M, Utsumi K. Mechanism and characteristics of stimuli-dependent ROS generation in undifferentiated HL-60 cells. *Antioxidants & Redox Signaling* 2005;7(9-10):1367-76.
37. Forehand JR, Pabst MJ, Phillips WA, Johnston RB, Jr. Lipopolysaccharide priming of human neutrophils for an enhanced respiratory burst. Role of intracellular free calcium. *Journal of Clinical Investigation* 1989;83(1):74-83.
38. Arnason BG. Immunologic therapy of multiple sclerosis. *Annu Rev Med* 1999;50:291-302.
39. Serhan CN, Drazen JM. Antiinflammatory potential of lipoxygenase-derived eicosanoids: a molecular switch at 5 and 15 positions? *J Clin Invest* 1997;99(6):1147-8.
40. Drummond GR, Selemidis S, Griendling KK, Sobey CG. Combating oxidative stress in vascular disease: NADPH oxidases as therapeutic targets. *Nature Reviews. Drug Discovery* 2011;10(6):453-71.
41. Frohman EM, Racke MK, Raine CS. Multiple sclerosis--the plaque and its pathogenesis. *N Engl J Med* 2006;354(9):942-55.
42. Cuadrado A, Rojo AI. Heme oxygenase-1 as a therapeutic target in neurodegenerative diseases and brain infections. *Curr Pharm Des* 2008;14(5):429-42.
43. Chao CC, Molitor TW, Hu S. Neuroprotective role of IL-4 against activated microglia. *Journal of Immunology* 1993;151(3):1473-81.
44. Finkelstein AE, Roisman FR, Batista V, de Nudelman FG, de Titto EH, Mizraji M, Walz DT. Oral chrysotherapy in rheumatoid arthritis: minimum effective dose. *J Rheumatol* 1980;7(2):160-8.
45. Walz DT, Dimartino MJ, Griswold DE, Intoccia AP, Flanagan TL. Biologic actions and pharmacokinetic studies of auranofin. *Am J Med* 1983;75(6A):90-108.
46. Zoriy M, Matuschb, A., Sprussc, T., Becker, J. S. Laser ablation inductively coupled plasma mass spectrometry for imaging of copper, zinc, and platinum in thin sections of a kidney from a mouse treated with cis-platin. *Int J Mass Spectrom* 2007;260(2-3):102-106.
47. Kim NH, Lee MY, Park SJ, Choi JS, Oh MK, Kim IS. Auranofin blocks interleukin-6 signalling by inhibiting phosphorylation of JAK1 and STAT3. *Immunology* 2007;122(4):607-14.
48. Kim NH, Oh MK, Park HJ, Kim IS. Auranofin, a gold(I)-containing antirheumatic compound, activates Keap1/Nrf2 signaling via Rac1/iNOS signal and mitogen-activated protein kinase activation. *J Pharmacol Sci* 2010;113(3):246-54.
49. Nakaya A, Sagawa M, Muto A, Uchida H, Ikeda Y, Kizaki M. The gold compound auranofin induces apoptosis of human multiple myeloma cells through both down-regulation of STAT3 and inhibition of NF-kappaB activity. *Leuk Res* 2011;35(2):243-9.
50. Stern I, Wataha JC, Lewis JB, Messer RL, Lockwood PE, Tseng WY. Anti-rheumatic gold compounds as sublethal modulators of monocytic LPS-induced cytokine secretion. *Toxicol In Vitro* 2005;19(3):365-71.
51. Yamashita M, Niki H, Yamada M, Watanabe-Kobayashi M, Mue S, Ohuchi K. Dual effects of auranofin on prostaglandin E2 production by rat peritoneal macrophages. *Eur J Pharmacol* 1997;325(2-3):221-7.

52. Danis VA, Kulesz AJ, Nelson DS, Brooks PM. The effect of gold sodium thiomalate and auranofin on lipopolysaccharide-induced interleukin-1 production by blood monocytes in vitro: variation in healthy subjects and patients with arthritis. *Clinical & Experimental Immunology* 1990;79(3):335-40.
53. Han S, Kim K, Kim H, Kwon J, Lee YH, Lee CK, Song Y, Lee SJ, Ha N. Auranofin inhibits overproduction of pro-inflammatory cytokines, cyclooxygenase expression and PGE2 production in macrophages. *Arch Pharm Res* 2008;31(1):67-74.
54. Dimartino MJ, Walz DT. Inhibition of lysosomal enzyme release from rat leukocytes by auranofin. A new chrysotherapeutic agent. *Inflammation* 1977;2(2):131-42.
55. Pham Huu T, Marquetty C, Amit N, Hakim J. Effect of degranulation on superoxide dismutase activity in human neutrophils. *Journal of Free Radicals in Biology & Medicine* 1986;2(3):213-7.
56. Elferink JG, de Koster BM. Potentiation and inhibition of migration of human neutrophils by auranofin. *Annals of the Rheumatic Diseases* 1993;52(8):595-8.
57. Jeon KI, Jeong JY, Jue DM. Thiol-reactive metal compounds inhibit NF-kappa B activation by blocking I kappa B kinase. *J Immunol* 2000;164(11):5981-9.
58. Park SJ, Kim IS. The role of p38 MAPK activation in auranofin-induced apoptosis of human promyelocytic leukaemia HL-60 cells. *Br J Pharmacol* 2005;146(4):506-13.
59. Greten FR, Karin M. The IKK/NF-kappaB activation pathway-a target for prevention and treatment of cancer. *Cancer Lett* 2004;206(2):193-9.
60. Yamamoto Y, Gaynor RB. Therapeutic potential of inhibition of the NF-kappaB pathway in the treatment of inflammation and cancer. *J Clin Invest* 2001;107(2):135-42.
61. Yamada R, Sano H, Hla T, Hashiramoto A, Fukui W, Miyazaki S, Kohno M, Tsubouchi Y, Kusaka Y, Kondo M. Auranofin inhibits interleukin-1beta-induced transcript of cyclooxygenase-2 on cultured human synoviocytes. *Euro J Pharmacol* 1999;385(1):71-9.
62. Hashioka S, Klegeris A, McGeer PL. Proton pump inhibitors reduce interferon-gamma-induced neurotoxicity and STAT3 phosphorylation of human astrocytes. *GLIA* 2011;59(5):833-40.
63. Hashioka S, Klegeris A, Qing H, McGeer PL. STAT3 inhibitors attenuate interferon-gamma-induced neurotoxicity and inflammatory molecule production by human astrocytes. *Neurobiology of Disease* 2011;41(2):299-307.
64. Terai K, Matsuo A, McGeer PL. Enhancement of immunoreactivity for NF-kappa B in the hippocampal formation and cerebral cortex of Alzheimer's disease. *Brain Research* 1996;735(1):159-68.
65. Griffioen AW, Molema G. Angiogenesis: potentials for pharmacologic intervention in the treatment of cancer, cardiovascular diseases, and chronic inflammation. *Pharmacol Rev* 2000;52(2):237-68.
66. Vagnucci AH, Jr., Li WW. Alzheimer's disease and angiogenesis. *Lancet* 2003;361(9357):605-8.
67. Saura R, Matsubara T, Mizuno K. Inhibition of neovascularization in vivo by gold compounds. *Rheumatol Int* 1994;14(1):1-7.
68. Park SJ, Lee AN, Youn HS. TBK1-targeted suppression of TRIF-dependent signaling pathway of toll-like receptor 3 by auranofin. *Arch Pharm Res* 2010;33(6):939-45.
69. Korherr C, Gille H, Schafer R, Koenig-Hoffmann K, Dixelius J, Eglund KA, Pastan I, Brinkmann U. Identification of proangiogenic genes and pathways by high-throughput functional genomics: TBK1 and the IRF3 pathway. *Proc Natl Acad Sci USA* 2006;103(11):4240-5.
70. Youn HS, Lee JY, Saitoh SI, Miyake K, Hwang DH. Auranofin, as an anti-rheumatic gold compound, suppresses LPS-induced homodimerization of TLR4. *Bioch Biophys Res Comm* 2006;350(4):866-71.
71. Mancek-Keber M, Gradisar H, Inigo Pestana M, Martinez de Tejada G, Jerala R. Free thiol group of MD-2 as the target for inhibition of the lipopolysaccharide-induced cell activation. *J Biol Chem* 2009;284(29):19493-500.

72. Kim IS, Jin JY, Lee IH, Park SJ. Auranofin induces apoptosis and when combined with retinoic acid enhances differentiation of acute promyelocytic leukaemia cells in vitro. *Br J Pharmacol* 2004;142(4):749-55.
73. Brown KK, Cox AG, Hampton MB. Mitochondrial respiratory chain involvement in peroxiredoxin 3 oxidation by phenethyl isothiocyanate and auranofin. *FEBS Letters* 2010;584(6):1257-62.
74. Cox AG, Brown KK, Arner ES, Hampton MB. The thioredoxin reductase inhibitor auranofin triggers apoptosis through a Bax/Bak-dependent process that involves peroxiredoxin 3 oxidation. *Biochem Pharmacol* 2008;76(9):1097-109.
75. Hill KE, McCollum GW, Boeglin ME, Burk RF. Thioredoxin reductase activity is decreased by selenium deficiency. *Biochem Biophys Res Commun* 1997;234(2):293-5.
76. Talbot S, Nelson R, Self WT. Arsenic trioxide and auranofin inhibit selenoprotein synthesis: implications for chemotherapy for acute promyelocytic leukaemia. *Br J Pharmacol* 2008;154(5):940-8.
77. van Oosten BW, Lai M, Barkhof F, Miller DH, Moseley IF, Thompson AJ, Hodgkinson S, Polman CH. A phase II trial of anti-CD4 antibodies in the treatment of multiple sclerosis. *Mult Scler* 1996;1(6):339-42.
78. Ashino T, Sugiuchi J, Uehara J, Naito-Yamamoto Y, Kenmotsu S, Iwakura Y, Shioda S, Numazawa S, Yoshida T. Auranofin protects against cocaine-induced hepatic injury through induction of heme oxygenase-1. *J Toxicol Sci* 2011;36(5):635-43.
79. Shabani F, McNeil J, Tippet L. The oxidative inactivation of tissue inhibitor of metalloproteinase-1 (TIMP-1) by hypochlorous acid (HOCl) is suppressed by anti-rheumatic drugs. *Free Radic Res* 1998;28(2):115-23.
80. Park CH, Lee MJ, Ahn J, Kim S, Kim HH, Kim KH, Eun HC, Chung JH. Heat shock-induced matrix metalloproteinase (MMP)-1 and MMP-3 are mediated through ERK and JNK activation and via an autocrine interleukin-6 loop. *J Invest Dermatol* 2004;123(6):1012-9.
81. Frears ER, Zhang Z, Blake DR, O'Connell JP, Winyard PG. Inactivation of tissue inhibitor of metalloproteinase-1 by peroxynitrite. *FEBS Lett* 1996;381(1-2):21-4.
82. Otterbein LE, Soares MP, Yamashita K, Bach FH. Heme oxygenase-1: unleashing the protective properties of heme. *Trends Immunol* 2003;24(8):449-55.
83. Zakhary R, Poss KD, Jaffrey SR, Ferris CD, Tonegawa S, Snyder SH. Targeted gene deletion of heme oxygenase 2 reveals neural role for carbon monoxide. *Proc Natl Acad Sci U S A* 1997;94(26):14848-53.
84. Yachie A, Niida Y, Wada T, Igarashi N, Kaneda H, Toma T, Ohta K, Kasahara Y, Koizumi S. Oxidative stress causes enhanced endothelial cell injury in human heme oxygenase-1 deficiency. *J Clin Invest* 1999;103(1):129-35.
85. Lee YJ, Han SB, Nam SY, Oh KW, Hong JT. Inflammation and Alzheimer's disease. *Arch Pharm Res* 2010;33(10):1539-56.
86. Klegeris A, Bissonnette CJ, McGeer PL. Reduction of human monocytic cell neurotoxicity and cytokine secretion by ligands of the cannabinoid-type CB2 receptor. *British Journal of Pharmacology* 2003;139(4):775-86.
87. Klegeris A, McGeer PL. Toxicity of human monocytic THP-1 cells and microglia toward SH-SY5Y neuroblastoma cells is reduced by inhibitors of 5-lipoxygenase and its activating protein FLAP. *J Leukoc Biol* 2003;73(3):369-78.
88. Bustin SA, Benes V, Garson JA, Hellemans J, Huggett J, Kubista M, Mueller R, Nolan T, Pfaffl MW, Shipley GL and others. The MIQE guidelines: minimum information for publication of quantitative real-time PCR experiments. *Clin Chem* 2009;55(4):611-22.
89. Rieu I, Powers SJ. Real-time quantitative RT-PCR: design, calculations, and statistics. *Plant Cell* 2009;21(4):1031-3.

90. Glass GV, Peckham PD, Sanders JR. Consequences of Failure to Meet Assumptions Underlying Fixed Effects Analyses of Variance and Covariance. *Review of Educational Research* 1972;42(3):237-288.
91. Klegeris A, Bissonnette CJ, McGeer PL. Modulation of human microglia and THP-1 cell toxicity by cytokines endogenous to the nervous system. *Neurobiology of Aging* 2005;26(5):673-82.
92. Hashioka S, Klegeris A, McGeer PL. Proton pump inhibitors exert anti-inflammatory effects and decrease human microglial and monocytic THP-1 cell neurotoxicity. *Exp Neurol* 2009;217(1):177-83.
93. Glennas A, Kvien TK, Andrup O, Clarke-Jenssen O, Karstensen B, Brodin U. Auranofin is safe and superior to placebo in elderly-onset rheumatoid arthritis. *Br J Rheumatol* 1997;36(8):870-7.
94. Roisman FR, Walz DT, Finkelstein AE. Superoxide radical production by human leukocytes exposed to immune complexes: inhibitory action of gold compounds. *Inflammation* 1983;7(4):355-62.
95. Crooke ST. A comparison of the molecular pharmacology of gold and platinum complexes. *J Rheumatol* 1982;9(SUPPL. 8):61-70.
96. Lee M, Sparatore A, Del Soldato P, McGeer E, McGeer PL. Hydrogen sulfide-releasing NSAIDs attenuate neuroinflammation induced by microglial and astrocytic activation. *Glia* 2010;58(1):103-13.
97. Polanski W, Reichmann H, Gille G. Stimulation, protection and regeneration of dopaminergic neurons by 9-methyl-beta-carboline: a new anti-Parkinson drug? *Expert Rev Neurother* 2011;11(6):845-60.
98. Klegeris A, McGeer PL. Cyclooxygenase and 5-lipoxygenase inhibitors protect against mononuclear phagocyte neurotoxicity. *Neurobiol Aging* 2002;23(5):787-94.
99. Klusa V, Klimaviciusa L, Duburs G, Poikans J, Zharkovsky A. Anti-neurotoxic effects of tauropyrone, a taurine analogue. *Adv Exp Med Biol* 2006;583:499-508.
100. Polanski W, Enzensperger C, Reichmann H, Gille G. The exceptional properties of 9-methyl-beta-carboline: stimulation, protection and regeneration of dopaminergic neurons coupled with anti-inflammatory effects. *J Neurochem* 2010;113(6):1659-75.
101. Klegeris A, McGeer PL. Non-steroidal anti-inflammatory drugs (NSAIDs) and other anti-inflammatory agents in the treatment of neurodegenerative disease. *Current Alzheimer Research* 2005;2(3):355-65.
102. de la Rosa EJ, de Pablo F. Proinsulin: from hormonal precursor to neuroprotective factor. *Front Mol Neurosci* 2011;4:20.
103. Dajas F, Rivera F, Blasina F, Arredondo F, Echeverry C, Lafon L, Morquio A, Heizen H. Cell culture protection and in vivo neuroprotective capacity of flavonoids. *Neurotox Res* 2003;5(6):425-32.
104. Hur JY, Soh Y, Kim BH, Suk K, Sohn NW, Kim HC, Kwon HC, Lee KR, Kim SY. Neuroprotective and neurotrophic effects of quinic acids from *Aster scaber* in PC12 cells. *Biol Pharm Bull* 2001;24(8):921-4.
105. Kim SS, Park RY, Jeon HJ, Kwon YS, Chun W. Neuroprotective effects of 3,5-dicaffeoylquinic acid on hydrogen peroxide-induced cell death in SH-SY5Y cells. *Phytother Res* 2005;19(3):243-5.
106. Angelucci F, Sayed AA, Williams DL, Boumis G, Brunori M, Dimastrogiovanni D, Miele AE, Pauly F, Bellelli A. Inhibition of *Schistosoma mansoni* thioredoxin-glutathione reductase by auranofin: structural and kinetic aspects. *J Biol Chem* 2009;284(42):28977-85.
107. Ellingsen T, Buus A, Stengaard-Pedersen K. Plasma monocyte chemoattractant protein 1 is a marker for joint inflammation in rheumatoid arthritis. *Journal of Rheumatology* 2001;28(1):41-6.
108. Miyachi Y, Yoshioka A, Imamura S, Niwa Y. Anti-oxidant effects of gold compounds. *British Journal of Dermatology* 1987;116(1):39-46.

109. Mirabelli CK, Johnson RK, Sung CM, Faucette L, Muirhead K, Crooke ST. Evaluation of the in vivo antitumor activity and in vitro cytotoxic properties of auranofin, a coordinated gold compound, in murine tumor models. *Cancer Research* 1985;45(1):32-9.
110. Moulton PJ, Hiran TS, Goldring MB, Hancock JT. Detection of protein and mRNA of various components of the NADPH oxidase complex in an immortalized human chondrocyte line. *Br J Rheumatol* 1997;36(5):522-9.
111. Van Dervort AL, Doerfler ME, Stuetz P, Danner RL. Antagonism of lipopolysaccharide-induced priming of human neutrophils by lipid A analogs. *J Immunol* 1992;149(1):359-66.
112. Abramson SL, Gallin JI. IL-4 inhibits superoxide production by human mononuclear phagocytes. *J Immunol* 1990;144(2):625-30.
113. Krause D, Suh HS, Tarassishin L, Cui QL, Durafourt BA, Choi N, Bauman A, Cosenza-Nashat M, Antel JP, Zhao ML and others. The tryptophan metabolite 3-hydroxyanthranilic acid plays anti-inflammatory and neuroprotective roles during inflammation: role of hemeoxygenase-1. *Am J Pathol* 2011;179(3):1360-72.
114. Wong K, Parente J, Prasad KV, Ng D. Auranofin modulated cytoplasmic free calcium in neutrophils by mobilizing intracellular calcium and inhibiting protein kinase. *Journal of Biological Chemistry* 1990;265(35):21454-61.
115. Means AR, Dedman JR. Calmodulin--an intracellular calcium receptor. *Nature* 1980;285(5760):73-7.
116. Chomarat P, Banchereau J. Interleukin-4 and interleukin-13: their similarities and discrepancies. *International Reviews of Immunology* 1998;17(1-4):1-52.
117. Brodie C, Goldreich N, Haiman T, Kazimirsky G. Functional IL-4 receptors on mouse astrocytes: IL-4 inhibits astrocyte activation and induces NGF secretion. *Journal of Neuroimmunology* 1998;81(1-2):20-30.
118. Curbo S, Gaudin R, Carlsten M, Malmberg KJ, Troye-Blomberg M, Ahlborg N, Karlsson A, Johansson M, Lundberg M. Regulation of interleukin-4 signaling by extracellular reduction of intramolecular disulfides. *Biochemical & Biophysical Research Communications* 2009;390(4):1272-7.
119. Blocka K. Auranofin versus injectable gold. Comparison of pharmacokinetic properties. *Am J Med* 1983;75(6A):114-22.
120. Bonilla M, Denicola A, Novoselov SV, Turanov AA, Protasio A, Izmendi D, Gladyshev VN, Salinas G. Platyhelminth mitochondrial and cytosolic redox homeostasis is controlled by a single thioredoxin glutathione reductase and dependent on selenium and glutathione. *J Biol Chem* 2008;283(26):17898-907.
121. Saijo K, Glass CK. Microglial cell origin and phenotypes in health and disease. *Nat Rev Immunol* 2011;11(11):775-87.
122. Kean WF, Forestier F, Kassam Y, Buchanan WW, Rooney PJ. The history of gold therapy in rheumatoid disease. *Seminars in Arthritis & Rheumatism* 1985;14(3):180-6.
123. Champion GD, Graham GG, Ziegler JB. The gold complexes. *Baillieres Clin Rheumatol* 1990;4(3):491-534.
124. Caroli A, Simeoni S, Lepore R, Tramontano A, Via A. Investigation of a potential mechanism for the inhibition of SmTGR by Auranofin and its implications for Plasmodium falciparum inhibition. *Biochem Biophys Res Commun* 2012;417(1):576-81.
125. Tepperman K, Finer R, Donovan S, Elder RC, Doi J, Ratliff D, Ng K. Intestinal uptake and metabolism of auranofin, a new oral gold-based antiarthritis drug. *Science* 1984;225(4660):430-2.
126. McKeage MJ, Berners-Price SJ, Galettis P, Bowen RJ, Brouwer W, Ding L, Zhuang L, Baguley BC. Role of lipophilicity in determining cellular uptake and antitumour activity of gold phosphine complexes. *Cancer Chemotherapy & Pharmacology* 2000;46(5):343-50.
127. Newman ZL, Sirianni N, Mawhinney C, Lee MS, Leppla SH, Moayeri M, Johansen LM. Auranofin protects against anthrax lethal toxin-induced activation of the Nlrp1b inflammasome. *Antimicrob Agents Chemother* 2011;55(3):1028-35.

128. Sannella AR, Casini A, Gabbiani C, Messori L, Bilia AR, Vincieri FF, Majori G, Severini C. New uses for old drugs. Auranofin, a clinically established antiarthritic metalloid drug, exhibits potent antimalarial effects in vitro: Mechanistic and pharmacological implications. *FEBS Letters* 2008;582(6):844-7.
129. Lewis MG, DaFonseca S, Chomont N, Palamara AT, Tardugno M, Mai A, Collins M, Wagner WL, Yalley-Ogunro J, Greenhouse J and others. Gold drug auranofin restricts the viral reservoir in the monkey AIDS model and induces containment of viral load following ART suspension. *AIDS* 2011;25(11):1347-56.
130. Balkwill F, Mantovani A. Inflammation and cancer: back to Virchow? *Lancet* 2001;357(9255):539-45.
131. Kelly MG, Alvero AB, Chen R, Silasi DA, Abrahams VM, Chan S, Visintin I, Rutherford T, Mor G. TLR-4 signaling promotes tumor growth and paclitaxel chemoresistance in ovarian cancer. *Cancer Res* 2006;66(7):3859-68.
132. Valko M, Rhodes CJ, Moncol J, Izakovic M, Mazur M. Free radicals, metals and antioxidants in oxidative stress-induced cancer. *Chem Biol Interact* 2006;160(1):1-40.
133. Brown NS, Bicknell R. Hypoxia and oxidative stress in breast cancer. Oxidative stress: its effects on the growth, metastatic potential and response to therapy of breast cancer. *Breast Cancer Research* 2001;3(5):323-7.
134. Marzano C, Gandin V, Folda A, Scutari G, Bindoli A, Rigobello MP. Inhibition of thioredoxin reductase by auranofin induces apoptosis in cisplatin-resistant human ovarian cancer cells. *Free Rad Biol Med* 2007;42(6):872-81.
135. Ichimura K, Pearson DM, Kocalkowski S, Backlund LM, Chan R, Jones DT, Collins VP. IDH1 mutations are present in the majority of common adult gliomas but rare in primary glioblastomas. *Neuro-Oncology* 2009;11(4):341-7.
136. Hileman EO, Liu J, Albitar M, Keating MJ, Huang P. Intrinsic oxidative stress in cancer cells: a biochemical basis for therapeutic selectivity. *Cancer Chemother Pharmacol* 2004;53(3):209-19.
137. Omata Y, Lewis JB, Lockwood PE, Tseng WY, Messer RL, Bouillaguet S, Wataha JC. Gold-induced reactive oxygen species (ROS) do not mediate suppression of monocytic mitochondrial or secretory function. *Toxicol in Vitro* 2006;20(5):625-33.
138. Stanley BA, Sivakumaran V, Shi S, McDonald I, Lloyd D, Watson WH, Aon MA, Paolocci N. Thioredoxin reductase-2 is essential for keeping low levels of H<sub>2</sub>O<sub>2</sub> emission from isolated heart mitochondria. *J Biol Chem* 2011;286(38):33669-77.
139. Chiellini C, Casini A, Cochet O, Gabbiani C, Ailhaud G, Dani C, Messori L, Amri EZ. The influence of auranofin, a clinically established antiarthritic gold drug, on bone metabolism: analysis of its effects on human multipotent adipose-derived stem cells, taken as a model. *Chem Biodivers* 2008;5(8):1513-20.
140. Debnath A, Parsonage D, Andrade RM, He C, Cobo ER, Hirata K, Chen S, Garcia-Rivera G, Orozco E, Martinez MB and others. A high-throughput drug screen for *Entamoeba histolytica* identifies a new lead and target. *Nat Med* 2012.
141. Jones JS. Life in the 21st century - a vision for all. *S Afr Med J* 1998;88(6):674.
142. Savioli L, Smith H, Thompson A. *Giardia* and *Cryptosporidium* join the 'Neglected Diseases Initiative'. *Trends in Parasitol* 2006;22(5):203-8.
143. Winzeler EA. Malaria research in the post-genomic era. *Nature* 2008;455(7214):751-6.
144. Martinez-Gonzalez JJ, Guevara-Flores A, Alvarez G, Rendon-Gomez JL, Del Arenal IP. In vitro killing action of auranofin on *Taenia crassiceps* metacestode (cysticerci) and inactivation of thioredoxin-glutathione reductase (TGR). *Parasitol Res* 2010;107(1):227-31.
145. Jackson-Rosario S, Cowart D, Myers A, Tarrien R, Levine RL, Scott RA, Self WT. Auranofin disrupts selenium metabolism in *Clostridium difficile* by forming a stable Au-Se adduct. *J Biol Inorg Chem* 2009;14(4):507-19.
146. Jackson-Rosario S, Self WT. Inhibition of selenium metabolism in the oral pathogen *Treponema denticola*. *J Bacteriol* 2009;191(12):4035-40.

147. Lo Vecchio A, Zacur GM. Clostridium difficile infection: an update on epidemiology, risk factors, and therapeutic options. *Curr Opin Gastroenterol* 2012;28(1):1-9.
148. Simonson LG, Goodman CH, Bial JJ, Morton HE. Quantitative relationship of Treponema denticola to severity of periodontal disease. *Infect Immun* 1988;56(4):726-8.
149. Moayeri M, Crown D, Dorward DW, Gardner D, Ward JM, Li Y, Cui X, Eichacker P, Leppa SH. The heart is an early target of anthrax lethal toxin in mice: a protective role for neuronal nitric oxide synthase (nNOS). *PLoS Pathog* 2009;5(5):e1000456.
150. Shapiro DL, Masci JR. Treatment of HIV associated psoriatic arthritis with oral gold. *J Rheumatol* 1996;23(10):1818-20.
151. Rabasseda X. A report from the XVIII International AIDS Conference. (July 18-23, 2010-Vienna, Austria). *Drugs Today (Barc)* 2011;46(12):945-57.
152. Fauci AS. Host factors and the pathogenesis of HIV-induced disease. *Nature* 1996;384(6609):529-34.
153. Fonteh PN, Keter FK, Meyer D. HIV therapeutic possibilities of gold compounds. *Biometals* 2010;23(2):185-96.
154. Chomont N, El-Far M, Ancuta P, Trautmann L, Procopio FA, Yassine-Diab B, Boucher G, Boulassel MR, Ghattas G, Brenchley JM and others. HIV reservoir size and persistence are driven by T cell survival and homeostatic proliferation. *Nat Med* 2009;15(8):893-900.
155. Berners-Price SJ, Filipovska A. Gold compounds as therapeutic agents for human diseases. *Metallomics* 2011;3(9):863-873.
156. Zilka N, Kazmerova Z, Jadhav S, Neradil P, Madari A, Obetkova D, Bugos O, Novak M. Who fans the flames of Alzheimer's disease brains? Misfolded tau on the crossroad of neurodegenerative and inflammatory pathways. *J Neuroinflammation* 2012;9(1):47.
157. Bruze M, Bjorkner B, Moller H. Skin testing with gold sodium thiomalate and gold sodium thiosulfate. *Contact Dermat* 1995;32(1):5-8.
158. Mosmann T. Rapid colorimetric assay for cellular growth and survival: application to proliferation and cytotoxicity assays. *Journal of Immunological Methods* 1983;65(1-2):55-63.
159. Hansen MB, Nielsen SE, Berg K. Re-examination and further development of a precise and rapid dye method for measuring cell growth/cell kill. *Journal of Immunological Methods* 1989;119(2):203-10.
160. Skehan P, Storeng R, Scudiero D, Monks A, McMahon J, Vistica D, Warren JT, Bokesch H, Kenney S, Boyd MR. New colorimetric cytotoxicity assay for anticancer-drug screening. *J Natl Cancer Inst* 1990;82(13):1107-12.
161. Chien WL, Lee TR, Hung SY, Kang KH, Lee MJ, Fu WM. Impairment of oxidative stress-induced heme oxygenase-1 expression by the defect of Parkinson-related gene of PINK1. *J Neurochem* 2011;117(4):643-53.
162. Hayashi F, Means TK, Luster AD. Toll-like receptors stimulate human neutrophil function. *Blood* 2003;102(7):2660-9.
163. Madeira JM, Beloukhina N, Boudreau K, Boettcher TA, Gurley L, Walker DG, McNeil WS, Klegeris A. Cobalt(II) beta-ketoamino complexes as novel inhibitors of neuroinflammation. *Eur J Pharmacol* 2012;676(1-3):81-8.
164. Vos CM, Sjulson L, Nath A, McArthur JC, Pardo CA, Rothstein J, Conant K. Cytotoxicity by matrix metalloprotease-1 in organotypic spinal cord and dissociated neuronal cultures. *Exp Neurol* 2000;163(2):324-30.
165. Profenno LA, Porsteinsson AP, Faraone SV. Meta-analysis of Alzheimer's disease risk with obesity, diabetes, and related disorders. *Biol Psychiatry* 2010;67(6):505-12.
166. Panza F, Frisardi V, Capurso C, Imbimbo BP, Vendemiale G, Santamato A, D'Onofrio G, Seripa D, Sancarolo D, Pilotto A and others. Metabolic syndrome and cognitive impairment: current epidemiology and possible underlying mechanisms. *J Alzheimers Dis* 2010;21(3):691-724.
167. Whitmer RA, Gunderson EP, Quesenberry CP, Jr., Zhou J, Yaffe K. Body mass index in midlife and risk of Alzheimer disease and vascular dementia. *Curr Alzheimer Res* 2007;4(2):103-9.

168. Peila R, Rodriguez BL, Launer LJ. Type 2 diabetes, APOE gene, and the risk for dementia and related pathologies: The Honolulu-Asia Aging Study. *Diabetes* 2002;51(4):1256-62.
169. Block ML, Zecca L, Hong JS. Microglia-mediated neurotoxicity: uncovering the molecular mechanisms. *Nat Rev Neurosci* 2007;8(1):57-69.
170. Klegeris A, McGeer EG, McGeer PL. Therapeutic approaches to inflammation in neurodegenerative disease. *Curr Opin Neurol* 2007;20(3):351-7.
171. Mittendorfer B, Magkos F, Fabbrini E, Mohammed BS, Klein S. Relationship between body fat mass and free fatty acid kinetics in men and women. *Obesity (Silver Spring)* 2009;17(10):1872-7.
172. Jensen MD, Haymond MW, Rizza RA, Cryer PE, Miles JM. Influence of body fat distribution on free fatty acid metabolism in obesity. *J Clin Invest* 1989;83(4):1168-73.
173. Lee JY, Zhao L, Hwang DH. Modulation of pattern recognition receptor-mediated inflammation and risk of chronic diseases by dietary fatty acids. *Nutr Rev* 2010;68(1):38-61.
174. Dasu MR, Jialal I. Free fatty acids in the presence of high glucose amplify monocyte inflammation via Toll-like receptors. *Am J Physiol Endocrinol Metab* 2011;300(1):E145-54.
175. Haversen L, Danielsson KN, Fogelstrand L, Wiklund O. Induction of proinflammatory cytokines by long-chain saturated fatty acids in human macrophages. *Atherosclerosis* 2009;202(2):382-93.
176. Nguyen MT, Favelyukis S, Nguyen AK, Reichart D, Scott PA, Jenn A, Liu-Bryan R, Glass CK, Neels JG, Olefsky JM. A subpopulation of macrophages infiltrates hypertrophic adipose tissue and is activated by free fatty acids via Toll-like receptors 2 and 4 and JNK-dependent pathways. *J Biol Chem* 2007;282(48):35279-92.
177. Karmi A, Iozzo P, Viljanen A, Hirvonen J, Fielding BA, Virtanen K, Oikonen V, Kempainen J, Viljanen T, Guiducci L and others. Increased brain fatty acid uptake in metabolic syndrome. *Diabetes* 2010;59(9):2171-7.
178. Klegeris A, Bissonnette CJ, McGeer PL. Modulation of human microglia and THP-1 cell toxicity by cytokines endogenous to the nervous system. *Neurobiol Aging* 2005;26(5):673-82.
179. Klegeris A, Bissonnette CJ, McGeer PL. Reduction of human monocytic cell neurotoxicity and cytokine secretion by ligands of the cannabinoid-type CB2 receptor. *Br J Pharmacol* 2003;139(4):775-86.
180. Klegeris A, Choi HB, McLarnon JG, McGeer PL. Functional ryanodine receptors are expressed by human microglia and THP-1 cells: Their possible involvement in modulation of neurotoxicity. *J Neurosci Res* 2007;85(10):2207-15.
181. Klegeris A, Pelech S, Giasson BI, Maguire J, Zhang H, McGeer EG, McGeer PL. Alpha-synuclein activates stress signaling protein kinases in THP-1 cells and microglia. *Neurobiol Aging* 2008;29(5):739-52.
182. Bamberger ME, Harris ME, McDonald DR, Husemann J, Landreth GE. A cell surface receptor complex for fibrillar beta-amyloid mediates microglial activation. *J Neurosci* 2003;23(7):2665-74.
183. Si Q, Zhao ML, Morgan AC, Brosnan CF, Lee SC. 15-deoxy-Delta12,14-prostaglandin J2 inhibits IFN-inducible protein 10/CXC chemokine ligand 10 expression in human microglia: mechanisms and implications. *J Immunol* 2004;173(5):3504-13.
184. Yuzefovych L, Wilson G, Racheck L. Different effects of oleate vs. palmitate on mitochondrial function, apoptosis, and insulin signaling in L6 skeletal muscle cells: role of oxidative stress. *Am J Physiol Endocrinol Metab* 2010;299(6):E1096-105.
185. Decker T, Lohmann-Matthes ML. A quick and simple method for the quantitation of lactate dehydrogenase release in measurements of cellular cytotoxicity and tumor necrosis factor (TNF) activity. *J Immunol Methods* 1988;115(1):61-9.
186. Bennett BL, Sasaki DT, Murray BW, O'Leary EC, Sakata ST, Xu W, Leisten JC, Motiwala A, Pierce S, Satoh Y and others. SP600125, an anthrapyrazolone inhibitor of Jun N-terminal kinase. *Proc Natl Acad Sci U S A* 2001;98(24):13681-6.
187. Schwartz EA, Zhang WY, Karnik SK, Borwege S, Anand VR, Laine PS, Su Y, Reaven PD. Nutrient modification of the innate immune response: a novel mechanism by which saturated

- fatty acids greatly amplify monocyte inflammation. *Arterioscler Thromb Vasc Biol* 2010;30(4):802-8.
188. Hu W, Ross J, Geng T, Brice SE, Cowart LA. Differential regulation of dihydroceramide desaturase by palmitate versus monounsaturated fatty acids: implications for insulin resistance. *J Biol Chem* 2011;286(19):16596-605.
189. Kravka JM, Li L, Szulc ZM, Bielawski J, Ogretmen B, Hannun YA, Obeid LM, Bielawska A. Involvement of dihydroceramide desaturase in cell cycle progression in human neuroblastoma cells. *J Biol Chem* 2007;282(23):16718-28.
190. Morris MC, Evans DA, Bienias JL, Tangney CC, Wilson RS. Dietary fat intake and 6-year cognitive change in an older biracial community population. *Neurology* 2004;62(9):1573-9.
191. Morris MC, Evans DA, Bienias JL, Tangney CC, Bennett DA, Aggarwal N, Schneider J, Wilson RS. Dietary fats and the risk of incident Alzheimer disease. *Arch Neurol* 2003;60(2):194-200.
192. Morris MC, Evans DA, Bienias JL, Tangney CC, Bennett DA, Wilson RS, Aggarwal N, Schneider J. Consumption of fish and n-3 fatty acids and risk of incident Alzheimer disease. *Arch Neurol* 2003;60(7):940-6.
193. Hotamisligil GS. Role of endoplasmic reticulum stress and c-Jun NH2-terminal kinase pathways in inflammation and origin of obesity and diabetes. *Diabetes* 2005;54 Suppl 2:S73-8.
194. Solinas G, Vilcu C, Neels JG, Bandyopadhyay GK, Luo JL, Naugler W, Grivennikov S, Wynshaw-Boris A, Scadeng M, Olefsky JM and others. JNK1 in hematopoietically derived cells contributes to diet-induced inflammation and insulin resistance without affecting obesity. *Cell Metab* 2007;6(5):386-97.
195. Assmann A, Mohlig M, Osterhoff M, Pfeiffer AF, Spranger J. Fatty acids differentially modify the expression of urokinase type plasminogen activator receptor in monocytes. *Biochem Biophys Res Commun* 2008;376(1):196-9.
196. Bilbo SD, Tsang V. Enduring consequences of maternal obesity for brain inflammation and behavior of offspring. *FASEB J* 2010;24(6):2104-15.
197. Tapia-Gonzalez S, Garcia-Segura LM, Tena-Sempere M, Frago LM, Castellano JM, Fuente-Martin E, Garcia-Caceres C, Argente J, Chowen JA. Activation of microglia in specific hypothalamic nuclei and the cerebellum of adult rats exposed to neonatal overnutrition. *J Neuroendocrinol* 2011;23(4):365-70.

## Figure Legends

**Fig. 1.** Palmitate induces MCP-1 and IL-8 secretion from THP-1 monocytes. Cytokine concentrations were measured by ELISA after 48 h incubation with BSA alone or BSA complexed with 125  $\mu$ M and 250  $\mu$ M palmitate. Data from 4 independent experiments are presented; \* $p$ <0.001 vs. unstimulated THP-1 cell cultures.

**Fig. 2.** Palmitate induces human THP-1 monocytic cell toxicity towards SH-SY5Y neuronal cells that is ameliorated by inhibition of c-Jun NH<sub>2</sub>-terminal kinase (JNK). **(A)** SH-SY5Y cell viability was assessed by the LDH assay after 72 h treatment with conditioned media from THP-1 cells, which had been incubated for 48 h with BSA alone or BSA complexed with palmitate, oleate, or linoleate at the indicated concentrations. **(B)** Treatment of THP-1 cells with 10  $\mu$ M of the JNK inhibitor SP600125 significantly reduced palmitate-induced THP-1 neurotoxicity. Data from 3-5 independent experiments are presented; \* $p$ <0.001 vs. treatment with unstimulated THP-1 cell conditioned media.

Figure 1

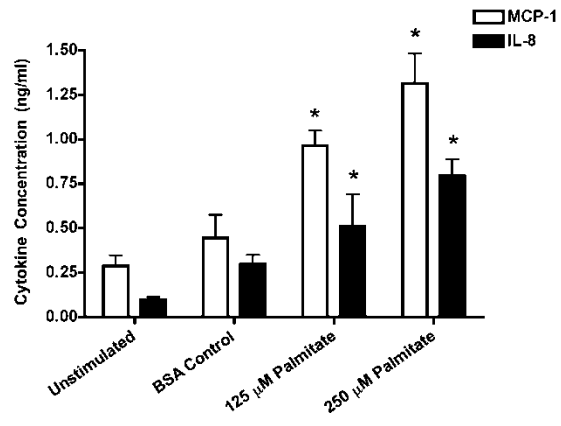


Figure 2

